G4625
K9-1

GEOTECHNICAL ENGINEERING

THE PROPERTIES OF SAN FRANCISCO BAY MUD AT HAMILTON AIR FORCE BASE, CALIFORNIA

by

Rudolph Bonaparte
and
James K. Mitchell

April 1979

Department of Civil Engineering

University of California, Berkeley

TABLE OF CONTENTS

Section	Title	Page
1	Geology	1
	A) San Francisco Bay Mud	3
	B) Hamilton Air Force Base Site	8
2	Composition and Engineering Properties	12
	A) Soil Description	12
	B) Composition	12
	C) Particle Size Determination and Soil Activity	13
	D) Specific Gravity	15
	E) Unit Weight	15
	F) Atterberg Limits and Water Contents - Liquidity Index	17
	G) Organic Content	17
3	Compressibility	21
	A) General	21
	B) Consolidation Tests	21
	C) Summary	43
4	In-Situ Measurements of Soil Properties	48
	A) Introduction	48
	B) Field Vane Shear Tests	48
	C) Cone Penetration Test	56
	D) Self Boring Pressuremeter	62
	E) Discussion of In-Situ Shear Strength Test Results	65
	F) Evaluation of In-situ Lateral Stresses	69
5	Laboratory Strength Tests	76
	A) Effective Stress Strength Parameters	76
	B) IC-U Triaxial Tests	83
	1) Normalized Behavior	96
	2) Behavior of Remolded Bay Mud	96
	3) Strain Rate Effects in IC-U Tests	100
	C) AC-U Triaxial Tests	110
	D) Summary of IC-U and AC-U Triaxial Test Results	122
	E) Effect of Overconsolidation	122
	F) UU and Laboratory Vane Tests	126
	G) Plane Strain Tests	131
6	Stress-Strain-Time Behavior	144
	A) Introduction	144
	B) Creep Behavior of Bay Mud	144
	C) Creep Behavior-Remolded Bay Mud	161
	D) Creep Rupture	161
7	Summary	168

Section	Title	Page
	Bibliography	171
Appendix 1	Corrections to Strength Test Data	174

ABSTRACT

The Hamilton Air Force Base in Novato, California underlain by a 55 to 60 ft. thick homogeneous deposit of soft gray silty clay known locally as the San Francisco Bay Mud. This soil has been the subject of much study through the years and a substantial body of information has been accumulated on its engineering properties. This report brings together much of this information. The Bay Mud's compositional, index, compressibility, deformation and strength properties, as determined from in-situ and laboratory tests, are presented in the accompanying table. Where appropriate, these properties have been compared with those of Bay Mud from other locations around the Bay, as well as with established soil property correlations that can be found in the literature.

SUMMARY OF ENGINEERING PROPERTIES OF S.F. BAY MUD AT THE UNIVERSITY OF CALIFORNIA HAMILTON AIR FORCE BASE TEST SITE

Property	Value
Thickness of Deposit	55-58 ft
Depth of Water Table	0-12 ft
Winter Average	4-6 ft
Summer Average	8 ft
Saturated Unit Weight	94 pcf
Natural Water Content (%)	90
Liquid Limit (%)	88
Plasticity Index (%)	40
Liquidity Index (%)	1
Organic Content (Total carbon - %)	1.5
Compression Index C_c	
Just past p_p'	1.2-1.8 (1.5~average)
For $p' > 2$-3 kg/cm^2	.8-.9
Recompression Index C_r	.10-.15
Coefficient of Secondary Compression C_α	.01-.02
Coefficient of Consolidation, C_v	8-10 ft^2/year
Effective Stress Friction Angle, ϕ'	
Consolidated undrained triaxial	32.5°-35° (34° average)
Vertical Plane Strain C-U	38°
Horizontal Plane Strain C-U	35°
Consolidated Drained	31°
Undrained Strength Ratio $S_u/\bar{p}$	
IC-U	.34
AC-U (K_o)	.35
UU	.32
Field Vane	.31-.32
Cone Penetrometer	.31-.32
Self Boring Pressuremeter	.40
IC-U Data Extrapolated (to an OCR of 1.1-1.5)	.36-.42

SUMMARY OF ENGINEERING PROPERTIES OF S.F. BAY MUD AT THE UNIVERSITY OF CALIFORNIA HAMILTON AIR FORCE BASE TEST SITE (CONTD.)

Property	Value
Undrained Strength Ratio-Continued	
Vertical Plane Strain	.29
Horizontal Plane Strain	.37
Creep Parameters (Undrained Creep on CU Samples)	
α	4.45
A	.0035%/minute
m	.7-.8
Overconsolidation Ratio	
Crust	3
"Normally Consolidated Zone	1.0-1.5
In-Situ Lateral Stresses	See Text
Modulus Multiplier M ($E = MS_u$)	See Text

1. GEOLOGY

The San Francisco Bay occupies a depression situated between uplifted regions which lie to the east and west. Associated with both of the uplifted regions are active faults. To the east of the Bay stand the Berkeley Hills, along the base of which lies the Hayward Fault. To the west of the Bay lies a series of mountains, including the Montara Mountains, through the center of which passes the San Andreas Fault.

The Franciscan formation comprises the primary bedrock unit beneath the Bay and the surrounding areas. This formation, which is of Jurassic age, consists primarily of graywacke (sandstone), but also contains shale, siltstone, chert, greenstone and serpentine. Prior to the deposition of the various Bay sediments, the Franciscan formation underwent considerable faulting, deformation and erosion. Consequently, the erosional unconformity between the Franciscan and the overlying sediments shows considerable relief.

Overlying bedrock are the San Francisco Bay sediments, a series of five sedimentary formations, the youngest of which is the San Francisco Bay Mud. Descriptions of these five formations, are given in Table 1. The Bay sediments are of late Quaternary age and consist of materials washed out of the surrounding hills and from sediments brought down the Sacramento River and other smaller rivers that enter the Bay. The diversity of the source rock from which Bay sediments are derived accounts for the wide variety of minerals found in them.

The Alameda, San Antonio and Posey formations, the oldest of the Bay sediments are alluvial in nature, having been deposited above sea level. These formations are composed of moderately stiff to very stiff clays, sandy clays, sands and fine gravels. Collectively they are known as the Older

TABLE 1 CORRELATION CHART OF SEDIMENTS OF SAN FRANCISCO BAY
From Denby (1978)

<table>
<tr><th>TRASK and ROLSTON (1951)</th><th colspan="2">TREASHER (1961)</th></tr>
<tr><td>BAY MUD

Formation A

Member A-1 Soft mud up to 65 ft. thick composed of silty clay and occasional interbedded thin sand layers

A-2 Fine to medium grained silty sand up to 40 ft. thick

A-3 Silty clay, firmer and less sandy than zone A-1, up to 45 ft. thick</td><td>Younger Bay Mud</td><td>Normally consolidated member

Semi-consolidated member</td></tr>
<tr><td>MERRITT SAND

Wind-blown sand up to 60 ft. thick</td><td colspan="2">SAND DEPOSITS

Including Merritt Sand</td></tr>
<tr><td>POSEY FORMATION

A mixture of sand and sandy clay up to 50 ft. thick</td><td colspan="2" rowspan="3">OLDER BAY MUD</td></tr>
<tr><td>SAN ANTONIO FORMATION

A sequence of moderately firm clays, sands and gravels between 15 and 120 ft. thick</td></tr>
<tr><td>ALAMEDA FORMATION

This formation varies from very firm clay through sandy clay to sand and gravel. It varies up to 200 ft. in thickness</td></tr>
<tr><td>BEDROCK</td><td colspan="2">BEDROCK</td></tr>
</table>

Bay Mud and comprise a competent foundation material. For instance, the caissons for the section of the Bay Bridge between Yerba Buena Island and Oakland are founded in the Alameda Formation.

Throughout the geologic history of the San Francisco Bay there have been periodic changes in the level of the oceans. These risings and lowerings of the sea level were principally associated with the great glacial advances and retreats that occurred during the late Pleistocene Epoch. With each drop in sea level the hydraulic gradients of the rivers and streams entering the Bay were increased. The increased gradients caused intense erosion near the mouths of these rivers and streams. The result of this action was the creation of valleys in the Bay sediments. As the sea level eventually rose these valleys were either partially or totally filled with new sediment resulting in the existence of a series of erosional unconformities between the various sedimentary formations. The most pronounced unconformity is the one lying between the Posey Formation and the Merritt Sand. It is associated with the last major glacial advance and a drop in sea level of about 200-300 feet. Valleys up to 1000 feet wide were eroded into the Posey formation. With time, the aeolian Merritt Sand partially filled these valleys and covered the flats between valleys. As the sea level continued to rise the nature of the material being deposited in the Bay changed from a sand to a fine-grained sediment. The topmost fine-grained material comprises the deposit known as Bay Mud.

San Francisco Bay Mud

Because of the already mentioned erosional unconformities the thickness of the Bay Mud deposit varies considerably. Where it has filled the preexisting valleys in the Merritt Sand and the Posey Formation its thickness

may exceed 100 feet. In the flat areas between valleys the thickness of the deposit may be only 10 to 20 feet. The Bay Mud is composed of dark gray silty clay, with thin layers of silt and fine to medium grained sands, small amounts of organic material and shell fragments. Where it is exposed at the surface it is fairly stiff and somewhat desiccated. At depth it is very nearly normally consolidated.

As with the thickness of the Bay Mud deposit, the engineering properties of this soil vary from point to point across the Bay Area. Denby (1978) compiled a partial list of the engineering properties of Bay Mud at various locations around the Bay (this table is based on a similar earlier table developed by Mitchell (1963)). This list has been expanded with material that has been obtained during this study and is shown in Table 2. The locations of most of the sites from which the data used in Table 2 was obtained are shown on a map of the San Francisco Bay Area, which is presented in Figure 1. Note the differences in the thickness of the Bay Mud deposit, in-situ water contents and unit weights, Atterberg Limits, compressibility and strength characteristics for the different sites listed. Values for the liquid limit range from 41.5% at the Bridge Oakland Mole, to 90% at the Hamilton Air Force Base (HAFB), to a high of 119% at Candlestick Cove. The normalized strength parameter $s_u/\bar{p}$ (S_u = undrained shear strength; $\bar{p}$ = effective overburden pressure) varies between .11 and .40. The high value for $S_u/\bar{p}$ may be due to ageing effects (discussed later), water table changes or unloading. Denby (1978) postulates that the very low value of $S_u/\bar{p}$ = .11 at the Islais Creek site may be due to the fact that the soil at that particular site is very young geologically, compared to Bay Mud deposits in other locations, and consequently has not undergone the ageing effects

TABLE 2 COMPARISON OF ENGINEERING PROPERTIES OF BAY MUD

Location	Reference	Thickness of mud (feet)	Natural water content (percent)	Liquid limit (percent)	Plastic limit (percent)	Unit weight lb/ft^3	Mean diameter D_{50} in microns	Shear Strength lb/ft^2	Compression index C_c	$S_u/\bar{p}$	S_u/ft psf/ft
Proposed Southern Crossing	Trask and Rolston (1951)	0-45				94-107	1.4-10.5				
Proposed parallel Crossing	Trask and Rolston (1951)	0-65	35-80	47-68	--	93-113	3.7-13.5	200-400	--		
Oakland Estuary	Trask and Rolston (1951)	0-45				96-101	3.6-5.8				
Adjacent to Bridge Oakland Mole	Seed and Reese (1957)	20	35-50	41.5	23.5	112	--	100-500	0.36-0.45		
Islais Creek Basin	Lee (1953)	128	52-62	--	--	102-107	--	100-1000	--		
Candlestick Cove	Private Communication	>65	50-75	65-119	28-35	98-108	2-10	150-800	0.5-1.0		
Hamilton Air Force Base	Duncan (1965)	60	90	88	43	93-96	--	400-1200	1.1	0.32	10
Lash Terminal, Port of San Francisco	Duncan and Buchignani (1973)	100	55	50	30	100	--	200-700	--	0.27	10
Islais Creek S1	Clough and Sitar (1977)	50	55-95	75-100	30-45	105	--	400-1000	--	0.40	17
Islais Creek S2	Clough and Sitar (1977)	120	75-95	75-110	30-45	99	--	400-500	--	0.11	4
Ferry Building	Private Communication (1965)	--	--	--	--	98	--	--	--	0.24	10
Embarcadero Center	Private Communication (1971)	--	--	--	--	110	--	400-1500	--	0.27	13
Hamilton	Denby (1978)	58	86-90	85-88	38-40	94	--	400-1300	.8-1.1	0.34	10.7
Menlo Park	Holzer et al., (1973)		86-97	99	47				~1.1		
South S.F. Bay	Arulanandan et al., (1971)		96-103	93	45	90.5					

SAN FRANCISCO BAY

LOCATION MAP

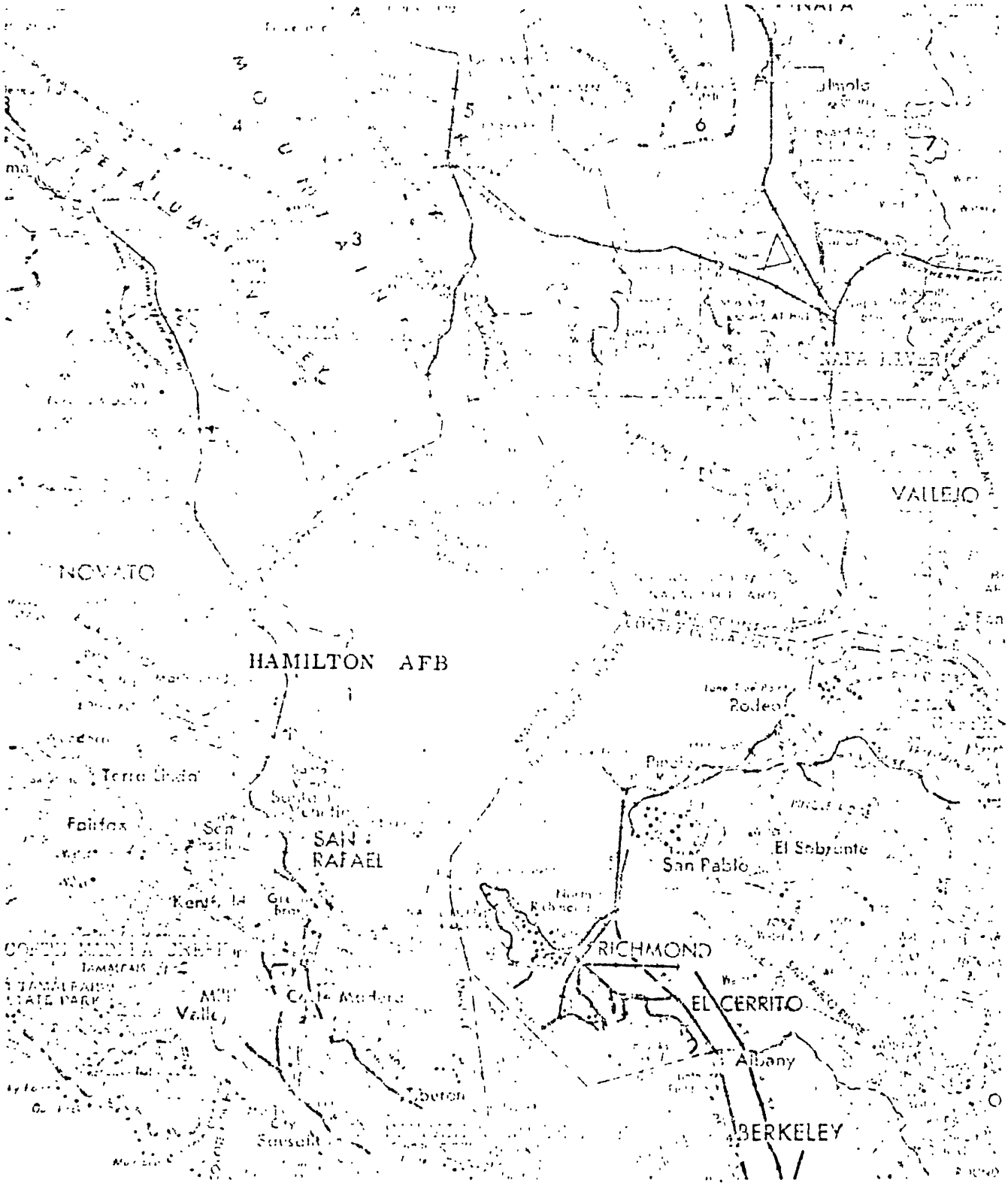
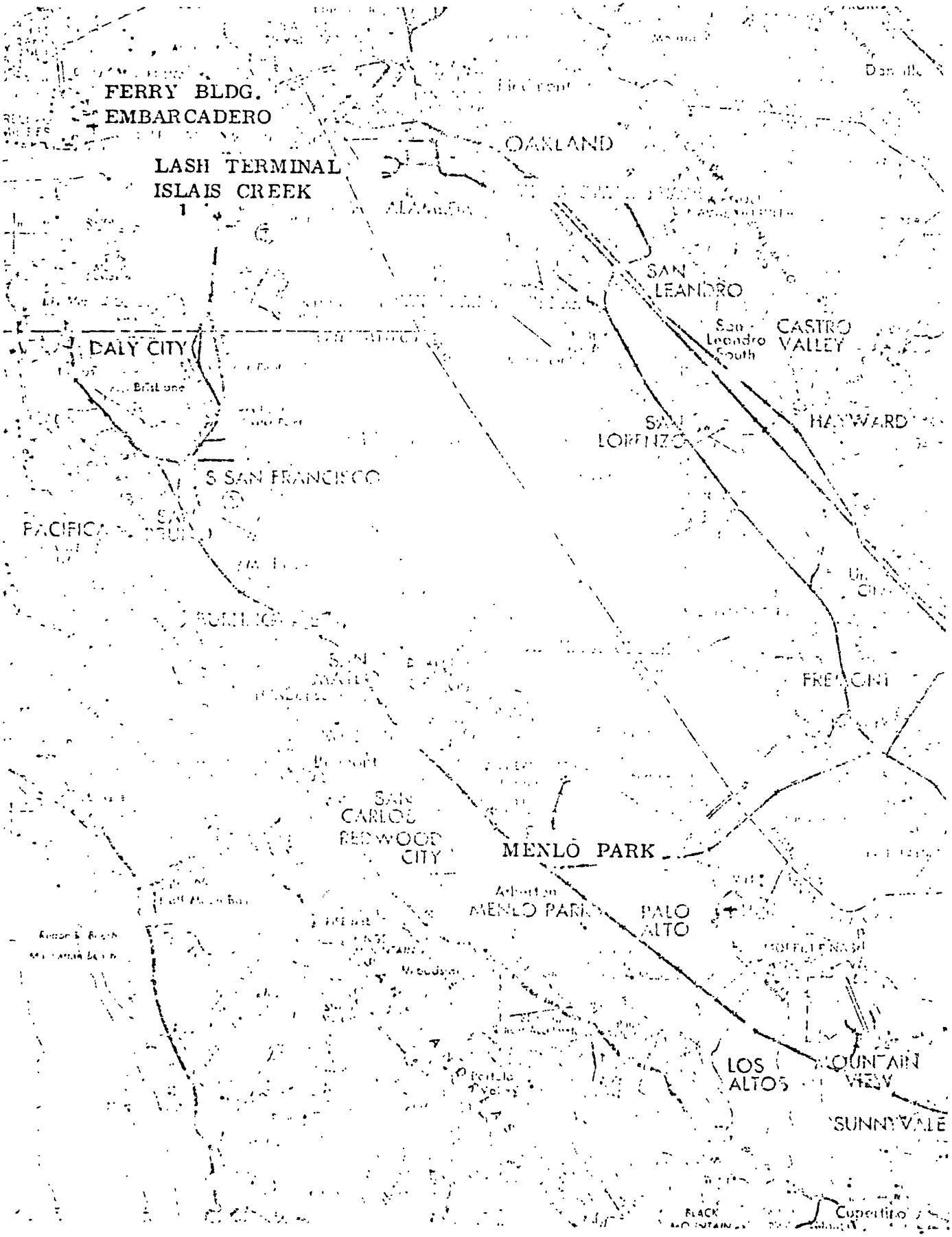


FIGURE 1 NORTH SAN FRANCISCO BAY

FIGURE 1 (Continued) SOUTH SAN FRANCISCO BAY



associated with the older soils. Conceivably, the soil at this particular location is underconsolidated.

Stratton (1975) attempted to correlate Atterberg Limits, water content, specific gravity, undrained shear strength and compressibility with location throughout the San Francisco Bay. He concluded "test values varied greatly and even average site values showed no correlation." He indicated that on the average the compressibility of the Bay Mud at the southern end of the Bay is slightly greater than at the northern end or in the San Pablo Bay Area. There was however, considerable scatter in his results.

Hamilton Air Force Base Site

The remainder of this report will be concerned primarily with the engineering properties of the Bay Mud that underlies the Hamilton Air Force Base, which lies near the northwestern shore of San Francisco Bay, as indicated in Figure 1. The Bay Mud at this site has properties that fall between the extremes reported at other locations around the Bay. It extends from the ground surface to a depth of about 58 ft. The top part of the deposit has been oxidized, weathered and desiccated and has a light to medium gray color. The stiff desiccated zone extends to a depth of about 10 ft. Below this upper zone the Bay Mud is a soft dark gray silty clay with various silt and fine sand lenses. It contains numerous very small shell fragments and small amounts of organic material.

The log of a recent soil boring taken from the HAFB site is presented in Figure 2. The boring was drilled on August 4, 1977 by the United States Geological Survey. The samples were extruded and recorded at Stanford University, and reported by Denby (1978). The approximate location of the

soil boring within the base is shown in Figure 3. Almost all of the geotechnical studies which have been carried out at HAFB have been located within 150 feet of this boring. The depth of the water table varies seasonally at the site. During the summer the water table may drop to 11 or 12 feet below the ground surface. In the winter it may be near the surface. The average depth of the water table throughout the year lies between 6 and 8 ft.

For a more complete description of the Bay and its geology the papers by Trask and Rolston (1961), Treasher (1963), Mitchell (1963), Oakeshott (1966) and Schlocker (1974) should be consulted.

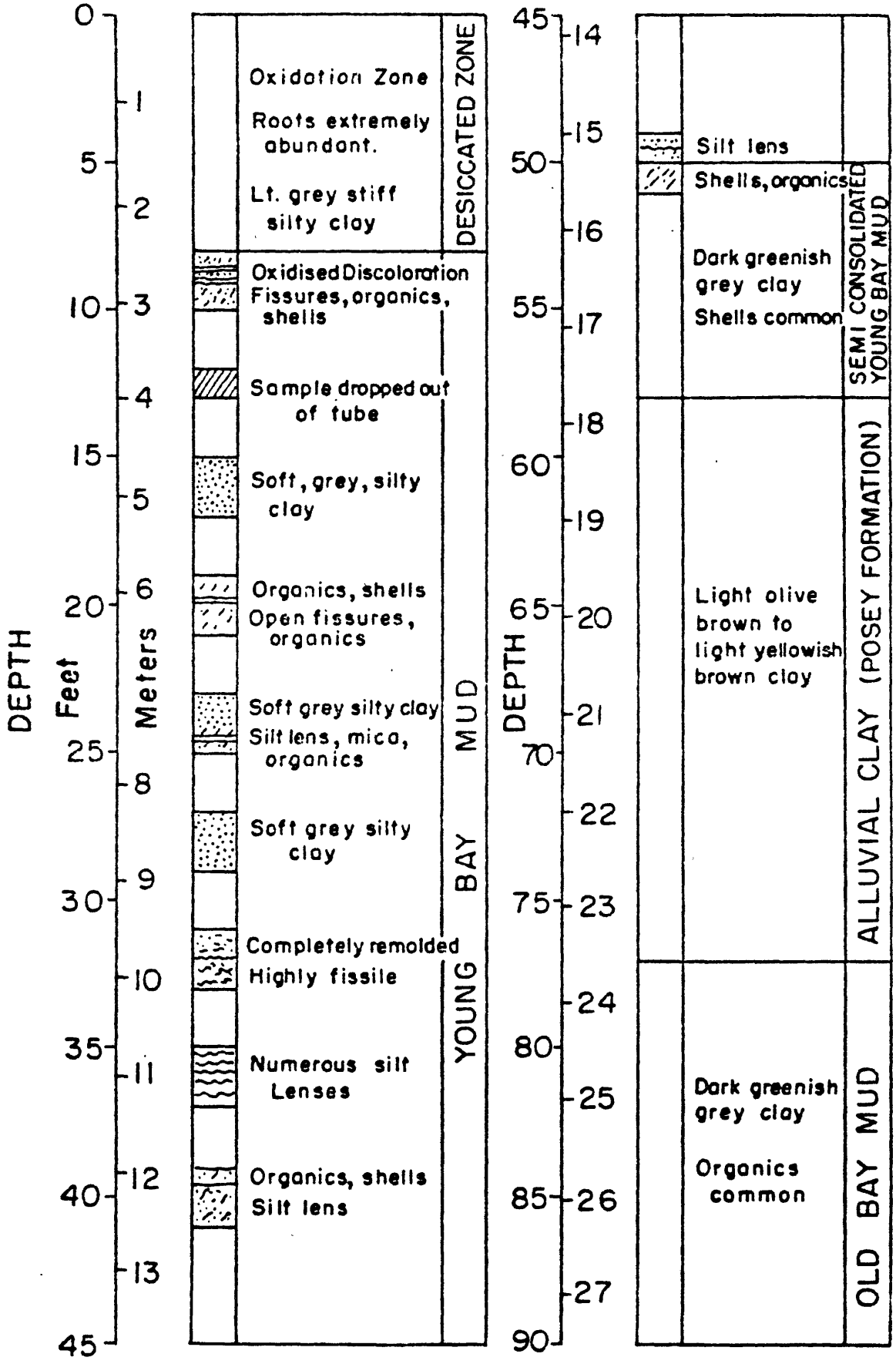


FIGURE 2 LOG OF BOREHOLE AT HAMILTON AIR FORCE BASE

From Denby (1978)

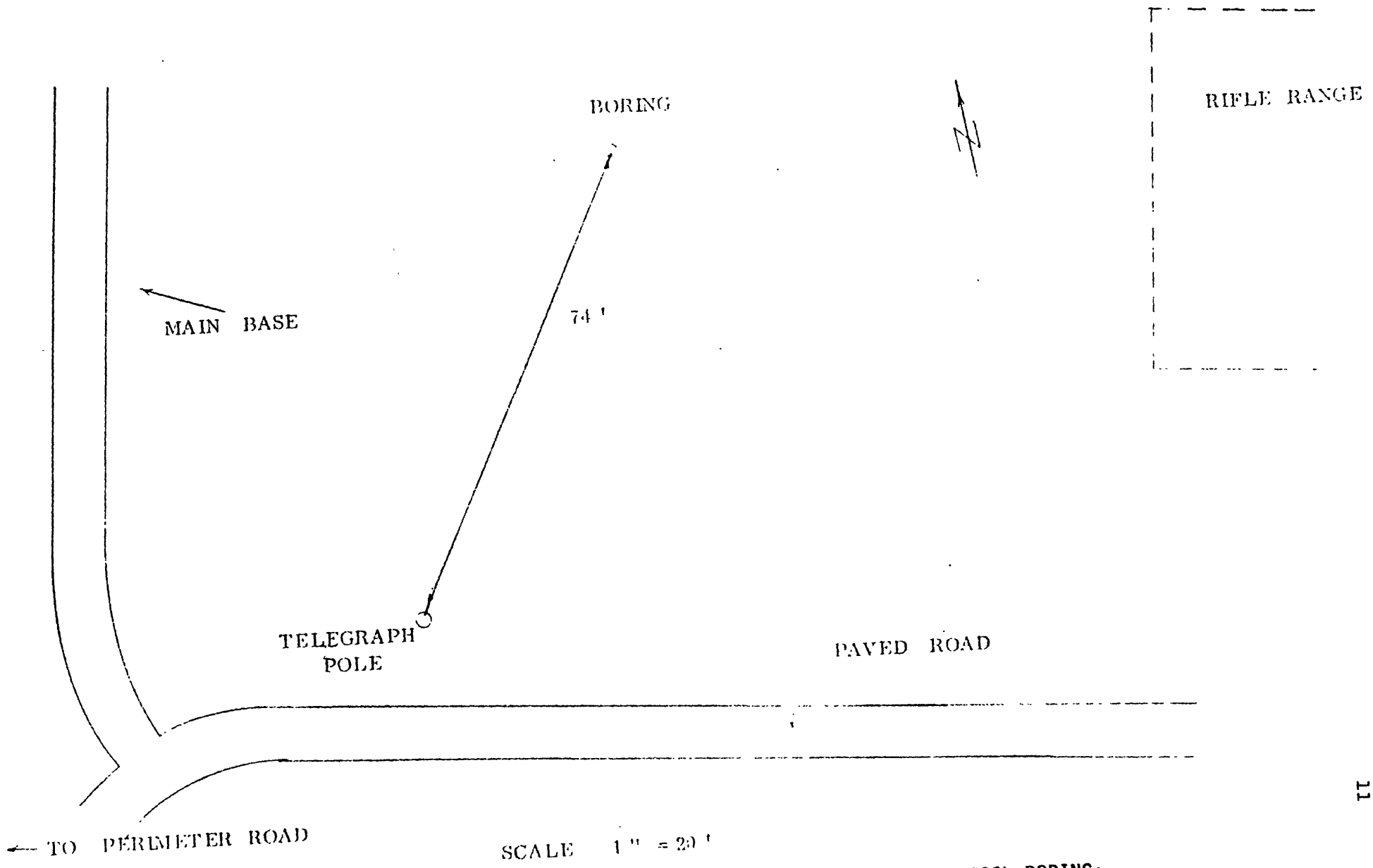


FIGURE 3 APPROXIMATE LOCATION OF UNITED STATES GEOLOGICAL SURVEY SOIL BORING; HAMILTON AIR FORCE BASE, CALIFORNIA

2. COMPOSITION AND ENGINEERING INDEX PROPERTIES

Soil Description

Mitchell (1963) gives the following general engineering description of Bay Mud.

> "A medium to dark gray, soft, silty clay becoming firmer with depth, containing varying amounts of shells and organic matter. In some areas, the upper part of the mud contains interbedded, thin lenses of fine to medium sand. The material is moderately sensitive to remolding; has a low undisturbed strength; is very compressible; and possesses a medium to high plasticity."

Composition

Mitchell (1963) and Tringale (1978) performed X-ray diffraction analyses on Bay Mud. A wide variety of minerals were found to be present in the soil, a fact which is a consequence of the wide variety of rocks from which the bay sediments are derived. Mitchell's analysis indicated the presence of montmorillonite (smectite), kaolin, vermiculite, mica, illite (hydrous mica) and quartz. He also noted that the kaolin mineral present may be halloysite. Tringale found the same mineral constituents as Mitchell plus small amounts of chlorite. Both Duncan (1966) and Tringale (1978) report a total electrolyte concentration in the Bay Mud pore fluid of about 17g/liter total dissolved solids taken as equivalent NaCl. This value is about one half the value of sea water. Below the water table sodium is the predominant cation in the pore fluid salts with lesser amounts of magnesium, potassium and calcium. Above the water table sodium is still the predominant cation although its

concentration is reduced to about one fifth of the value it had below the water table. The potassium ion concentration is reduced by about one third above the water table, while the concentration of magnesium decreases only slightly. The concentration of calcium ions increases by a factor of 1.5 in moving from below the water table to above it. The pH of the Bay Mud at the HAFB site was measured to be approximately 8 (measured at a water content w = 200%) below the water table and about 4 (w = 200%) in the weathered, desiccated zone above the water table.

The sensitivity of Bay Mud has been reported to range between 2 to 10 with values of 5 to 8 being most common. Duncan (1966) reported a value of 8 for the HAFB site while in-situ test results (reported in the section on in-situ tests) indicate the sensitivity to be about 5 or 6. The combination of pore fluid salt concentration and soil sensitivity obtained for the Bay Mud agrees well with values reported by Bjerrum (1954) and shown in Figure 4, for Norwegian marine clays. Also, as noted by Mitchell (1976), Bjerrum (1954) and others, clays of high sensitivity exhibit relatively high in-situ water contents in relation to their liquid limit. A measure of the relative value of the water content with respect to the liquid limit is obtained through the use of the liquidity index, defined as $LI = \frac{w\% - PL\%}{LL\% - PL\%}$. For Bay Mud the liquidity index is slightly greater than 1, which as Figure 5 indicates, is typical of values of LI obtained by Bjerrum for Norwegian marine clays with sensitivities similar to that of Bay Mud.

Particle Size Determination and Soil Activity

The results of 22 grain size analyses of soil from the HAFB site were

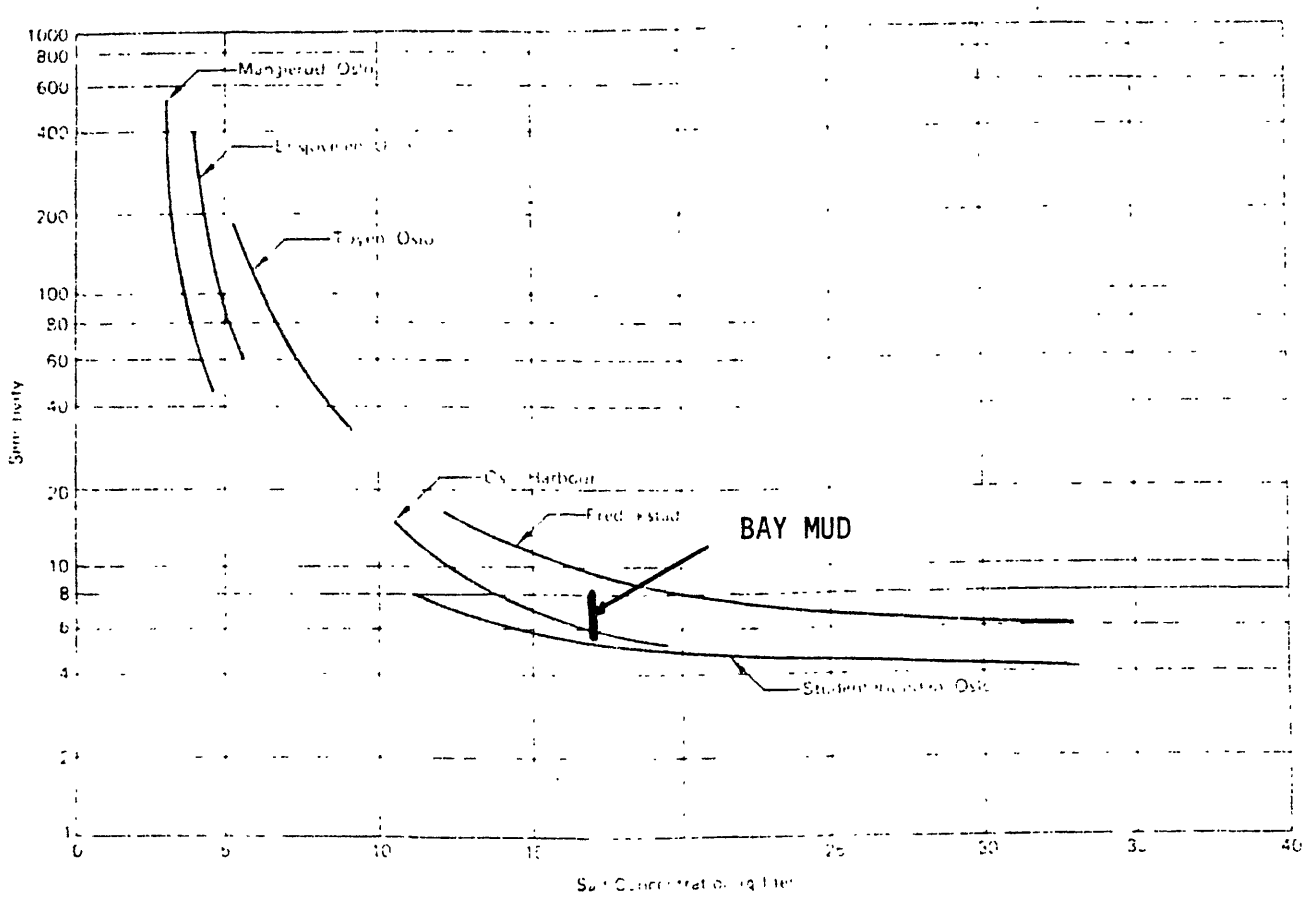


FIGURE 4 RELATIONSHIP BETWEEN SENSITIVITY AND SALT CONCENTRATION FOR SOME NORWEGIAN CLAY DEPOSITS (Bjerrum, 1954)

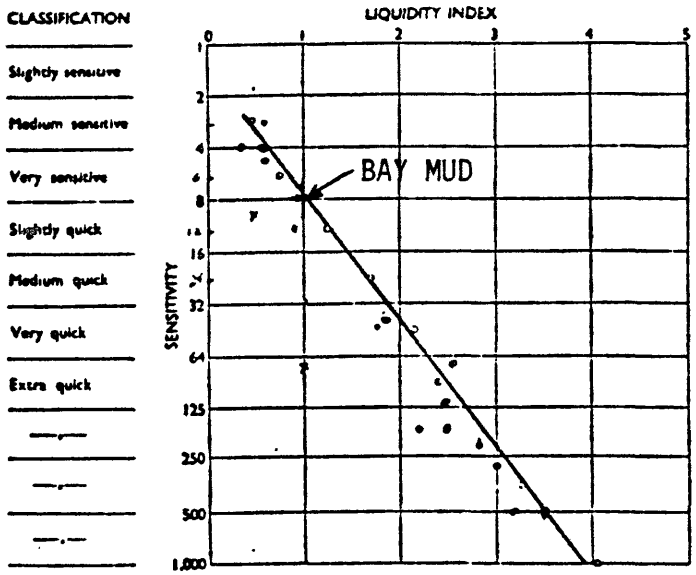


FIGURE 5 RELATIONSHIP BETWEEN SENSITIVITY AND LIQUIDITY INDEX FOR SOME NORWEGIAN CLAY DEPOSITS (Bjerrum, 1954)

summarized by Denby (1978). He noted that the Bay Mud had a consistent gradation through the entire depth of the deposit. The average percentage of the soil finer than 2 microns was between 44% and 48%. For Bay Mud with a clay fraction of 46% and a plasticity index of 43% the activity is about 1.1 which is between the range of values for illitic clays (A = .5 to 1) and smectites (1-7). (For ranges of activities for various clay minerals see Mitchell (1976).)

Specific Gravity

Air pycnometer determinations of specific gravity were conducted by Kavazanjian (1978) and resulted in a mean value for the dry soil of 2.71. Denby (1978) reported specific gravities ranging from 2.52 at 5 ft to 2.65 at 50 ft. Below 75 ft he reported a constant specific gravity of 2.75. Based on weight volume relationships and measured values for total unit weight and water content, specific gravities falling between 2.69 and 2.73 are calculated.

Unit Weight

Average values for the total unit weight of Bay Mud were reported by Denby (1978) based on field tests at HAFB by the USGS and measurements in the laboratory at Stanford University. The values reported were 90 PCF (1.44 g/cm^3) and 94 PCF (1.51 g/cm^3), respectively. Denby indicated that the laboratory determinations were probably more accurate than those in the field because of the more careful trimming techniques used in the lab. The total unit weight of the soil was found to be fairly constant with depth, as seen in Figure 6. Total unit weights are slightly higher near the surface, the denser soil state being the result of desiccation.

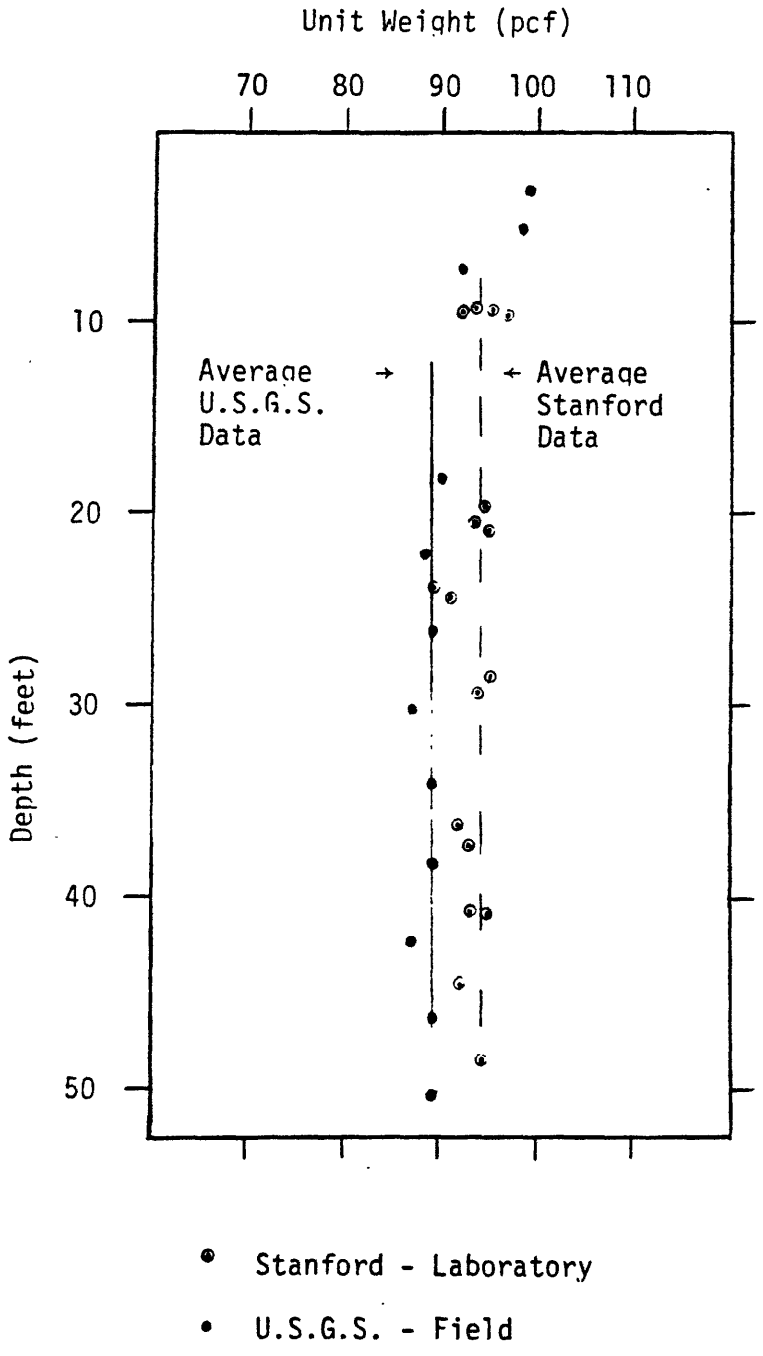


Figure 6 Comparison of Laboratory and Field Determined Total Unit Weights, Hamilton Air Force Base Data from Denby (1978)

Atterberg Limits, Water Contents and Liquidity Index

A summary of the average values of water content, liquid limit, plastic limit, plasticity index and liquidity index obtained by various researchers on Bay Mud from the HAFB site is given in Table 3. Generally the results are very consistent. Liquid limits are about 88%± and water contents are slightly higher at about 90%±.

Plots of liquid limit, plastic limit and water content versus depth are shown in Figure 7. The liquid and plastic limit show small local variations but do not exhibit any major fluctuations with depth. Similarly little variation in water content is found with depth, although some might be expected due to variations in effective consolidation pressure with depth.

Organic Content

The United States Geological Survey (Denby, 1978) measured the percentage total carbon present in the soil at the HAFB site. As Figure 8 illustrates, values ranged between 1 and 2 percent through the depth of the Bay Mud deposit. Denby notes that the organic matter appears in two stages of decomposition, "an older form consisting of black specs of carbon and a younger form consisting of yellow blades of marsh weeds."

TABLE 3. w%, L.L., P.L., P.I. AND L.I. AVERAGE VALUES - HAMILTON AIR FORCE BASE

Researcher	w%	LL%	PL%	PI%	LI
Seed et al. (1963)	88-93	88	43	45	1.04-1.11
Duncan (1966)	90	88	43	45	1.04
USGS (Denby, 1978)	89.8	87.6	40.4	47.2	1.05
Stanford (Denby, 1978)	86	85	38.3	46.7	1.02
Kavazanjian (1978)	90-96%	88±1%	35-44	43-54	~1

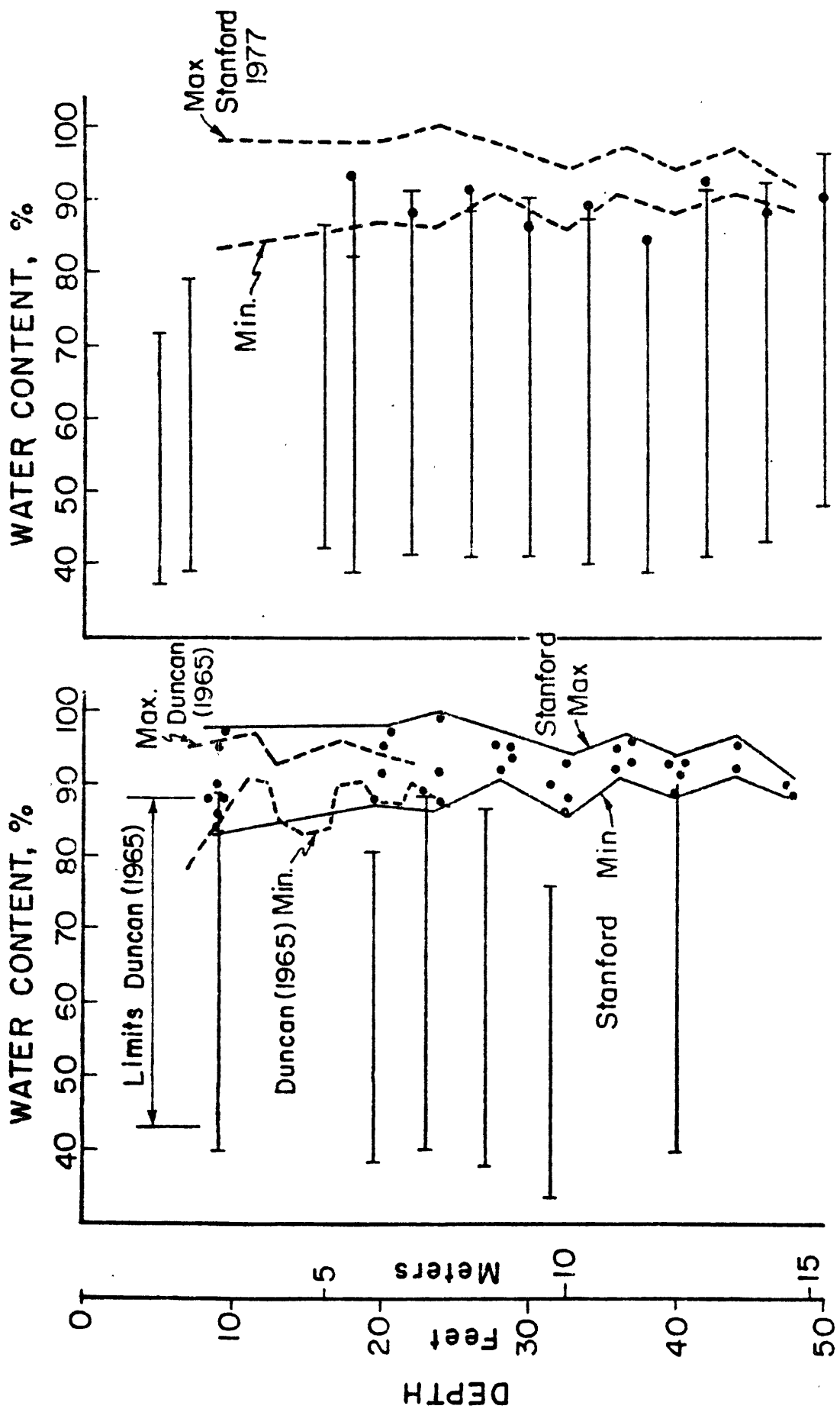


FIGURE 7 COMPARISON OF ATTERBERG LIMITS AND NATURAL WATER CONTENTS AT HAMILTON A. F. BASE
From Denby (1978)

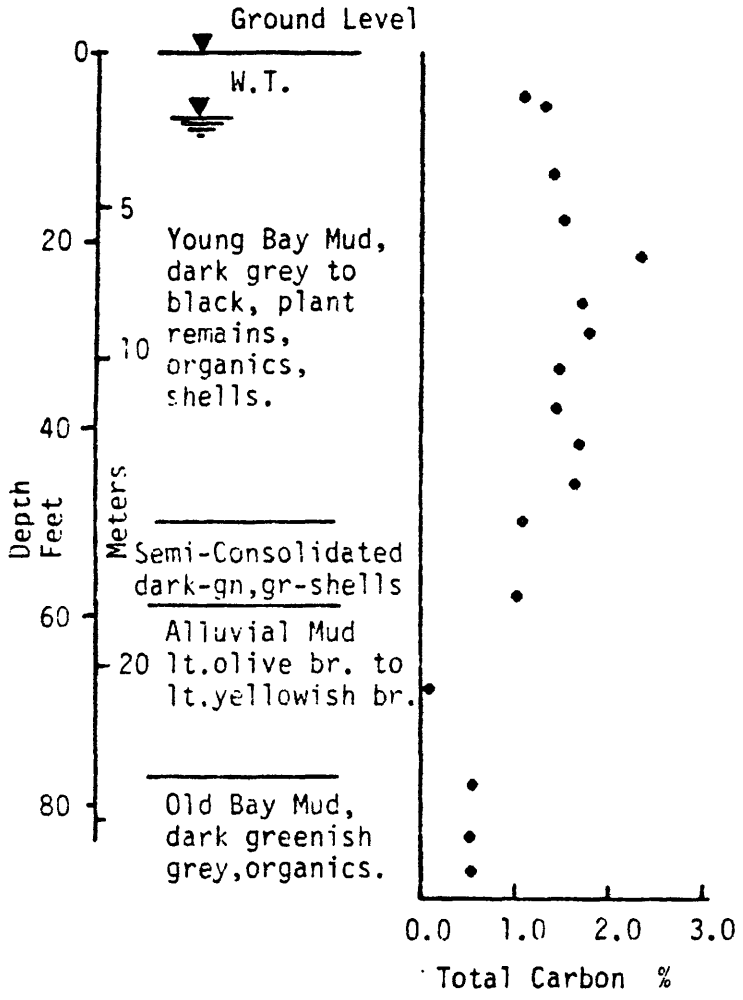


FIGURE 8 TOTAL CARBON CONTENT - BAY MUD,
HAMILTON AIR FORCE BASE From Denby (1978)

3. COMPRESSIBILITY

General

The Bay Mud at the HAFB site can be broken into two distinct zones. Near the surface the soil deposit has been weathered and overconsolidated, probably by desiccation. It is easily identified by its brownish gray color. Measured preconsolidation pressures and shear strength data indicate that this zone extends to a depth of about 10-12 ft. Below about 18 ft the soil is normally to slightly overconsolidated, having an OCR in the range of 1.1 to 1.5. Between the desiccated zone and the normally consolidated part of the deposit is a transition zone through which soil shear strengths are a minimum.

Consolidation Tests

Denby (1978) ran two conventional stress controlled consolidation tests and six strain controlled consolidation tests on samples of Bay Mud from HAFB. His objective was to accurately determine the relationship between preconsolidation pressure and depth as part of a SHANSEP (Ladd and Foott, 1974) analysis of the soil. A summary of his test results is given in Table 4, and the e-log $\bar{p}$ curves derived from the tests are given in Figures 9 and 10. Denby noted that the virgin compression curves from the e-log $\bar{p}$ plots were slightly non-linear, being concave upwards, a result that has been reported by others (Houston, 1979). His results showed the average value of the compression index, C_c, for the initial portion of the virgin compression curve to be 1.52. For the latter, flatter part of the curve the compression index dropped to a value of .81. As can be seen in

TABLE 4 RESULTS OF OEDOMETER TESTS
From Denby (1978)

NUMBER	TYPE OF TEST	DEPTH ft.	m/c %	γ pcf	STRAIN RATE ins/min	p_o psi	p_c psi	p_c/p_o	Cc initial	Cc final
HCON 1	Stress controlled	9.25	87.9	91.8	--	5.2	17.0	3.3 - 3.4	1.59	0.94
HCON 2	Stress controlled	9.0	84.0	92.9	--	5.16	16.2	3.1 - 3.3	1.67	0.83
CRSC 1	Strain controlled	36.0	91.6	92.0	0.0001	10.7	13.4	1.2 - 1.3	1.39	0.86
CRSC 2	Strain controlled	20.3	94.6	92.9	0.0001	7.5	11.3	1.45 - 1.55	1.77	0.80
CRSC 3	Strain controlled	40.3	91.3	93.1	0.0001	11.6	15.8	1.3 - 1.4	1.48	0.81
CRSC 4	Strain controlled	24.3	99.3	90.7	0.00005	8.3	9.5	1.1 - 1.2	1.38	0.76
CRSC 5	Strain controlled	9.5	92.8	91.2	0.00024	5.26	15.2	2.9 - 3.1	1.33	0.63
CRSC 7	Strain controlled	50.0	88.6	94.2	0.0001	13.6	21.4	1.5 - 1.6	2.21	0.88
								Averages:	1.52	0.81

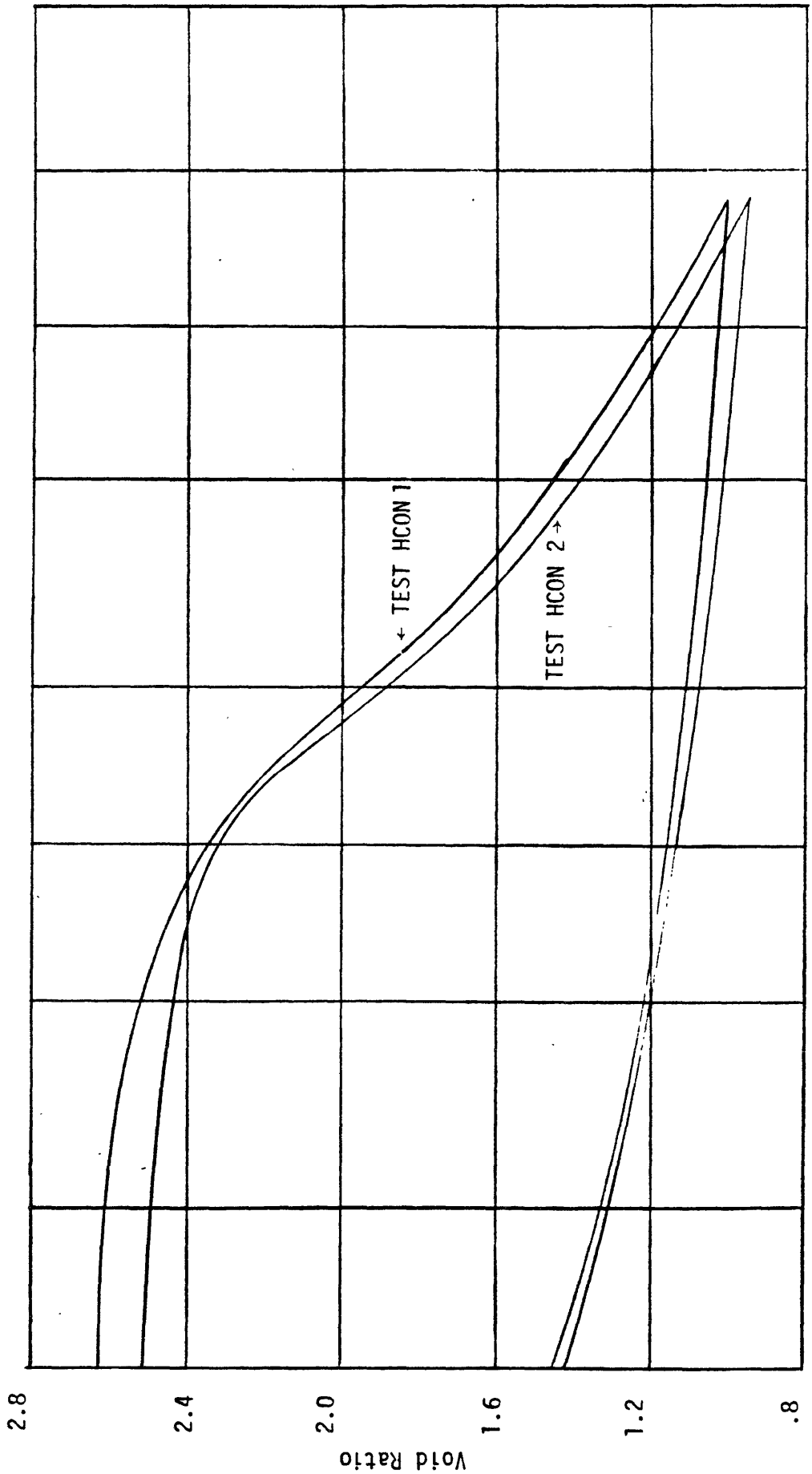


FIGURE 9 STRESS CONTROLLED CONSOLIDATION TESTS PERFORMED BY DENBY (1978)

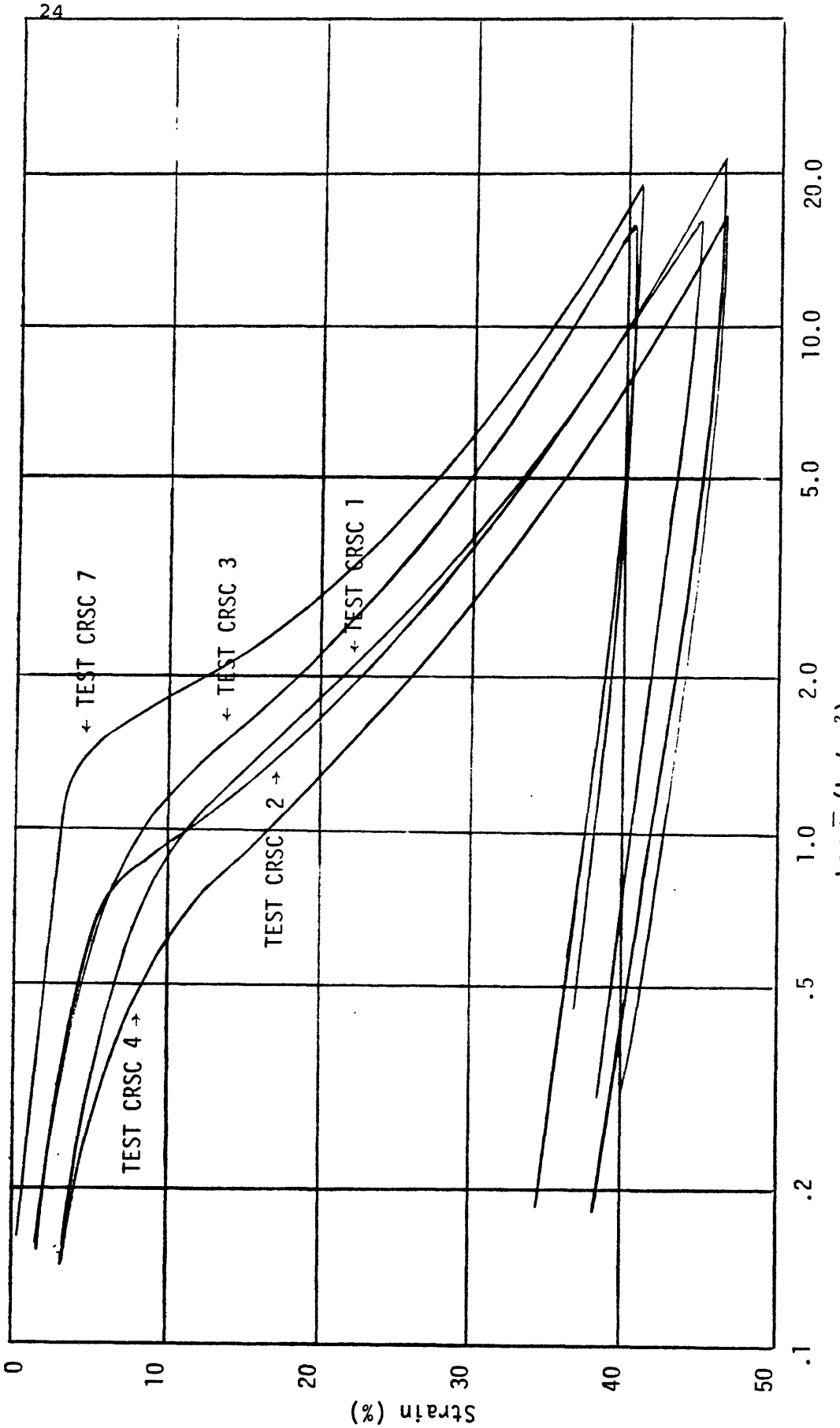


FIGURE 10 STRAIN CONTROLLED CONSOLIDATION TESTS PERFORMED BY DENBY (1978)

Figures 9 and 10, the slope of the virgin compression curve begins a progressive flattening at an effective consolidation pressure of about 2 kg/cm^2. Ladd (1971) has pointed out that non-linear e-log $\bar{p}$ curves are fairly common in sensitive clays. Values for the recompression index C_r average about .15.

Duncan (1962, 1963) performed a series of conventional stress controlled consolidation tests on the Bay Mud from HAFB. His results are given in Figures 11 through 14. Figures 11 and 12 show the consolidation curves obtained from six of his tests. Figure 13 shows the coefficient of consolidation as a function of consolidation pressure for the consolidation test performed on the soil that came from a depth of 17.2 feet. Figure 14 shows a plot of soil permeability versus void ratio for both the loading and unloading portions of the same consolidation test.

Duncan's results, like Denby's, show the Bay Mud to have a virgin compression curve that is concave upward. Values of the compression index for the early portion of the virgin compression curve vary between .9 and 1.25 with most values being close to 1.2. The value of C_c drops to about .80 for the latter, flatter portion of the curve. The effective consolidation pressure at the point at which the compression curves begin to flatten out falls between 1.5 and 2 kg/cm^2. Values of the recompression index lie between .08 and .15 with an average of .12. The value of the coefficient of consolidation, C_v, for Bay Mud when normally consolidated varied between 5 and 10 ft^2/year with an average of 8 ft^2/year. This value agrees well with results for C_v reported by Houston (1979). Houston found the coefficient of consolidation of Bay Mud to be about 10±2 ft^2/year at the HAFB and throughout most of the Bay Area. His results were based on laboratory consolidation tests and field observed settlement rates.

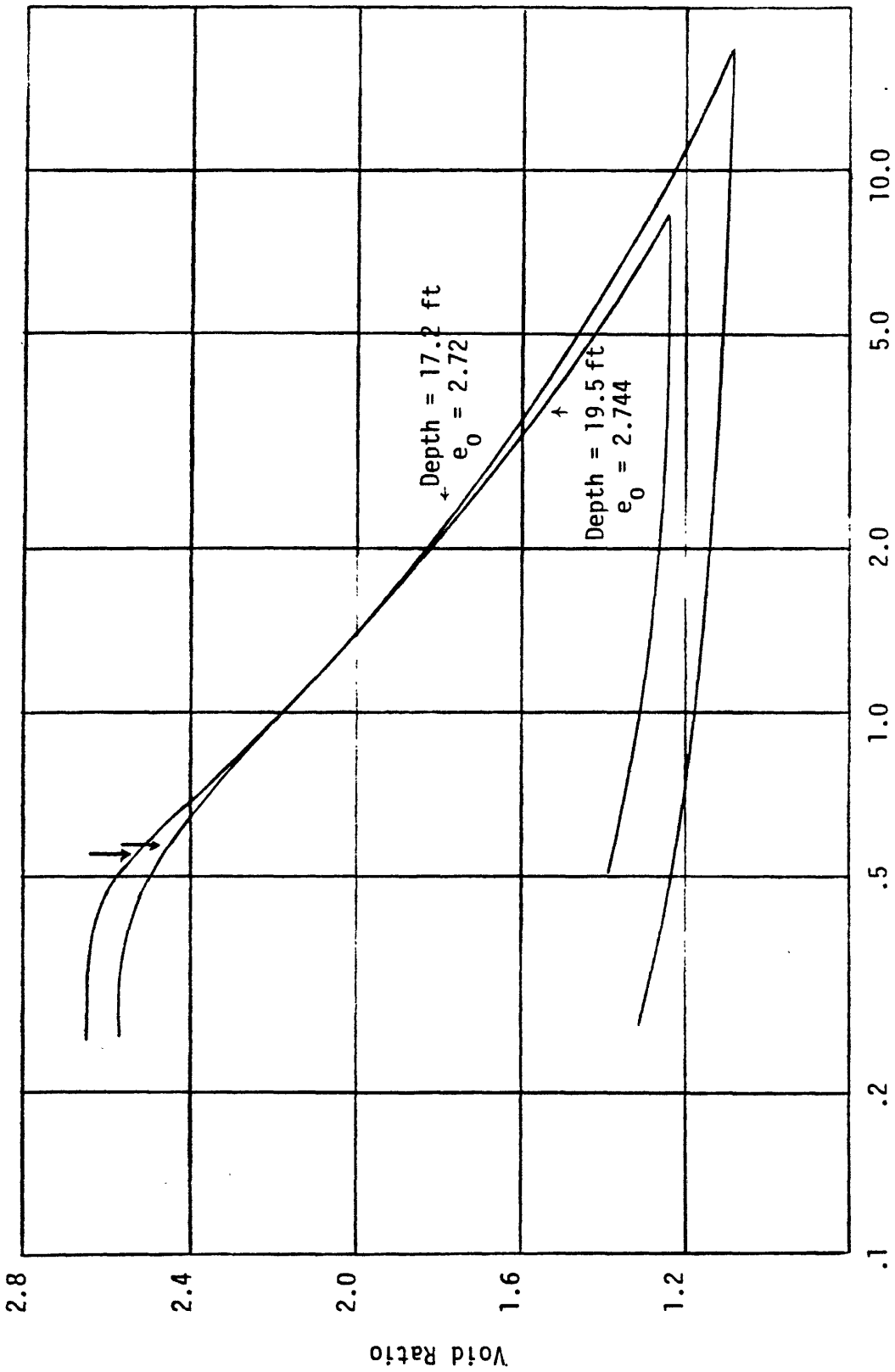


FIGURE 11 STRESS CONTROLLED CONSOLIDATION TESTS PERFORMED BY DUNCAN (1962)

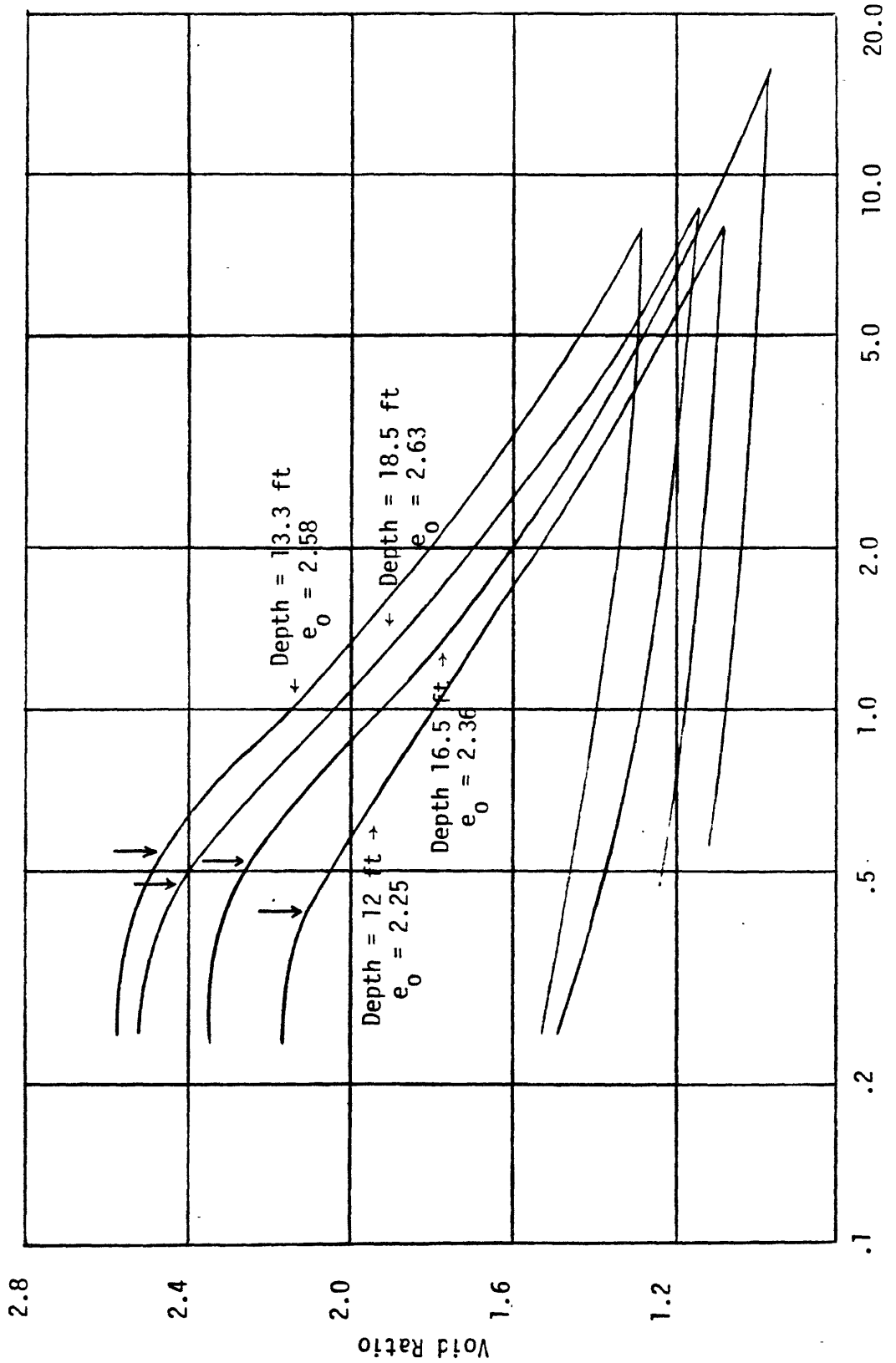


FIGURE 12 STRESS CONTROLLED CONSOLIDATION TESTS PERFORMED BY DUNCAN (1962)

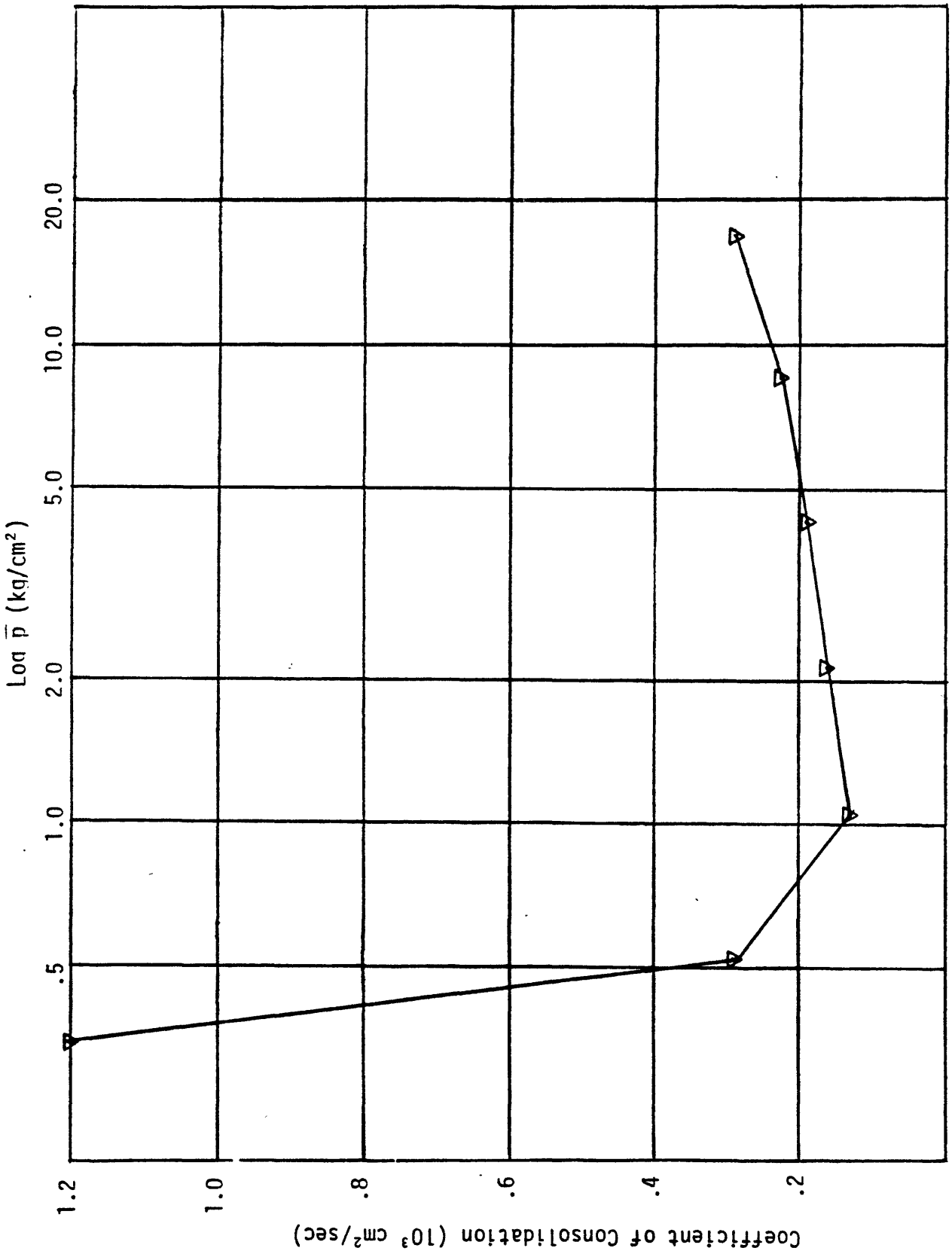


FIGURE 13 COEFFICIENT OF CONSOLIDATION - OBTAINED FROM THE STRESS CONTROLLED CONSOLIDATION TEST PERFORMED BY DUNCAN (1962) ON SOIL FROM A DEPTH OF 17.2 FEET

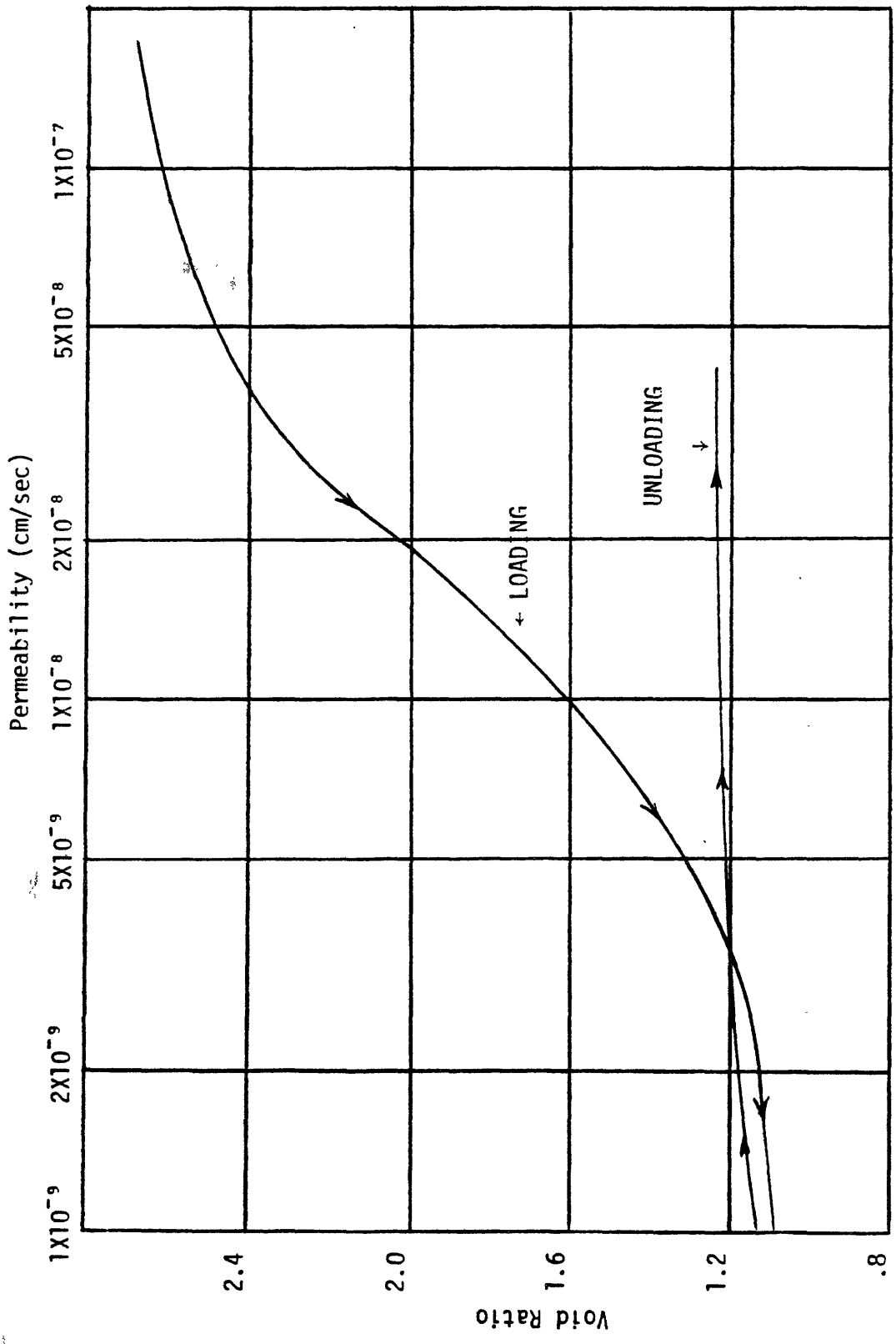


FIGURE 14 PERMEABILITY - OBTAINED FROM THE STRESS CONTROLLED CONSOLIDATION TEST PERFORMED BY DUNCAN (1962) ON SOIL FROM A DEPTH OF 17.2 FEET

Mejia (1979) ran three different types of consolidation tests on the Bay Mud from HAFB. These were; 1) Conventional consolidation test by incremental loading, 2) Constant ultimate rate of strain consolidation test. This test is similar to the conventional test except that instead of having the duration of the load increment fixed, as is done in the conventional test, a load increment is added as soon as the soil sample reaches some predetermined rate of strain. The ultimate strain rate used in Mejia's test was .02%/minute. 3) The third type of consolidation test used was a constant rate of strain test. Two of these tests were performed, one at a strain rate of .008%/minute, the other at a strain rate of .014%/minute.

The results of Mejia's tests are given in Figures 15 through 18. Figures 15 and 16 show the consolidation curves for the three different types of consolidation tests. As with the previous tests reported, these results show the virgin curve to be somewhat nonlinear in e-log $\bar{p}$ space. The initial value of compression index was measured to be about 1.6-1.8, while for effective stresses above 3 kg/cm^2 the compression index was .9. The recompression index, C_r was .14. The values reported above are those derived from the conventional incremental loading test. Values from the other test types were found to be quite similar.

The coefficient of consolidation from the conventional consolidation test performed by Mejia is shown in Figure 17. The value of C_v ranges between about 4 and 20 ft^2/year with a value of 10 ft^2/year being average. A plot of the coefficient of secondary compression, C_α (strain per log cycle time following completion of primary consolidation), is given in Figure 18. Values for C_α range from about .0015 to .0045 for pressures below p'_p to .01 to .02 for soil that is on the virgin compression curve.

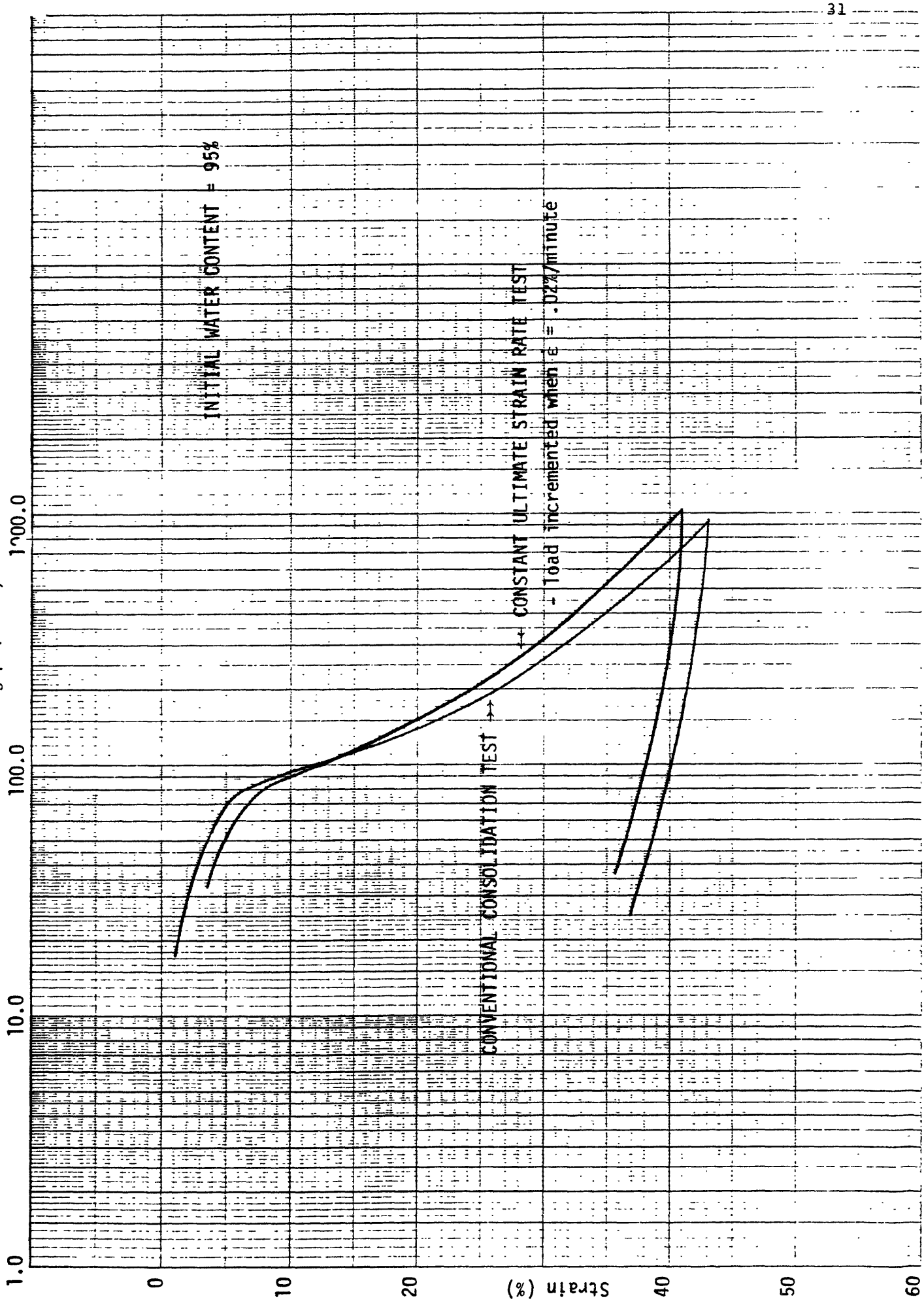


FIGURE 15 RESULTS OF CONSOLIDATION TESTS PERFORMED BY MEJIA (1979)

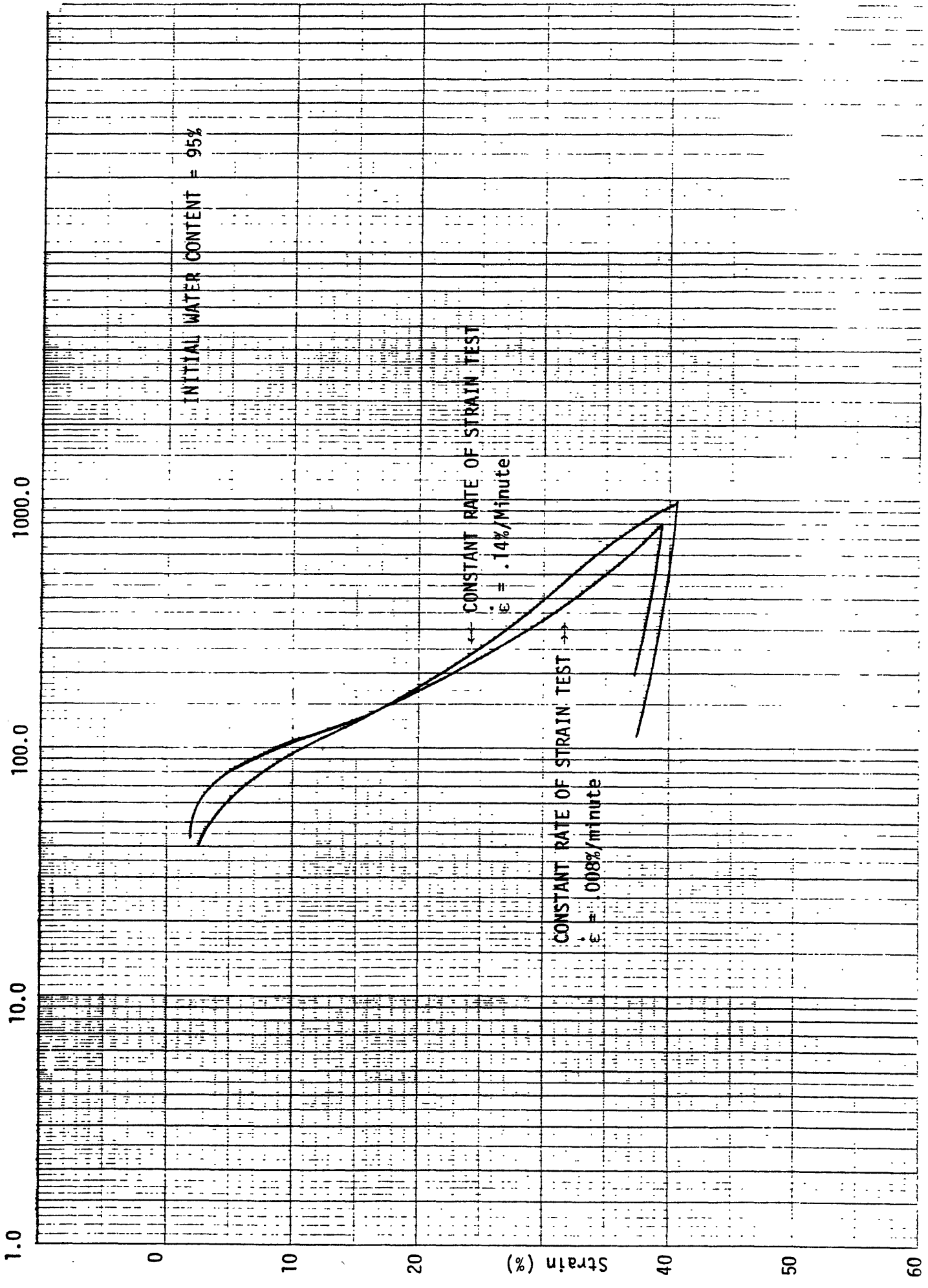


FIGURE 16 RESULTS OF CONSOLIDATION TESTS PERFORMED BY MEJIA (1979)

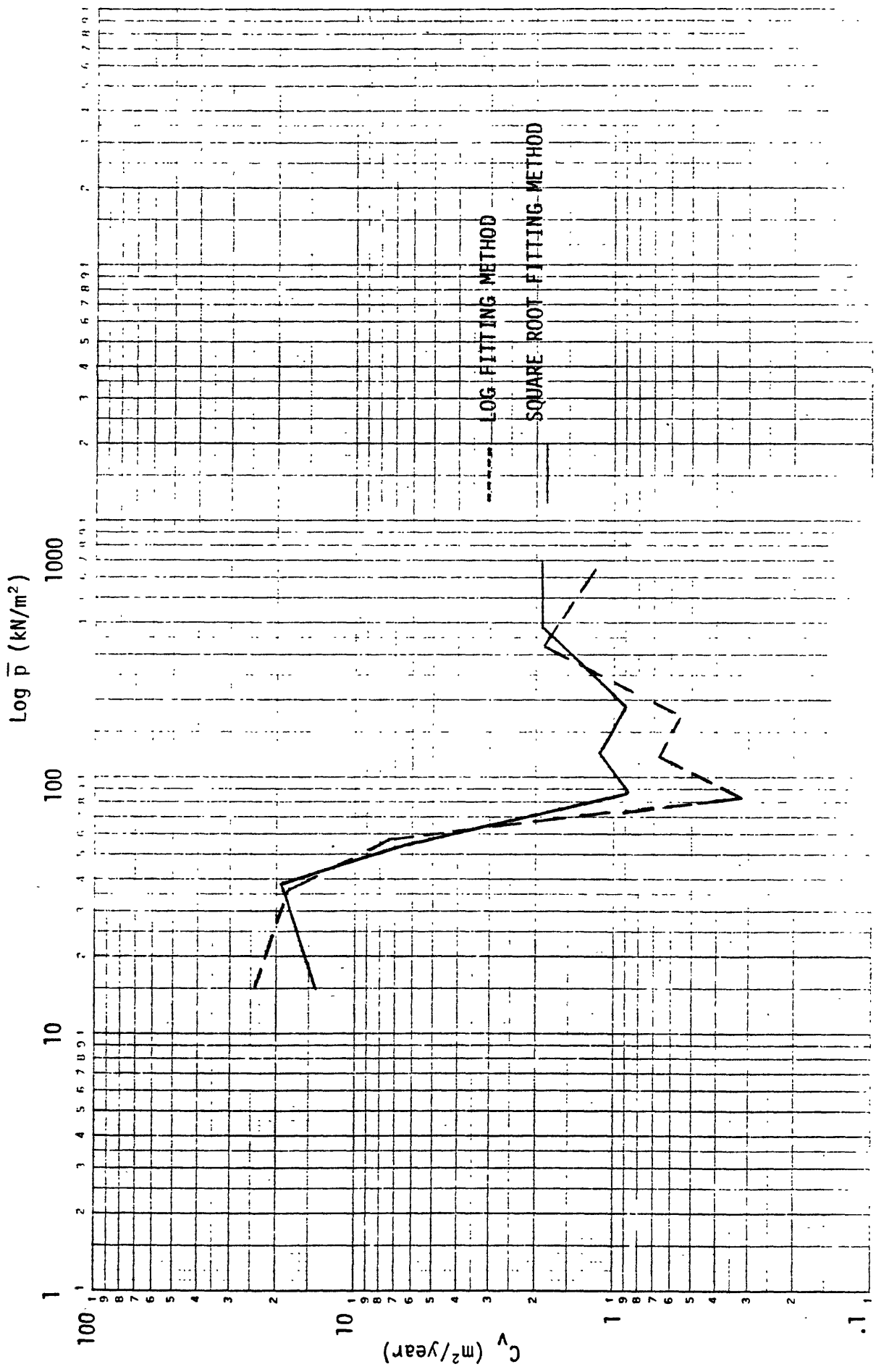
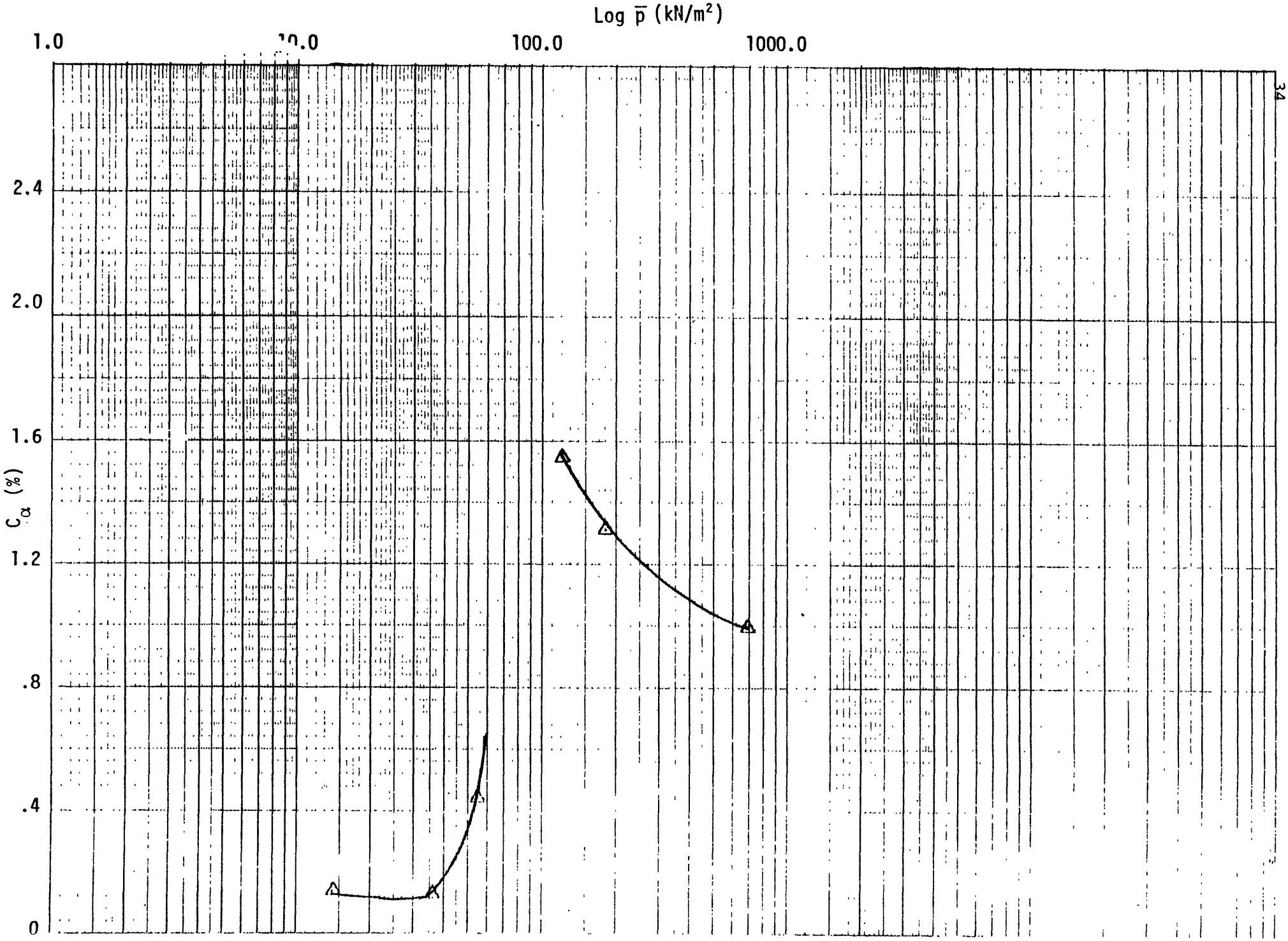


FIGURE 17 COEFFICIENT OF CONSOLIDATION OBTAINED FROM THE CONVENTIONAL CONSOLIDATION TEST PERFORMED BY MEJIA (1979)

CONSOLIDATION EST PERFORMED BY MEJI... (1979)



As can be seen in Figure 19, these values for C_α agree well with those obtained for other soils when C_α is taken as a function of natural water content. Based on a classification proposed by Duncan and Buchignani (1976), and given in Table 5, the secondary compressibility of Bay Mud would be classified as being high.

The values of the preconsolidation pressure obtained from Denby's, Duncan's and Mejia's data were determined using the standard Casagrande construction. Using the values for preconsolidation pressure obtained from these constructions and the values for the total unit weight of Bay Mud that were given previously (Figure 6), Figure 20 has been constructed. This figure shows plots of total stress, effective stress, preconsolidation pressure and OCR versus depth. At a depth of about 8 ft the soil exhibits an OCR close to 3, the large preconsolidation pressures being indicative of the desiccated zone. Below 18 feet the OCR is low, varying between 1.0 and 1.5. Since the Bay Mud is often described as a normally consolidated soil deposit it may seem surprising that the values obtained for the OCR are greater than one.

There exist several possible explanations for the values of OCR obtained. First, the level of the water table is not constant but changes with time. Typically the water table is located at a depth of about 8 ft. During the winter it may rise to within a few feet of the surface. During the summer the water table drops somewhat. Duncan (1965) reported that the water table may have dropped to a level 12 feet below the surface some time in the recent past. Changes in the water table level at HAFB will change the effective stress regime and hence, the consolidation pressures.

A second possible explanation for the slight overconsolidation noted is the ageing effect reported by Bjerrum (1967). This effect is the result

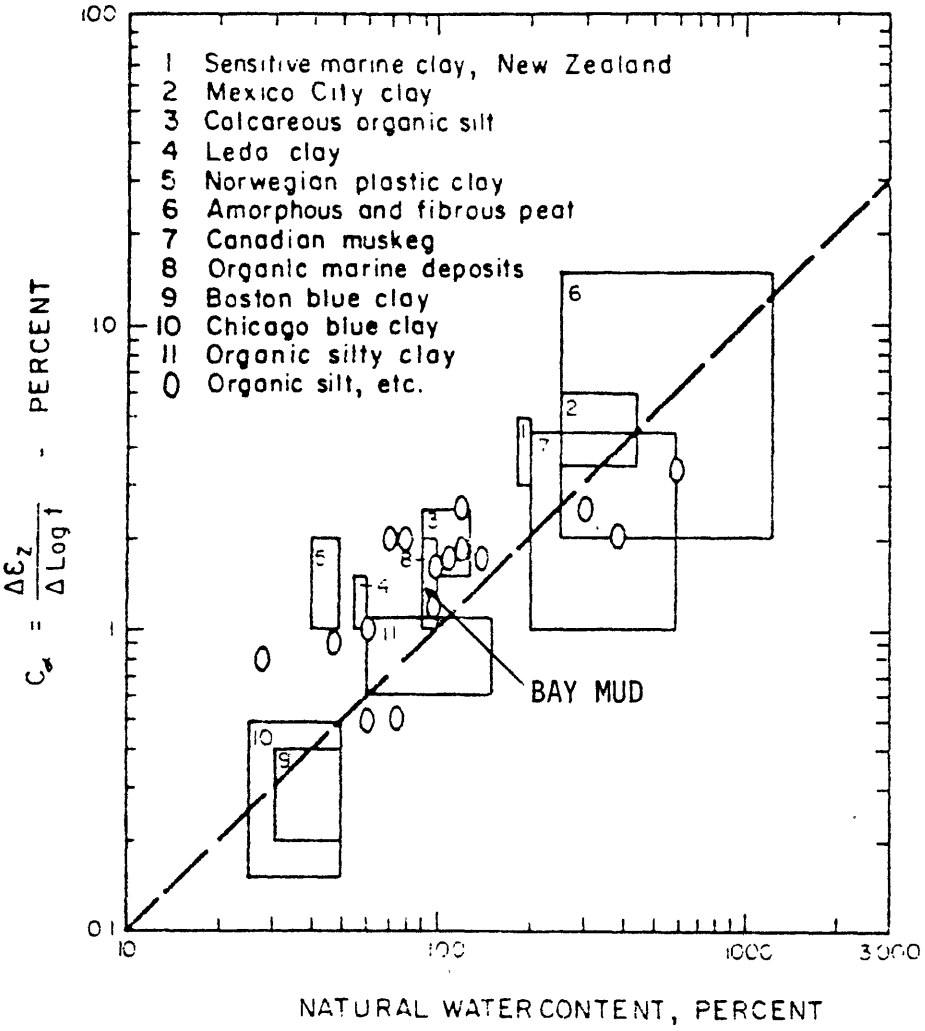


FIGURE 19 CORRELATION BETWEEN C_α AND NATURAL WATER CONTENT

From Duncan and Buchignani (1976)

TABLE 5 SECONDARY COMPRESSION RATES

From Duncan and Buchignani (1976)

Coefficient of Secondary Compression, C_α	Secondary Compressibility
0.002	very low
0.004	low
0.008	medium
0.016	high
0.032	very high
0.064	extremely high

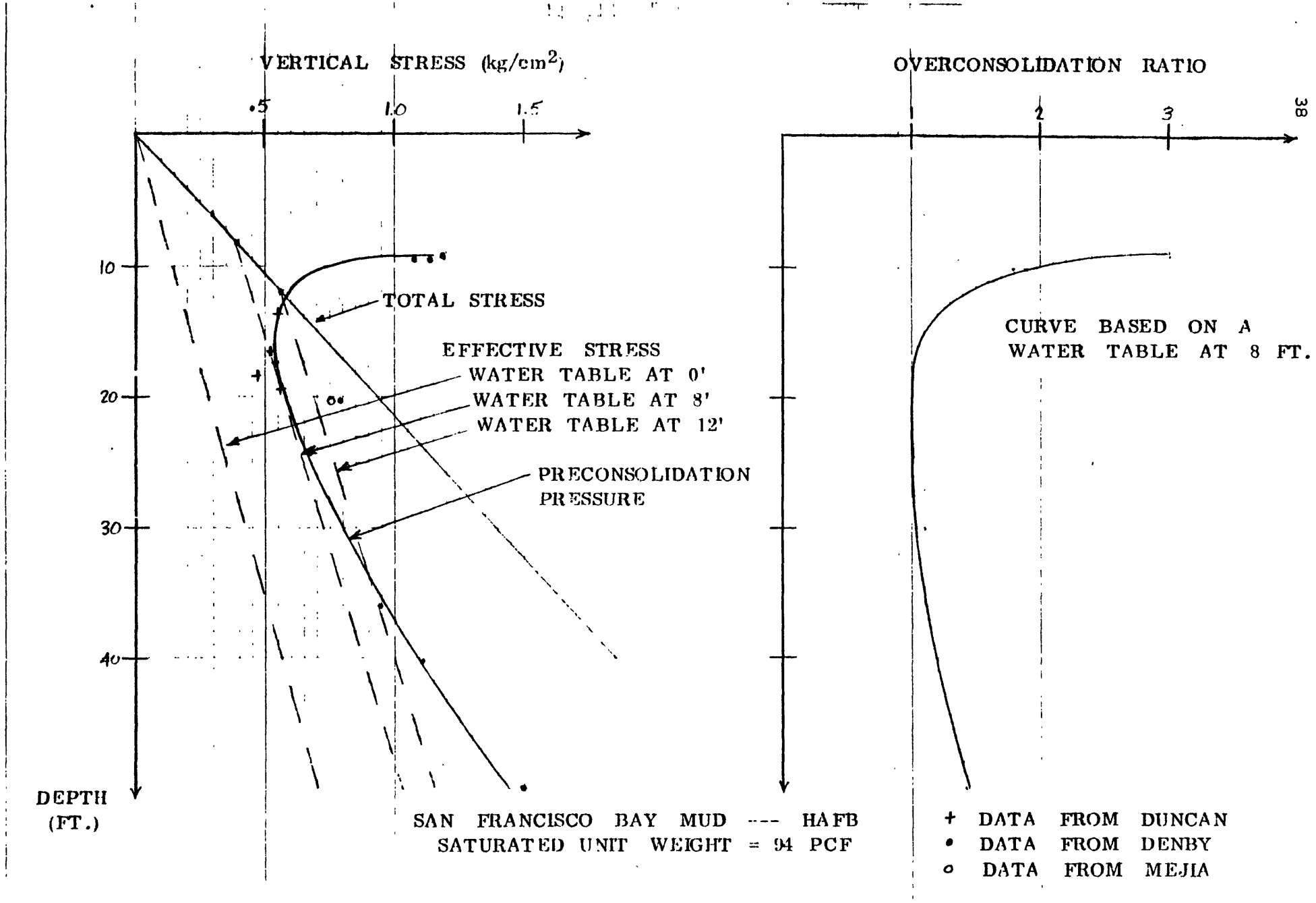


FIGURE 20 TOTAL STRESS, EFFECTIVE STRESS AND OCR VERSUS DEPTH, HAMILTON AIR FORCE BASE

of secondary compression, or more precisely, the time dependent, delayed component of one dimensional deformation. This deformation occurs at constant effective stress and results in a more stable soil structure, a decrease in void ratio and compressibility and an increase in shear strength and preconsolidation pressure. Figure 21 shows, in e-log $\bar{p}$ space, how the delayed component of consolidation decreases the void ratio and increases the shear strength and preconsolidation pressure.

To see the possible effect of ageing on the preconsolidation pressures of Bay Mud, use can be made of a correlation developed by Bjerrum (1973) and presented in Figure 22. Denby (1978) indicates that the Bay Mud at the HAFB site is between 6000 and 8000 years old, an amount of time in which some, but not complete ageing, would have occurred. For Bay Mud with a P.I. of about 45 the ageing effect alone could cause the soil to have an OCR between 1.0 and 1.7.

While ageing effects and water table fluctuations explain why the OCR may be greater than 1, they do not adequately explain why it changes with depth. The effect of ageing on the OCR should be approximately constant with depth. Changes in the OCR due to changes in the water table level diminish with increasing depth. Therefore neither effect could be used to explain the curvature in the OCR curve between the depths of 30 and 50 feet. It is felt that additional consolidation tests are needed from depths greater than 30 feet to better evaluate whether or not the OCR curve actually changes as the data in Figure 20 seem to indicate.

Kavazanjian (1978) ran isotropic consolidation tests on remolded Bay Mud. Figure 23 shows the virgin consolidation curve obtained from his test results. Also shown in the figure are the consolidation curves corresponding

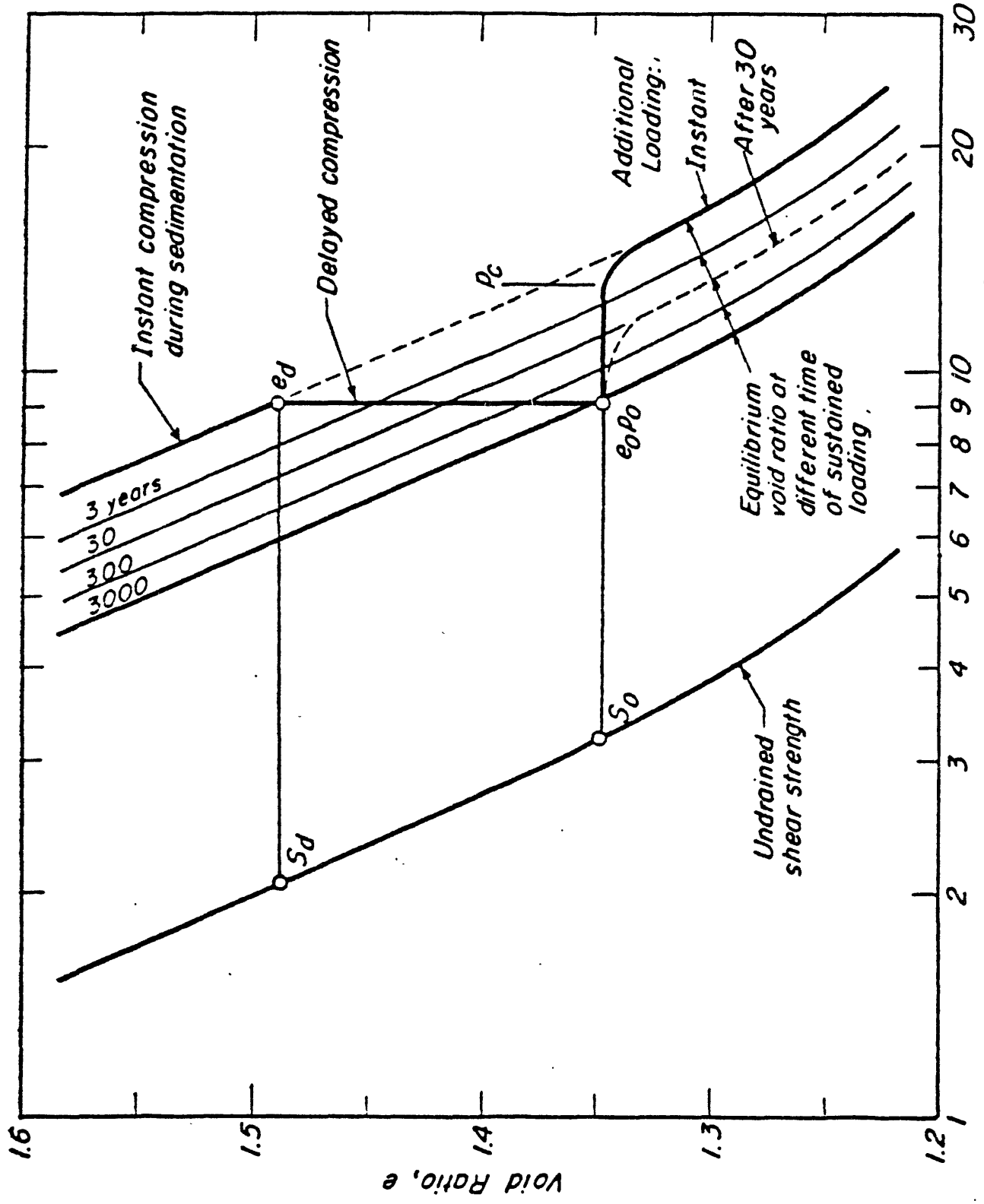


FIGURE 21 BJERRUM'S MODEL FOR ONE-DIMENSIONAL COMPRESSION
From Kavazanjian (1978)

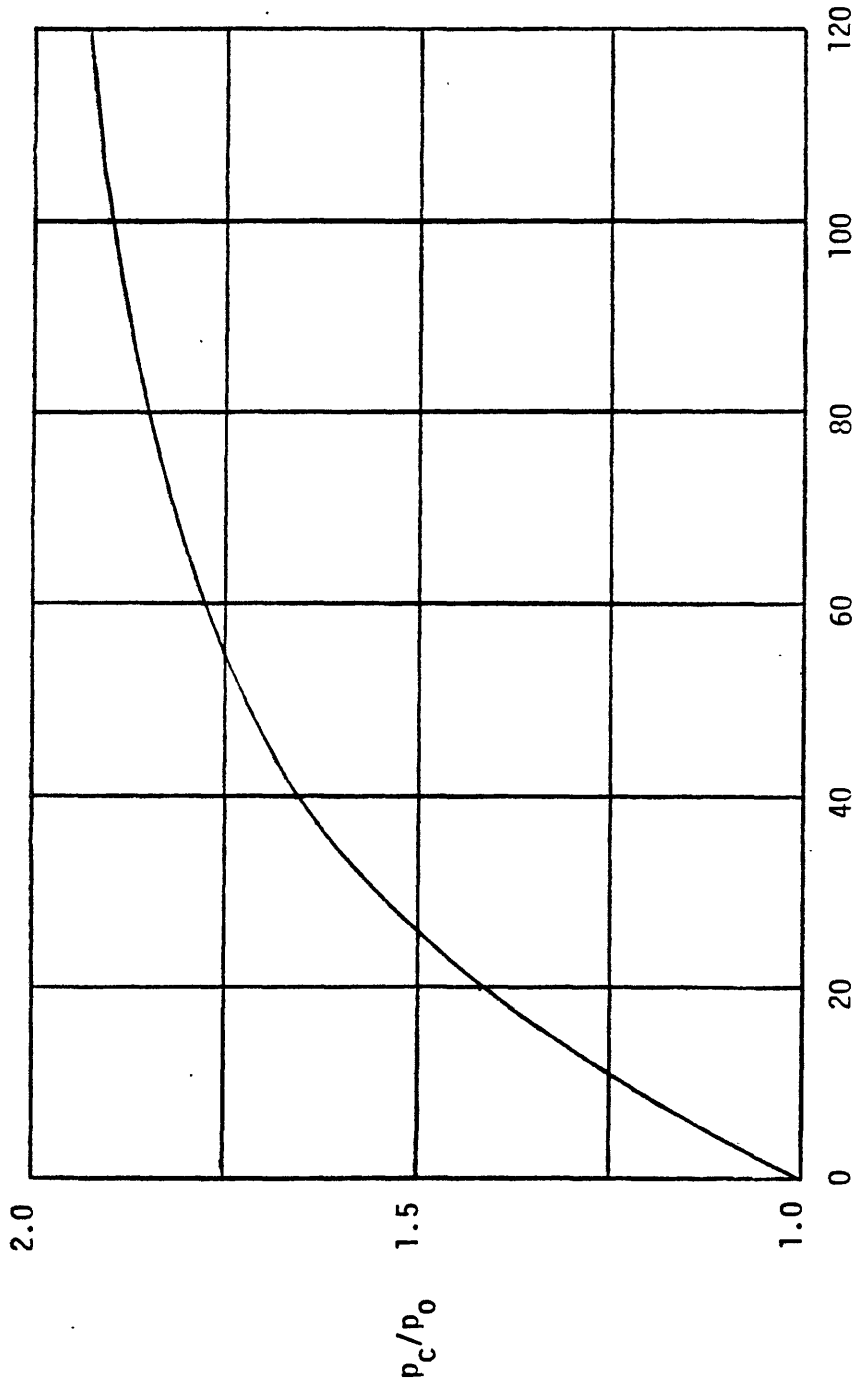


FIGURE 22 INCREASE IN PRECONSOLIDATION PRESSURE DUE TO AGEING
Bjerrum (1973)

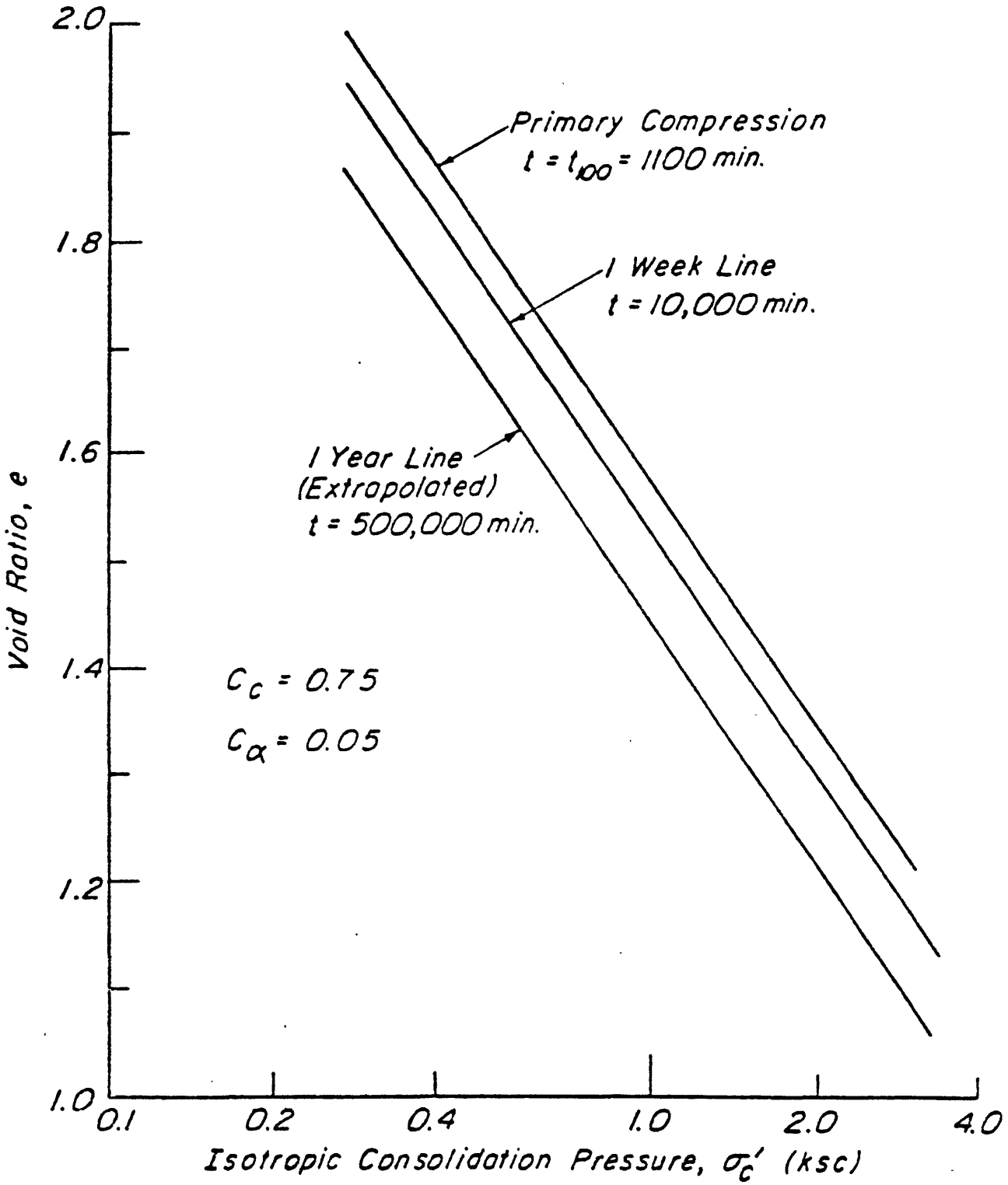


FIGURE 23 PRIMARY COMPRESSION LINE WITH PARALLEL ISOCHRONES FOR REMOLDED SAN FRANCISCO BAY MUD

From Kavazanjian (1978)

to the state of Bay Mud after it had been in the delayed isotropic compression mode for given periods of time (based on C_α = .05). The value of the compression index obtained from his tests is .75. The secondary compression index was measured to be .05. Figure 24 shows the unloading behavior of remolded Bay Mud. Kavazanjian measured a swelling index equal to .10. The isotropic consolidation behavior of undisturbed Bay Mud was obtained indirectly from the results of several isotropically consolidated-undrained triaxial tests. The void ratios and consolidation pressures at the end of the consolidation phase of the triaxial tests were plotted, and it was found that the value of the compression index obtained from the consolidation phase of the $\overline{\text{IC-U}}$ tests is about .8.

Figure 25 is a correlation between compression index and liquid limit which was compiled by McClelland (1967). Figure 26 is a correlation between the virgin compression ratio ($C_c/1 + e_o$) and natural water content presented by Lambe and Whitman (1969). As can be seen in both of these figures Bay Mud plots within the established data bands but in both cases plots above the average values for soils with similar index properties. The wide range of compression index values that Bay Mud encompasses in Figures 25 and 26 is a reflection of the curvature of the virgin compression line.

Summary

The results of the various consolidation tests discussed above are presented in Table 6. Also included for comparative purposes are two commonly used empirical relations for C_c which have been developed by Skempton.

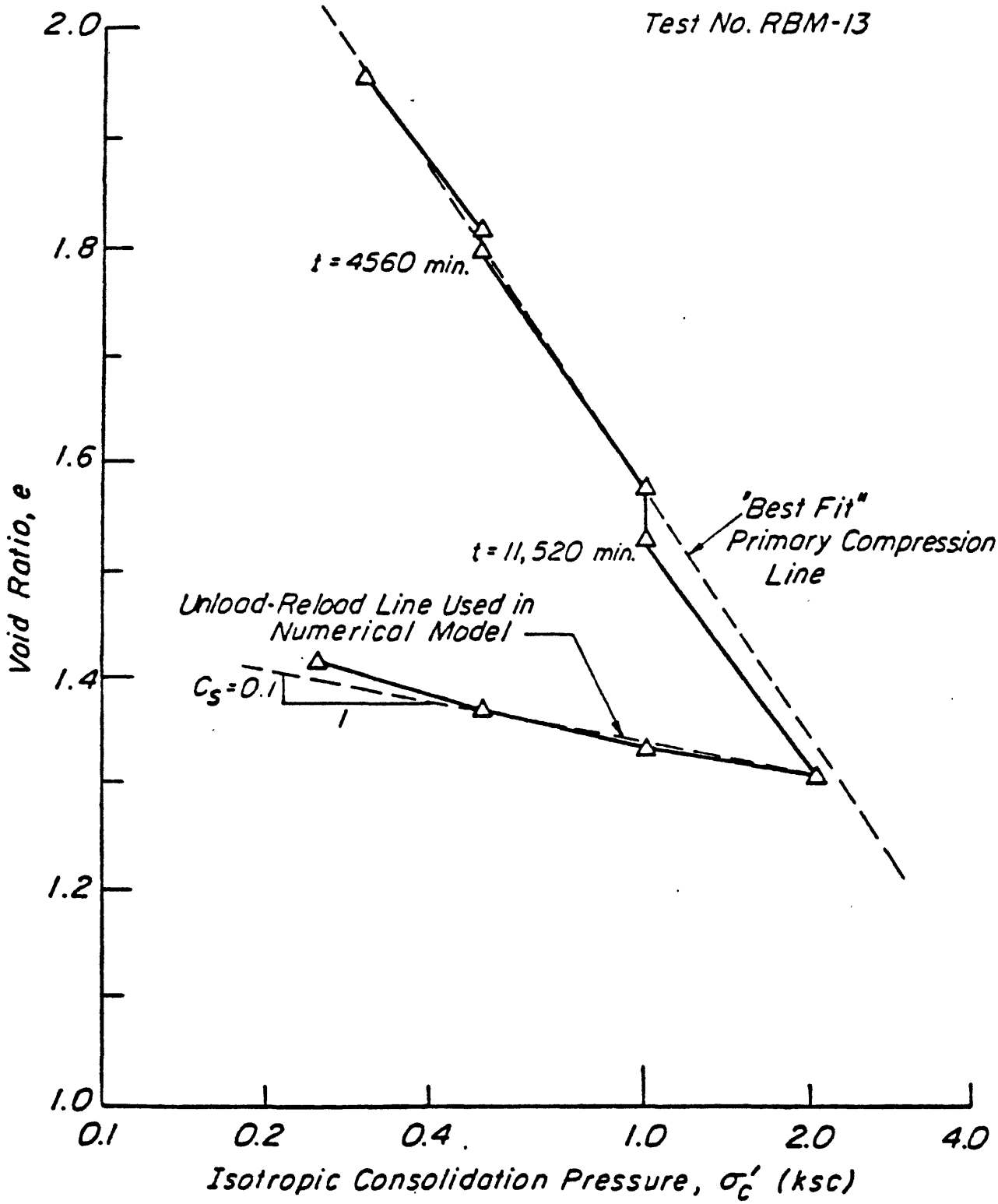


FIGURE 24 VOLUMETRIC UNLOADING BEHAVIOR OF REMOLDED SAN FRANCISCO BAY MUD

From Kavazanjian (1978)

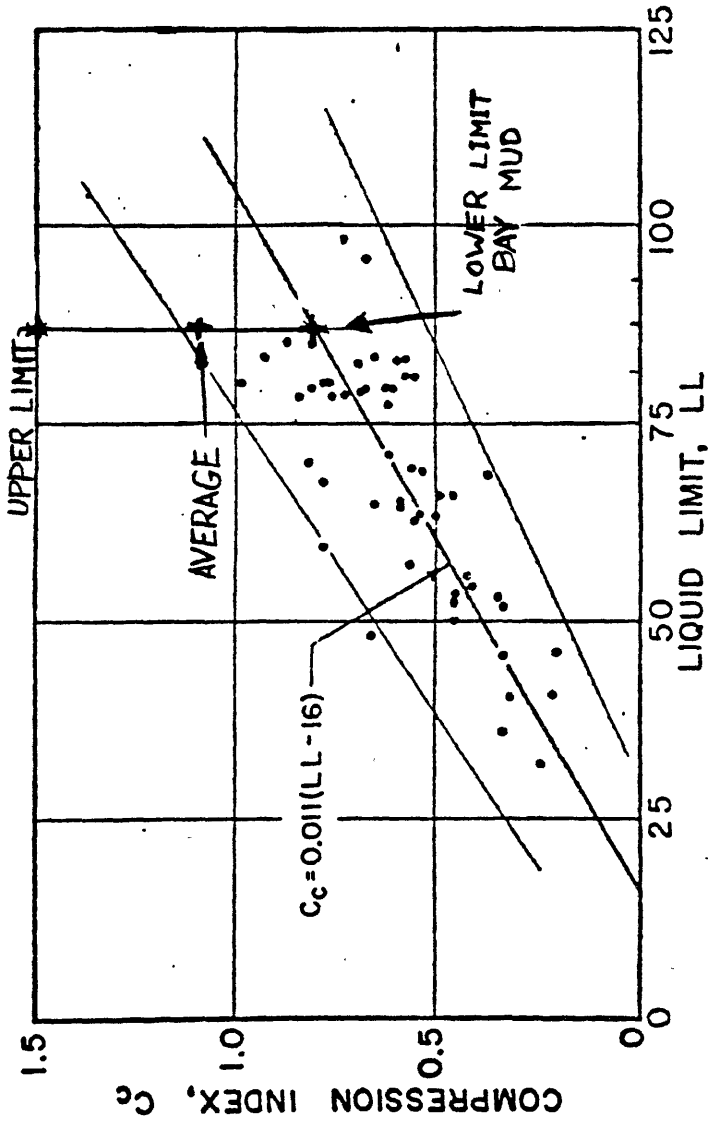


FIGURE 25 CORRELATION OF COMPRESSION INDEX WITH LIQUID LIMIT
McClelland (1967)

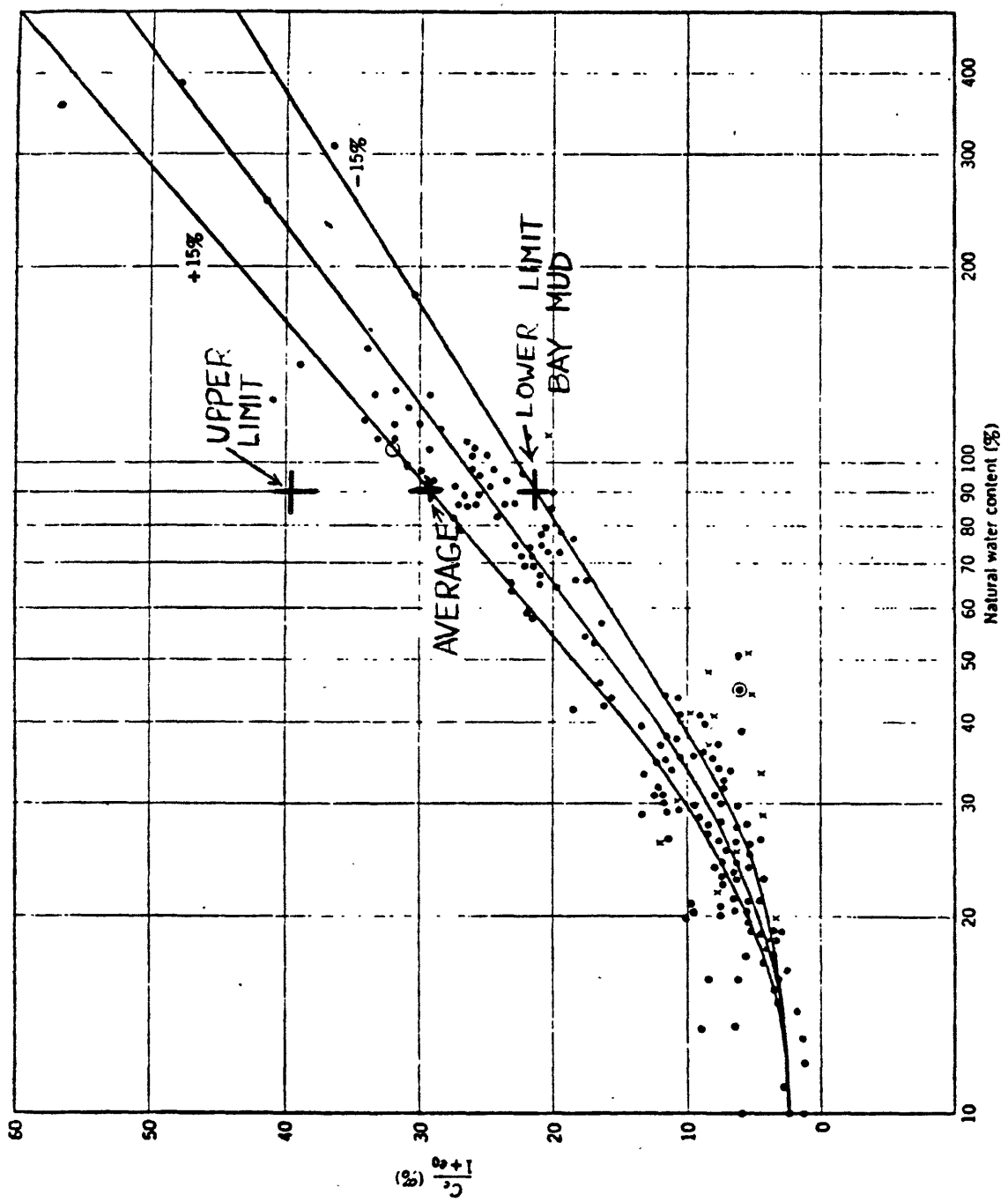


FIGURE 26 RELATION BETWEEN COMPRESSION RATIO AND NATURAL WATER CONTENT
After Lambe and Whitman (1969)

TABLE 6

Researcher	Soil State	Type of Consolidation	C_c	C_R	C_α	C_v ft^2/year
Duncan (1962,63)	Undisturbed	K_o	1.2/.8	.12	.12	8
Mejia (1979)	"	"	1.6-1.8/.9	.14	.01-.02	10
Denby	"	"	1.52/.81	.15		
Kavazanjian	Remolded	Isotropic	.75	.10	.05	
Various $\overline{ICU}$ Tests	Undisturbed	"	.80			
Skempton $C_c = .009$ (L.L.-10%)	"	K_o	.70			
Skempton $C_c = .007$ (L.L.-10%)	Remolded	K_o	.55			

4. IN-SITU MEASUREMENTS OF SOIL PROPERTIES

Introduction

Presented in this chapter are the results of various in-situ tests which were carried out in the Bay Mud deposit at HAFB. The following testing techniques were used to yield a variety of information.

1) Vane Shear Test
2) Quasi-Static Cone Penetration Test
3) Self Boring Pressuremeter Test
4) Glötzl Cell.

For discussions of these in-situ test methods reference should be made to the ASCE Geotechnical Engineering Division Specialty Conference on In-situ Measurement of Soil Properties (1975) and to the report on in-situ measurement of soil properties by Mitchell et al. (1978).

Field Vane Shear Test

The results of vane shear tests at HAFB are presented from work done by Tringale (1978), Mitchell and Lunne (1977), and Duncan (1965). Also presented are the results of vane shear tests given by Duncan and Buchignani (1973) for Bay Mud at the LASH Terminal, Port of San Francisco. Pertinent information concerning vane dimensions, rotation rates and installation procedures for the above-mentioned tests are given in Table 7.

Figure 27 shows the results of the vane shear tests performed by Tringale. In this figure the soil's shear strength was calculated from the measured torque by assuming that the soil failed along a cylindrical surface passing through the outer edge of the vane. Furthermore, a parabolic shear stress distribution was assumed to act along the top and bottom of the failure

TABLE 7

FIELD VANE TEST PROCEDURES

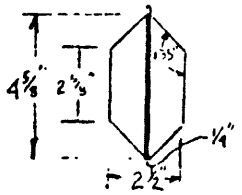
1) Duncan (1965)

Installation - auger to within 1/2 meter and then push vane

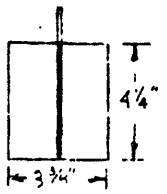
2) Tringale (1978)

A) Vane configurations

VANE # 1



VANE # 2



B) Rate of rotation 6°/minute

C) Installation - auger to within 1/2 meter and push vane

3) Mitchell & Lunne (1976)

A) Vane configurations

3 Rectangular Vanes

Size	Height (mm)	Dia. (mm)	Thick. (mm)
Small	50.5	101	3
Med.	107	50.5	3
Large	152	76	3

B) Rotation rate 6°/minute

C) Push vane from surface to desired depth. Connecting rods and vane are connected by a slip coupling and are disengaged at the start of the test. First the connecting rods are rotated and the shaft friction is measured. Then the slip coupling is engaged and the shaft and vane are rotated together. The friction of the coupling rods is subtracted from the measured vane resistance to obtain the actual vane resistance.

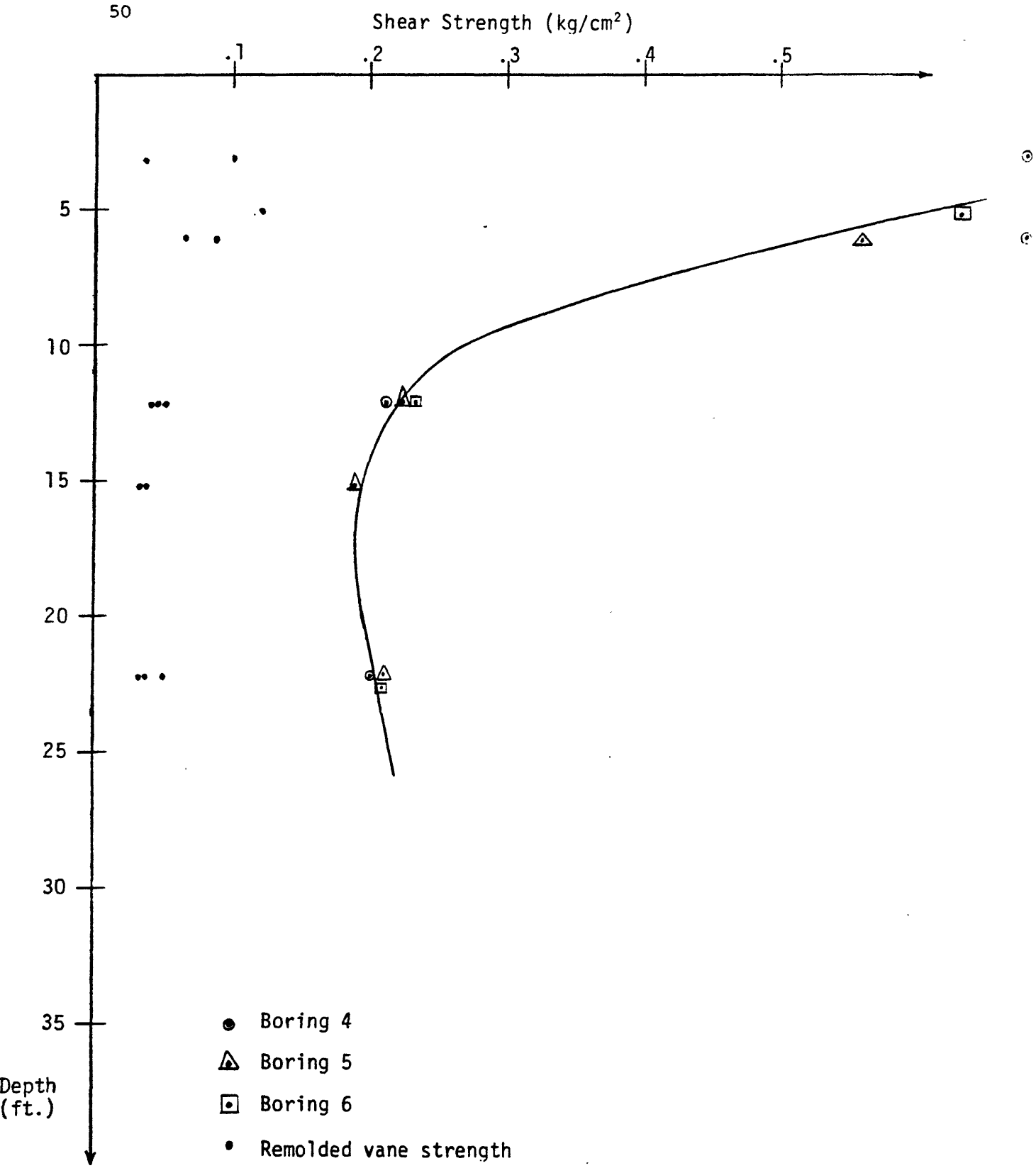


FIGURE 27 FIELD VANE SHEAR TEST RESULTS FROM TESTS PERFORMED BY TRINGALE (1978)

cylinder. His results show the Bay Mud having a stiff crust extending to a depth of about 12 feet. From about 12 to 17 feet the shear strength is at a minimum, being about 400 PSF. At about 18 feet the shear strength begins to increase linearly with depth. The tests indicate that the vane shear strength increases in proportion to the effective overburden pressure, the constant of proportionality ($S_u/\bar{p}$) being .31. Also shown on Figure 27 are values for the remolded shear strength. The remolded strength was obtained by continually rotating the vane until a minimum shear strength was obtained. As can be seen, except in the weathered desiccated zone where strengths are slightly higher, the remolded shear strength of Bay Mud is about 100 PSF and is constant with depth. Figure 28 shows the results of the vane shear tests run by Mitchell and Lunne (1977) and Figure 29 shows both vane and laboratory UU triaxial test results obtained by Duncan (1965). The shear strength values shown in these figures were obtained from the measured torques in the same way that the values in Figure 27 were obtained, the only difference being that for these figures uniform shear stress distributions were assumed to act along the top and bottom of the failure cylinder. The combined results from Figures 27 through 29 are shown in Figure 30. The agreement between the different tests is excellent. All test results fall close to each other and show the same trends as exhibited by Tringale's data; an upper desiccated zone, followed by a zone of minimum shear strength, below which the soil shear strength increases linearly with depth. The rate of strength increase in this lowest zone as measured by the undrained strength ratio $S_u/\bar{p}$, equals .31 to .32.

Figure 31 shows the results of vane shear tests presented by Duncan and Buchignani for the LASH Terminal, Port of San Francisco. The Bay Mud at this site has a liquid limit of 50 and a plastic limit of 20. It is

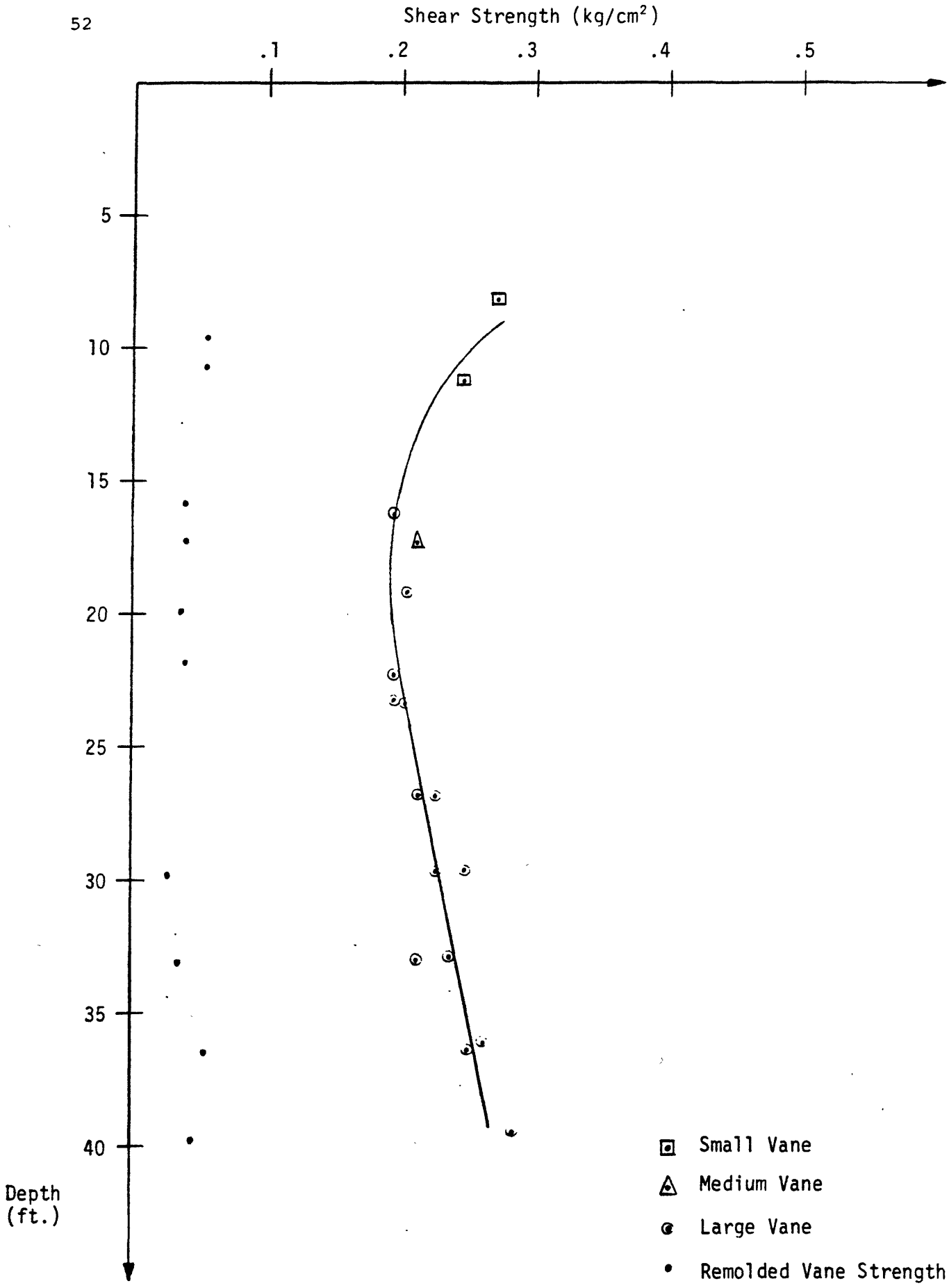


FIGURE 28 FIELD VANE SHEAR TEST RESULTS FROM TESTS PERFORMED BY MITCHELL AND LUNNE (1977)

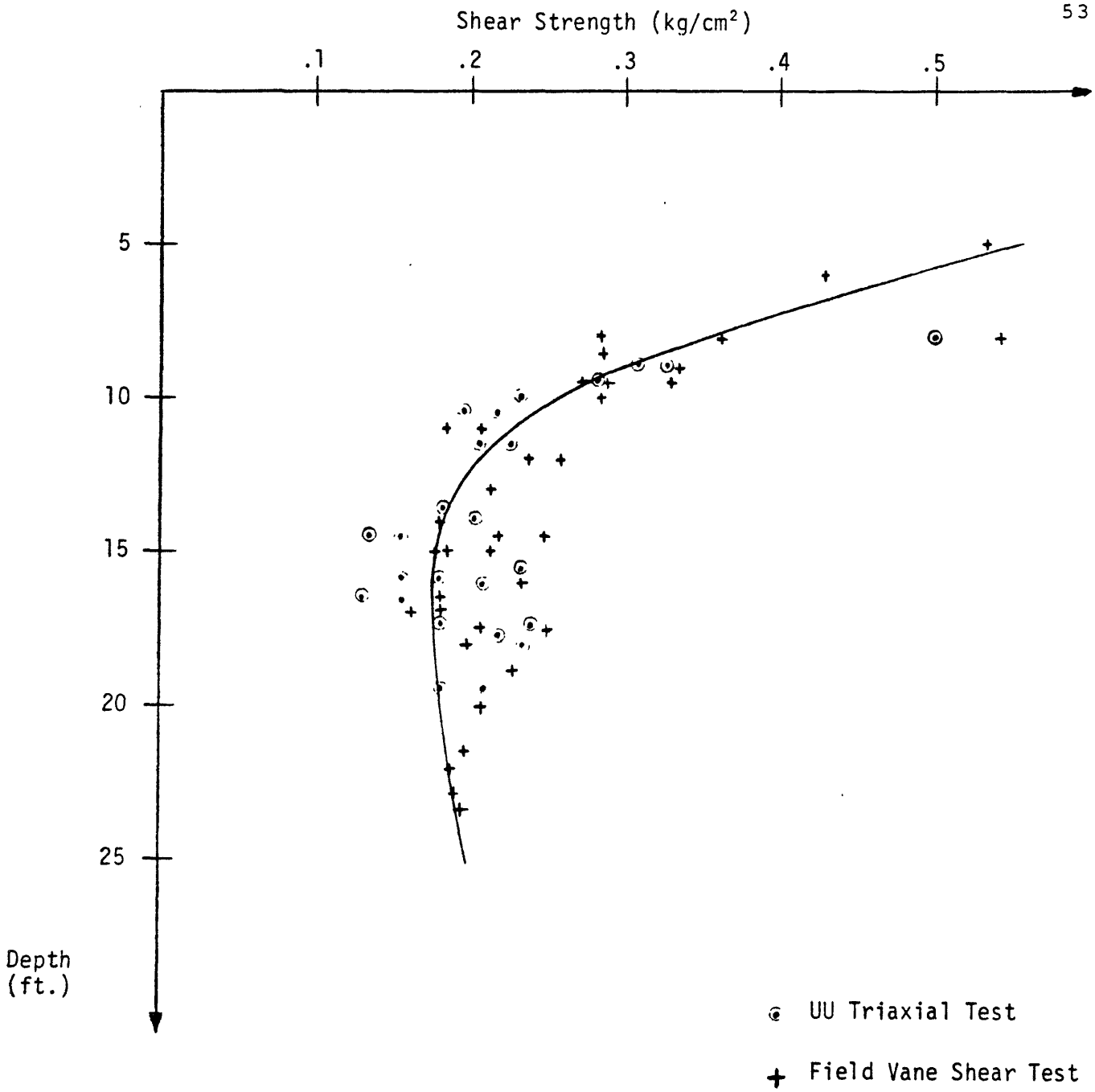


FIGURE 29 FIELD VANE SHEAR TEST RESULTS FROM TESTS PERFORMED BY DUNCAN (1965)

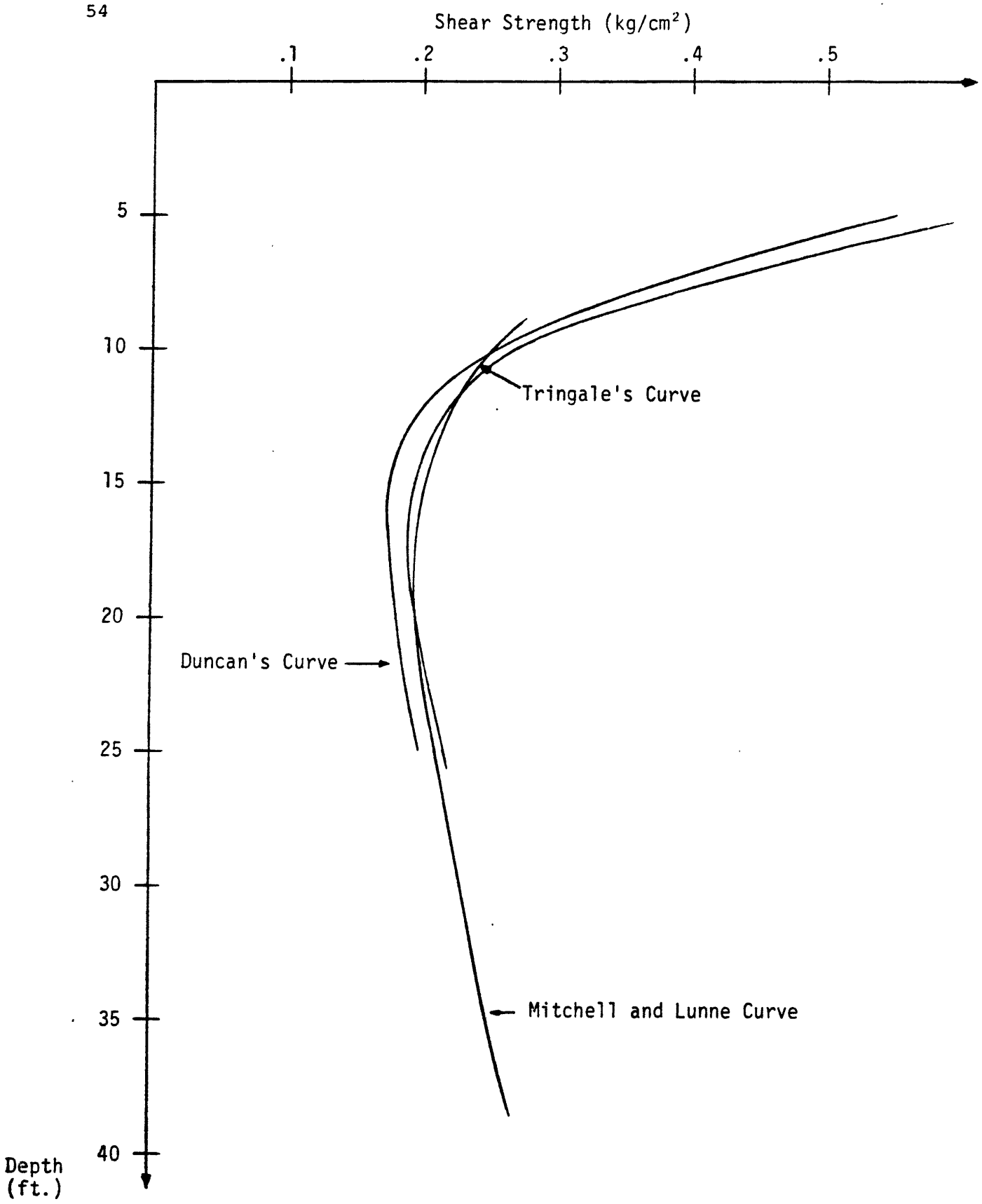


FIGURE 30 COMPARISON OF FIELD VANE SHEAR TEST RESULTS, HAMILTON AIR FORCE BASE

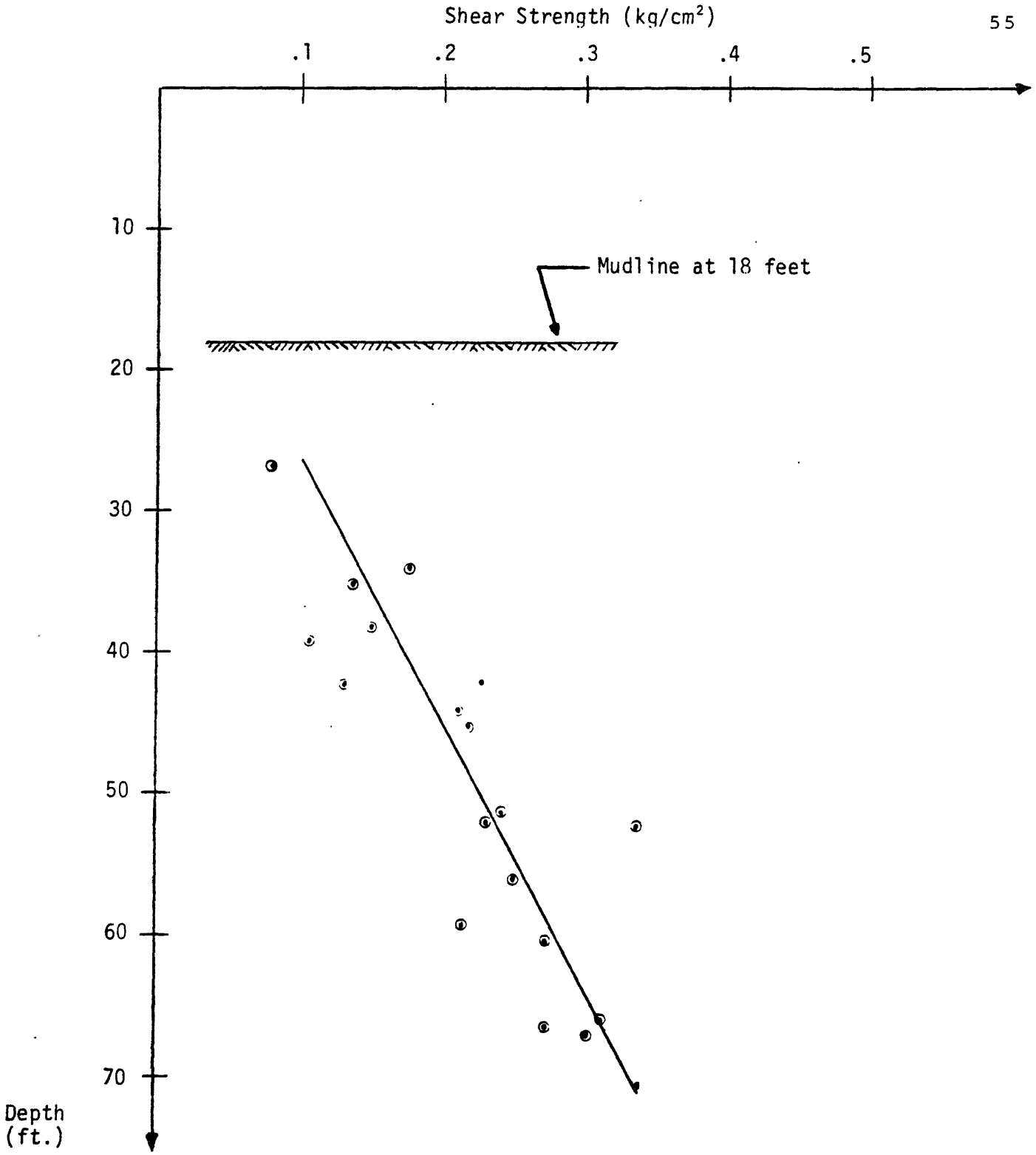


FIGURE 31 FIELD VANE SHEAR TEST RESULTS FROM THE LASH TERMINAL, PORT OF SAN FRANCISCO. REPORTED BY DUNCAN AND BUCHIGNANI (1973)

submerged under approximately 18 feet of water. These results show the Bay Mud to be consolidated under a lower effective stress than the soil at HAFB. As Figure 31 indicates however, the soils at this site exhibit an increase in vane shear strength with depth that is similar to the Bay Mud at the HAFB site. For both sites the $S_u/\overline{p}$ ratio is about .31 - .32.

The average value of remolded strength obtained by rotating the vane to very large strains is plotted in Figure 32, which shows a correlation between the remolded shear strength of several clay soils and the liquidity index. As can be seen the Bay Mud falls within the limits of the data band that has been developed for a number of clays. This result coupled with the liquidity index-sensitivity interrelationship of the Bay Mud (Figure 5) agrees with the concept (Mitchell, 1976) that a unique relationship between sensitivity, liquidity index and effective stress exists for a soil.

Cone Penetration Test

The shear strength of clays can be estimated from penetration resistances using the relationship

$$S_u = \frac{q_c - p}{N_c}$$

where: S_u = undrained shear strength

q_c = cone tip resistance

p = total overburden pressure

N_c = bearing capacity factor.

The bearing capacity factor is not a simple constant, and in cases where the soil shear strength has been determined by alternate means, back calculation has shown N_c to vary between 5 and 70. Schmertmann (1975) summarized the factors that influence N_c. Among these are the test method

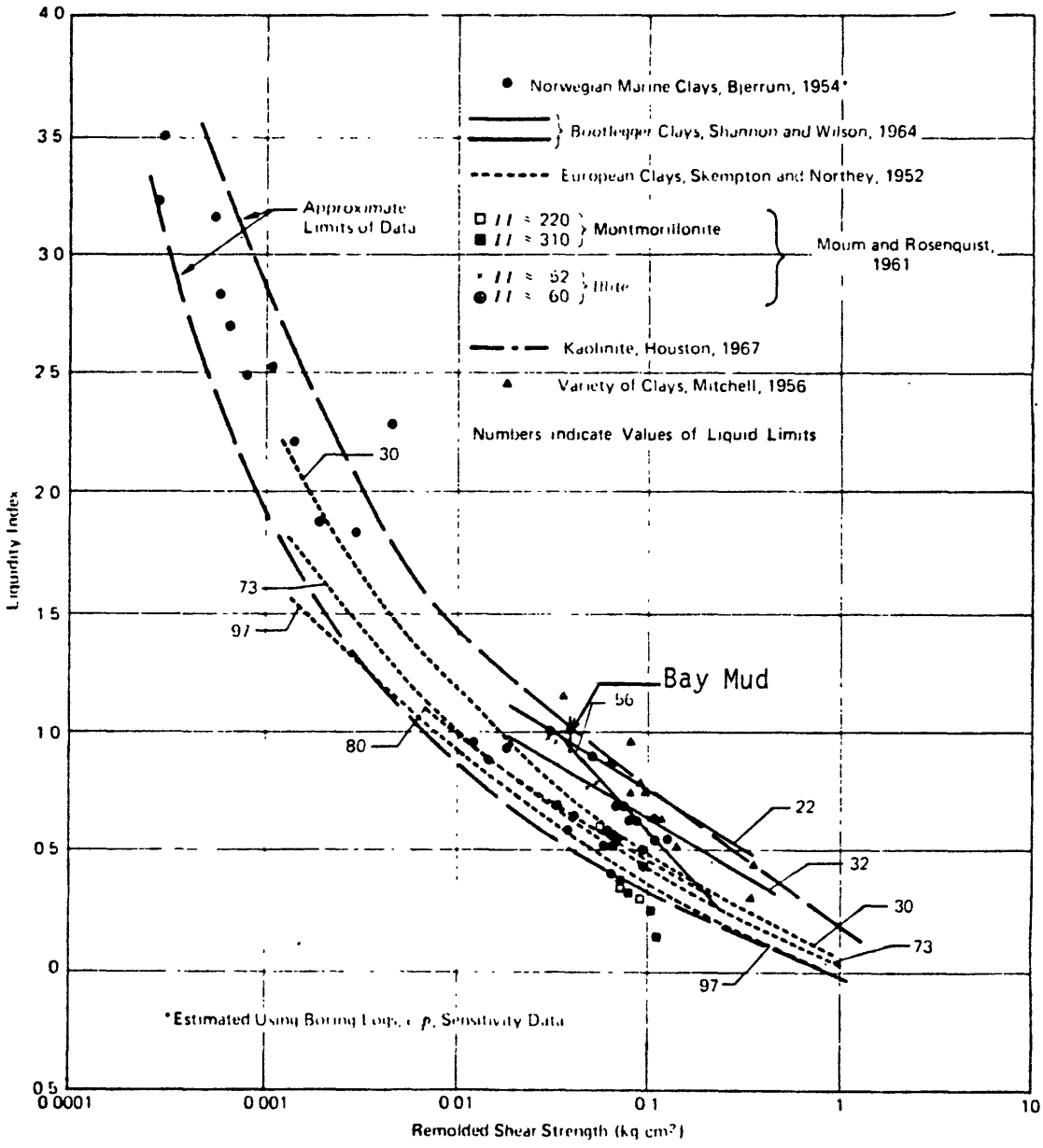


FIGURE 32 REMOLDED SHEAR STRENGTH VERSUS LIQUIDITY INDEX RELATIONSHIPS FOR SEVERAL CLAYS

From Mitchell (1976)

used, the clay stiffness ratio, G/S_u, the effective friction angle, ϕ', the overconsolidation ratio, the penetrometer tip shape and the rate of penetration. Mitchell et al. (1978) state, "The best approach (for finding N_c) for design purposes is to experimentally determine N_c for a given clay type, penetrometer apparatus, testing procedure and reference S_u." This technique was used to interpret the cone penetration resistances measured in the Bay Mud.

Mitchell and Lunne (1977) ran three cone penetration tests in the Bay Mud at the HAFB site. The average of the cone resistances for the three tests is shown in Figure 33. The tests were run using the electrical friction cone penetrometer developed at the Norwegian Geotechnical Institute, based on a design by the County Research Board, Melbourne, Australia. The cone tip has a base area of 10 cm^2 and an apex angle of 60°. These tip dimensions are identical to those of the standard Dutch cone. The overall dimensions and the geometry of the cone, which are illustrated in Figure 34 are the same as those of the Fugro electrical cone. Because of the low penetration resistance of the Bay Mud, the cone tip was stressed to only a fraction of its capacity, and consequently it was sensitive to fluctuations in temperature. Therefore, a thermistor was mounted inside the tip of the cone, which enabled the data to be corrected for temperature effects. The cone was pushed into the ground using a truck-mounted hydraulic cylinder. The rate of penetration was kept at about 20 mm/sec.

The first step in the analysis of the cone data is to back calculate N_c. Use Figure 33 to find the penetration resistance at a given depth. At 15 m, q_c = 5.0 kg/cm^2. The measurements were made in the spring, so assume the water table was at a depth of 6 ft.

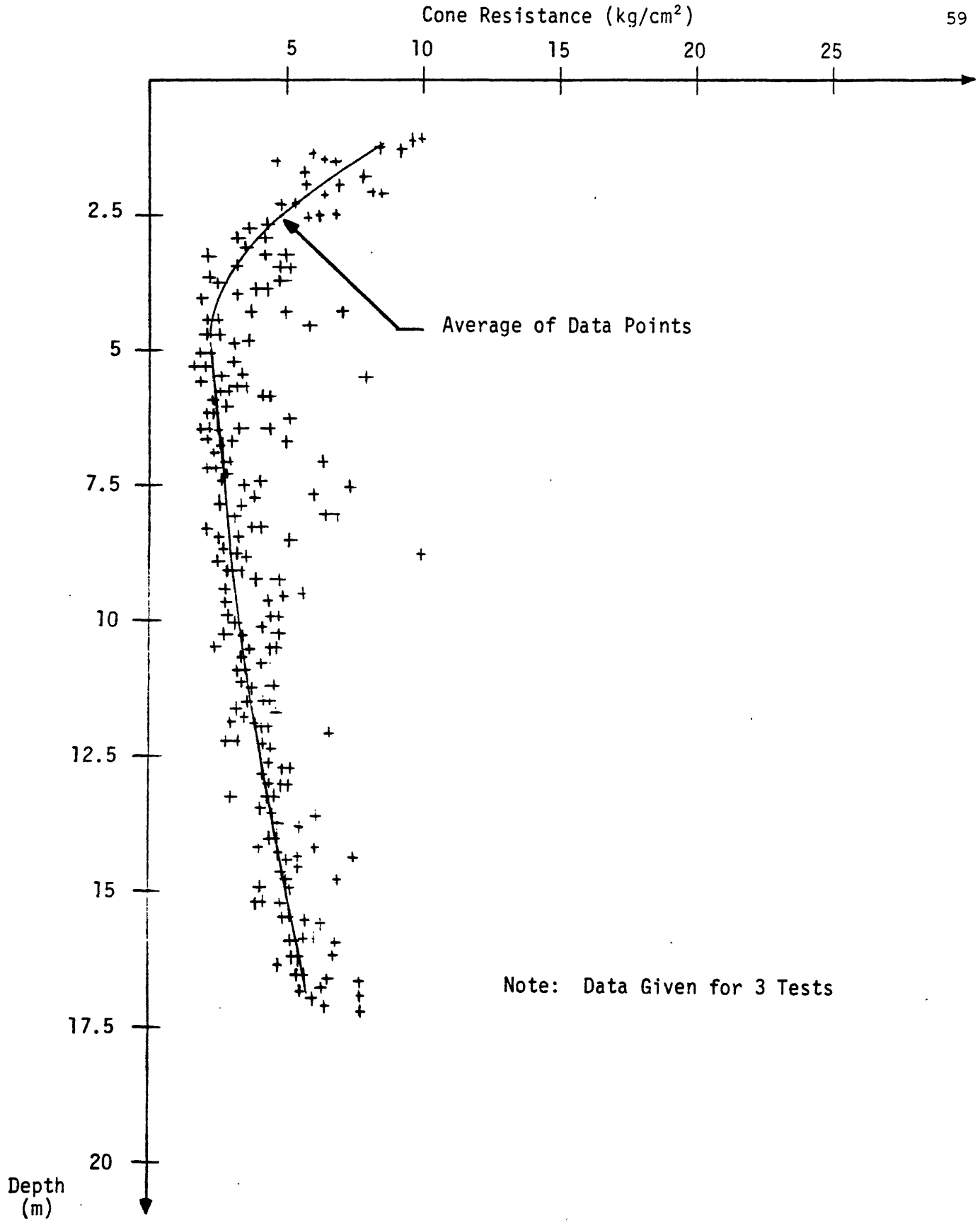


FIGURE 33 CONE PENETRATION TEST RESULTS ON BAY MUD FROM TESTS PERFORMED BY MITCHELL AND LUNNE (1976)

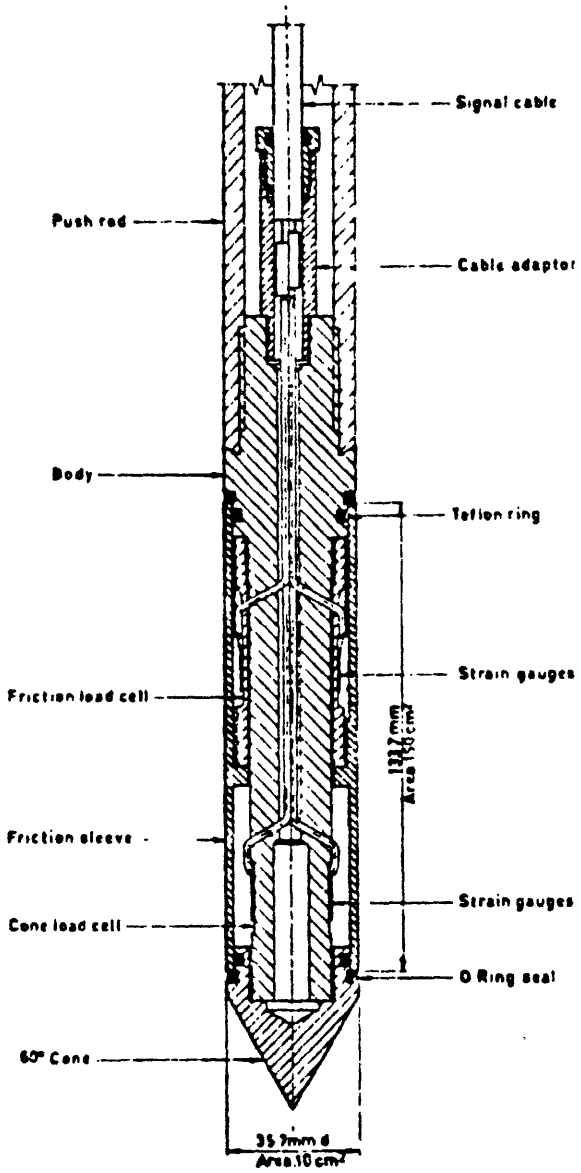


FIGURE 34 C.R.B. ELECTRICAL FRICTION CONE PENETROMETER USED BY MITCHELL AND LUNNE (1976) AT HAMILTON AIR FORCE BASE

σ(at 15 m) = 15m x 94 lb/ft^3 = 2.26 kg/cm^2

σ' (GWT = 1.83m) = 2.26 kg/cm^2 - (15m - 1.83m) = .94 kg/cm^2

To find S_u, the undrained shear strength, use the results of the field vane shear strength tests, which are given in Figure 30. These strengths are then reduced using a correction factor, u, first proposed by Bjerrum (1973). Bjerrum's correction factor is primarily to compensate for strain rate effects. For Bay Mud this factor is about .85. Local experience indicates that field vane shear strengths are about 15% higher than UU test results (Duncan and Buchignani (1973)), which agrees well with Bjerrum's correction factor.

At 15 meters

field vane shear strength from Figure 30 = .31 kg/cm^2

Bjerrum correction factor = .85

corrected field vane shear strength, S_u = .85 x .31 = .26 kg/cm^2

$$N_c = \frac{q_c - \sigma}{S_u} = \frac{(5.0 - 2.26)\ kg/cm^2}{.26\ kg/cm^2} = 10.5$$

Try 7.5 meters to make sure that the value for N_c just calculated is applicable to the entire soil profile.

At 7.5 m (GWT at 1.83 m)

q_c = 2.8 kg/cm^2

σ = 1.13 kg/cm^2

σ' = .56 kg/cm^2

field vane shear strength = .21 kg/cm^2

Bjerrum correction factor = .85

corrected field vane shear strength = .85 x .21 = .18 kg/cm^2

$$N_c = \frac{(2.8 - 1.13)\ kg/cm^2}{.18\ kg/cm^2} = 9.4$$

The value of N_c computed in this way is fairly constant and can be taken to be about 10. Figure 35 shows the shear strength profile based on the measured cone penetration resistances and $N_c = 10$. The shear strength profile obtained shows the same trends as the results of the field vane shear tests. An upper desiccated zone extends from the surface to a depth of about 15 feet, followed by a zone of minimum shear strength, below which the shear strength increases proportionally with depth.

Self Boring Pressuremeter Test

Denby (1978) ran a series of 33 tests using the self-boring pressuremeter at HAFB. The pressuremeter used in his tests was manufactured by Cambridge Insitu. It is cylindrical in shape and is about 75 mm in diameter and 800 mm long. The pressuremeter was pushed into the ground by two hydraulic jacks. As it was pushed downward the soil entering the tip of the instrument was chopped by a cutting edge and a chopping bit and then flushed to the surface. Ideally, the lateral stresses in the ground are not affected by the insertion process. Once seated, application of a nitrogen gas pressure expanded a rubber membrane against the sides of the borehole. The pressure was applied in 1/2 psi increments every 30 seconds.

From the results of the pressuremeter tests values for a soil's shear strength, in-situ lateral stress and stress-strain curve can be back calculated. To derive these quantities a "method of interpretation" is needed to relate the desired soil property to the actual test results. Denby developed a new method for pressuremeter test interpretation based on a modified hyperbolic stress-strain model (see Duncan and Chang (1970) for development of the hyperbolic stress-strain model). Using this new model and his test results he derived Figure 36, which shows the variation in

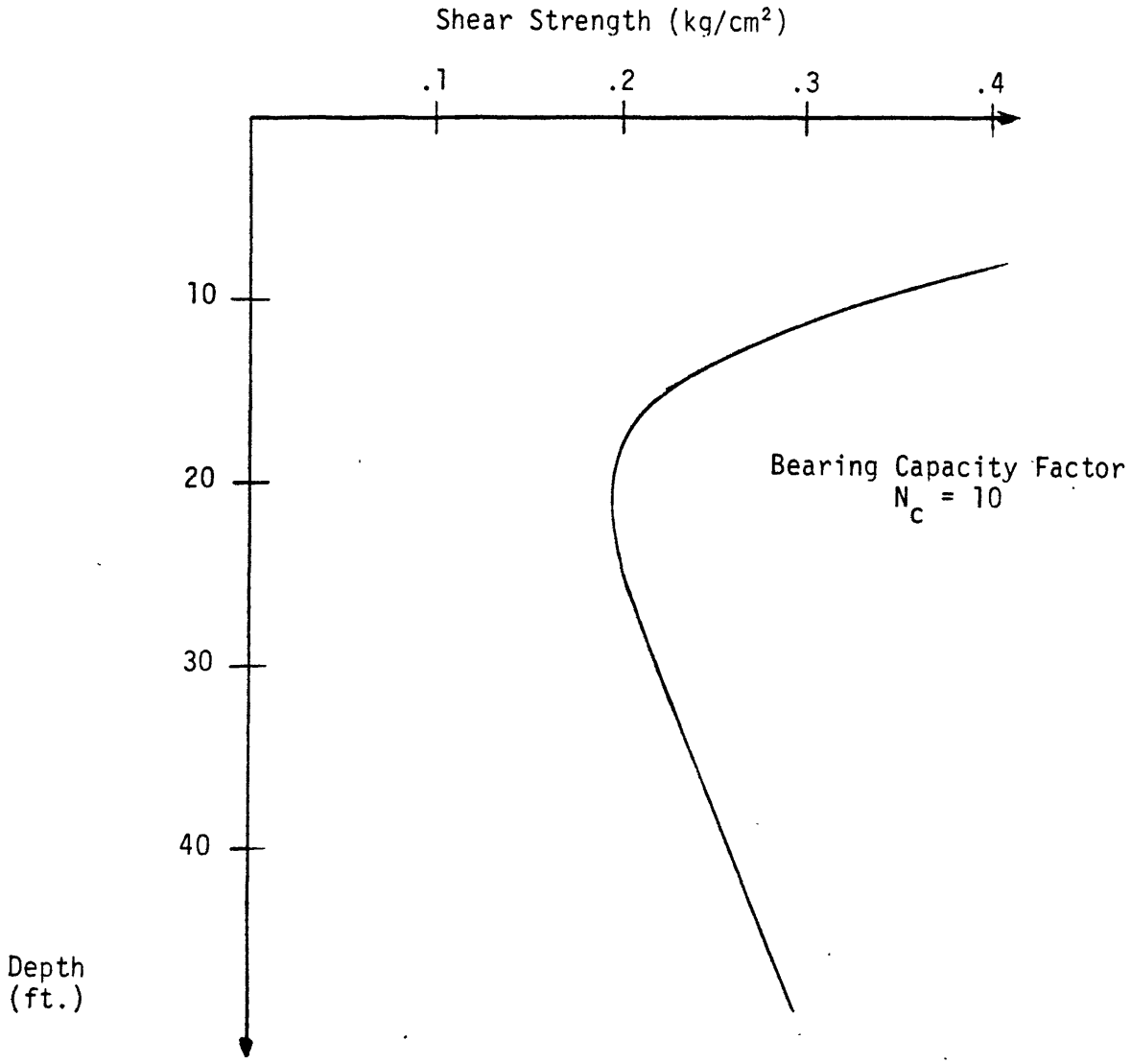


FIGURE 35 SOIL SHEAR STRENGTH AS DERIVED FROM THE CONE PENETRATION TEST RESULTS PRESENTED BY MITCHELL AND LUNNE (1976)

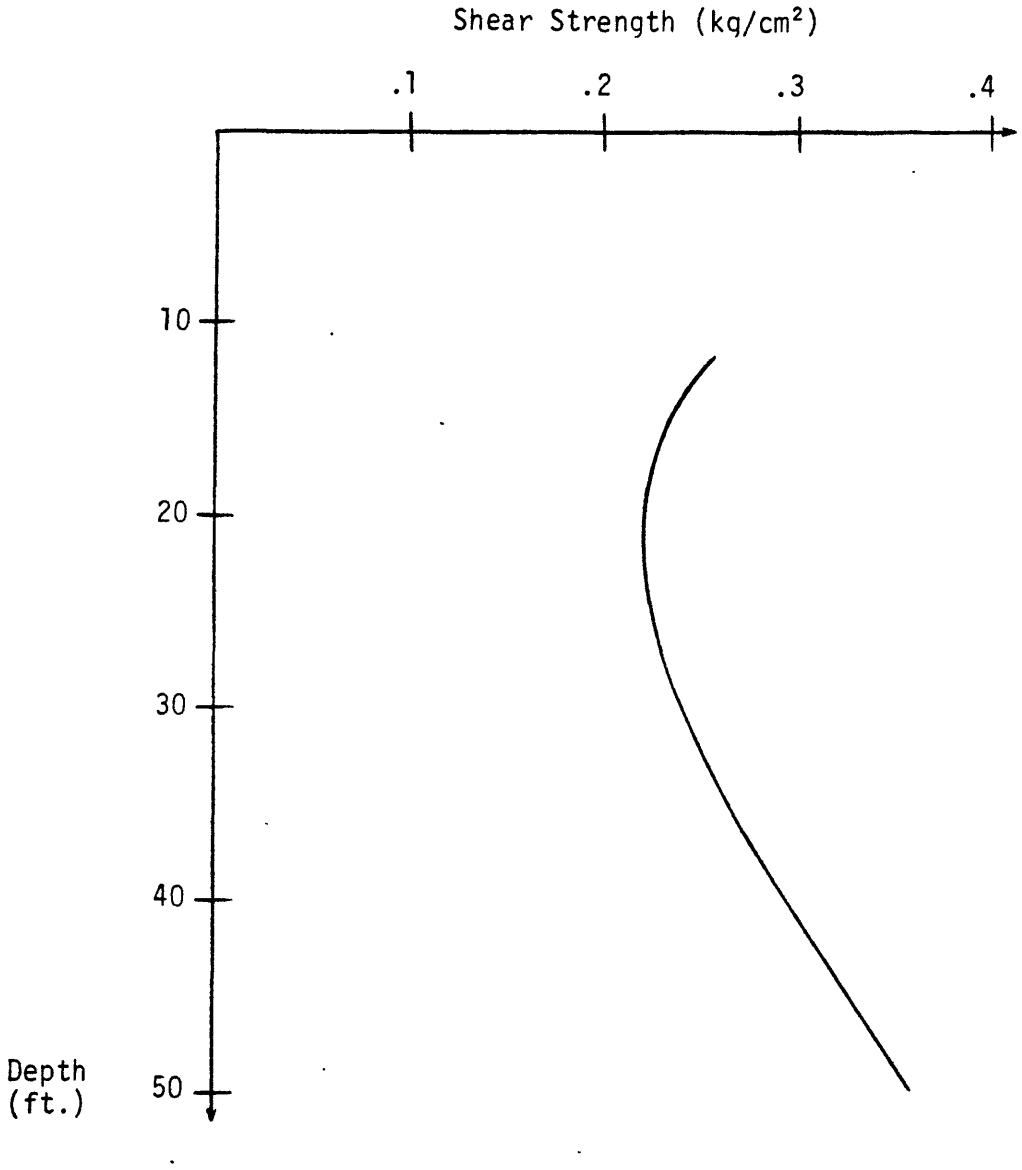


FIGURE 36 UNDRAINED SHEAR STRENGTH PROFILE DERIVED FROM THE SELF BORING PRESSUREMETER TESTS PERFORMED BY DENBY (1978)

undrained shear strength versus depth. These strength results will be discussed in the next section of this report where they will be compared to the field vane and cone penetrometer results.

Figure 37 shows values for the initial shear modulus G_i plotted as a function of depth. Also shown in this figure are values for the modulus multiplier M, defined by $E_i = MS_u$. E_i is the initial tangent modulus obtained from a soil's stress-strain curve. Both G_i and M increase with depth. The modulus multiplier M varies between about 600 and 1200. Denby reports measuring values of M as high as 2500 in $\overline{AC-U}$ triaxial tests. He attributes these differences to differences in the stress paths, failure surfaces and loading rates between the pressuremeter test and the triaxial test. Duncan and Buchignani (1976) presented a chart for estimating the modulus multiplier. It is based on field tests which "are not affected by disturbance," and is shown in Figure 38. Using the known PI and OCR of Bay Mud, Figure 38 indicates that the modulus multiplier should be close to 600.

Values for the in-situ lateral stresses obtained from the pressuremeter tests will be given in a subsequent section.

Discussion of In-Situ Shear Strength Test Results

The results of all in-situ tests which were used to measure the undrained shear strength of Bay Mud are shown in Figure 39. All test methods show the profile to have a desiccated crust followed by a zone of minimum shear strength. In this zone measured shear strengths ranged from a low of 370 PSF for the vane shear test to a high of 450 PSF for the pressuremeter test. Below 20 feet the shear strength increases linearly with depth. The $S_u/\overline{p}$ ratios for the field vane shear test and the cone penetration test are both about .32 while the $S_u/\overline{p}$ ratio for the self boring pressuremeter

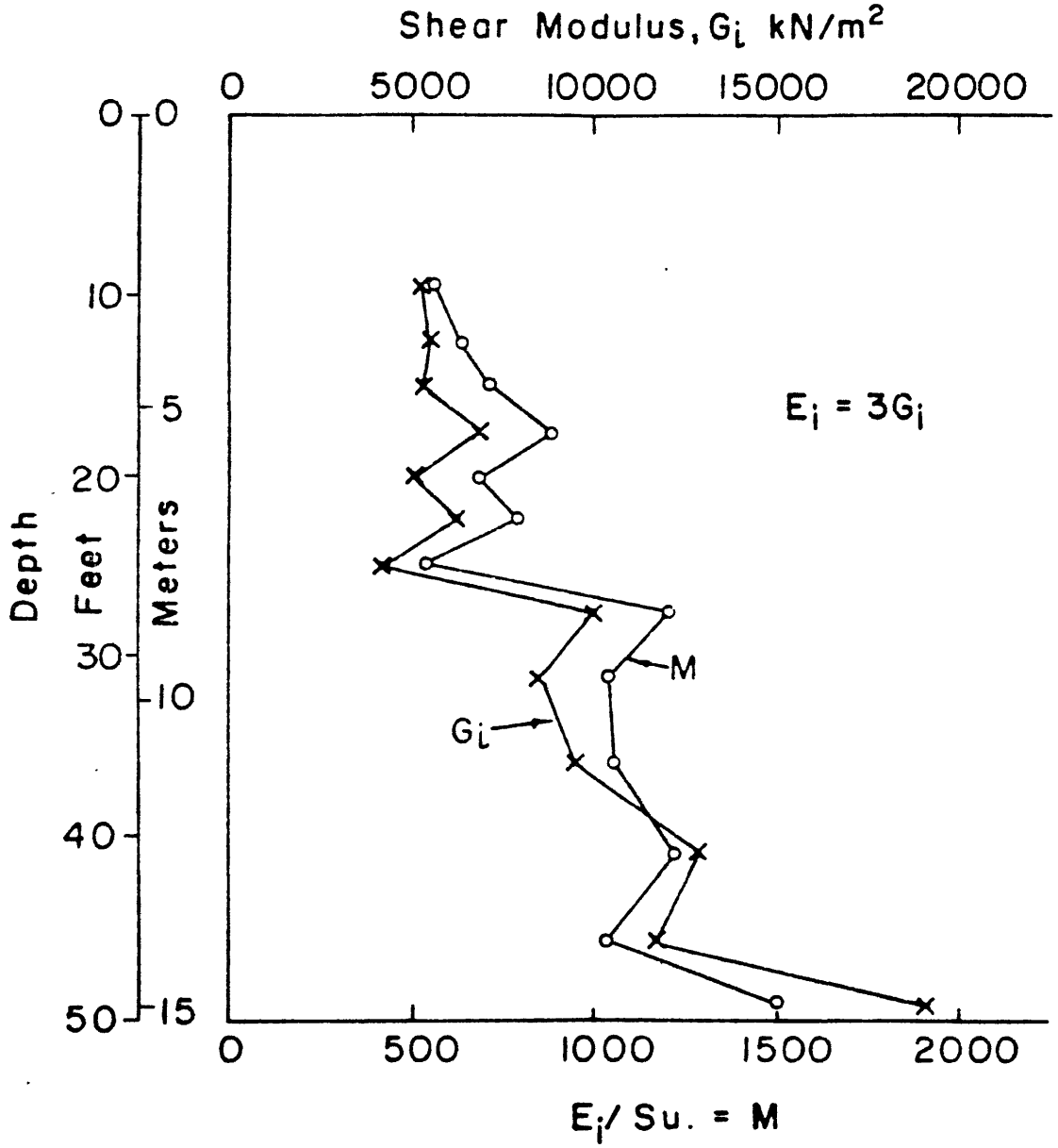
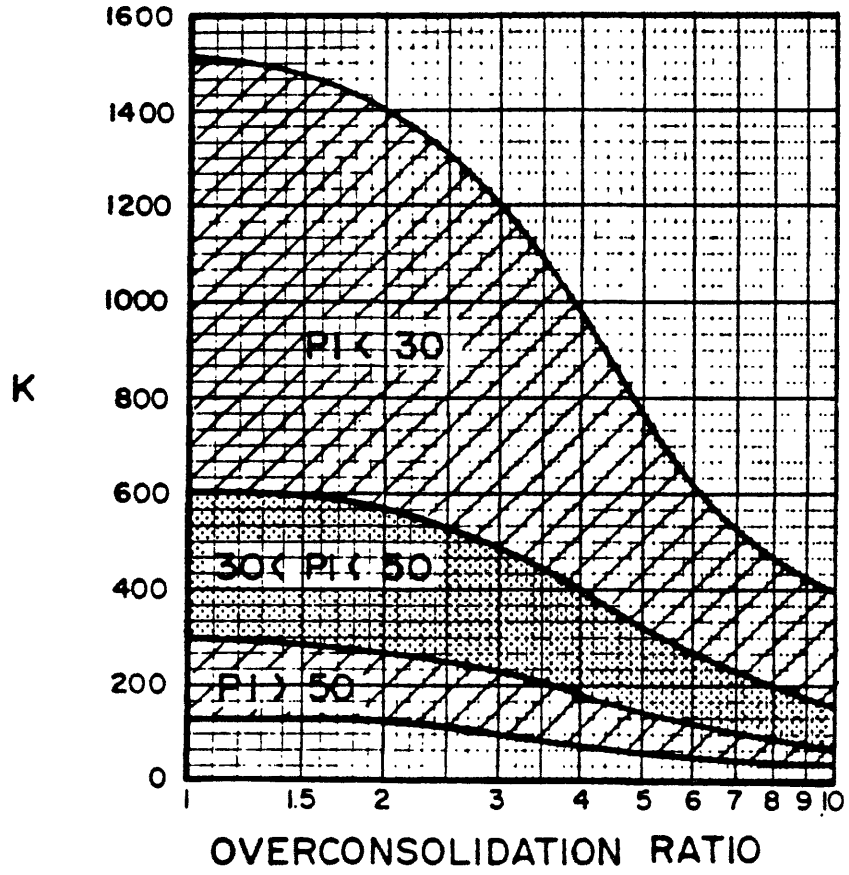


FIGURE 37 SHEAR MODULUS AND MODULUS MULTIPLIER (M) AS DERIVED FROM THE SELF-BORING PRESSUREMETER TEST BY DENBY (1978)



$E_u = KS_u$

E_u = UNDRAINED MODULUS OF CLAY

K = FACTOR FROM CHART ABOVE

S_u = UNDRAINED SHEAR STRENGTH OF CLAY

FIGURE 38 CHART FOR ESTIMATING THE UNDRAINED MODULUS MULTIPLIER (K) FOR CLAY

From Duncan and Buchignani (1976)

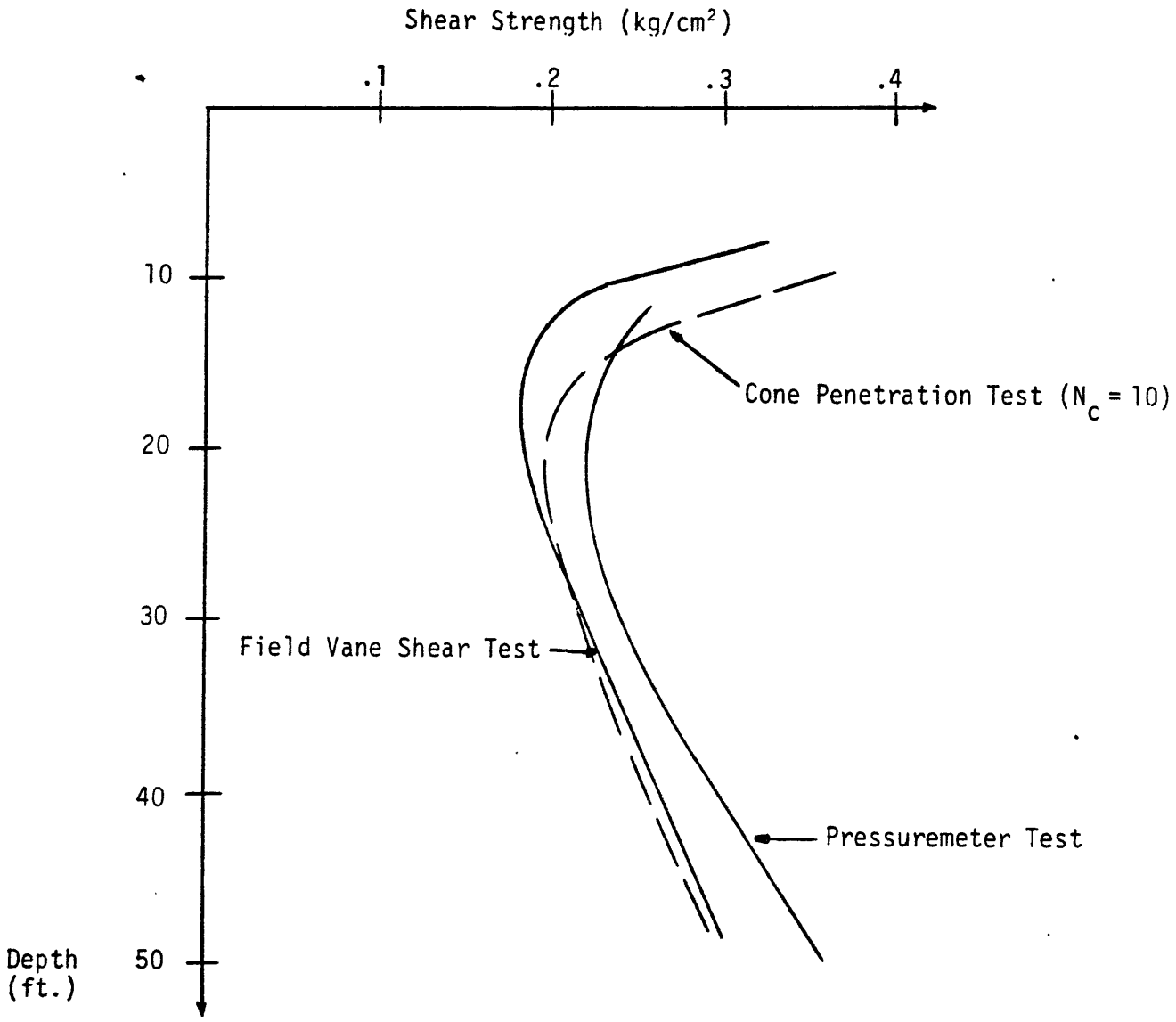


FIGURE 39 COMPARISON OF UNDRAINED SHEAR STRENGTH FROM VARIOUS IN-SITU TESTS

is .40 indicating strengths measured in the pressuremeter test are about 15% higher than the strengths measured in the other in-situ tests.

The fact that these in-situ test methods give somewhat differing answers is not surprising when the differences between the test methods are considered. Different failure modes, strain rates and stress conditions are developed during the different tests. Some of these differences have been summarized by Denby (1978) and are presented in Table 8. Research is needed in relating the results from the different in-situ shear strength tests, and in relating the results of these tests to the actual in-situ conditions.

Evaluation of In-Situ Lateral Stresses

The self boring pressuremeter and the Glötzl load cell have been used to obtain values for the total lateral stress acting at depth in the Bay Mud. The Glötzl cell, shown schematically in Figure 40, is a thin spade like unit that is inserted into the ground with its face perpendicular to the direction in which the stress is to be measured. The cell is filled with a fluid that has been prestressed at the time of manufacture. Once inserted the cell fluid transmits the earth pressure to a thin diaphragm. The amount of air pressure needed to just balance the fluid pressure against the diaphragm is measured. The earth pressure is calculated from the difference between the total stress measured and the calibration stress of the unloaded cell. The soil displacement during the insertion of the cell causes an increase in the lateral stress acting on the cell. This stress increment is allowed to dissipate before the earth pressure measurements are made. Equilibration of the stresses takes place in 3 to 5 days.

TABLE 8 DIFFERENCES IN IN-SITU TEST METHODS

From Denby (1978)

Type of Test	Loading Rate	Failure Surface	Stress Conditions
Self-Boring Pressuremeter	0.5 psi/0.5 min. Failure in 10-20 min. depending on s_u	Vertical	Major principal stress rotates 90° during test; all three principal stresses change in magnitude; progressive failure; non-uniform stress field
Vane (Lunne, 1977)	Vanes rotated at 6°/min; failure in about 2-4 mins. depending on s_u	Vertical and horizontal	Poorly defined; shear stress primarily increased on vertical plane; principal stresses rotated; progressive failure likely
Cone Penetrometer	Cone advanced at rate of 20 mm./ sec.	Curvilinear	Poorly defined; principal stresses rotated; progressive failure likely

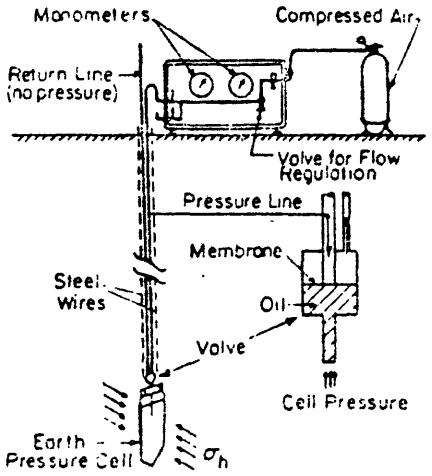


FIGURE 40 SCHEMATIC DIAGRAM SHOWING THE MEASUREMENT OF IN-SITU LATERAL PRESSURE USING THE GLÖTZL CELL

From Mitchell, Guzikowski and Villet (1978)

The Glötzl cell tests were run by Mitchell and Lunne (1977) and the self boring pressuremeter tests were run by Denby. The results of these tests, in terms of both total horizontal stress and the coefficient of lateral earth pressure at rest, $K_o' = \sigma_H'/\sigma_v'$, are given in Table 9. As can be seen, the differences between the lateral earth pressures measured by the two methods are rather significant and correspond to rather large differences in the calculated values of K_o'. This fact becomes clear when the results are plotted, as in Figure 41. In the normally consolidated zone of the Bay Mud deposit the pressuremeter test measures total lateral earth pressures that correspond to a K_o' equal to .5 at depths falling between 20 and 35 feet and .6 below 35 ft. The Glötzl cell measured a total lateral earth pressure that corresponded to a value for K_o' of .7 in the normally consolidated zone. Denby suggests that the high value of K_o' obtained with the Glötzl cell may be due to either an insufficient equilibration period or disturbance of the clay due to insertion of the cell.

Lacerda (1976) studied the change in K_o' with time due to the effect of stress relaxation in Bay Mud. He suggested that under conditions of constant vertical stress the lateral stress would increase with time so as to reduce the deviator stress acting on the soil. This process would be very slow and would occur at an ever decreasing rate. It follows directly that if the vertical stress is constant and the horizontal stress is increasing, then the value of K_o' must be increasing. Using a conventional triaxial apparatus, Lacerda measured variations in K_o' with time. His tests were of relatively short duration. The results showed that K_o' increased linearly with the logarithm of time. In one test K_o' increased from a value of .520 at 1000 minutes to .55 at 10,000 minutes. In a second test K_o' increased from .528 to .588 in the same period of time.

TABLE 9 COMPARISON OF PRESSUREMETER AND GLÖTZL LOAD CELL.IN-SITU HORIZONTAL STRESSES AT HAMILTON TEST SITE

From Denby (1978)

		PRESSUREMETER			GLOTZL LOAD CELL		
DEPTH FT.	W.T. FT.	TEST NO.	P_H kN/m^2	K_o'	P_H kN/m^2	K_o'	SOIL PROFILE
9.5	6.3	HPR14	38.6	0.83			
11.3	4.70				52.5	1.02	G.L.
12.4	6.3	15	40.0	0.55			
15.0	6.4	16	50.4	0.57			γ = 100 pcf (1.6 Kg/cc)
16.4	4.7				66.5	0.80	
17.3	6.4	17	54.5	0.47			
20.0	6.4	18	64.1	0.47			W.T.
22.2	6.4	19	73.1	0.48			
22.9	4.7				89.0	0.70	$\gamma_{Sat.}$ = 94 pcf (1.5 Kg/cc)
24.9	6.7	20	82.8	0.49			
27.5	6.7	21	95.2	0.53			
31.1	6.7	22	107.1	0.50			
36.0	6.7	23	132.4	0.60			
40.9	6.8	24	152.4	0.61			
45.8	6.8	25	173.8	0.64			
49.1	6.8	26	187.6	0.65			

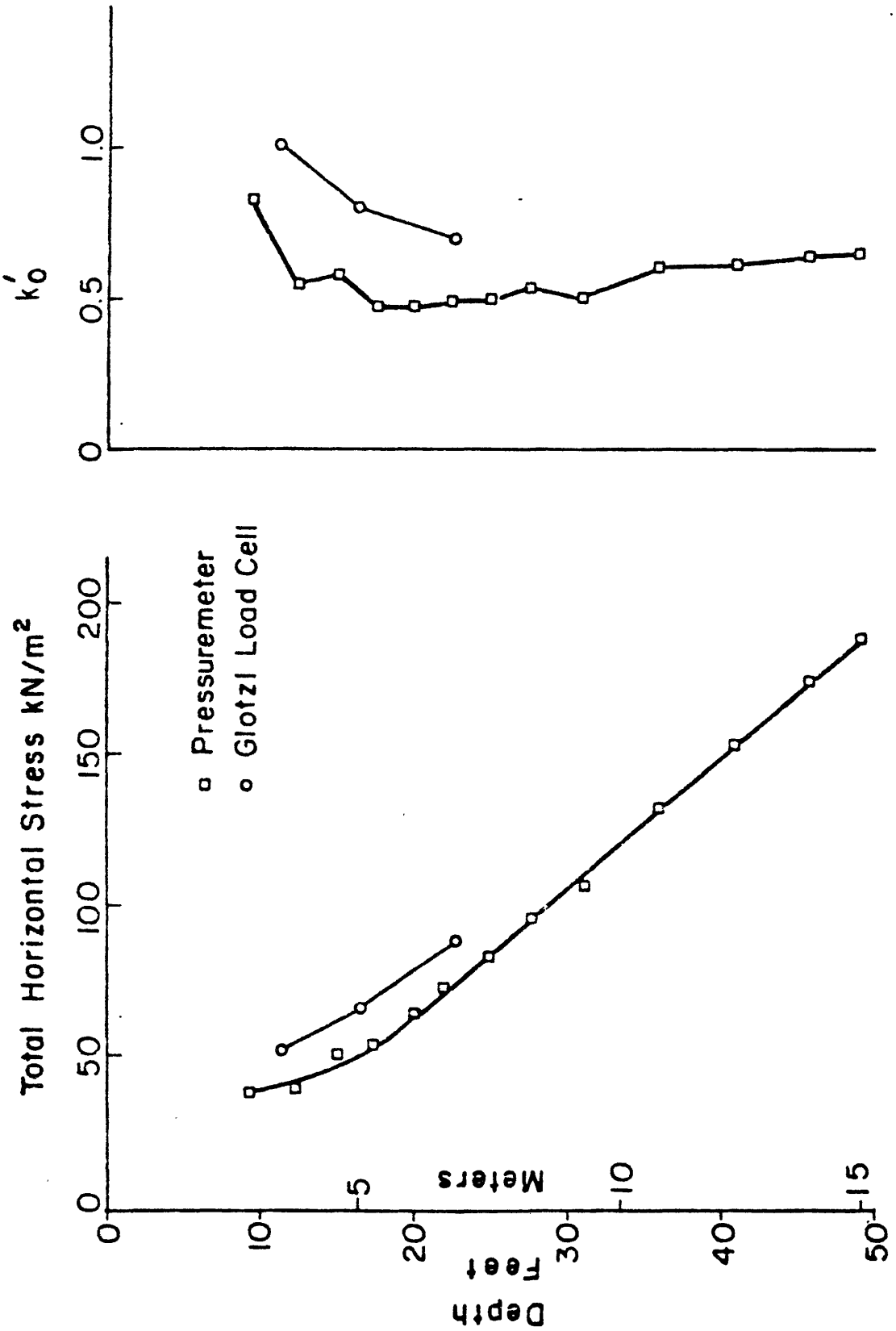


FIG. 41 COMPARISON OF TOTAL HORIZONTAL STRESS AND K_o' VALUES DETERMINED BY THE PRESSUREMETER AND GLÖTZL LOAD CELLS

From Denby (1978)

For normally consolidated soils the relationship $K_o' = 1 - \sin\phi'$ is often used to calculate K_o'. It will be shown in a later section that the angle of internal friction, ϕ', for Bay Mud as measured in $\overline{IC-U}$ triaxial tests is about 34.5°. The value of K_o' calculated using $\phi' = 34.5°$ is .434.

5. LABORATORY STRENGTH TESTS

Effective Stress Strength Parameters

When comparing results from consolidated-drained tests or consolidated-undrained tests with pore pressure measurement, there exist at least two ways of presenting the effective stress strength data. These are: 1) at maximum deviatoric stress difference; and 2) at maximum obliquity, i.e. at the maximum value of σ_1'/σ_3'. For soft normally consolidated soils with increasing pore pressure parameter $\bar{A}$ at failure, ϕ' at maximum obliquity will be larger than ϕ' at maximum deviatoric stress difference. For sensitive clays and K_o consolidation, Ladd (1971) reports that the difference in ϕ' can approach 5 to 10°.

The effective stress strength parameters of Bay Mud have been reported by a number of investigators. Several types of shear strength tests were used to obtain values for the effective stress friction angle ϕ' and the effective stress cohesion intercept c'. These tests included consolidated-drained triaxial tests (CD), isotropic and anisotropic consolidated-undrained triaxial tests with pore pressure measurement ($\overline{\text{IC-U}}$, $\overline{\text{AC-U}}$) and vertical and horizontal plane strain tests with pore pressure measurement ($\overline{\text{VPS}}$, $\overline{\text{HPS}}$).

All test results show that the effective stress cohesion intercept, c', of Bay Mud is 0. The results of measurements of the effective stress friction angle, ϕ', are given in Table 10. Several points should be noted relative to the values given in this table. 1) Values of ϕ' are given at maximum deviator stress. Most of the tests reviewed were stopped shortly after $(\sigma_1 - \sigma_3)_{max}$ was reached and before the maximum value of (σ_1'/σ_3') was obtained (it typically takes several percent more strain to reach the

TABLE 10

EFFECTIVE STRESS FRICTION ANGLE - BAY MUD

Researcher	Test Type		ϕ'	ε_f
Seed et al. (1964)	$\overline{\text{AC-U}}$	$\sigma_{rc}' = .5\ \sigma_{AC}'$	33°-35°	~5%
Duncan (1965)	$\overline{\text{VPS}}$		38°	~5%
	$\overline{\text{HPS}}$		35°	~10%
	$\overline{\text{AC-U}}$	$\sigma_{rc}' = .54\ \sigma_{AC}'$	34.3°	~6%
	$\overline{\text{AC-U}}$	$\sigma_{AC}' = .65\ \sigma_{rc}'$	34.5°	~13%
	$\overline{\text{IC-U}}$			10-12%
Lacerda (1976)	C-D		31°	~30%
Berkeley (CE 273) 1977	$\overline{\text{ICU}}$		34.5°	8%
Denby (1978)	$\overline{\text{AC-U}}$	$\sigma_{rc}' = .7\ \sigma_{AC}'$	29.5°	4%
Berkeley (CE 270L) 1978	$\overline{\text{IC-U}}$		32.4°	10%

Note: 1) ϕ' measured at maximum deviator stress

2) σ_{rc}' = effective radial stress at the end of consolidation

3) σ_{AC}' = effective axial stress at the end of consolidation

4) ε_f = axial strain at maximum deviator stress

σ_1'/σ_3' failure criteria in soft clays). Therefore, values of ϕ' at maximum obliquity have not been reported. Judging from the data that are available it appears that ϕ' at maximum obliquity is about 3° to 4° greater than ϕ' at maximum deviator stress. 2) There is a considerable variation in the values measured for ϕ'. Variations due to different testing conditions are to be expected. For instance, ϕ' from a $\overline{\text{VPS}}$ (38°) is expected to be larger than ϕ' from a $\overline{\text{HPS}}$ (35°), while $\overline{\text{HPS}}$ (35°) results should be slightly larger than $\overline{\text{IC-U}}$ (34°-35°) results. However, for a given test type there exists considerable variation in the measured values of ϕ'. In $\overline{\text{AC-U}}$ tests ϕ' varied between 29.5° and 35°, while in $\overline{\text{IC-U}}$ tests ϕ' varied between 32.4° and 34.5°. In review, the reasons for these variations are not obvious. Differences could develop due to several causes, among them differences in test equipment and test procedures and variability in the properties of Bay Mud. Figures 42 through 44 present the effective stress failure envelopes obtained from several sets of tests.

It is interesting to compare the value of ϕ' obtained for Bay Mud with empirical correlations for clays from other parts of the world. Figure 45 shows a plot of ϕ' versus plasticity index. As can be seen ϕ' for Bay Mud plots a few degrees higher than is typical for clays with the same plasticity index as Bay Mud. The reason for the high value of ϕ' obtained for Bay Mud has not been ascertained, although it is possible that the presence of microscopic fragments of shells, coccoliths and other materials play a role.

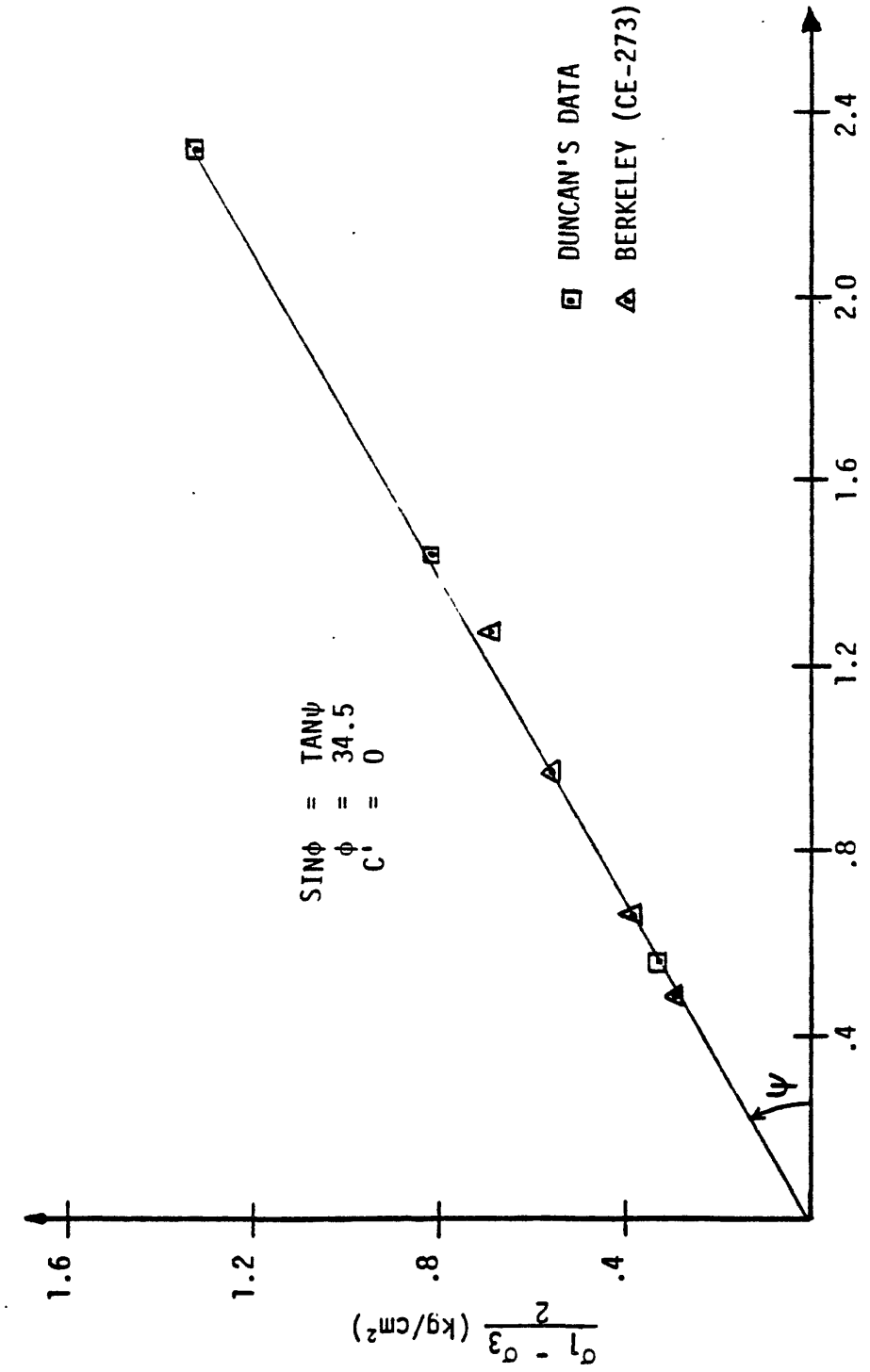


FIGURE 42 $\overline{IC\text{-}U}$ TRIAXIAL TEST EFFECTIVE STRESS STRENGTH ENVELOPE FOR UNDISTURBED SAN FRANCISCO BAY MUD

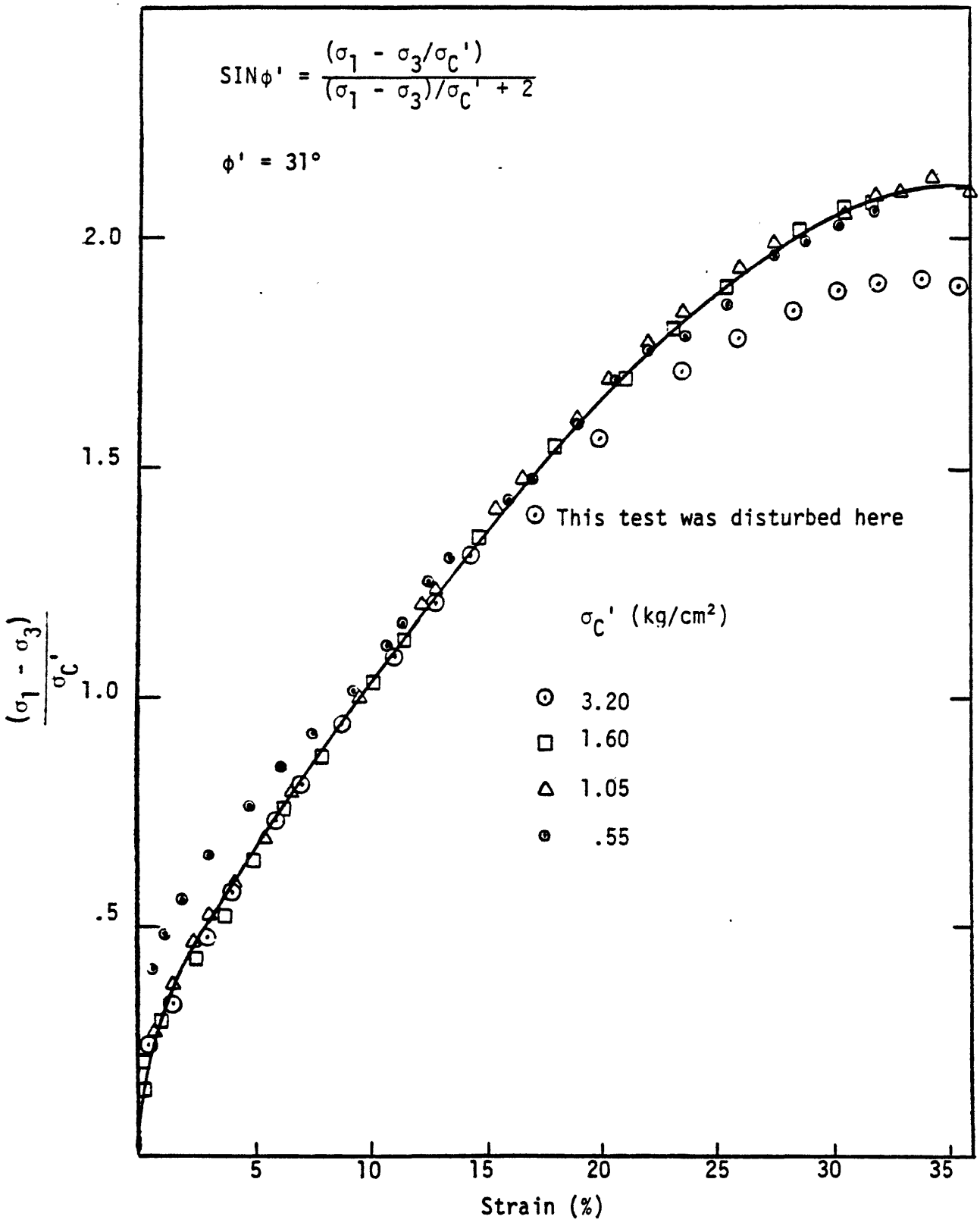


FIGURE 43 NORMALIZED PLOT FROM ISOTROPICALLY CONSOLIDATED DRAINED TRIAXIAL TESTS ON UNDISTURBED BAY MUD

From Lacerda (1977)

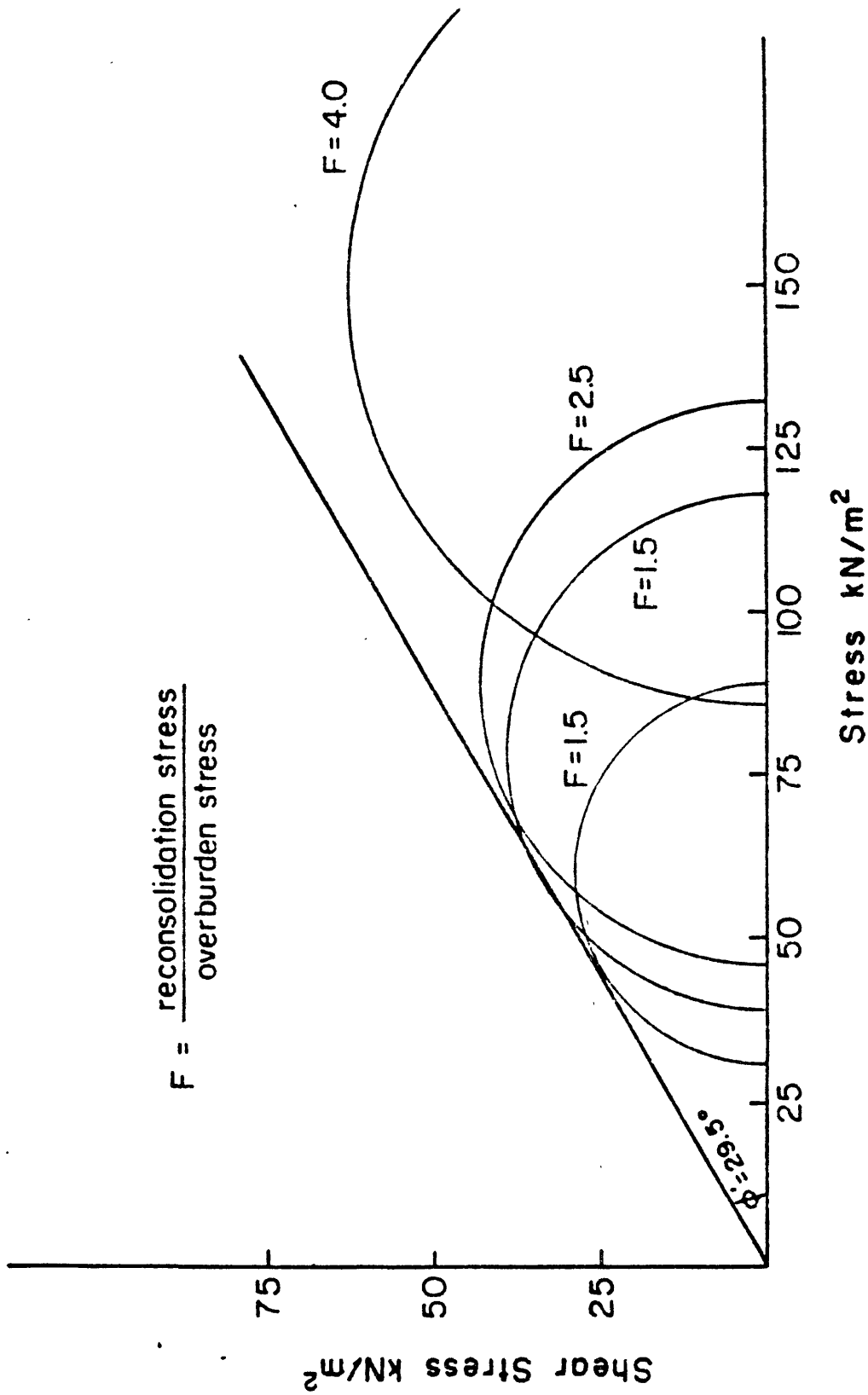


FIGURE 44 EFFECTIVE STRESS FAILURE ENVELOPE FROM AC-Ū TRIAXIAL TESTS PERFORMED BY DENBY (1978)

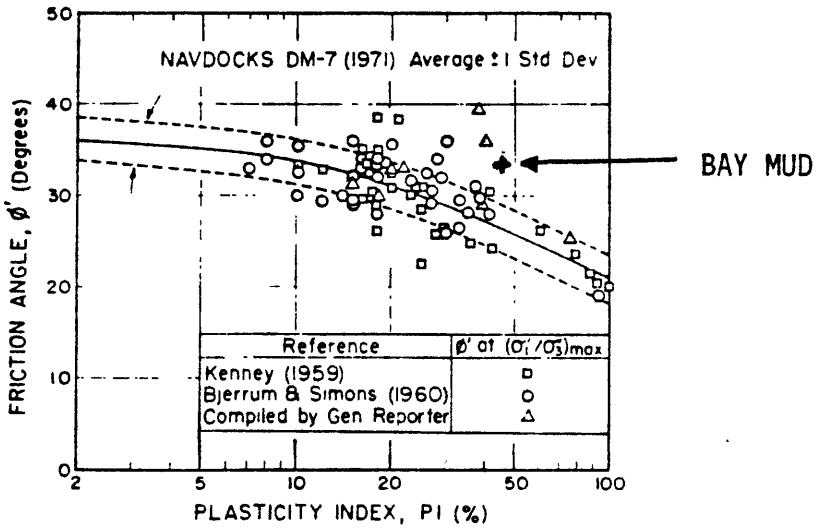


FIGURE 45 EMPIRICAL CORRELATION BETWEEN EFFECTIVE STRESS FRICTION ANGLE AND PLASTICITY INDEX FROM TRIAXIAL COMPRESSION TESTS ON NORMALLY CONSOLIDATED UNDISTURBED CLAYS

From Ladd (1977)

$\overline{\text{IC-U}}$ Triaxial Tests

Results of isotropically consolidated undrained triaxial tests on Bay Mud at the HAFB site are reported from the work of Duncan (1965) and several groups at U.C., Berkeley (CE 273 - 1977, CE 270L - 1978). Duncan (1965) ran three $\overline{\text{IC-U}}$ tests. Undisturbed samples were taken from HAFB, trimmed and placed in a triaxial cell and consolidated to effective stresses that were larger than those they were subjected to in the field. Consolidating the Bay Mud from its field condition to effective stresses larger than those existing in the field has the effect of bringing the soil from its in-situ state of being slightly overconsolidated (OCR = 1.1 to 1.5), past its maximum past pressure, p_c', and down the virgin compression curve. This procedure has the effect of removing much of the soil disturbance, which is an inevitable consequence of the sampling process. However, because the small amount of overconsolidation has been lost by the consolidation onto the virgin curve, values for the normalized strength parameter, $S_u/\overline{p}$, may be slightly smaller than those that exist in-situ.

The results of Duncan's tests are summarized in Table 11 and the stress-strain curves obtained from the tests are shown in Figure 46. These results have been corrected for the effects of piston friction, load carried by the filter paper drains and load carried by the rubber membranes. The corrections applied to the strength test data are given in Appendix 1 at the end of this report. Inspection of Figure 46 will show that the quantity $\sigma_1 - \sigma_3$ is not zero at zero strain, it has some small negative value. This fact is a ramification of the differences in the test corrections that are applied during the consolidation phase of the $\overline{\text{IC-U}}$ test. The correction applied to the axial stress is greater than that applied to

TABLE 11 SUMMARY OF RESULTS OF CONSOLIDATED UNDRAINED TRIAXIAL TESTS ON UNDISTURBED SAN FRANCISCO BAY MUD

Sample	Depth (feet)	Initial w/c (percent)	σ'_{ac} (kg/cm^2)	σ'_{rc} (kg/cm^2)	$\left(\frac{\sigma'_a}{\sigma'_r}\right)$	Consol. w/c (percent)	$\left(\frac{\Delta V}{V}\right)_c$	ε_{ac}	$\Delta(\sigma_a - \sigma_r)_f$ (kg/cm^2)	Δu_f (kg/cm^2)
IC-U-1	19	87.7	0.87	1.00	0.87	67.7	0.147	0.041	0.79	0.77
IC-U-2	19	87.5	2.33	2.48	0.94	55.3	0.248	0.097	1.77	1.86
IC-U-3	19	85.6	3.81	3.98	0.96	49.0	0.297	0.123	2.81	2.96

Sample	Depth (feet)	$\bar{A}_f$	$(\sigma_1 - \sigma_3)_f$ (kg/cm^2)	$\left(\frac{\sigma'_1}{\sigma'_3}\right)_f$	ε_{af} (%)	Time to Failure (hours)	σ'_{1f} (kg/cm^2)	σ'_{3f} (kg/cm^2)	$\frac{(\sigma_1 - \sigma_3)_f}{2}$ (kg/cm^2)	$\frac{(\sigma'_1 + \sigma'_3)_f}{2}$ (kg/cm^2)
IC-U-1	19	0.98	0.66	3.87	11.3	5	0.89	0.23	0.33	0.56
IC-U-2	19	1.05	1.62	3.58	11.0	5	0.89	0.23	0.33	1.44
IC-U-3	19	1.05	2.64	3.56	12.6	5	3.65	1.01	1.32	2.33

FROM DUNCAN (1965)

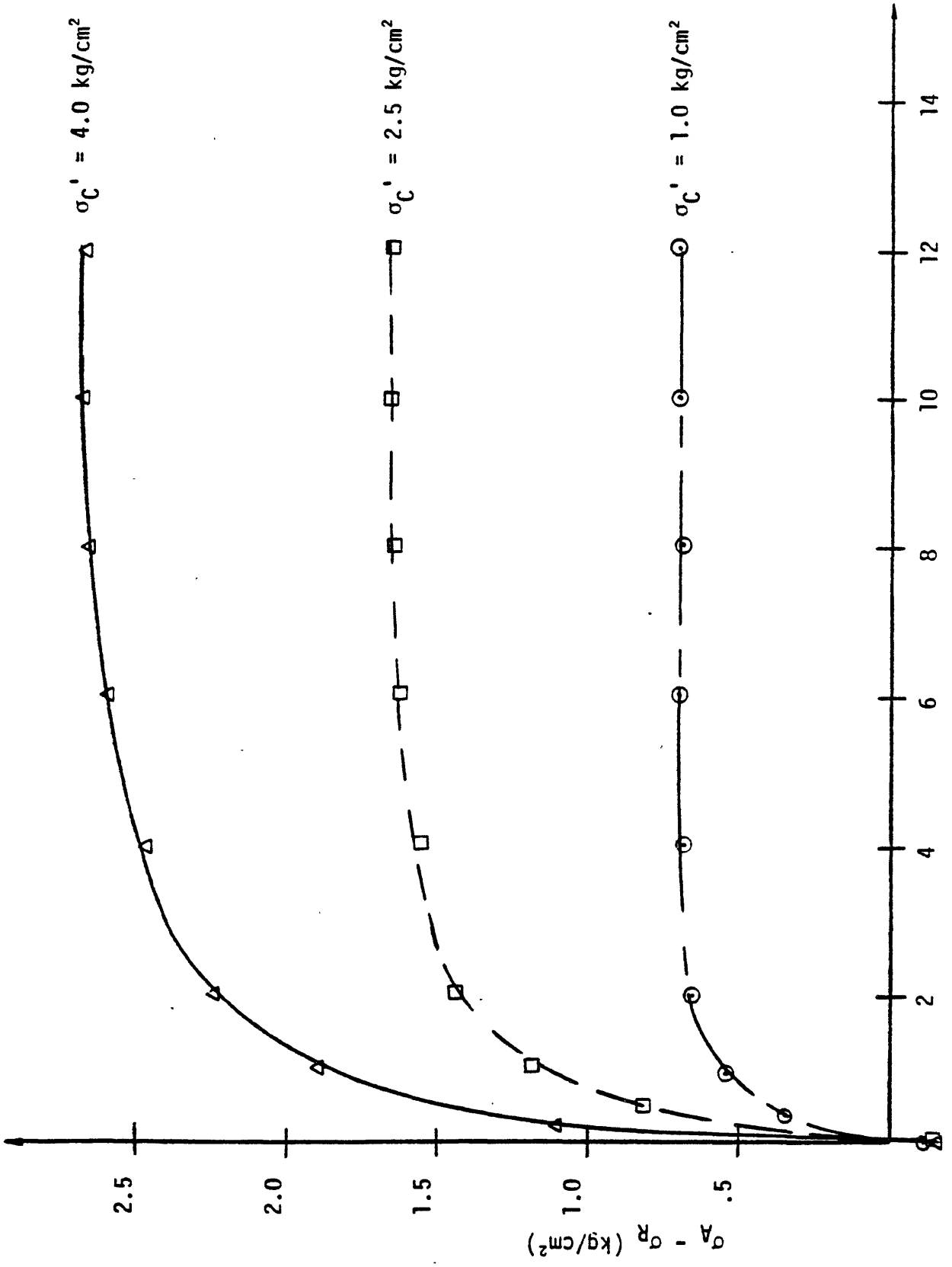
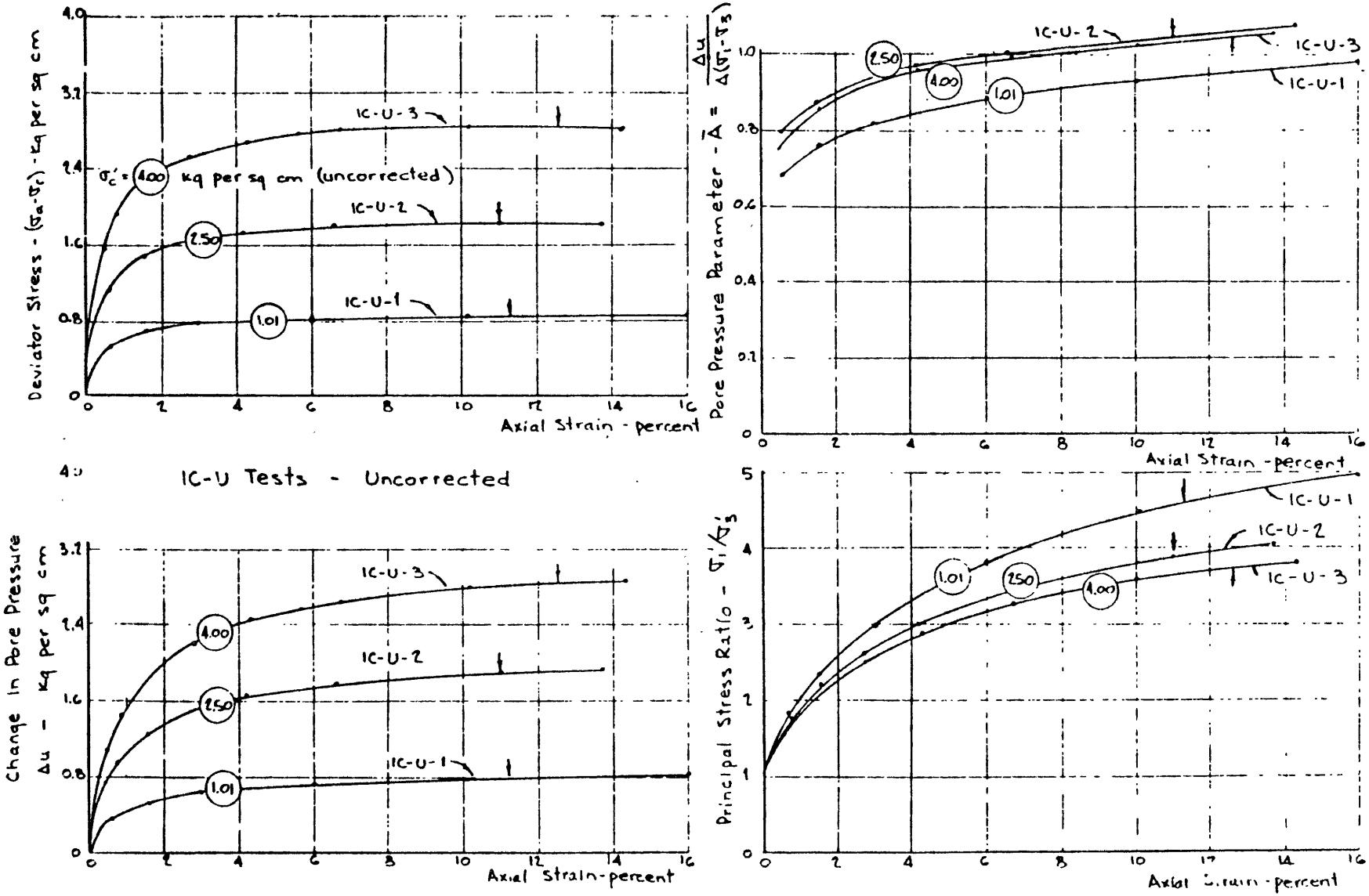


FIGURE 46 RESULTS OF $\overline{\text{IC-U}}$ TRIAXIAL TESTS ON UNDISTURBED BAY MUD TEST DATA FROM DUNCAN (1965)

the radial stress. This leads to a condition at the end of consolidation in which the soil is consolidated under a slightly anisotropic stress state, with the actual radial stress acting on the soil being a little larger than the actual axial stress acting on the soil. Examination of the correction factors given in Appendix 1 will make this point clear. Figure 47 shows uncorrected plots of deviator stress vs. strain, pore pressure vs. strain, pore pressure parameter $\bar{A}$ vs. strain and effective principal stress ratio vs. strain.

Figures 48 and 49 give the results of $\overline{IC-U}$ tests run at Berkeley during 1977 and 1978. Figure 48 gives the corrected stress-strain curve for an $\overline{IC-U}$ test run by the CE 270L graduate laboratory testing class. Figure 49 gives uncorrected plots of deviator stress, pore pressure, pore pressure parameter $\bar{A}$ and effective principal stress ratio versus strain. The results of this test are very similar to the results obtained by Duncan. Shown in Figure 50 is the effective stress-strain path that the Bay Mud followed during the test. Note that $\bar{A}_f$, the value of the pore pressure parameter $\bar{A}$ at failure is very close to one. The type of behavior exhibited by this stress path is typical of results obtained for soft normally consolidated clay.

Figures 51 and 52 show the results of 4 $\overline{IC-U}$ triaxial tests run at Berkeley in 1977 by the CE 273 graduate soil behavior class. Figure 51 shows the uncorrected plots of deviator stress versus strain while Figure 52 shows the uncorrected plots of pore pressure versus strain. Values for the total deviator stress and the major and minor principal stresses at failure, corrected for the loads carried by filter paper drains and rubber membranes, are presented below. Values of the corrections applied to the test data are given in the appendix at the end of this report.



VARIATIONS OF DEVIATOR STRESS, PORE-WATER PRESSURE, PORE PRESSURE COEFFICIENT $\bar{A}$, AND EFFECTNE PRINCIPAL STRESS RATIO WITH AXIAL STRAIN FOR $\overline{IC\text{-}U}$ TRIAXIAL TESTS ON UNDISTURBED SAN FRANCISCO BAY MUD.

FIGURE 47 $\overline{IC\text{-}U}$ TEST RESULTS

From Duncan (1965)

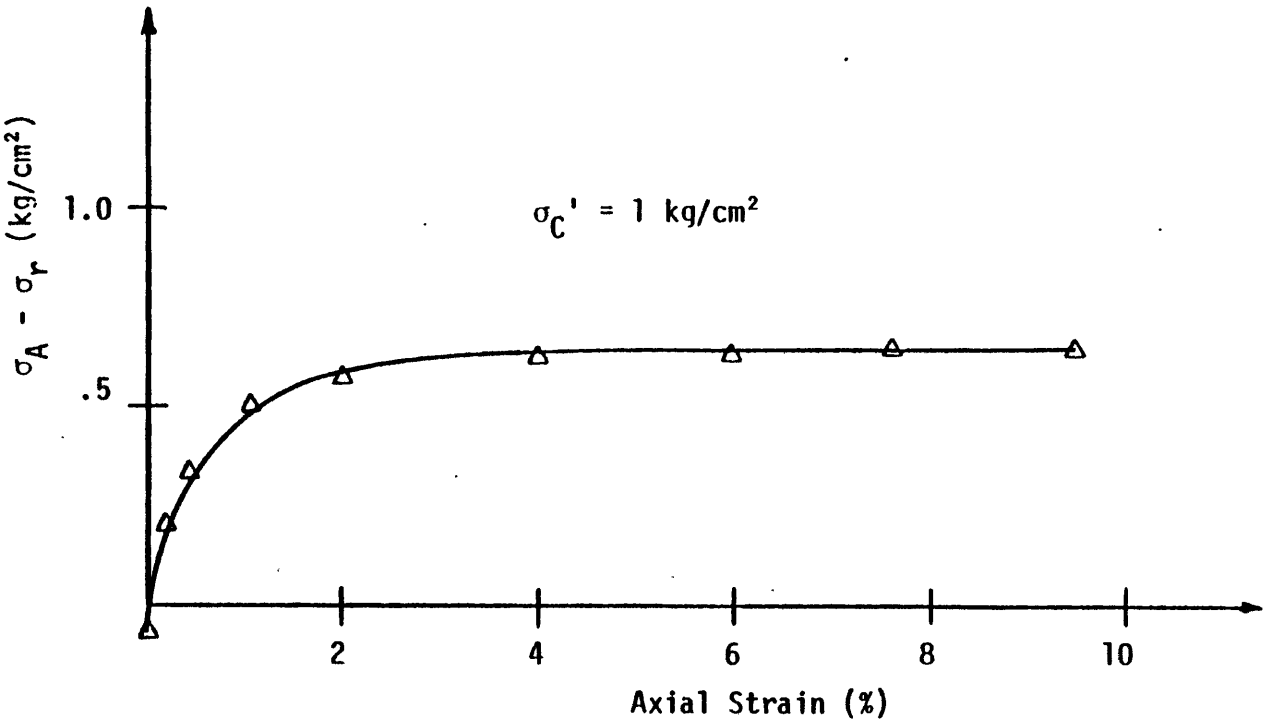
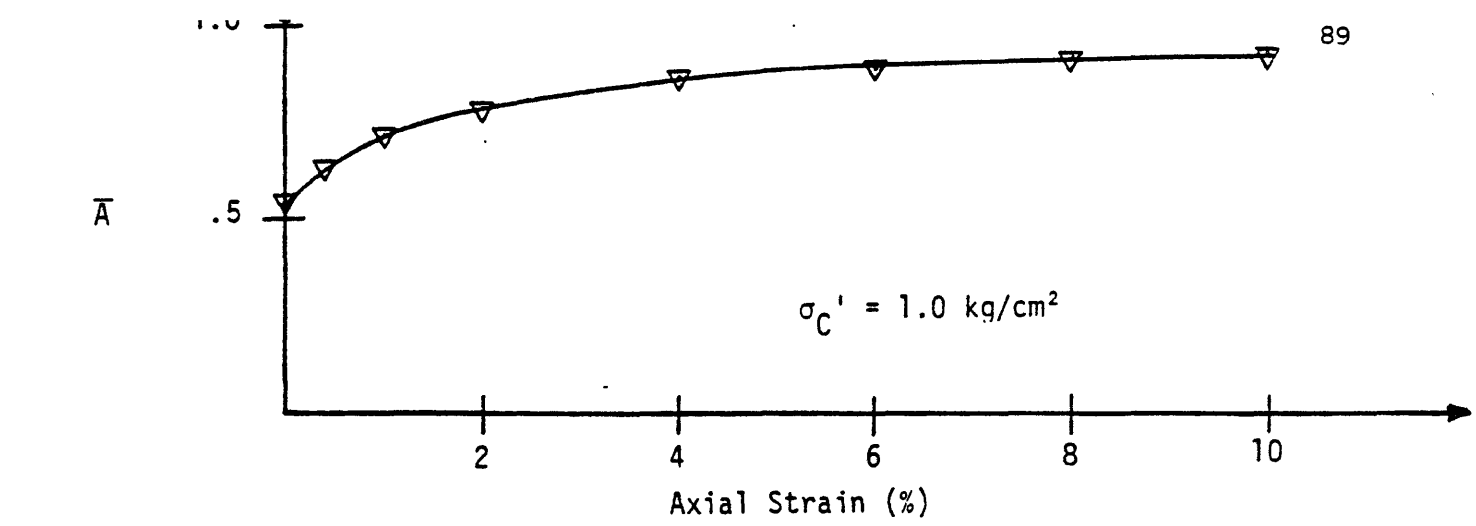
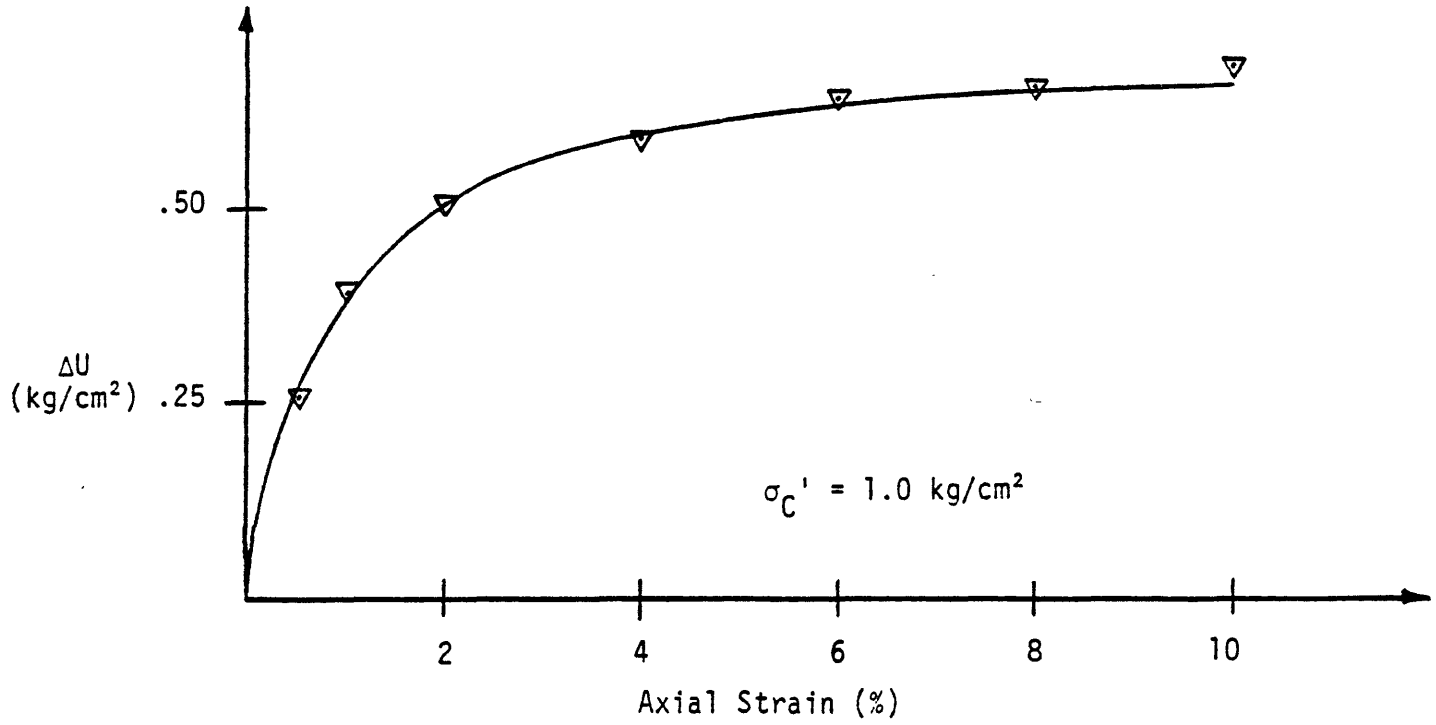


FIGURE 48 $\overline{IC-U}$ TRIAXIAL TEST ON UNDISTURBED BAY MUD
TEST PERFORMED AT UCB (CE-270L, 1978)





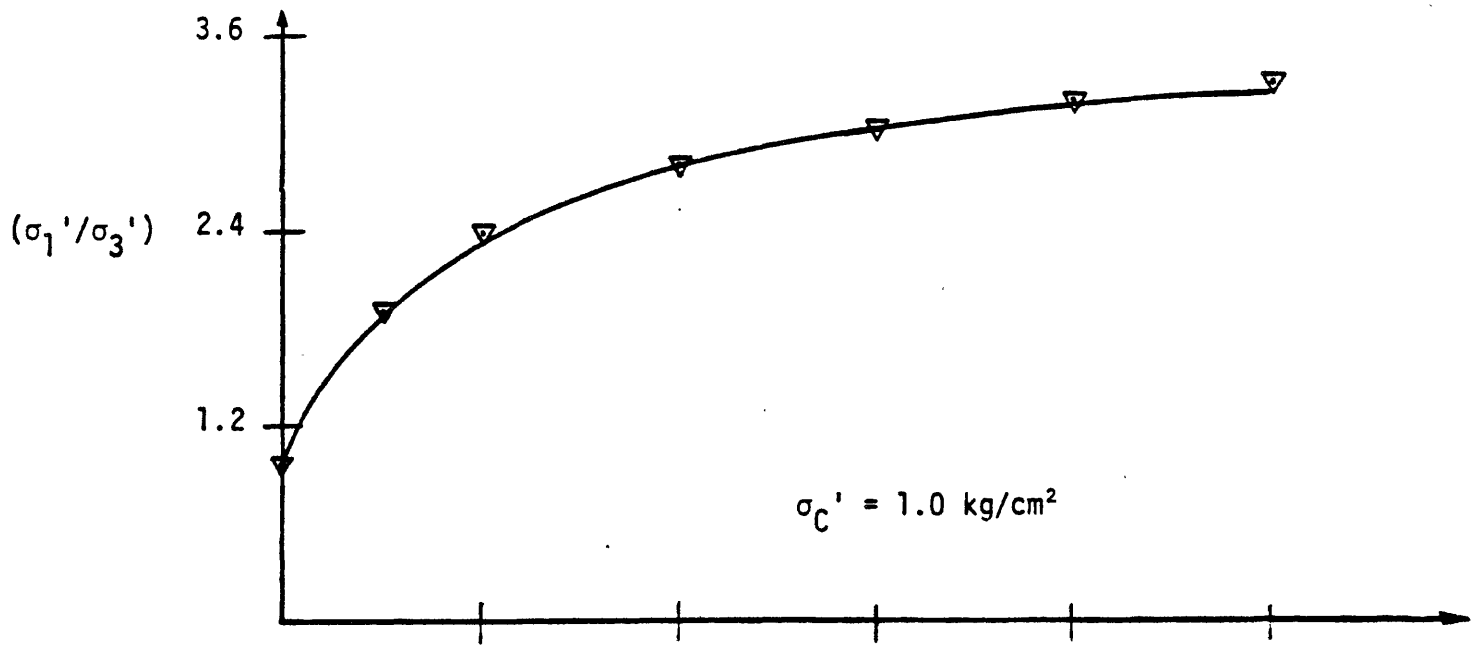


FIGURE 49 FURTHER RESULTS FROM THE $\overline{\text{IC-U}}$ TRIAXIAL TEST PRESENTED IN FIGURE 48

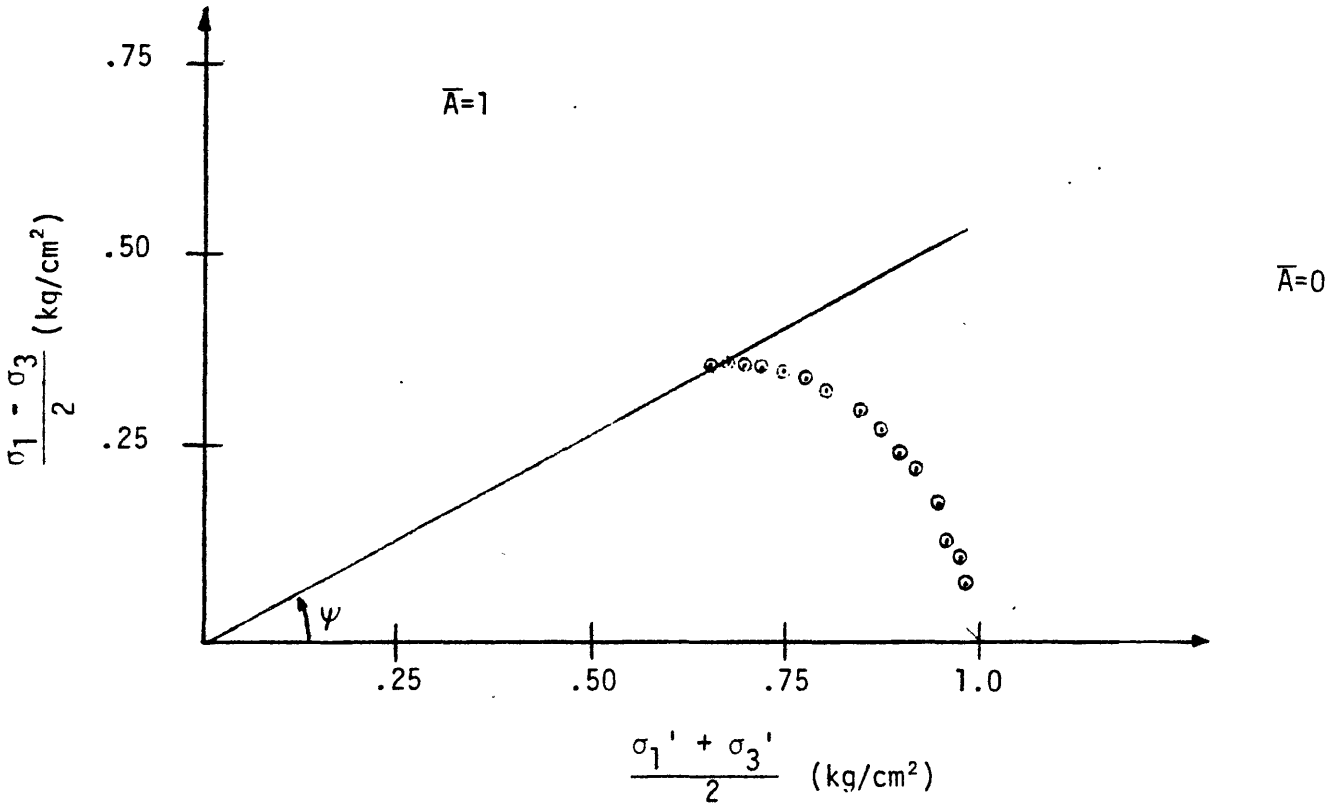


FIGURE 50 EFFECTIVE STRESS-PATH FOLLOWED BY BAY MUD DURING THE $\overline{\text{IC-U}}$ TRIAXIAL TEST SHOWN IN FIGURES 48 AND 49

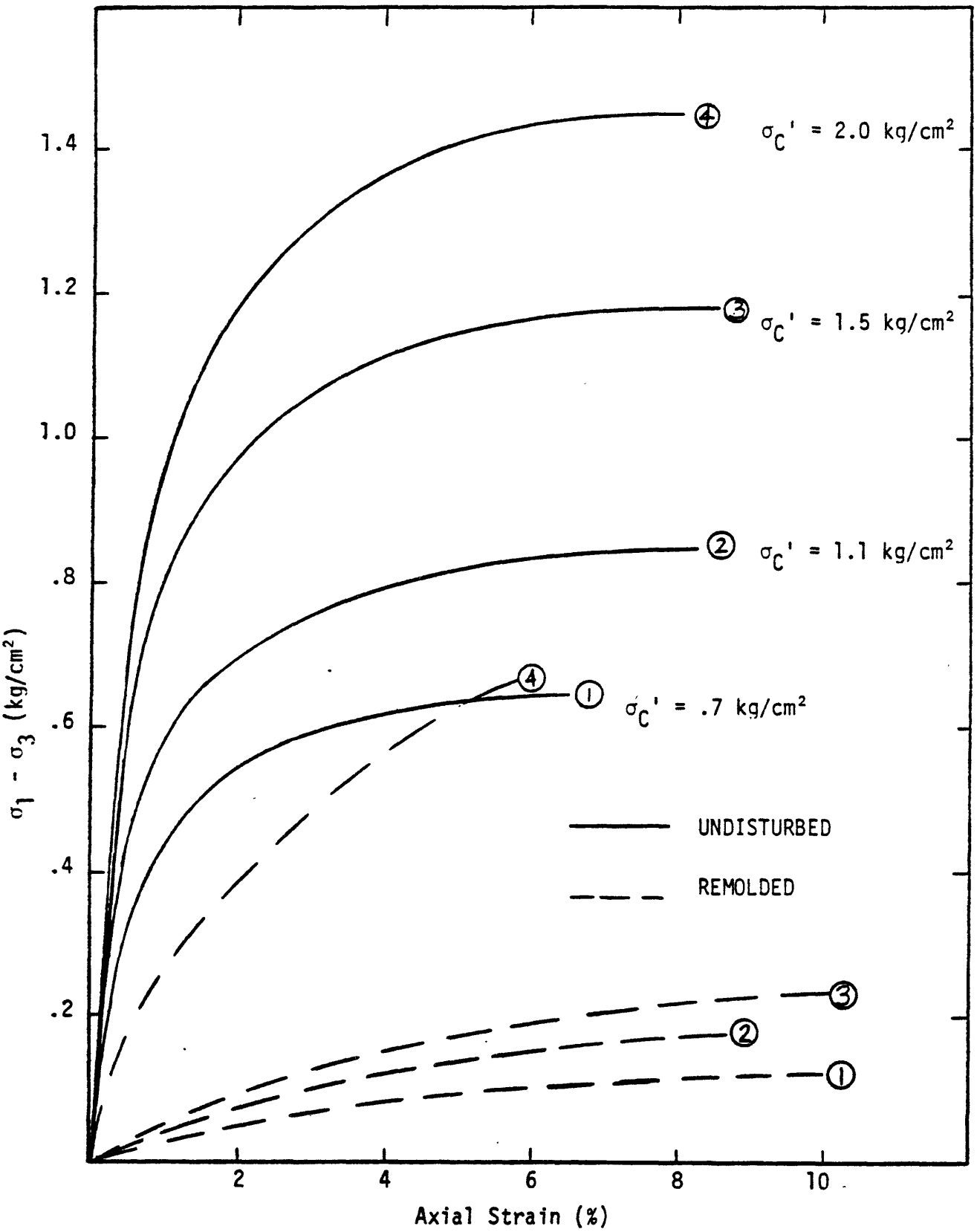


FIGURE 51 RESULTS OF $\overline{\text{IC-U}}$ TRIAXIAL TESTS ON UNDISTURBED AND REMOLDED BAY MUD. PERFORMED AT UCB (CE-273, 1977)

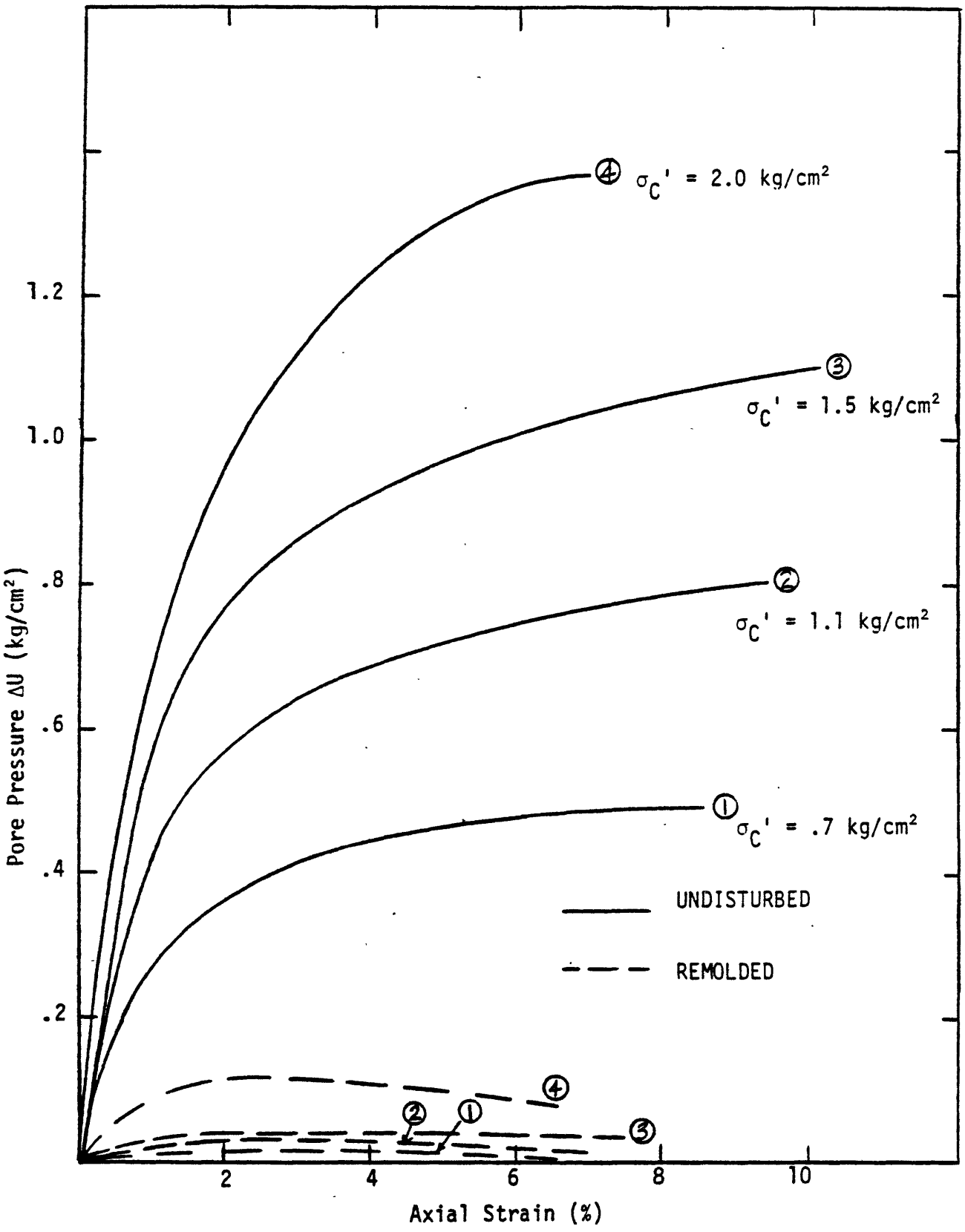


FIGURE 52 RESULTS OF $\overline{IC\text{-}U}$ TRIAXIAL TESTS ON UNDISTURBED AND REMOLDED BAY MUD. PERFORMED AT UCB (CE-273, 1977)

Corrected Results of $\overline{IC-U}$ Tests CE 273 (1977)			
Test	σ_c' (kg/cm^2)	$\left(\frac{\sigma_1 - \sigma_3}{2}\right)_f$ (kg/cm^2)	$\left(\frac{\sigma_1' + \sigma_3'}{2}\right)_f$ kg/cm^2
1	.68	.28	.49
2	1.08	.38	.67
3	1.47	.55	.95
4	1.97	.67	1.28

Shown in Figure 53 is a plot of undrained shear strength S_u ($S_u = 1/2\ (\sigma_1 - \sigma_3)_{MAX}$) versus effective consolidation pressure, σ_{1c}', for the three sets of $\overline{IC-U}$ tests already discussed. The data falls on a line with a slope of about .34, indicating that for Bay Mud in isotropic compression the $S_u/\overline{p}$ ratio is equal to .34. It is instructive to compare this value of $S_u/\overline{p}$ with correlations developed by others. Figure 54 shows a correlation developed by Skempton for the $S_u/\overline{p}$ ratio versus plasticity index and Figure 55 shows a correlation developed by Bjerrum and Simons (1960) for $S_u/\overline{p}$ as a function of liquidity index. As with the effective angle of internal friction the $S_u/\overline{p}$ value for Bay Mud plots above the established correlations, indicating that for a soil with its particular index properties, its strength, under both drained and undrained conditions is higher than would be expected for a "typical" clay with the same index properties.

In summary, the results of the $\overline{IC-U}$ triaxial tests on Bay Mud indicate that the soil has an $S_u/\overline{p}$ ratio of .34 and reaches its peak shear strength ($1/2(\sigma_1 - \sigma_3)_{max}$) at axial strains of between 8% and 12% (10% ~ average). At failure the pore pressure parameter, $\overline{A}$, is about 1 and the effective principal stress ratio (σ_1'/σ_3') is about 3.6.

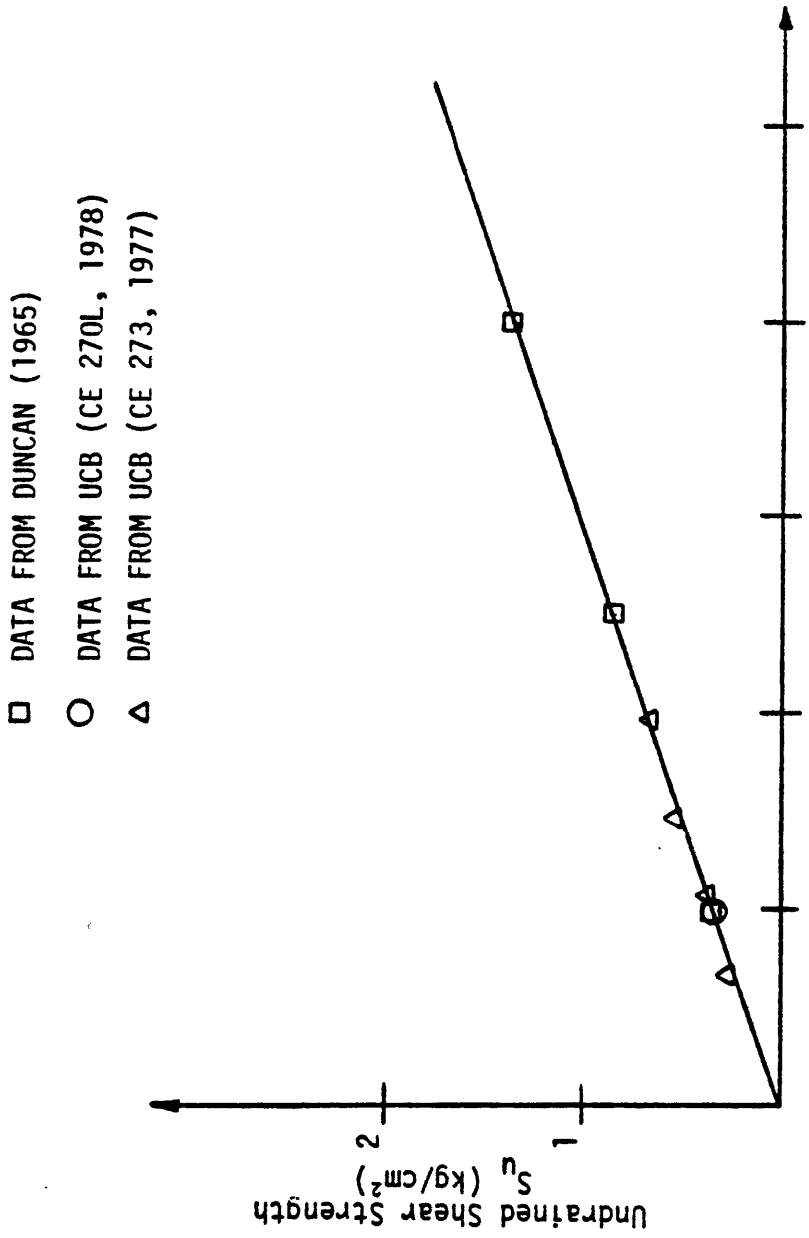


FIGURE 53 UNDRAINED SHEAR STRENGTH OF UNDISTURBED BAY MUD FROM $\overline{IC-U}$ TRIAXIAL TESTS

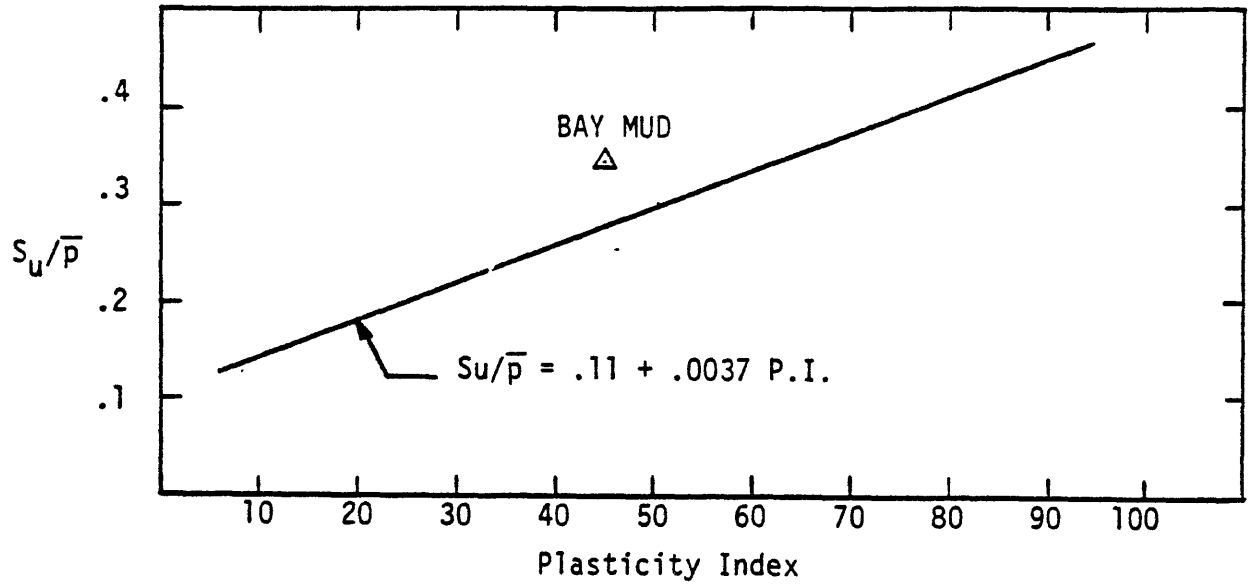


FIGURE 54 EMPIRICAL CORRELATION OF UNDRAINED STRENGTH RATIO VERSUS PLASTICITY INDEX. PLOT ORIGINALLY FROM SKEMPTON

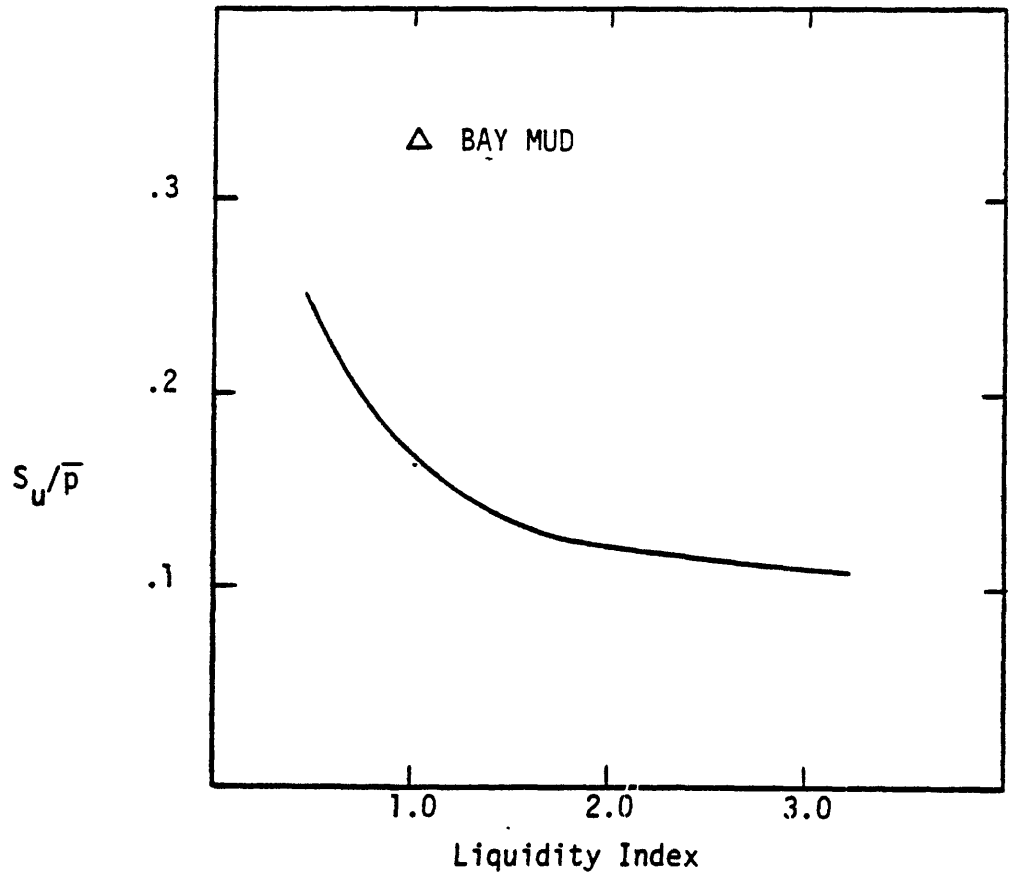


FIGURE 55 EMPIRICAL RELATIONSHIP BETWEEN THE UNDRAINED STRENGTH RATIO AND LIQUIDITY INDEX. FROM BJERRUM AND SIMONS (1960)

Normalized Behavior

Ladd and Foott (1974) showed that a variety of clay soil properties could be "normalized" with respect to the consolidation pressure to which the soil had been subjected. One aspect of normalized behavior is the classical $S_u/\bar{p}$ ratio which has been discussed already. Several other soil properties can be normalized with respect to consolidation pressure including a soil's stress-strain curve and pore pressure-strain curve. Figures 56 and 57 present such curves. Figure 56 shows the corrected normalized stress-strain curves for Bay Mud during the $\overline{\text{IC-U}}$ triaxial tests performed by Duncan. As can be seen, the curves don't normalize perfectly, which reflects inhomogeneities in the Bay Mud, sample disturbance, imperfect sample preparation, testing techniques, etc. Still, the maximum difference in normalized strength between the data is only about 7% and the stress strain curves are all similar. Figure 57 shows the results of the $\overline{\text{IC-U}}$ tests run at Berkeley (CE 273) normalized with respect to σ_c'. These tests too, show the normalizing ability of Bay Mud. Three of the four tests fall into a narrow band when normalized. The fourth test, run with a confining pressure of .7 kg/cm^2 shows a higher strength, which is probably a reflection of its overconsolidation ratio being greater than 1.

Behavior of Remolded Bay Mud in $\overline{\text{IC-U}}$ Tests

The results of $\overline{\text{IC-U}}$ triaxial tests on samples of Bay Mud from the HAFB site which were completely remolded and then reconsolidated under various isotropic confining pressures are shown in Figure 58. These test results were originally presented by Kavazanjian (1978). They are plotted in normalized form. Mitchell (1976) presented stress-strain and pore pressure-strain curves from triaxial tests on undisturbed and remolded Bay Mud.

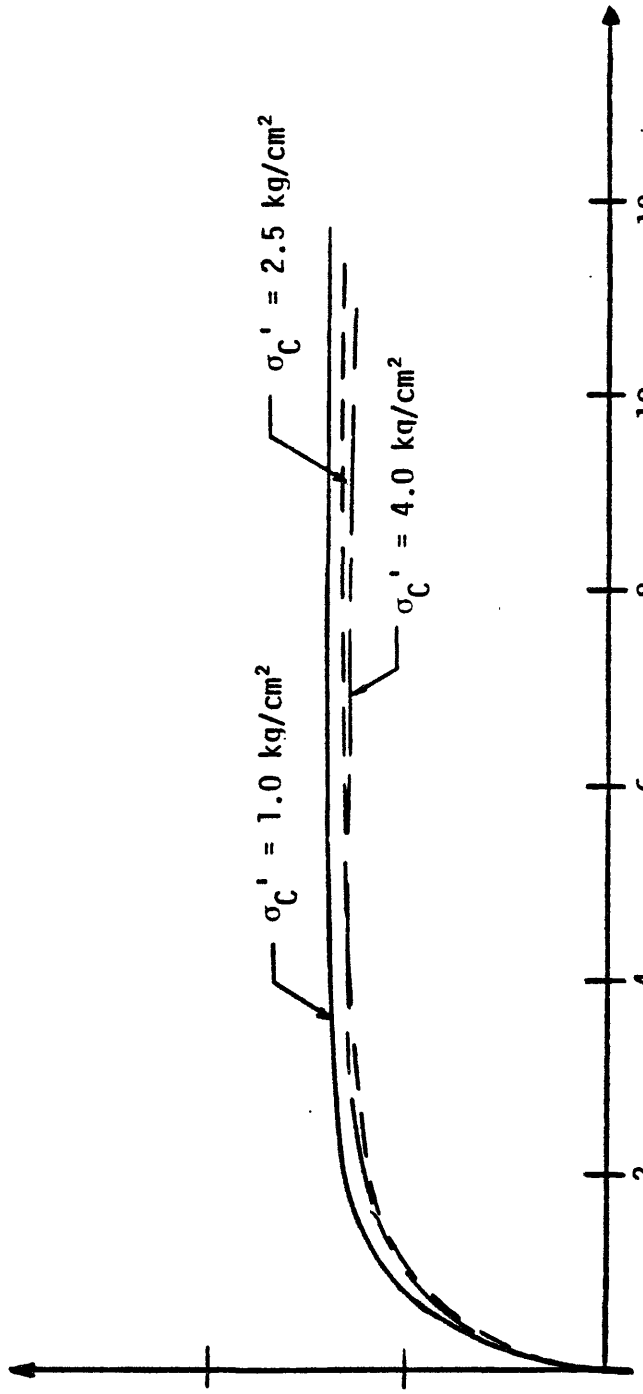


FIGURE 56 NORMALIZED STRESS-STRAIN CURVES OBTAINED FROM $\overline{IC-U}$ TRIAXIAL TESTS ON UNDISTURBED BAY MUD. TESTS PERFORMED BY DUNCAN (1965)

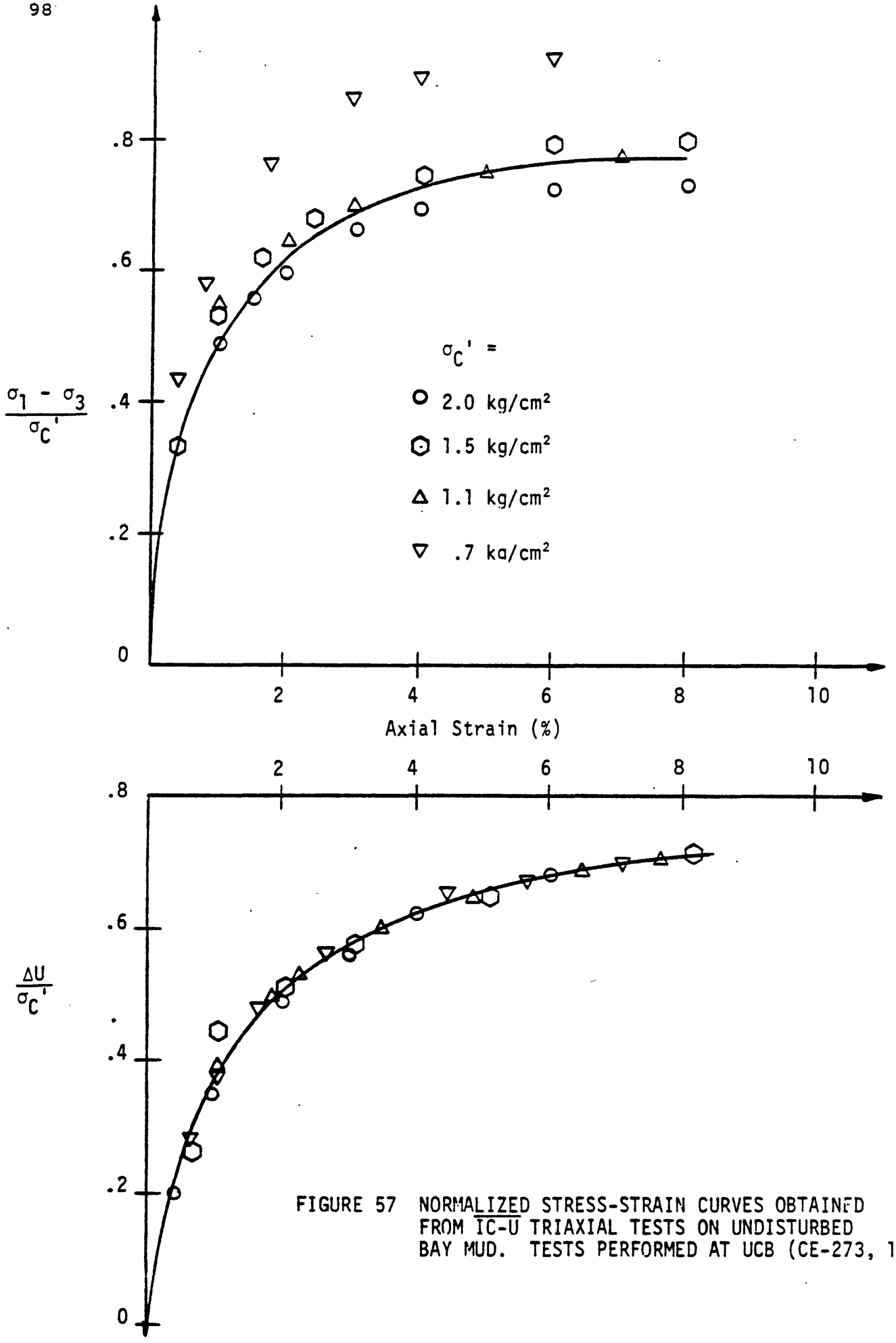


FIGURE 57 NORMALIZED STRESS-STRAIN CURVES OBTAINED FROM IC-U TRIAXIAL TESTS ON UNDISTURBED BAY MUD. TESTS PERFORMED AT UCB (CE-273, 1977)

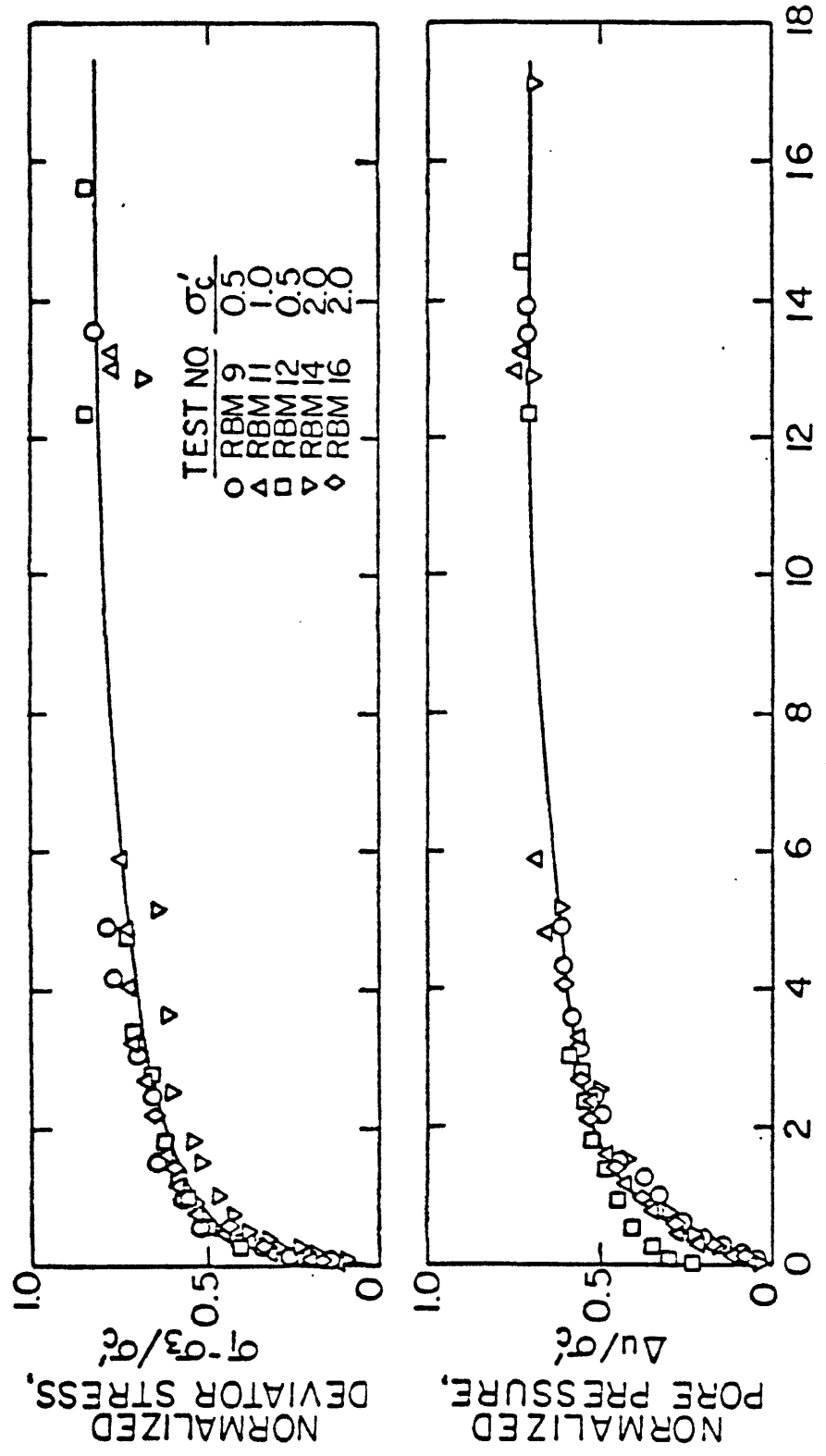


FIGURE 58 NORMALIZED DEVIATORIC BEHAVIOR OF REMOLDED SAN FRANCISCO BAY MUD

From Kavazanjian (1978)

These tests were run by first performing an $\overline{IC-U}$ triaxial test on an undisturbed sample. After undrained loading to failure the sample was remolded in the triaxial cell. Pore pressures were measured and the sample was then sheared. The results of these tests are shown in Figure 59a and the stress paths for one of the tests is shown in Figure 59b. The data presented in Figures 59a and 59 b have not been corrected for the load carried by filter paper drains and rubber membranes. The corrections to be applied to these test data to obtain their true behavior in the triaxial tests are found in Appendix 1.

Strain Rate Effects

The decrease in undrained strength with increasing time to failure is a time dependent phenomenon that would normally be grouped with soil creep, stress relaxation and other such properties discussed later in this report. However, since most strain rate data has been accumulated from $\overline{IC-U}$ tests, this topic is presented here so that comparisons can be made with the "conventional" $\overline{IC-U}$ test results.

Lacerda (1976) ran a series of $\overline{IC-U}$ tests on Bay Mud at strain rates that were both higher and lower than those usually recommended for undrained tests. Tests that are run too quickly don't allow time for pore pressure equalization, while undrained creep becomes a factor for tests with very low strain rates. Lacerda ran tests at rates between .04%/hour (7.3×10^{-4}%/minute) and 210%/hr (3.5%/minute). For comparison with the $\overline{IC-U}$ test which were performed at conventional strain rates (~ .5%/hr), the stress strain curves for Bay Mud sheared at a variety of strain rates are given in Figure 60. It can be seen that an increase in strain rate by a factor of 8 leads to an increase in shear strength of approximately 8%. The soil

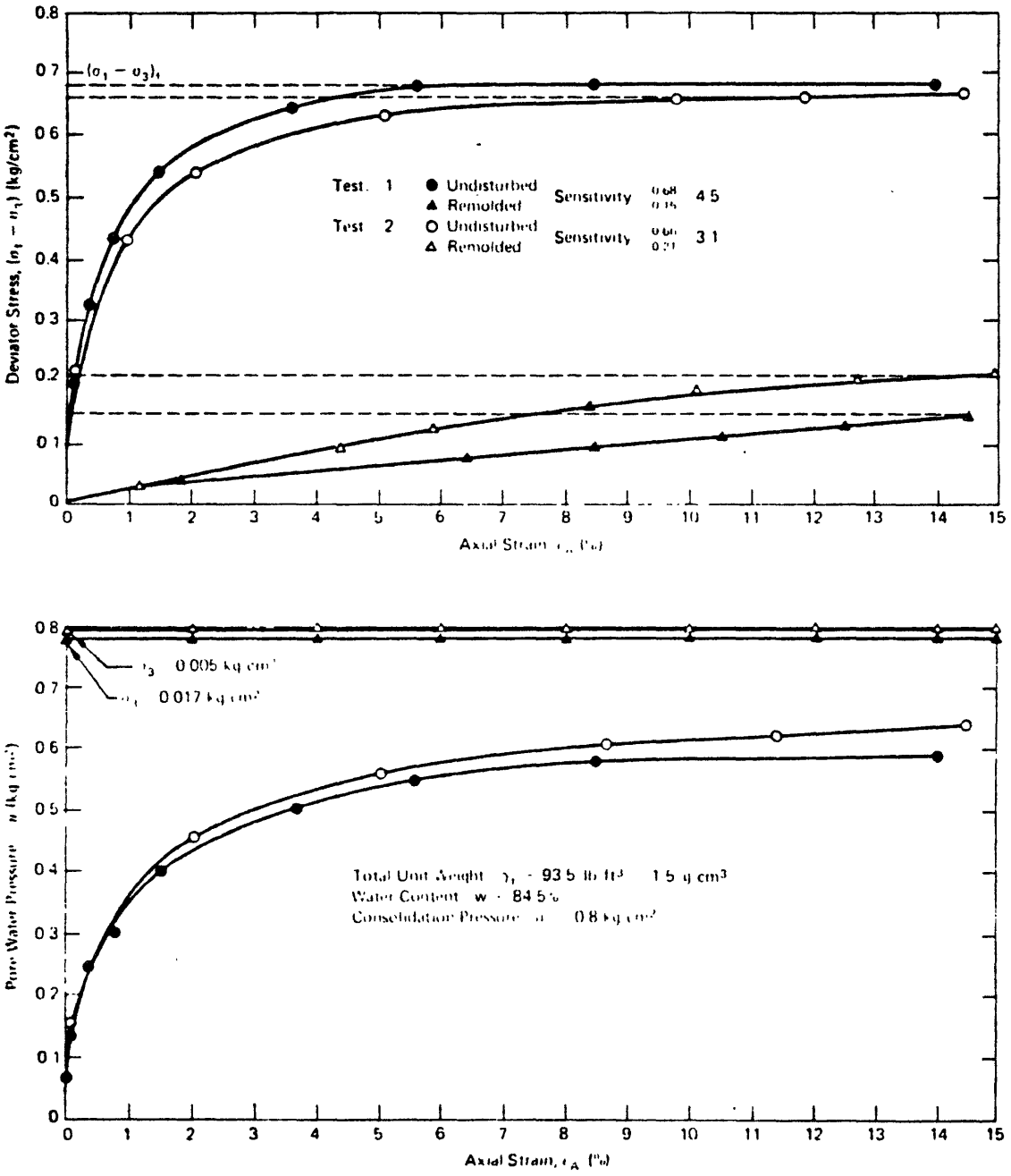


FIGURE 59a EFFECT OF REMOLDING ON UNDRAINED STRENGTH AND PORE WATER PRESSURES IN SAN FRANCISCO BAY MUD

From Mitchell (1976)

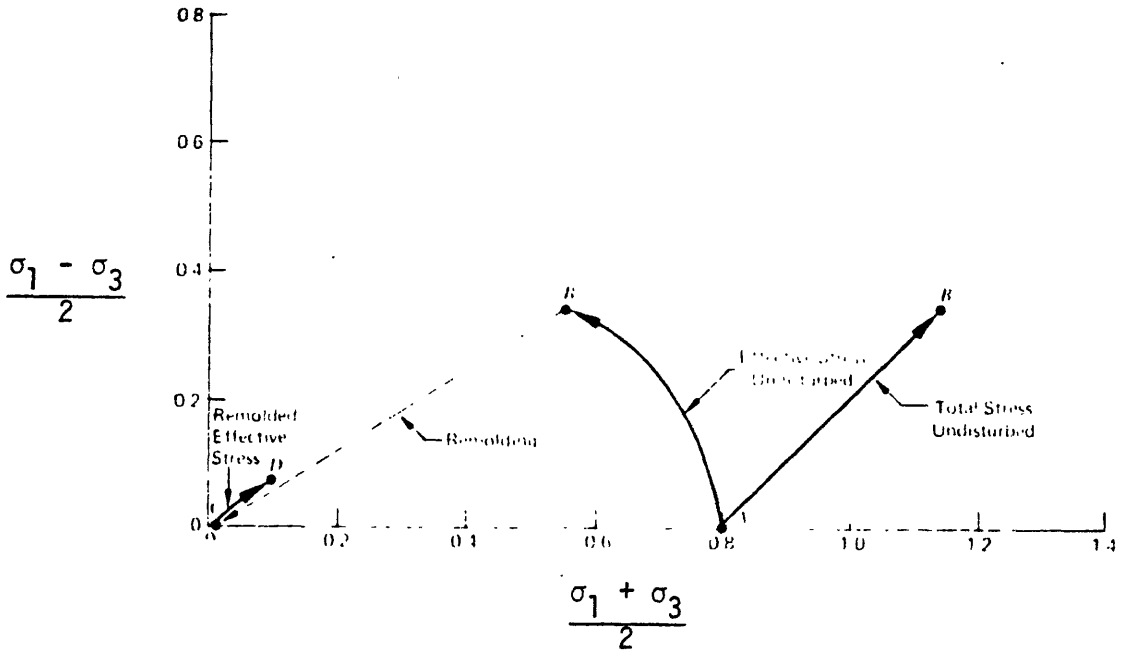


FIGURE 59b STRESS PATHS FOR TRIAXIAL COMPRESSION TESTS ON UNDISTURBED AND REMOLDED SAMPLES OF SAN FRANCISCO BAY MUD

From Mitchell (1976)

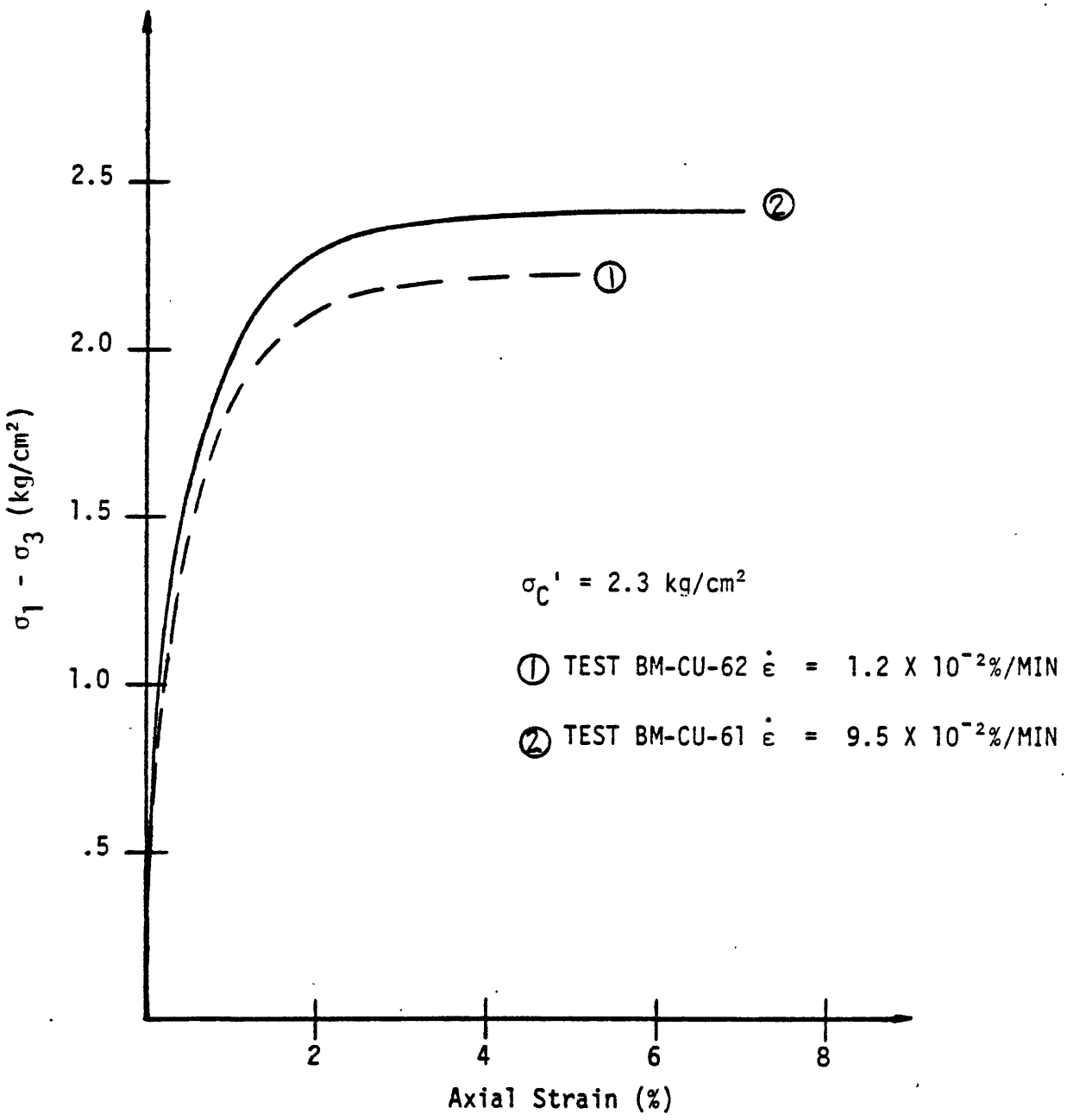


FIGURE 60 EFFECT OF STRAIN RATE DURING $\overline{IC-U}$ TRIAXIAL TEST ON THE STRESS-STRAIN BEHAVIOR OF UNDISTURBED BAY MUD. TESTS PERFORMED BY LACERDA (1976)

stiffness also increases with increasing strain rate. These results compare favorably with work done by Bjerrum (1973) which indicated that for an order of magnitude increase in strain rate there is about a 10-15% increase in undrained strength.

Table 12 summarizes the results of the $\overline{\text{IC-U}}$ and UU triaxial tests run by Lacerda. The results of these tests are plotted in Figures 61 through 63. Figure 61 shows the deviator stress at failure versus the logarithm of strain rate during shear for UU samples and $\overline{\text{IC-U}}$ samples consolidated to .8 kg/cm^2. Figure 62 shows the same thing for samples consolidated to 3.2 kg/cm^2. The fact that the data points plot on a straight line indicates that the shear strength is proportional to the logarithm of time to failure, which agrees well with work by others (Ladd, 1971). It can be seen that Lacerda's results agree with those obtained in the "conventional" $\overline{\text{IC-U}}$ tests by noting that at a strain rate of .5%/hour Figures 61 and 62 indicate that the shear strength at these rates corresponds to an $S_u/\overline{p}$ ratio equal to .34. Figure 63 illustrates the effect of strain rate on the results obtained from UU triaxial tests.

An interesting point worth noting is that although the stress-strain curve obtained from a test is a function of the strain rate used during the test, it appears as if the pore pressure-strain curve is not. This can be seen by comparing the stress-strain curves shown in Figure 60 with the pore pressure strain curves for the same tests, which are given in Figure 64. While the stress-strain curves are markedly different, the pore pressure-strain curves overlap. Lacerda states, "This behavior was found in all tests with Bay Mud; that is, the stress-strain curves are strain rate dependent while the pore pressure buildup is not." These results agree with results presented by Lo (1969) for Brobekkvein Clay that show that the pore

TABLE 12 CU AND UU TESTS ON SAN FRANCISCO BAY MUD-STRENGTH DATA

Test	σ_c kg/cm^2	$\dot{\varepsilon}$ %/min	E_i kg/cm^2	D_f kg/cm^2
SR-1-8	0.8	7.3×10^{-4}	192	.485
SR-1-8		1.9×10^{-1}	-	.640
SR-1-8		3.5 -	-	.712
SR-1-8		9.2×10^{-1}	-	.685
SR-1-8		7.4×10^{-3}	-	.551
		1.25×10^{-1}	-	.660
UBM-2	UU	1.35	50	0.376
UBM-4	UU	7.3×10^{-3}	26	0.300
SR-I-9	3.2	1.37×10^{-1}	-	2.26
SR-I-9		1.66×10^{-2}	-	2.10
SR-I-9		3.2	-	2.6
BM-CU-61	3.2	9.5×10^{-2}	909	2.42
BM-CU-61	3.2	3.3×10^{-3}	-	2.12
BM-CU-62	3.2	1.2×10^{-2}	-	2.25
FP-4	0.8	6×10^{-2}	245.	.630
SR-1-5	0.8	1.1	245.	.750
SR-1-6	0.8	1.62×10^{-2}	208	.620

FROM LACERDA (1977)

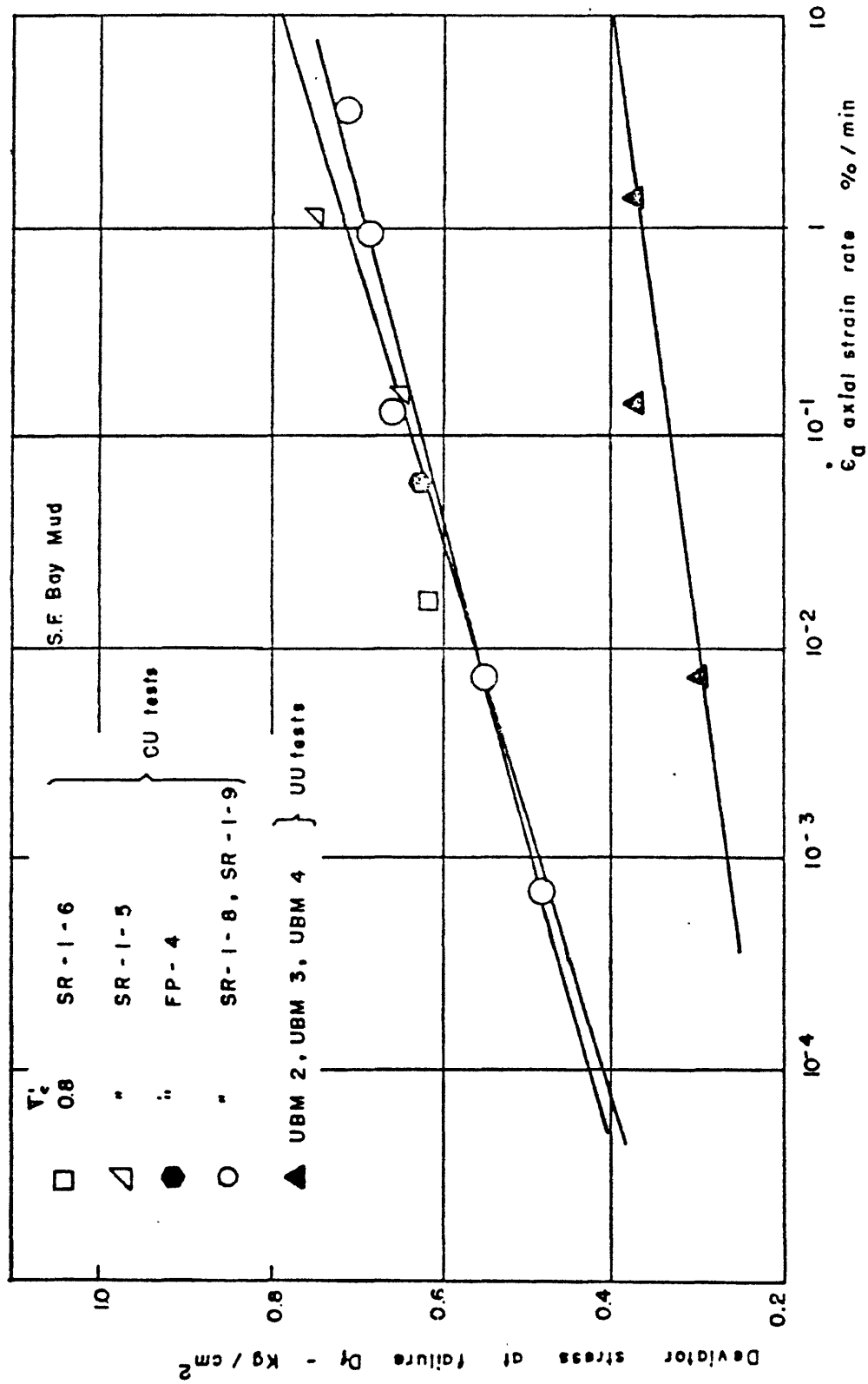


FIGURE 61 EFFECT OF STRAIN RATE ON THE MAXIMUM DEVIATOR STRESS MEASURED IN $\overline{IC-U}$ AND UU TRIAXIAL TESTS. TESTS PERFORMED BY LACERDA (1976)

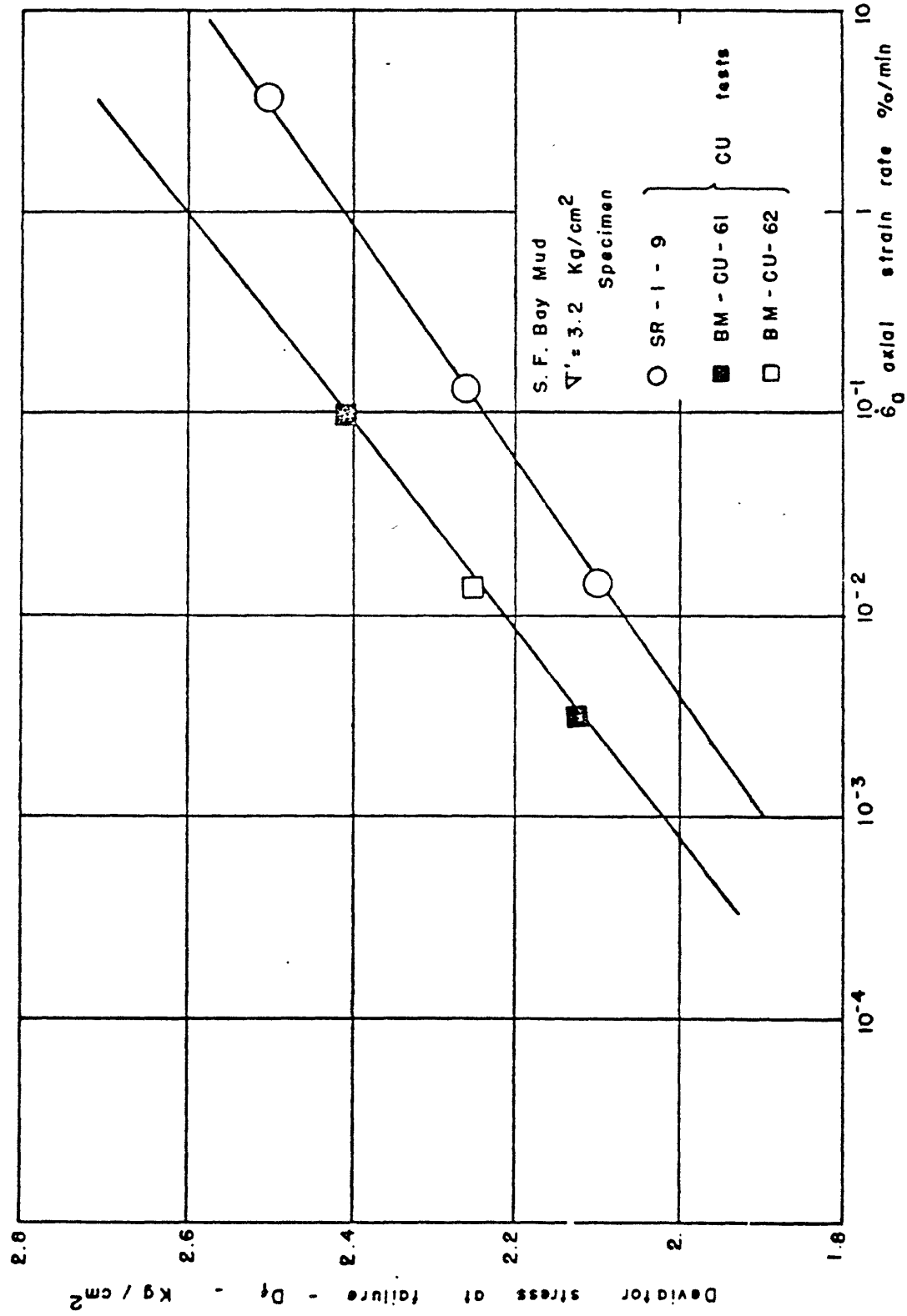


FIGURE 62 EFFECT OF STRAIN RATE ON THE MAXIMUM DEVIATOR STRESS MEASURED IN $\overline{IC-U}$ TRIAXIAL TESTS. TESTS PERFORMED BY LACERDA (1976)

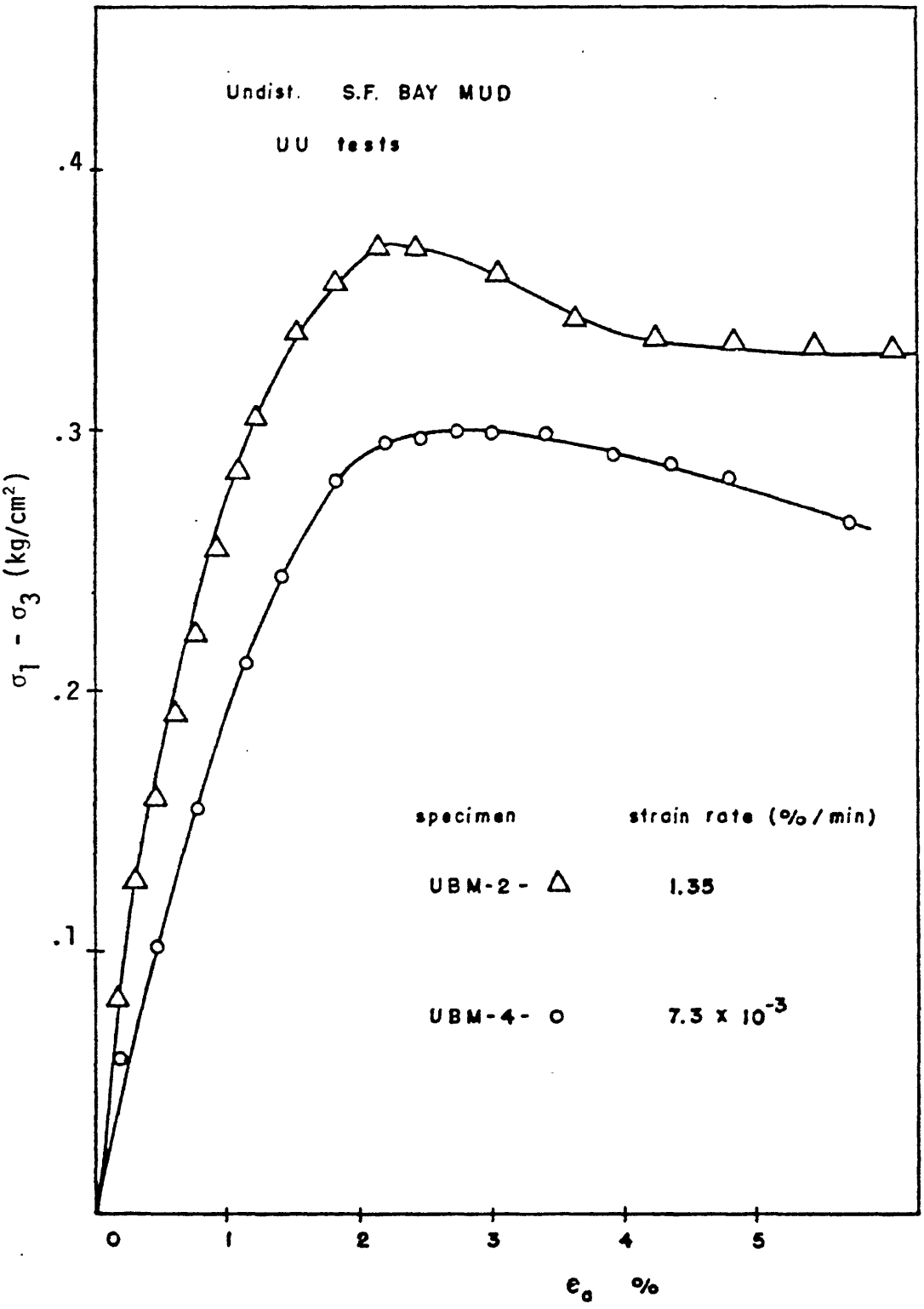


FIGURE 63 EFFECT OF STRAIN RATE DURING UU TRIAXIAL TESTS ON THE STRESS-STRAIN CURVE OBTAINED FOR UNDISTURBED BAY MUD. TESTS PERFORMED BY LACERDA (1976)

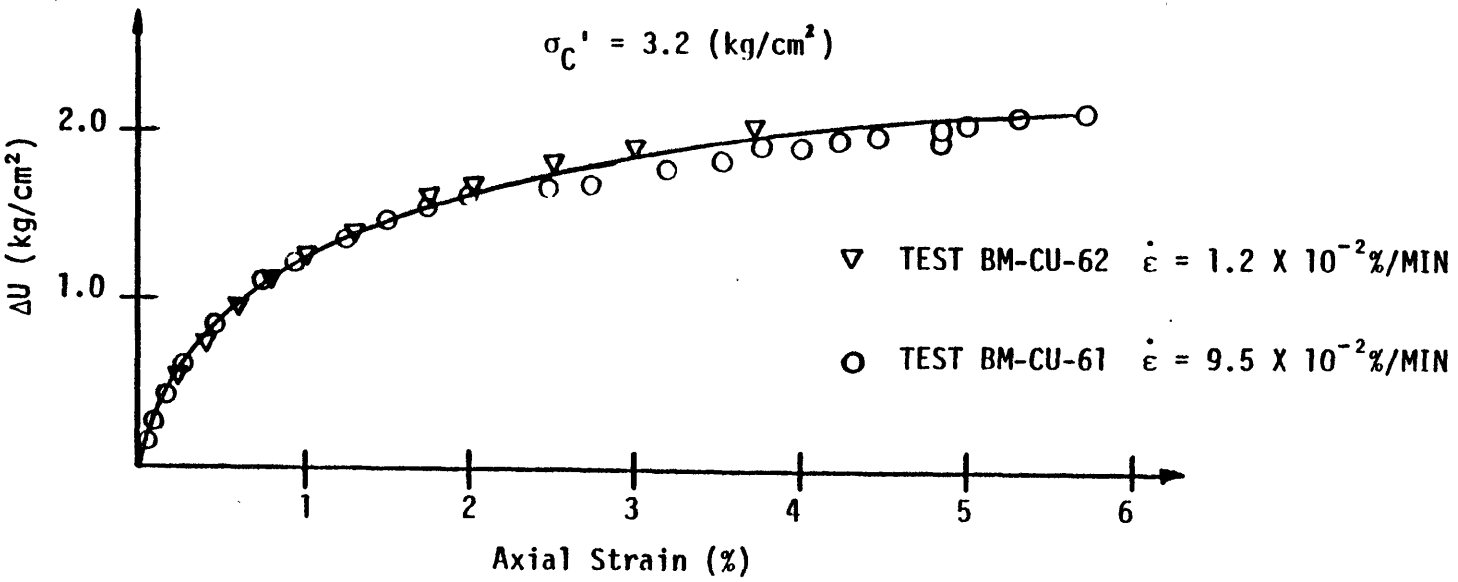


FIGURE 64 EFFECT OF STRAIN RATE ON THE PORE PRESSURE BUILDUP DURING $\overline{IC-U}$ TRIAXIAL TESTS ON UNDISTURBED BAY MUD. TEST PERFORMED BY LACERDA (1976) NOTE: SEE FIGURE 60 TO COMPARE THESE CURVES WITH THE STRESS-STRAIN CURVES OBTAINED FROM THE SAME TESTS

pressures developed during shear are primarily a function of the amount of strain that has taken place and are not a function of the rate at which shearing took place.

$\overline{\text{AC-U}}$ Triaxial Tests

Results of $\overline{\text{AC-U}}$ triaxial tests on Bay Mud are reported here, from the work of Seed et al. (1964), Duncan (1965) and Denby (1978). Tests using anisotropic consolidation are designed to better simulate the in-situ soil stresses. The most usual condition simulated is the case where the horizontal consolidation pressure is K_o times the vertical consolidation pressure. Ladd (1971) presented several case studies which showed that anisotropic consolidation can significantly affect the engineering properties of a soil, particularly soft sensitive clays. Generally, when comparing K_o consolidation to isotropic consolidation, results show (Ladd, 1971) that the undrained strength ratio can change by ±10-15%, increasing with sensitive clays and decreasing with insensitive ones. Strains at failure decrease markedly with anisotropic consolidation. Values of ϕ' measured at maximum deviator stress are typically one to three degrees lower, although ϕ' measured at maximum obliquity does not change significantly due to K_o consolidation.

A summary of the results of the $\overline{\text{AC-U}}$ tests run by Duncan is given in Table 13. These results have been corrected for the load carried by filter paper drains, rubber membranes and piston friction, as have the stress-strain curves given in Figure 65. Sample AC-U-1 represents a soil element consolidated without lateral strain (K_o condition) and with the major principal stress vertical. The soil was sheared by increasing the axial compressive stress until failure. Sample AC-U-2 represents a soil element in which the

TABLE 13 SUMMARY OF RESULTS OF CONSOLIDATED UNDRAINED TRIAXIAL TESTS ON UNDISTURBED SAN FRANCISCO BAY MUD

Sample	Depth (feet)	Initial w/c (percent)	σ'_{ac} (kg/cm^2)	σ'_{rc} (kg/cm^2)	$\left(\frac{\sigma_a'}{\sigma_r'}\right)$	Consol. w/c (percent)	$\left(\frac{\Delta V}{V}\right)_c$	ε_{ac}	$\Delta(\sigma_a - \sigma_r)_f$ (kg/cm^2)	Δu_f (kg/cm^2)
AC-U-1	15.5	92.2	2.91	1.58	1.84	55.0	0.262	0.236	0.71	0.79
AC-U-2	15.5	-	2.07	3.18	0.65	55.4	0.262	0.012	2.97	2.44

Sample	Depth (feet)	$\bar{A}_f$	$(\sigma_1 - \sigma_3)_f$ (kg/cm^2)	$\left(\frac{\sigma_1'}{\sigma_3'}\right)_f$	ε_{af} (%)	Time to Failure (hours)	σ'_{1f} (kg/cm^2)	σ'_{3f} (kg/cm^2)	$\frac{(\sigma_1 - \sigma_3)_f}{2}$ (kg/cm^2)	$\frac{(\sigma_1' + \sigma_3')_f}{2}$ (kg/cm^2)
AC-U-1	15.5	1.11	2.04	3.58	6.2	4.2	2.83	0.79	1.02	1.81
AC-U-2	15.5	0.82	1.86	3.62	12.9	3.5	2.57	0.71	0.93	1.64

FROM DUNCAN (1965)

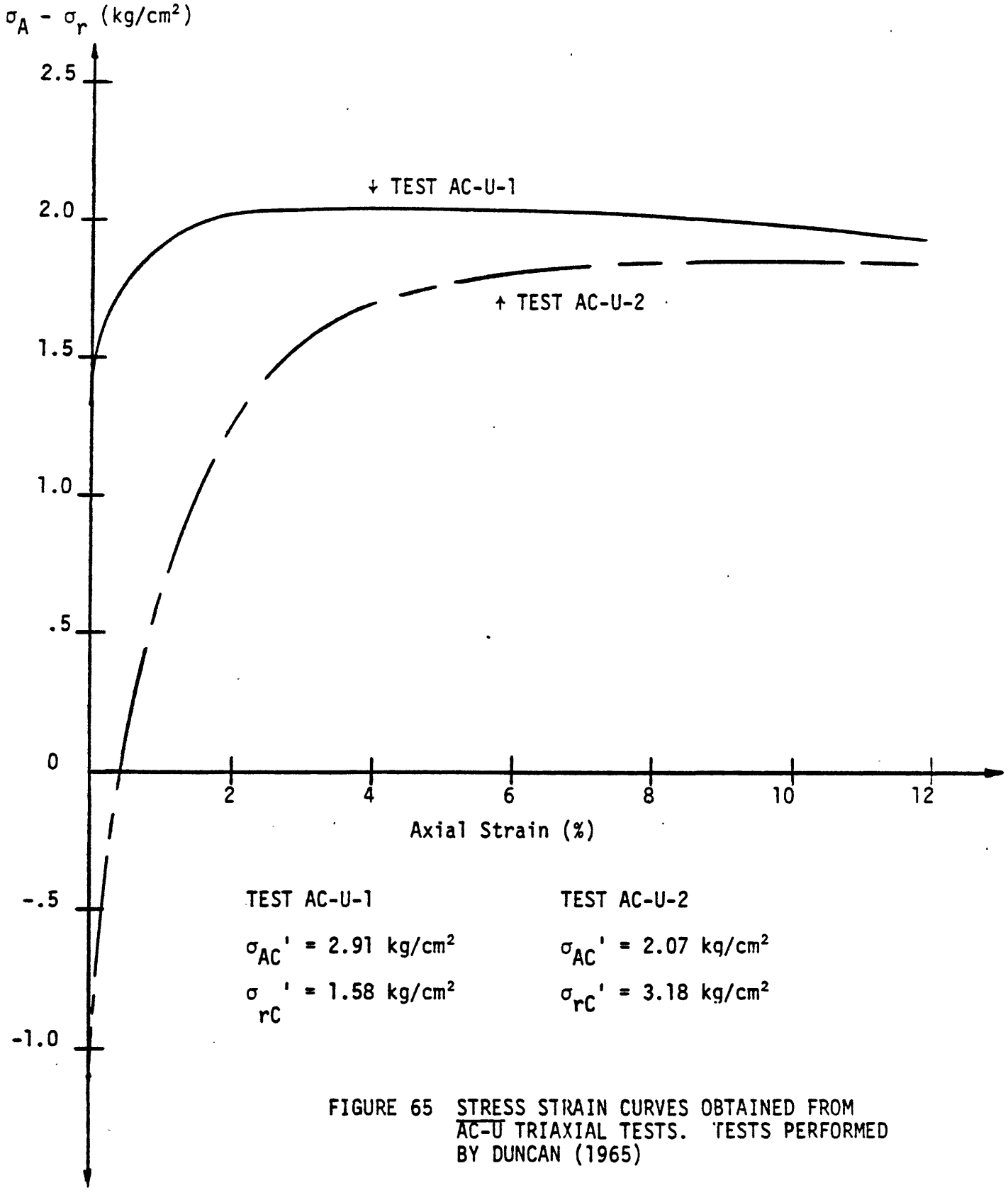


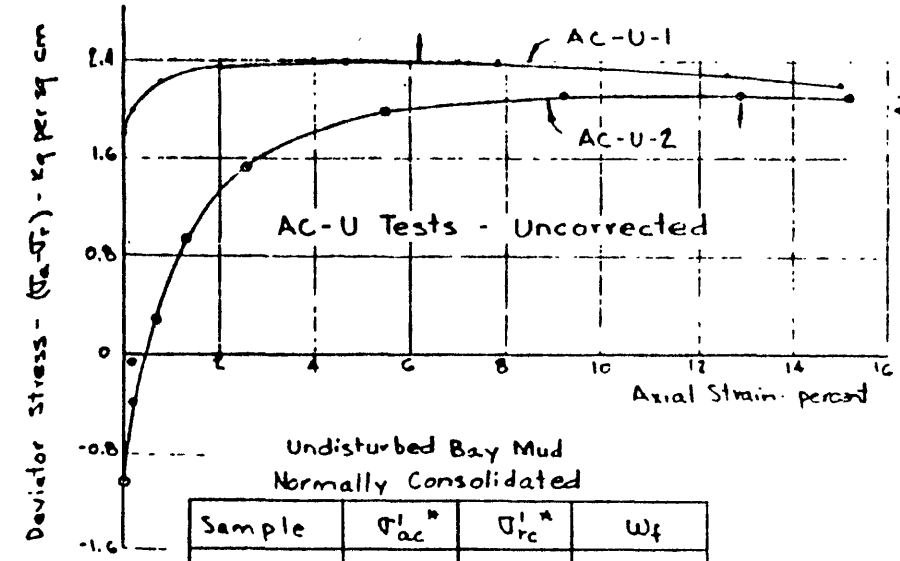
FIGURE 65 STRESS STRAIN CURVES OBTAINED FROM AC-U TRIAXIAL TESTS. TESTS PERFORMED BY DUNCAN (1965)

major principal stress acts in the lateral direction during consolidation and in the vertical direction as it is sheared to failure. Obviously, a rotation of 90° occurs in the direction of the principal stresses as the AC-U-2 sample is sheared to failure. This condition might represent an element near the foot of a slope that has failed, an exception being that the laboratory sample failed radially symmetrically while the element of soil in the field would fail under plane strain conditions.

Values of the undrained strength ratio S_u/σ_{1c}' (σ_{1c}' = maximum effective consolidation pressure) obtained from these tests range between .35 for sample AC-U-1 and .29 for AC-U-2. Strains at failure $(\sigma_1 - \sigma_3)_{max}$ are twice as high for test AC-U-2 than they are for AC-U-1. The differences in behavior observed during the two tests is primarily a function of the anisotropy, of $\bar{A}_f$ and the difference in reorientation of stresses between the two tests. These differences in response of the Bay Mud can be seen in the uncorrected curves of Figure 66, which show plots of deviator stress, pore pressure, $\bar{A}$ and principal stress ratio versus strain.

Denby (1978) ran a series of $\overline{AC-U}$ triaxial tests in which a K_o = .7 was used. Table 14 gives a summary of Denby's test results. All of his test data has been corrected for the load carried by the rubber membranes and filter paper drains. Figure 67 shows the stress-strain curves obtained from the tests run on soil from the normally consolidated unweathered zone of the Bay Mud profile. These results have been normalized with respect to the major principal confining pressure, and are in agreement with the results obtained by Duncan for test AC-U-1. The S_u/σ_{1c}' ratio is about .35 and the strain at failure is about 2%-3%.

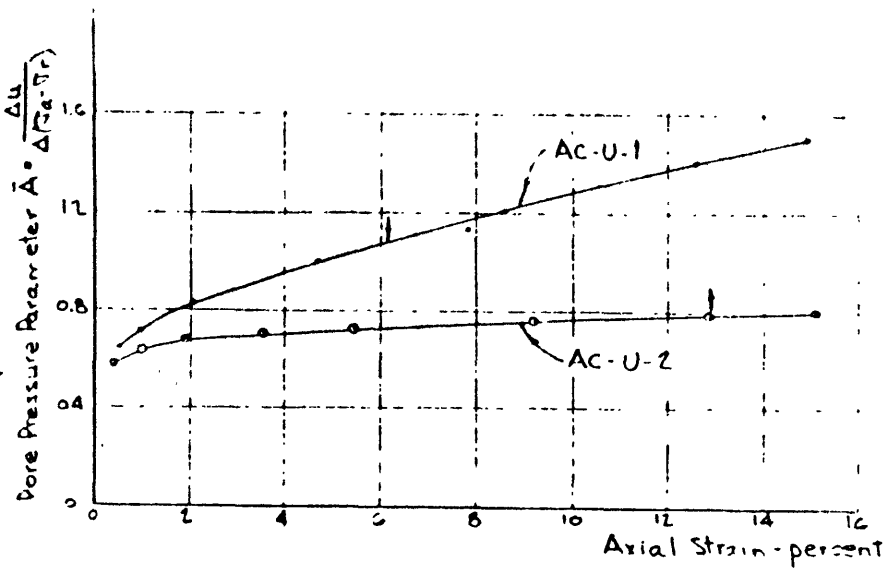
Seed et al. (1964) ran a series of 4 sets of $\overline{\overline{AC-U}}$ triaxial tests on Bay Mud. Each test set consisted of two tests, a "field condition" test

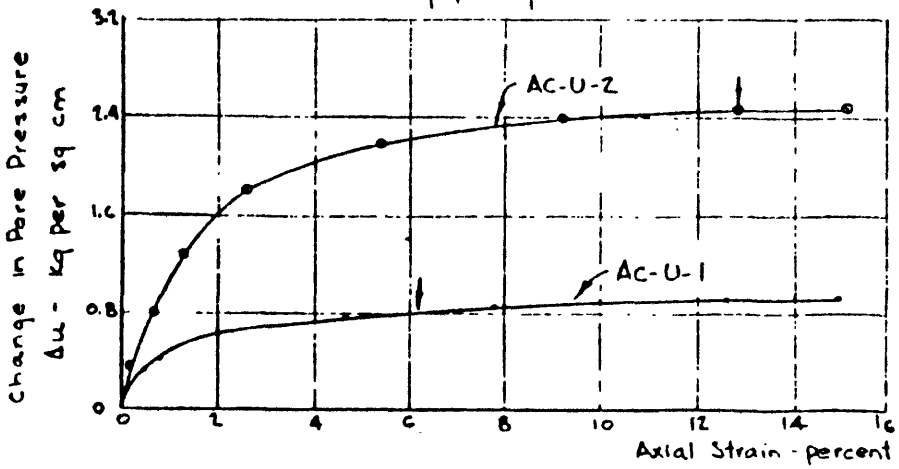


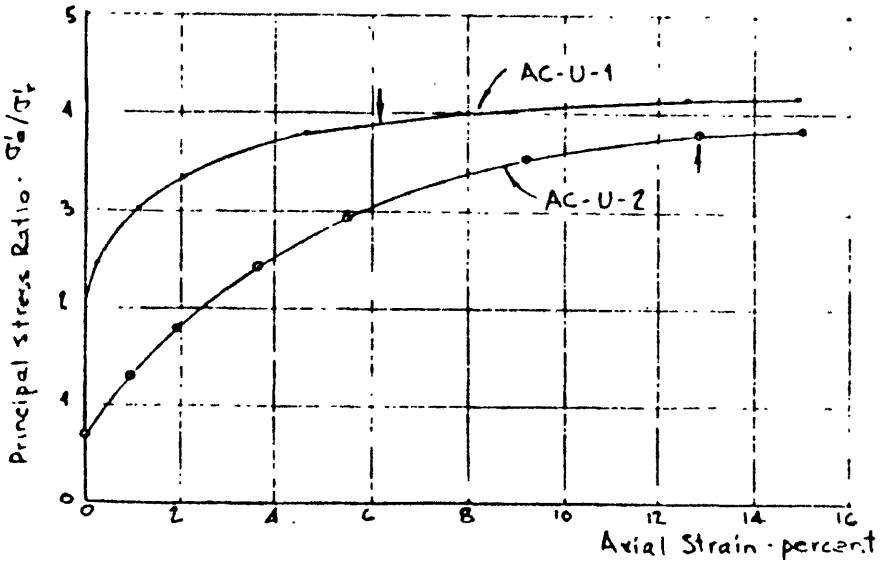
Undisturbed Bay Mud
Normally Consolidated

Sample	σ'_{ac}*	σ'_{rc}*	w_f
AC-U-1	3.21	1.60	55.0
AC-U-2	2.14	3.20	55.4

*Pressures are kg per sq cm







VARIATIONS OF DEVIATOR STRESS, PORE WATER PRESSURE, PORE PRESSURE COEFFICIENT Ā, AND EFFECTIVE PRINCIPAL STRESS RATIO WITH AXIAL STRAIN FOR $\overline{AC-U}$ TRIAXIAL TESTS ON UNDISTURBED SAN FRANCISCO BAY MUD.

FIGURE 66 $\overline{AC-U}$ TRIAXIAL TEST RESULTS. FROM DUNCAN (1965)

TABLE 14 SHANSEP TEST RESULTS

Test No.	Depth	p_o psi	k_o	$\sigma_c/k_o p_o$	s_u kN/m^2	ε_f %	$s_u/\bar{p}$
HSHAN 4	8'9"	5.1	1.0	3.0*	33.2	3.2	0.31
HSHAN 5	9'6"	5.3	1.0	3.0*	23.2	2.6	0.21**
HSHAN 6	36'7"	10.8	0.7	1.5	38.9	2.3	0.35
HSHAN 7	20'6"	7.6	0.7	1.5	28.0	1.9	0.36
HSHAN 10	19'9"	7.4	0.7	2.5	42.8	1.8	0.34

* Samples from desiccated zone, OCR = 3

** Sample tilted during shear

FROM DENBY (1978)

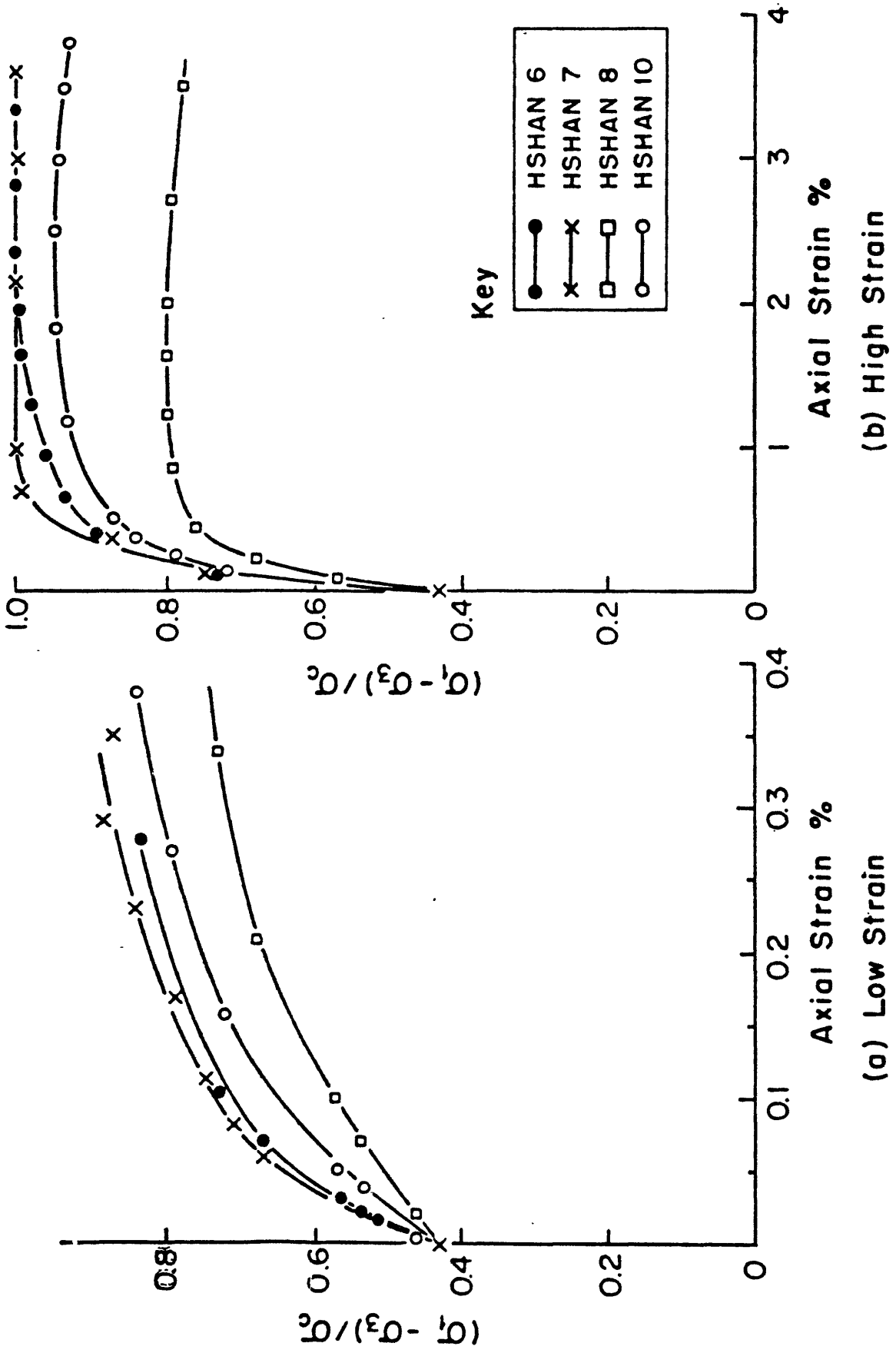
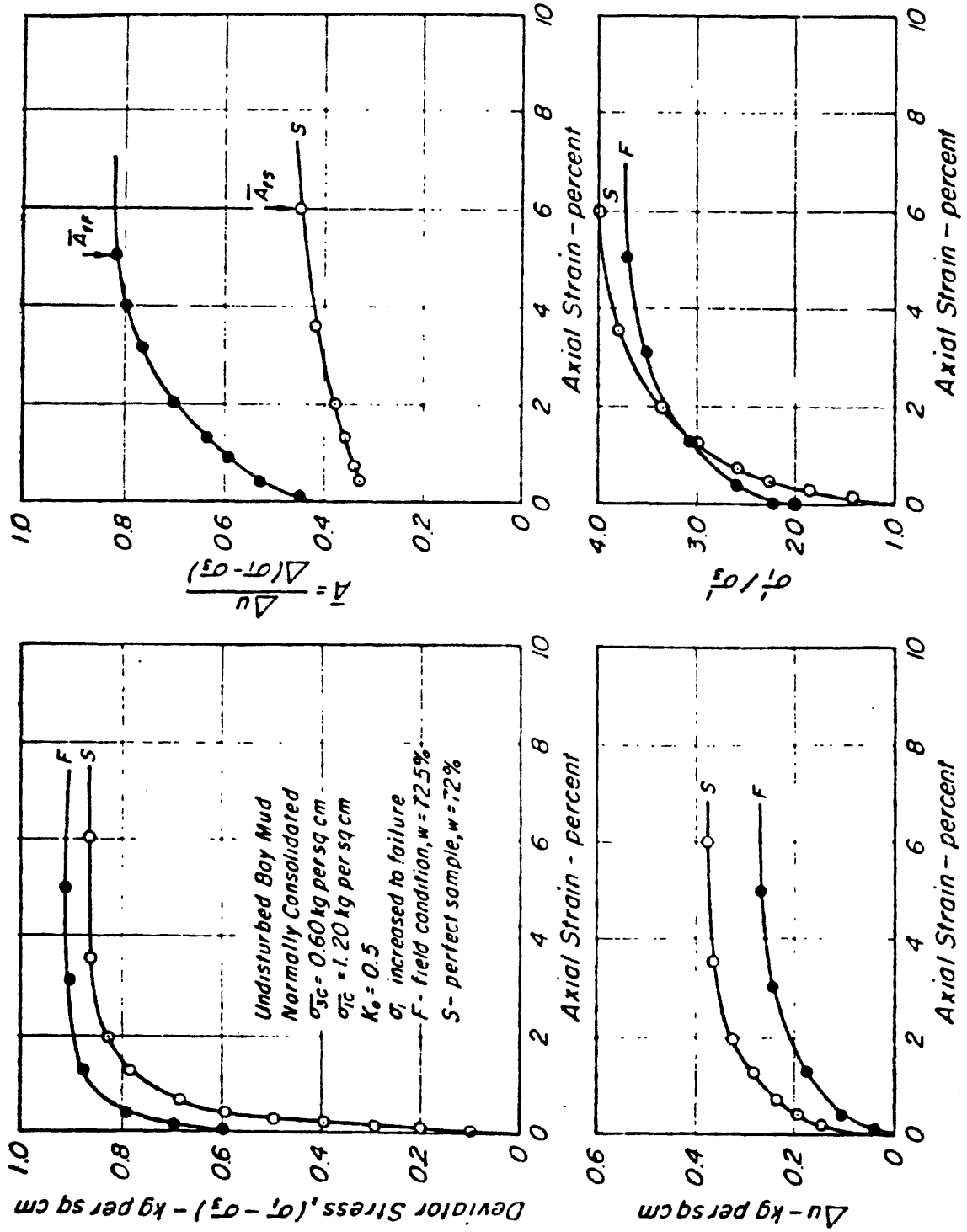


FIGURE 67 RESULTS OF $\overline{AC-U}$ TRIAXIAL TESTS ON UNDISTURBED BAY MUD. TESTS PERFORMED BY DENBY (1978) NOTE: SEE TABLE 14 FOR PERTINENT TEST DATA

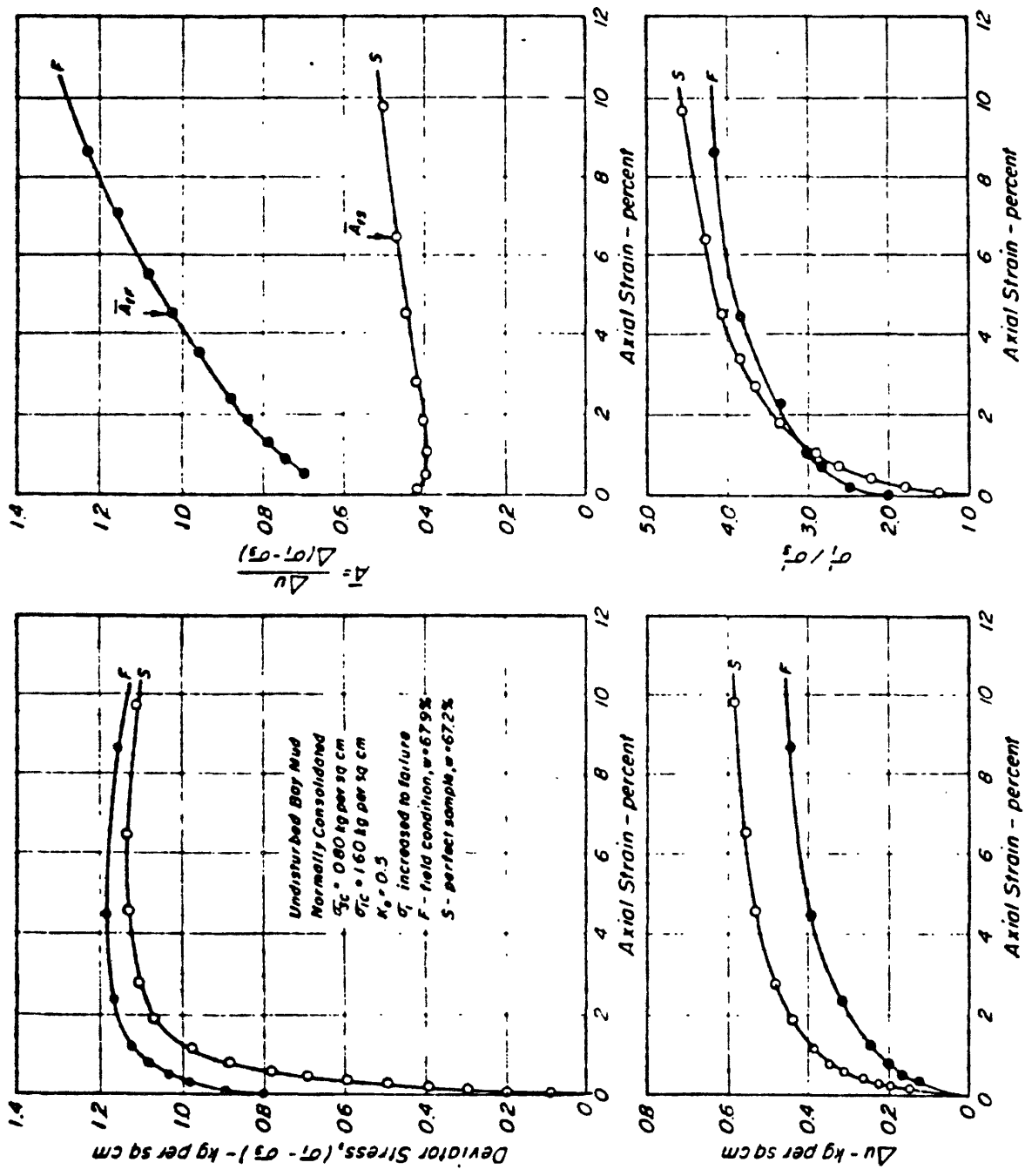
and a "perfect sample" test. All tests were carried out under $K_o = .5$ conditions. For each test set two identical samples were trimmed side by side and then consolidated anisotropically. The consolidation stresses were built up in small increments of $\Delta\sigma_3 = .10$ kg/cm^2 and $\Delta\sigma_1 = .20$ kg/cm^2. After completion of consolidation the drainage lines on the triaxial cells were closed and the deviator stress on one of the samples was increased to failure. This specimen simulated the field condition and the stress path it followed is similar to those followed in Denby's tests and in Duncan's test AC-U-1. The stresses σ_1 and σ_3 acting on the second sample were then removed, resulting in a decrease in porewater pressure. This step was intended to simulate a perfect sampling operation ("the removal of the anisotropic field stresses in the element while no remolding or change in water content occurred.") Next, a deviator stress was applied to the sample and was increased until failure occurred.

The results of the four test sets are shown in Figures 68 to 71. Figures 68 and 69 illustrate tests in which the deviator stress was applied by increasing the axial stress and Figures 70 and 71 show the results of tests in which the deviator stress was applied by decreasing the lateral stress acting on the sample. The test results presented in these figures have not been corrected for the loads carried by filter paper drains, rubber membranes and piston friction. Because corrections have not been applied small differences will appear when comparing the results of the tests representing the field conditions with the $\overline{AC-U}$ tests performed by Denby and Duncan. For instance, the S_u/σ_{1c}' ratio, which is about .37-.38 is slightly higher for these tests than for the other $\overline{AC-U}$ tests. Similarly, the pore pressure paramter $\bar{A}_f$ is slightly lower. The strains at failure which are not changed by any corrections, agree well with the previous



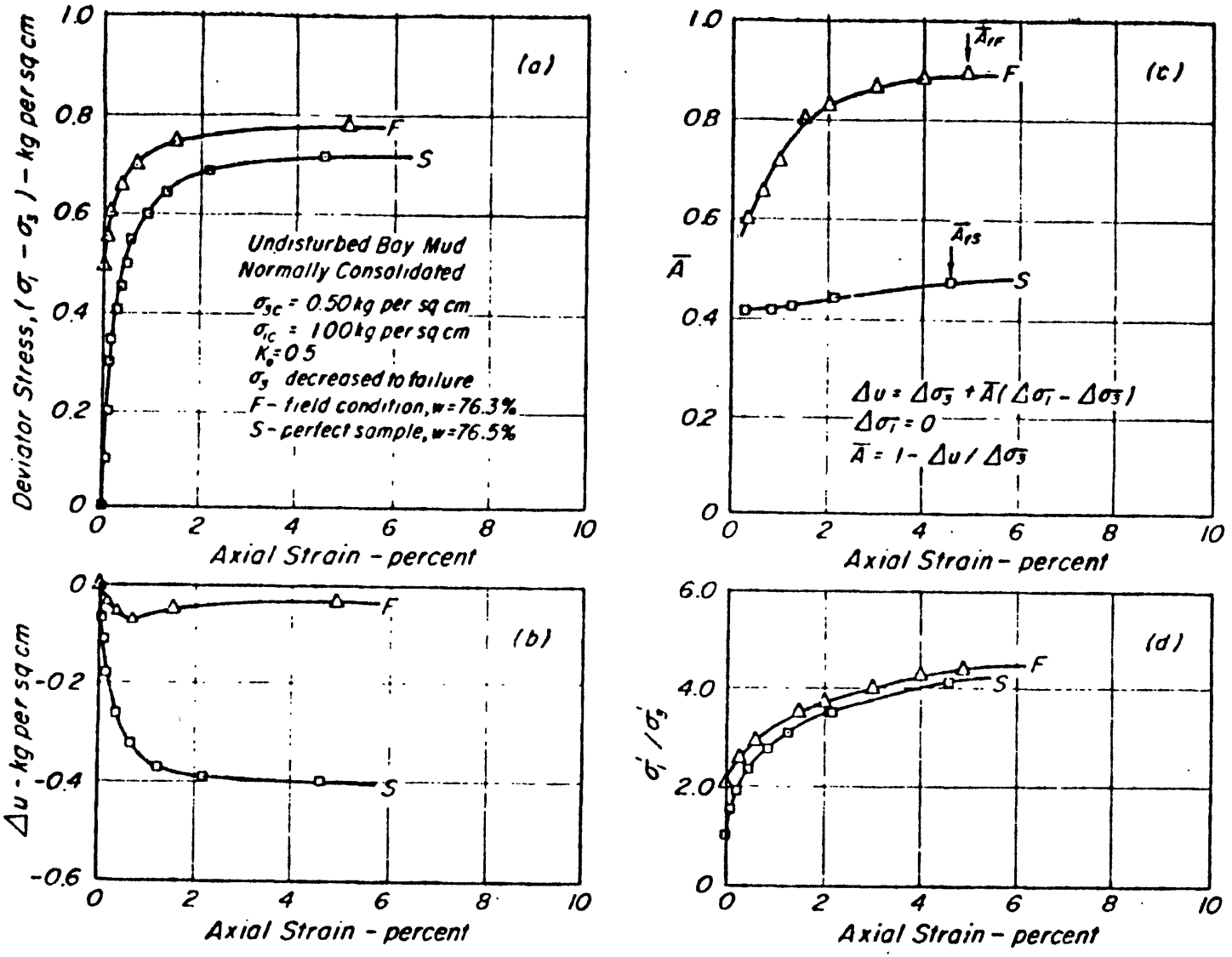
VARIATIONS OF DEVIATOR STRESS, PORE-WATER PRESSURE, PORE PRESSURE COEFFICIENT $\bar{A}$ AND EFFECTIVE PRINCIPAL STRESS RATIO WITH AXIAL STRAIN FOR "FIELD" AND "PERFECT SAMPLE" CONDITIONS.

FIGURE 68 $\overline{AC}$-$\overline{U}$ TESTS PERFORMED BY SEED ET AL. (1964)



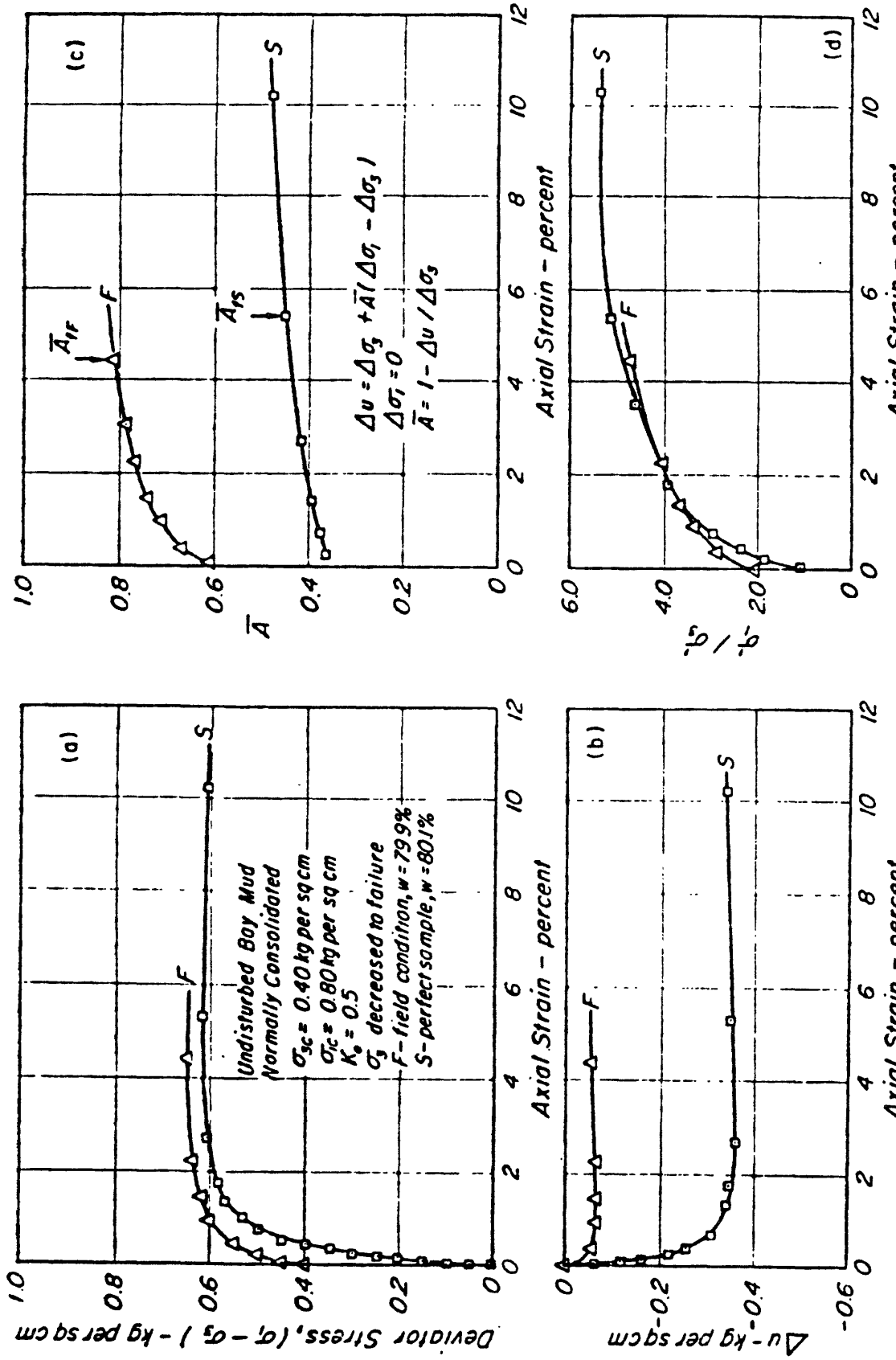
VARIATIONS OF DEVIATOR STRESS, PORE-WATER PRESSURE, PORE-PRESSURE COEFFICIENT $\bar{A}$ AND EFFECTIVE PRINCIPAL STRESS RATIO WITH AXIAL STRAIN FOR "FIELD" AND "PERFECT SAMPLE" CONDITIONS.

FIGURE 69 $\overline{AC}$-$\overline{U}$ TESTS PERFORMED BY SEED ET AL. (1964)



VARIATIONS OF THE DEVIATOR STRESS, PORE-WATER PRESSURE, PORE PRESSURE COEFFICIENT $\bar{A}$, AND THE EFFECTIVE PRINCIPAL STRESS RATIO, WITH AXIAL STRAIN FOR "FIELD" AND "PERFECT SAMPLE" CONDITIONS.

FIGURE 70 $\overline{AC-U}$ TESTS PERFORMED BY SEED ET AL. (1964)



VARIATIONS OF THE DEVIATOR STRESS, PORE-WATER PRESSURE, PORE PRESSURE COEFFICIENT $\bar{A}$, AND THE EFFECTIVE PRINCIPAL STRESS RATIO, WITH AXIAL STRAIN FOR "FIELD" AND "PERFECT SAMPLE" CONDITIONS.

FIGURE 71 $\overline{AC-U}$ TESTS PERFORMED BY SEED ET AL. (1964)

results, being about 4%-5% at maximum deviator stress.

The results of Seed et al. show that the strength measured on the anisotropically consolidated samples representing the field condition is higher than the strength of the "completely undisturbed samples of the same soil at the same water content tested under isotropic conditions in the laboratory". The magnitude of this strength difference was between 4% and 8%. The most pronounced effect of the perfect sampling procedure was on the pore pressure response during loading. The pore pressure parameter $\bar{A}$ was higher at all levels of strain for the field condition than it was for the perfect sample. At failure $\bar{A}$ was greater by a factor of almost 2.

Summary of $\overline{\text{IC-U}}$ and $\overline{\text{AC-U}}$ Triaxial Test Results

Table 15 summarizes the results of the $\overline{\text{IC-U}}$ and $\overline{\text{AC-U}}$ triaxial tests. Figures 72 and 73 show examples of typical effective stress-stress paths that the Bay Mud followed during both types of tests. These stress paths have been normalized with respect to the major principal confining pressure. It is noted that the behavior exhibited by the soil is fairly consistent, strengths are slightly higher in the $\overline{\text{AC-U}}$ tests than in the $\overline{\text{IC-U}}$ tests while strains at failure are considerably lower. The stress paths are consistent with results obtained for other sensitive normally consolidated soils.

Effect of Overconsolidation

In running the consolidated undrained triaxial tests all samples were consolidated past their preconsolidation pressure until they were normally consolidated. As previously discussed the actual field OCR is between 1.1 and 1.5. Although changes in $S_u/\bar{p}$ with OCR have not been studied for Bay

TABLE 15 SUMMARY OF CONSOLIDATED-UNDRAINED TRIAXIAL TESTS

Test	K_o	S_u/σ_{1c}'	ε_f	$\bar{A}_f$	Reference
$\overline{\text{IC-U}}$	1	.34	10-12%	~1	Duncan (1965)
$\overline{\text{IC-U}}$	1	.34	10%	~1	Berkeley (1978)
$\overline{\text{IC-U}}$*	1	.34	8%	.9-1	Berkeley (1977)
$\overline{\text{AC-U}}$	.54	.35	6%	1.1	Duncan (1965)
$\overline{\text{AC-U}}$	1.54	.29	13%	.8	Duncan (1965)
$\overline{\text{AC-U}}$	.7	.35	2-3%	.8-1	Denby (1978)
$\overline{\text{AC-U}}$*	.5	.37	4-5%	.8-1.1	Seed et al. (1964)

*These results have not been corrected for the effects of filter paper drains, etc. on test results.

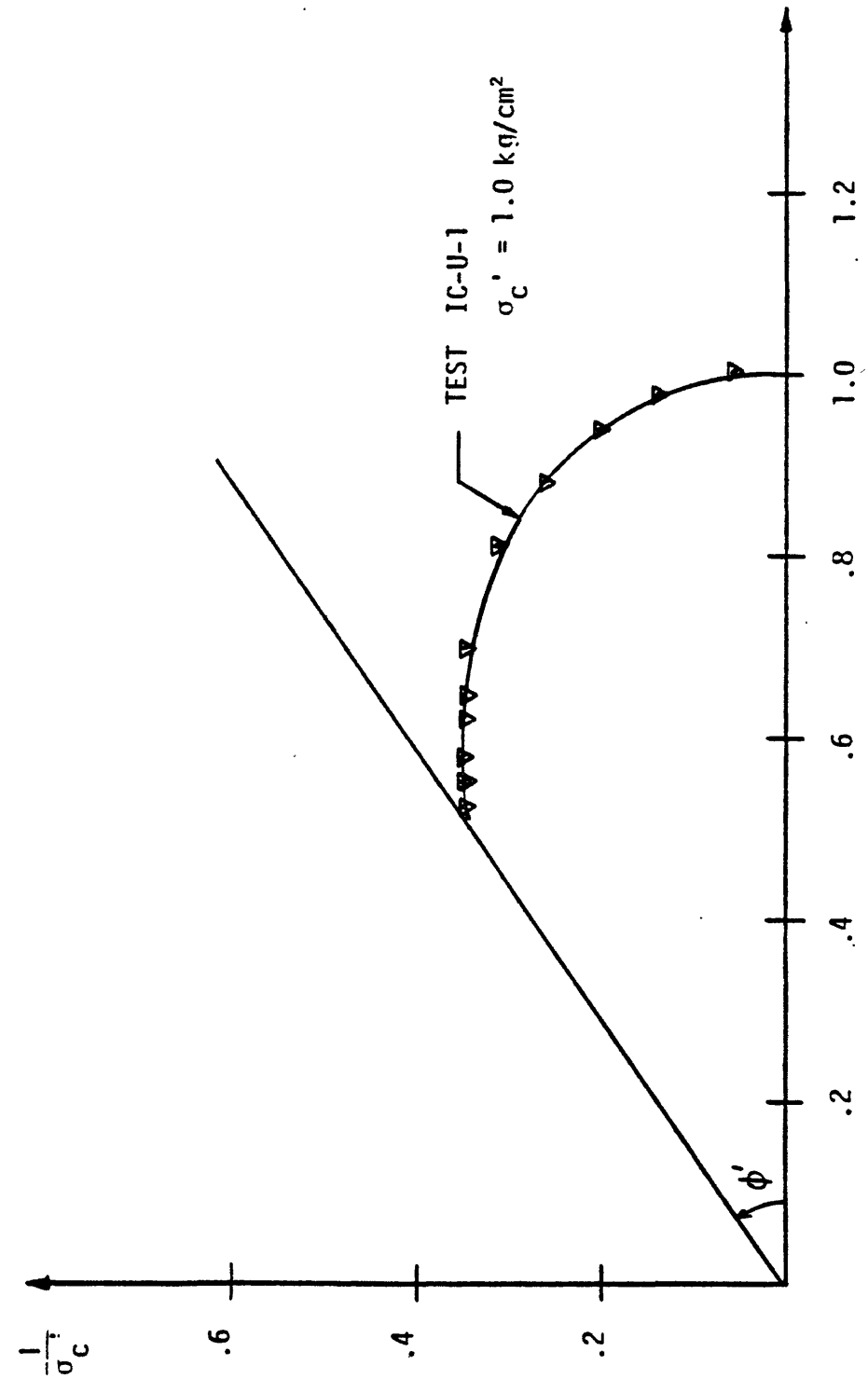


FIGURE 72 NORMALIZED EFFECTIVE STRESS PATH FOR $\overline{IC\text{-}U}$ TRIAXIAL TEST IC-U-1. TESTS PERFORMED BY DUNCAN (1965)

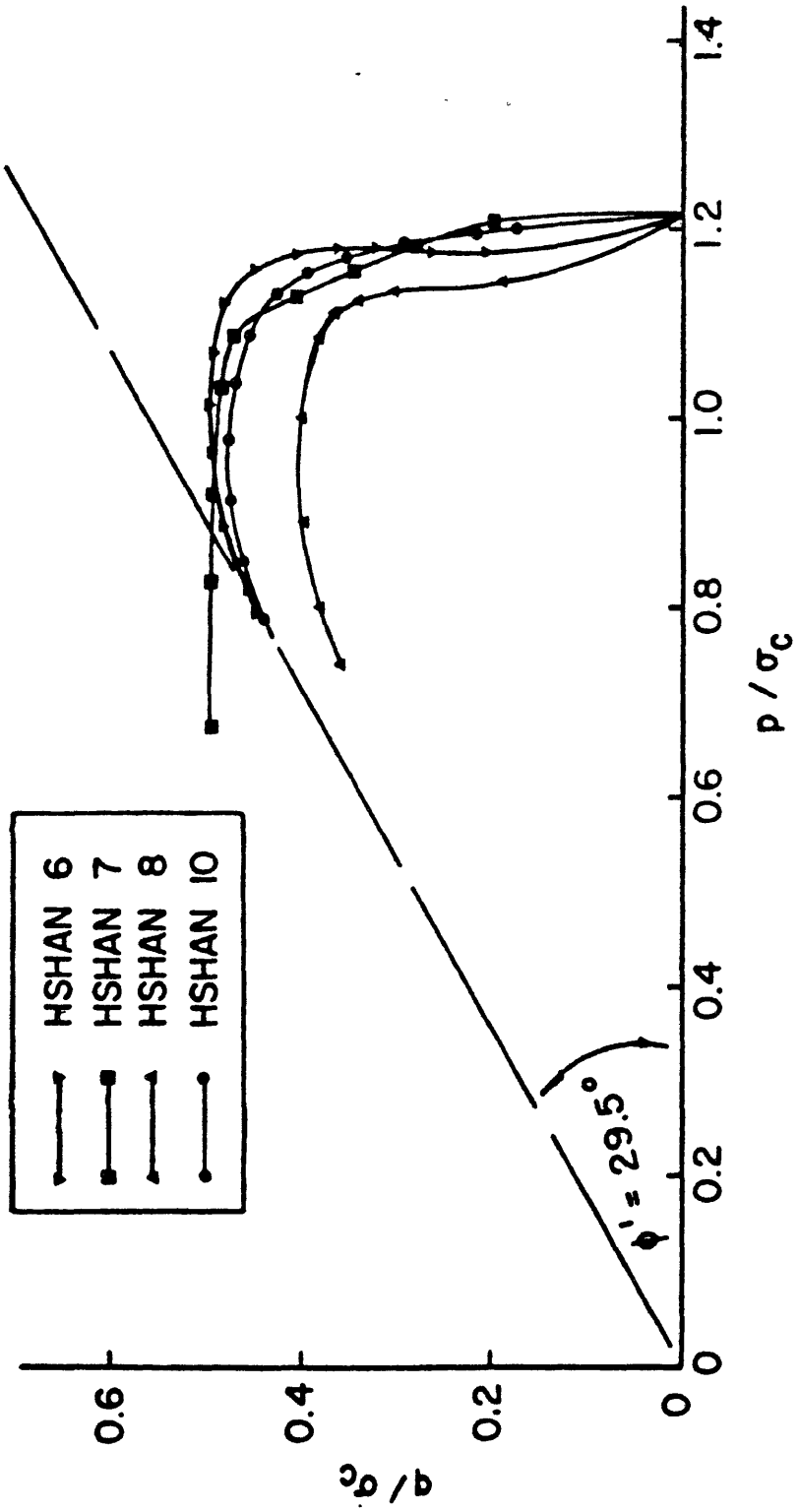


FIGURE 73 NORMALIZED EFFECTIVE STRESS PATHS FOR $\overline{AC}$-$\overline{U}$ TESTS ON BAY MUD.
TESTS PERFORMED BY DENBY (1978)

Mud results presented by Ladd (1977), and given in Figure 74, for Boston Blue Clay indicate an increase in $S_u/\bar{p}$ of about 10 to 30% for increases in OCR from 1 to 1.1 to 1.5. Although more study is needed on the normalized behavior of Bay Mud, these results give an idea of size of the change needed to convert laboratory shear strengths into field shear strengths for cases where no significant consolidation of the soil will take place before the soil is sheared.

If it is assumed that data for Bay Mud would plot parallel to the data for the other clays listed in Figure 74, and have an intercept of $S_u/\bar{p}$ = .34 at an OCR = 1, then $S_u/\bar{p}$ ratios for OCR's varying between 1.1 and 1.5 can be calculated. At an OCR of 1.1 a value of $S_u/\bar{p}$ = .36 is obtained, while an $S_u/\bar{p}$ value of .42 corresponds to an OCR equal to 1.5. These values of $S_u/\bar{p}$ are compared with the values of $S_u/\bar{p}$ obtained from the various in-situ test methods in Table 16. It is interesting to note that while the shear strengths obtained from the field vane and cone penetration tests are smaller than those obtained by extrapolating the data in Figure 74, the self boring pressuremeter test gives results that are in close agreement.

Unconsolidated Undrained and Laboratory Vane Tests

Unconsolidated undrained triaxial tests were run by Duncan (1965) and Tringale (1978) and laboratory vane shear tests were run by Stanford University and the U.S.G.S. (Denby (1978)).

Results of laboratory vane tests run at Stanford are given in Figure 75 and the results of the U.S.G.S. tests are given in Figure 76. The U.S.G.S. data show little increase in strength with depth until a depth of 45 feet is reached. The Stanford laboratory vane data give very

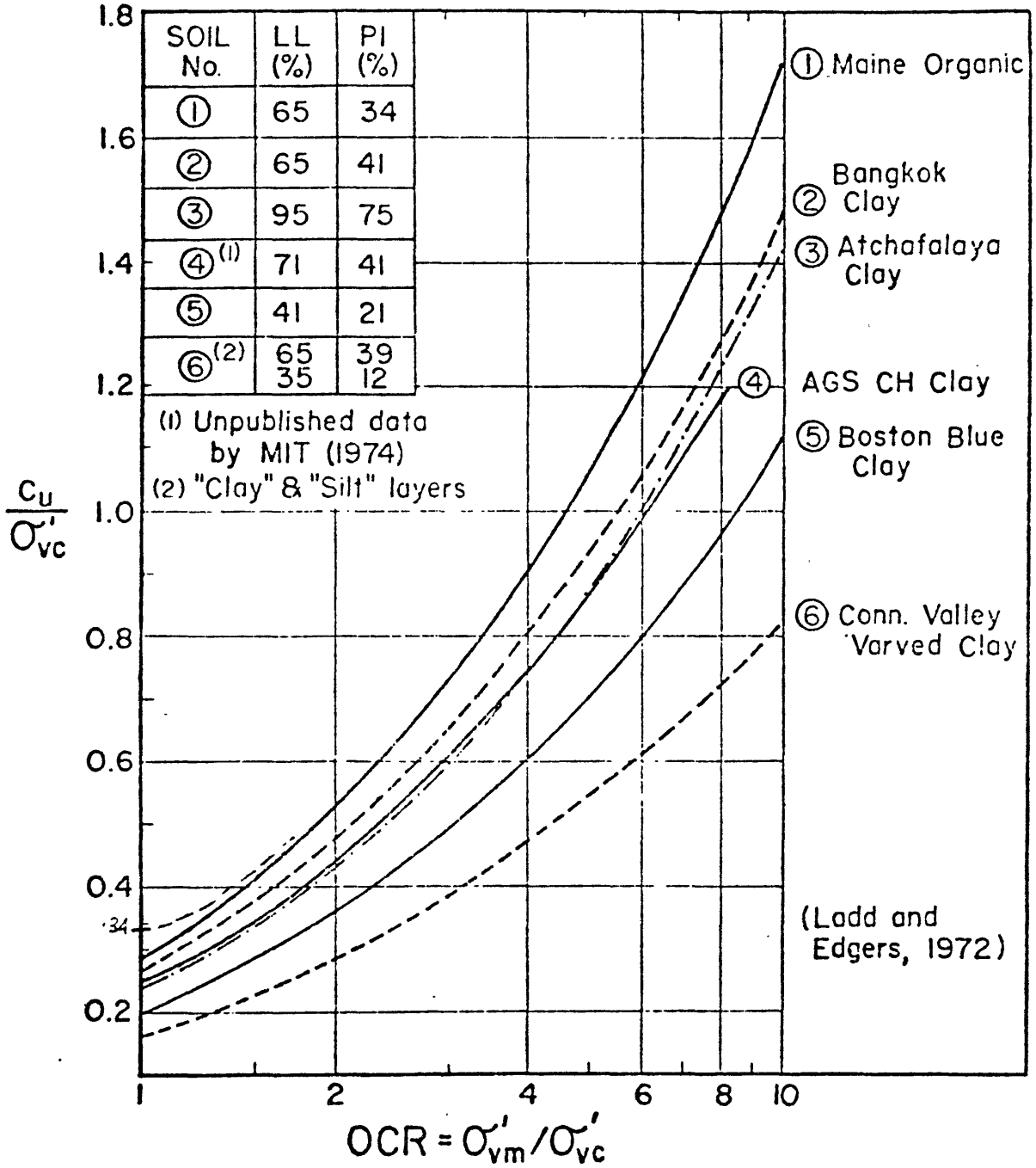


FIGURE 74 UNDRAINED STRENGTH RATIO VERSUS OCR FROM AC-U DIRECT SIMPLE SHEAR TESTS.

From Ladd et al. (1977)

TABLE 16 EFFECT OF OCR ON UNDRAINED SHEAR STRENGTH OF SAN FRANCISCO BAY MUD

Method of Obtaining $S_u/\overline{p}$	OCR	$S_u/\overline{p}$
1 Laboratory Tests		
$\overline{\text{IC-U}}$	1	.34
$\overline{\text{AC-U}}$	1	.35
UU	1.0-1.5	.31-.32
2 Extrapolation of $\overline{\text{IC-U}}$ Data in Figure 74	1.1-1.5	.36-.42
3 In-situ Tests		
Self Boring Pressuremeter	1.0-1.5	.40
Cone Pentrometer	1.0-1.5	.32
Field Vane	1.0-1.5	.32

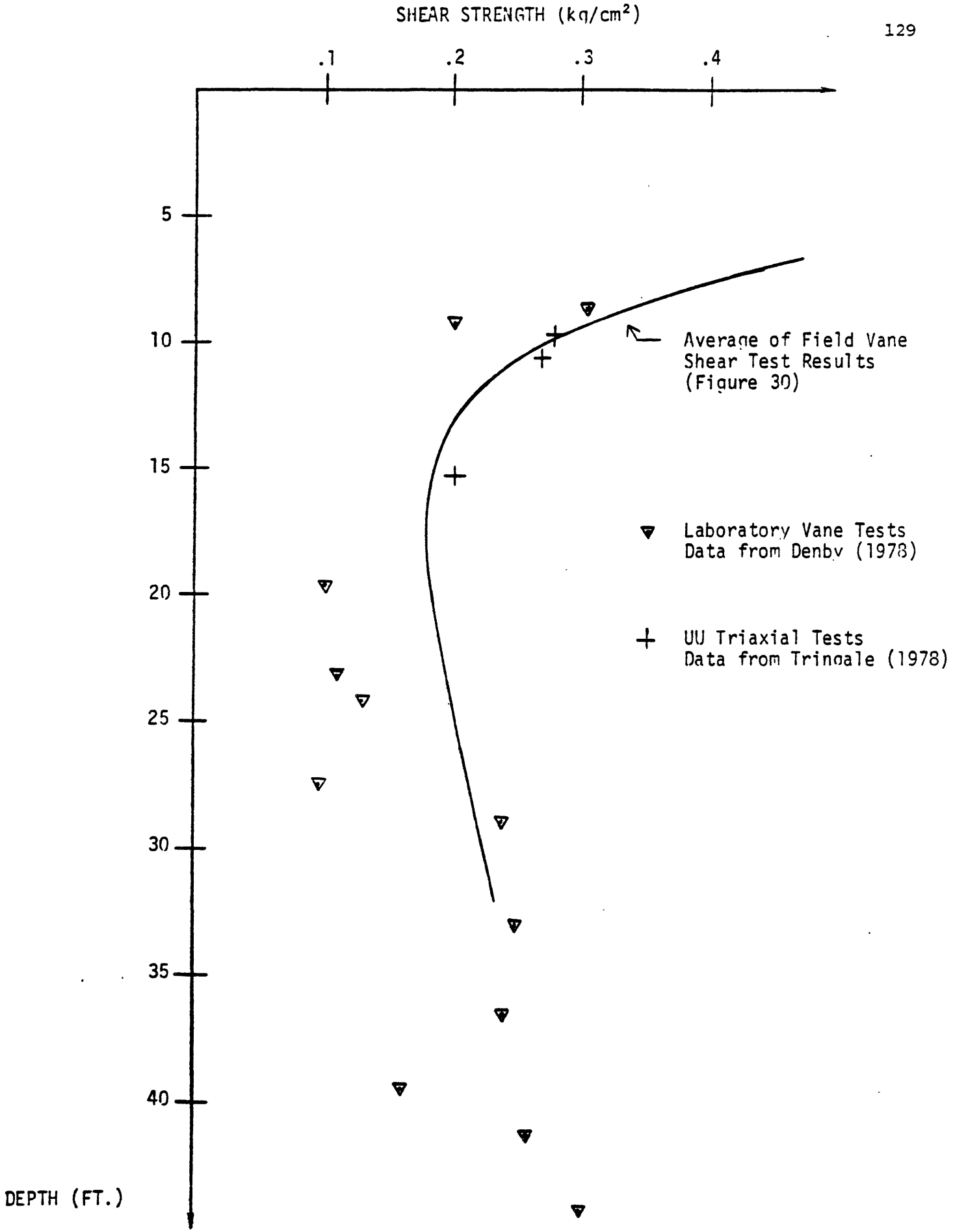


FIGURE 75 LABORATORY VANE AND UU TRIAXIAL TEST RESULTS

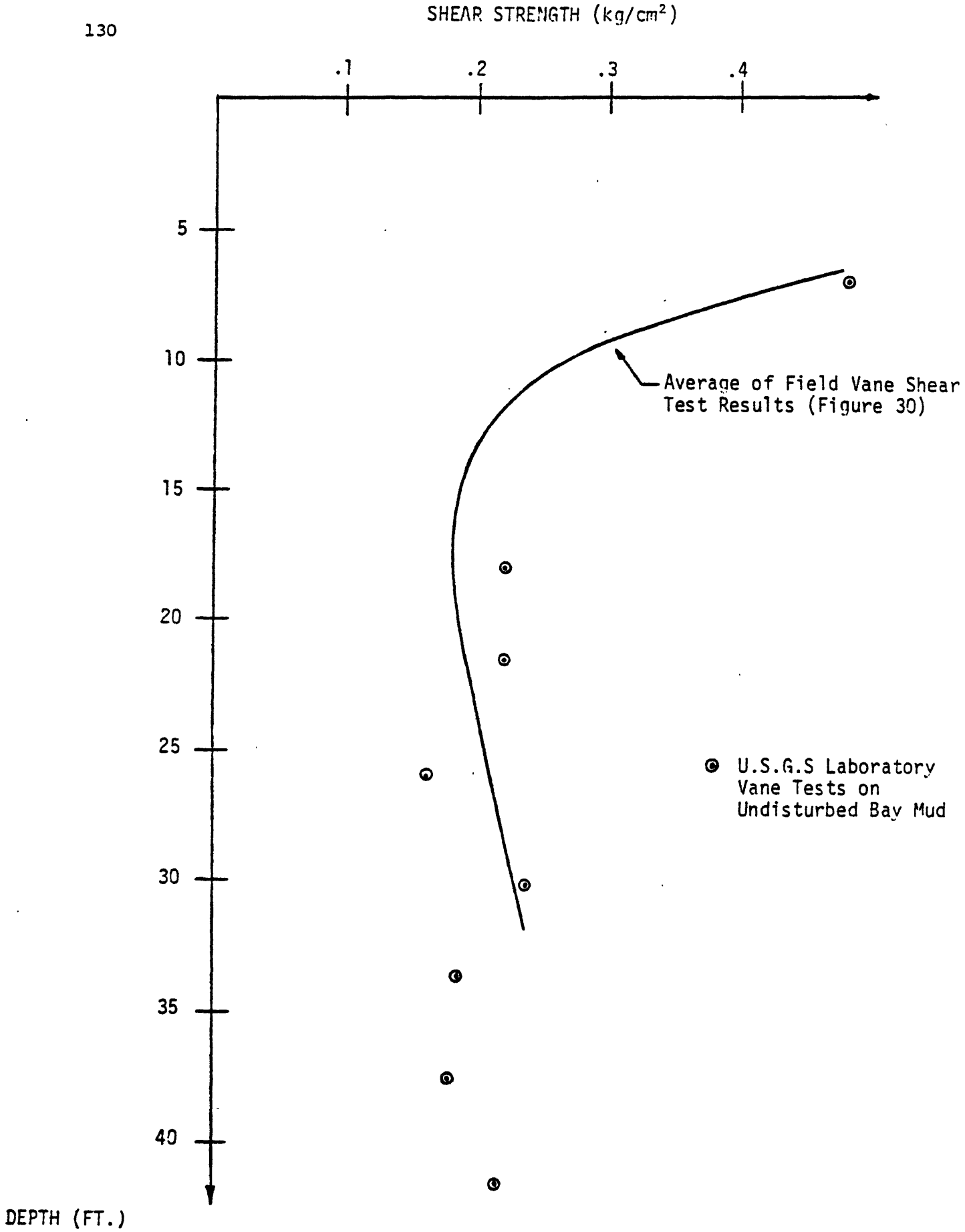


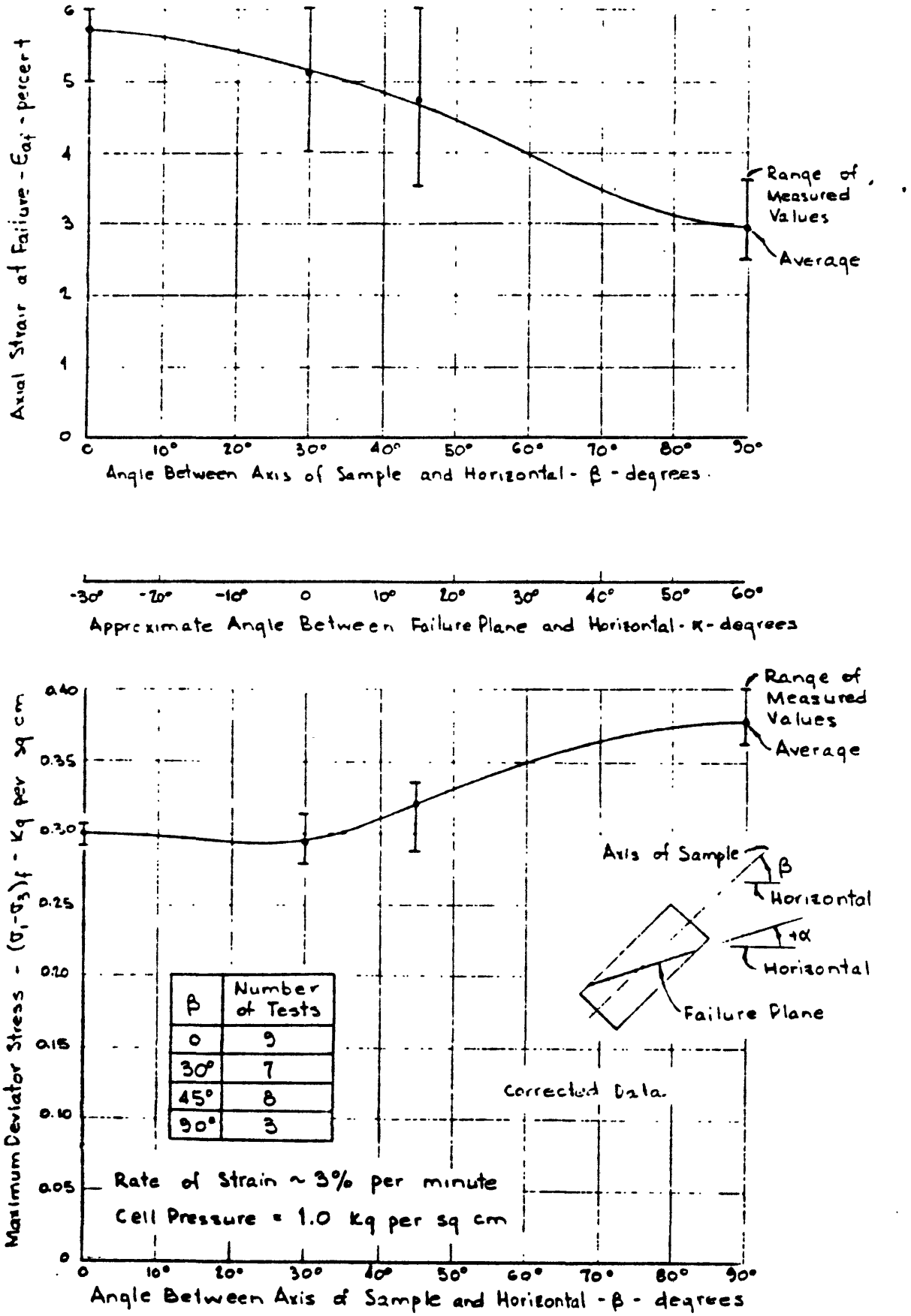
FIGURE 76 LABORATORY VANE TEST RESULTS. TESTS PERFORMED BY THE U.S.G.S. AND REPORTED BY DENBY (1978)

low shear strengths (~.1 kg/cm^2) between 20 and 30 feet, being only about half the value reported by the U.S.G.S. between those same depths. Below 30 feet the Stanford values increase linearly at a slope of $S_u/\bar{p}$ equal to .31-.32. The results of the UU tests by Duncan were given earlier in this report (Figure 29). He concluded that the $S_u/\bar{p}$ ratio from the UU tests was .32. Tringale's UU test results are shown in Figure 75 and correlate well with the results of Duncan.

Duncan carried out a second series of UU tests on samples of Bay Mud trimmed with their axes in different directions. The purpose of these tests was to determine the relationship between laboratory undrained strength and orientation of the failure plane. The variation of strength and axial strain at failure and orientation of the failure plane is shown in Figure 77. The results show that a strength variation of about 20% can occur in UU tests due solely to changes in the orientation of the failure plane. The minimum strength is associated with samples inclined at about 30°, a condition in which the failure plane coincides approximately with the horizontal. The maximum strength is associated with vertical samples. Note also that the average strain at failure for the vertical samples is only about half of that for the horizontal ones.

Plane Strain Test

Duncan (1965) ran $\overline{\text{AC-U}}$ plane strain tests on Bay Mud. These test results are reported here for completeness but are not discussed in depth. Two types of tests were performed. In vertical plane strain tests samples are consolidated approximately one dimensionally with the major principal stress acting in the axial direction. Failure is caused by either increasing the axial stress or decreasing the lateral stress after



β	Number of Tests
0	9
30°	7
45°	8
90°	3

FIGURE 77 VARIATION OF MAXIMUM DEVIATOR STRESS AND STRAIN AT FAILURE WITH ORIENTATION OF THE FAILURE PLANE IN UU TRIAXIAL TESTS ON UNDISTURBED BAY MUD.

From Duncan (1965)

completion of consolidation. During horizontal plane strain tests, samples are consolidated with the major principal stress acting vertically and are then sheared to failure with the major principal stress acting in the horizontal direction. For a complete description of the testing procedures reference is made to Duncan and Seed (1966).

The data from the plane strain tests are summarized in Table 17 and Figures 78 through 82. These results show average values for S_u/σ_{1c}' ratios of .37 for the $\overline{VPS}$ tests and .29 for the $\overline{HPS}$ tests. These results give a good measure of the undrained strength anisotropy of the Bay Mud. It is easily seen that the strength of the $\overline{HPS}$ sample is .78 times the strength of the $\overline{VPS}$ sample. It is interesting to compare this value with the behavior of other clays. Figure 83 shows that the Bay Mud is fairly consistent with the other data in marking out a trend of decreasing anisotropy with increasing plasticity. Figure 84 shows the vector curves that the Bay Mud followed during the plane strain tests. Vector curves are similar to stress paths except that they are the locus of points representing successive combinations of shear and normal stresses on the failure plane, whereas stress paths represent combinations of stresses on the plane of maximum shear stress.

Strains at failure in the $\overline{VPS}$ tests are typically around 3-1/2%, while strains in $\overline{HPS}$ tests are about 10%. In part, this difference is due to the reorientation of principal stresses that takes place during the $\overline{HPS}$ tests but is absent from the $\overline{VPS}$ tests. The angle of internal friction ϕ' (at $(\sigma_1 - \sigma_3)_{max}$) was measured to be 38° in the VPS tests and 35° in the $\overline{HPS}$ tests.

It is interesting to note that the behavior of Bay Mud during the $\overline{VPS}$ test, which is equivalent to a plane strain active test, is similar to

TABLE 17 SUMMARY OF RESULTS OF "IN-SITU" PLANE STRAIN TESTS ON UNDISTURBED SAN FRANCISCO BAY MUD

Sample	Depth (feet)	Initial w/c (percent)	σ'_{ac} (kg/cm^2)	$\sigma'_{\ell c}$ (kg/cm^2)	$\left(\frac{\sigma_3'}{\sigma_1'}\right)_c$	Consol. w/c (percent)	$\left(\frac{\Delta V}{V}\right)_c$	$(\sigma_a - \sigma_\ell)$ (kg/cm^2)	$\Delta(\sigma_a - \sigma_\ell)$ (kg/cm^2)
VPS-3	18.5	87.5	3.67	1.81	0.49	52.9	0.256	2.70	0.84
VPS-4	18.5	85.3	0.64	0.35	0.55	77.4	0.042	0.51	0.22
VPS-5	18.5	87.3	1.39	0.70	0.50	64.3	0.169	1.03	0.34
VPS-6	19.0	89.5	2.14	1.07	0.50	59.1	0.207	1.58	0.51
VPS-8	19.0	87.7	2.90	1.44	0.50	53.7	0.255	2.12	0.66
VPS-9	21.0	91.0	3.72	1.77	0.48	51.8	0.283	2.76	0.81
HPS-4	17.0	93.1	0.69	1.61	0.43	65.2	0.191	0.81	1.73
HPS-5	17.0	85.8	1.20	3.15	0.38	52.1	0.243	1.65	3.60
HPS-6	16.5	90.1	0.34	0.81	0.42	74.8	0.093	0.41	0.88
HPS-7	16.5	89.3	0.99	2.40	0.41	57.5	0.226	1.28	2.69
HPS-9	15.5	88.8	1.47	3.98	0.37	51.1	0.277	2.23	4.74
HPS-11	19.0	92.3	1.66	4.00	0.42	52.8	0.282	2.24	4.68
HPS-12	20.5	85.5	1.52	3.18	0.48	52.5	0.238	1.77	3.43

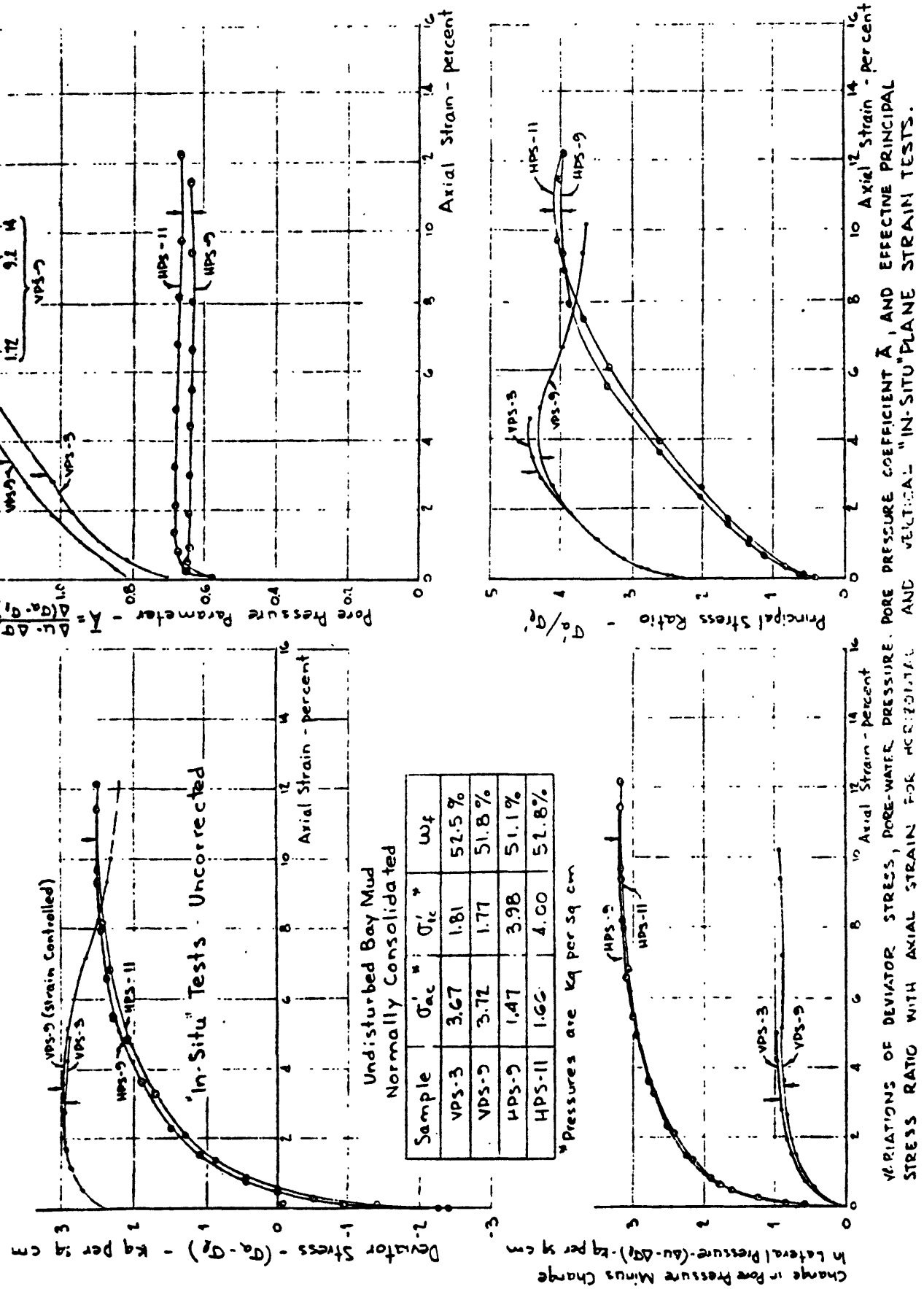
(Continued)

FROM DUNCAN (1965)

TABLE 17 CONTINUED

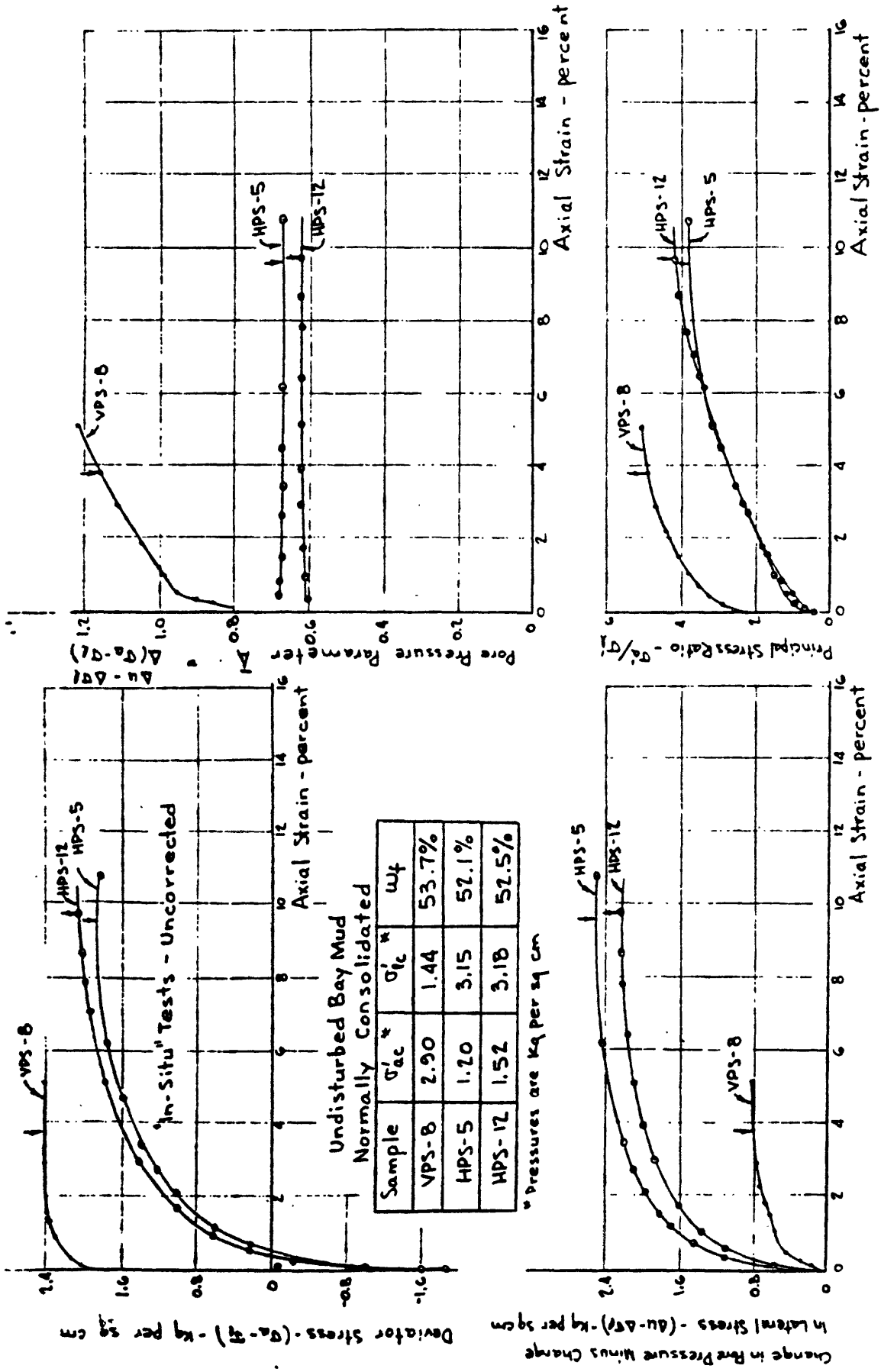
Sample	Depth (feet)	$(\Delta u - \Delta\sigma_\ell)_f$ (kg/cm^2)	$\bar{A}_f$	$\left(\frac{\sigma_1'}{\sigma_3'}\right)_f$	ε_{af} (percent)	Time to Failure (hours)	σ_{1f}' (kg/cm^2)	σ_{3f}' (kg/cm^2)	$(\sigma_1-\sigma_3)_f$ (kg/cm^2)	$(\sigma_1'+\sigma_3')_f$ (kg/cm^2)
VPS-3	18.5	0.90	1.07	3.97	3.1	5.25	3.61	0.91	1.35	2.26
VPS-4	18.5	0.20	0.91	4.40	4.0	5.75	0.66	0.15	0.26	0.41
VPS-5	18.5	0.39	1.15	4.33	3.2	6.0	1.34	0.31	0.52	0.83
VPS-6	19.0	0.58	1.14	4.22	4.2	7.0	2.07	0.49	0.79	1.28
VPS-8	19.0	0.78	1.18	4.27	3.8	6.75	2.77	0.65	1.06	1.71
VPS-9	21.0	0.87	1.07	4.07	3.5	4.5	3.66	0.90	1.38	2.28
HPS-4	17.0	1.30	0.75	3.61	11.1	4.50	1.12	0.31	0.41	0.72
HPS-5	17.0	2.52	0.70	3.62	9.6	4.50	2.28	0.63	0.83	1.46
HPS-6	16.5	0.61	0.69	3.05	9.0	5.0	0.61	0.20	0.21	0.41
HPS-7	16.5	1.94	0.72	3.91	10.0	5.25	1.72	0.44	0.64	1.08
HPS-9	15.5	3.17	0.67	3.76	10.6	5.25	3.04	0.81	1.12	1.93
HPS-11	19.0	3.20	0.68	3.80	10.6	4.50	3.04	0.80	1.12	1.92
HPS-12	20.5	2.24	0.65	3.68	9.8	5.25	2.43	0.66	0.89	1.55

FROM DUNCAN (1965)



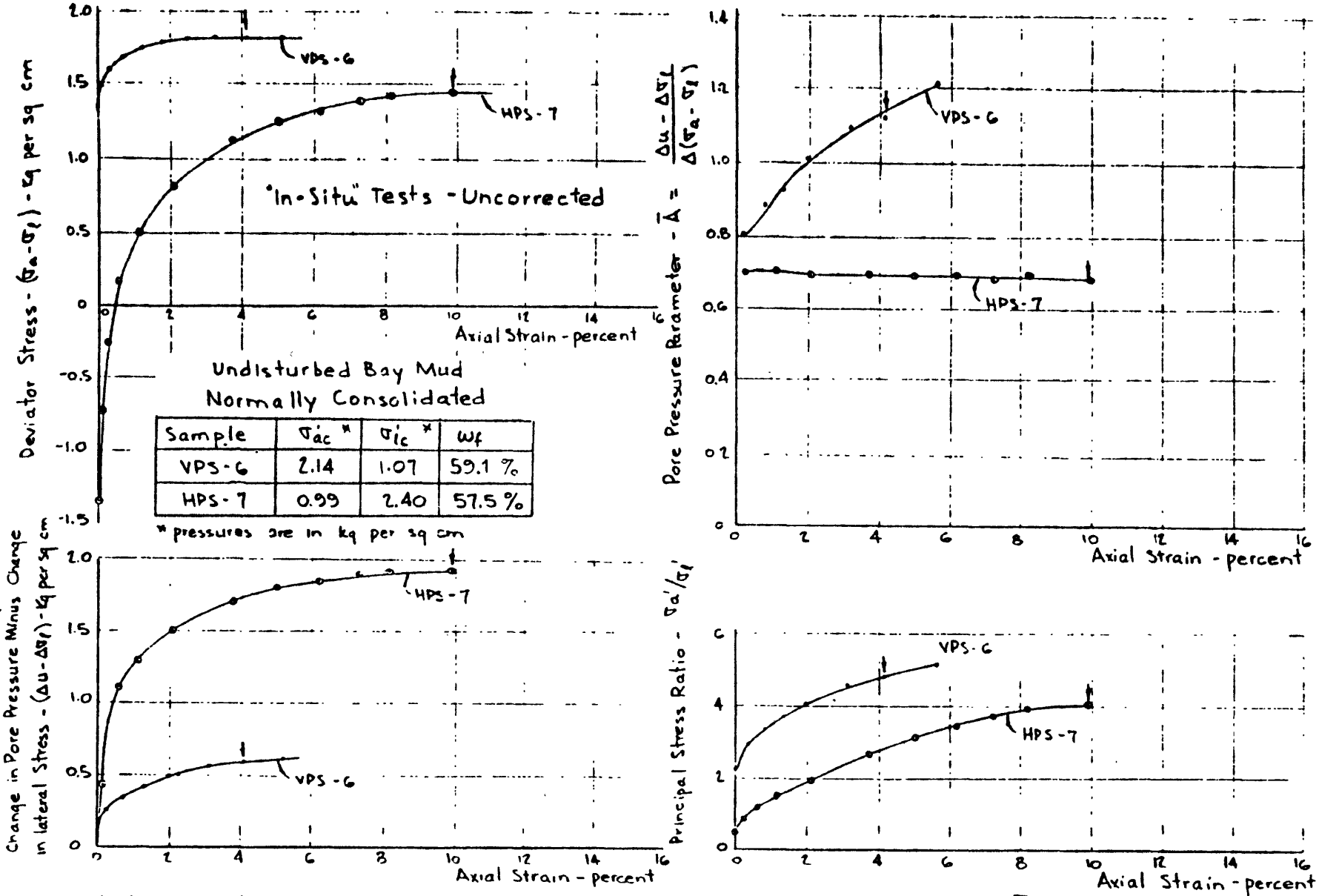
VARIATIONS OF DEVIATOR STRESS, PORE-WATER PRESSURE, PORE PRESSURE COEFFICIENT $\bar{A}$, AND EFFECTIVE PRINCIPAL STRESS RATIO WITH AXIAL STRAIN FOR HORIZONTAL AND VERTICAL "IN-SITU" PLANE STRAIN TESTS.

FIGURE 78 PLANE STRAIN $\overline{AC\text{-}U}$ TESTS PERFORMED BY DUNCAN (1965)



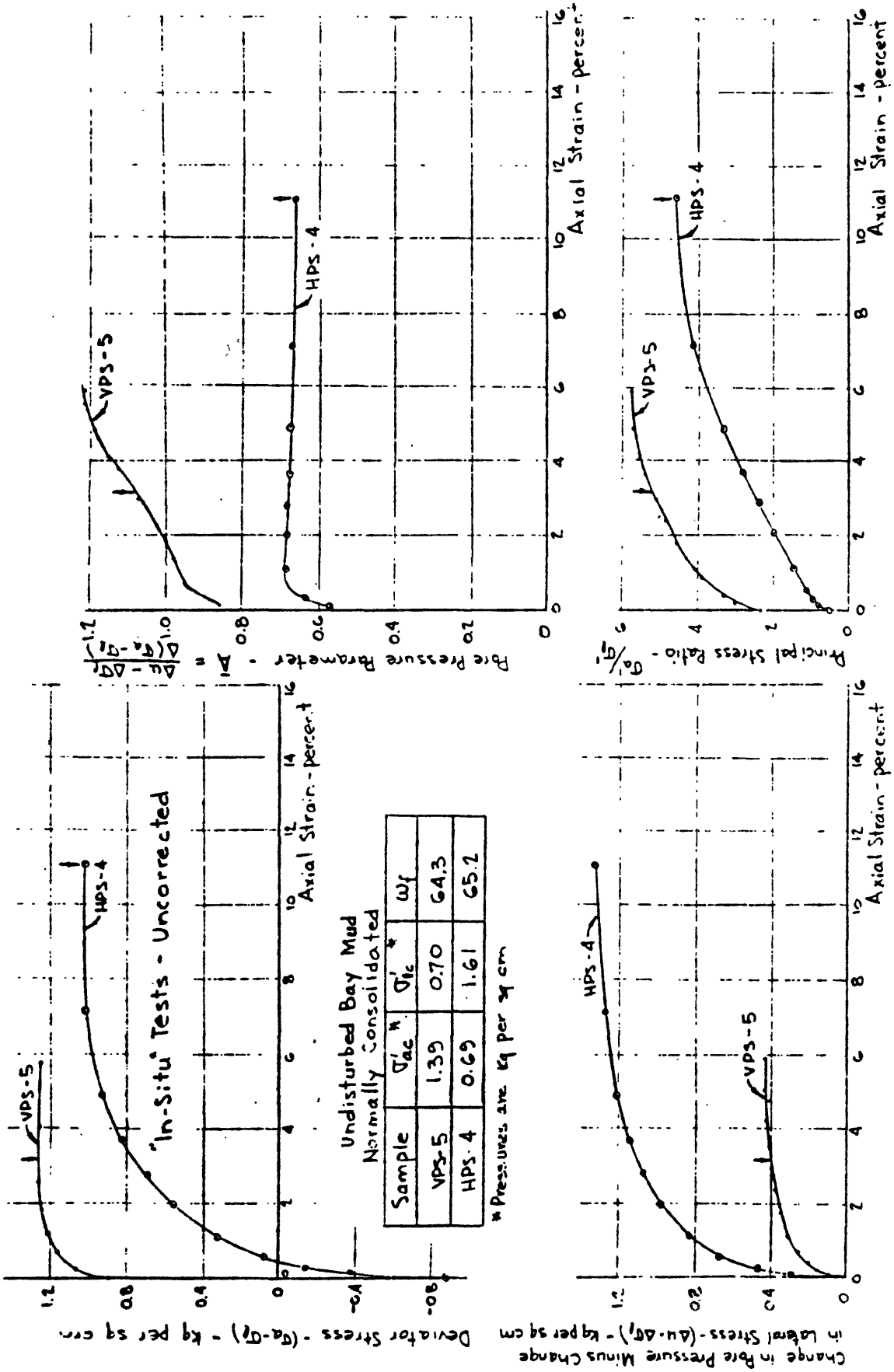
VARIATIONS OF DEVIATOR STRESS, PORE WATER PRESSURE, PORE PRESSURE COEFFICIENT $\bar{A}$, AND EFFECTIVE PRINCIPAL STRESS RATIO WITH AXIAL STRAIN FOR HORIZONTAL AND VERTICAL "IN-SITU" PLANE STRAIN TESTS.

FIGURE 79 PLANE STRAIN $\overline{AC\text{-}U}$ TESTS PERFORMED BY DUNCAN (1965)



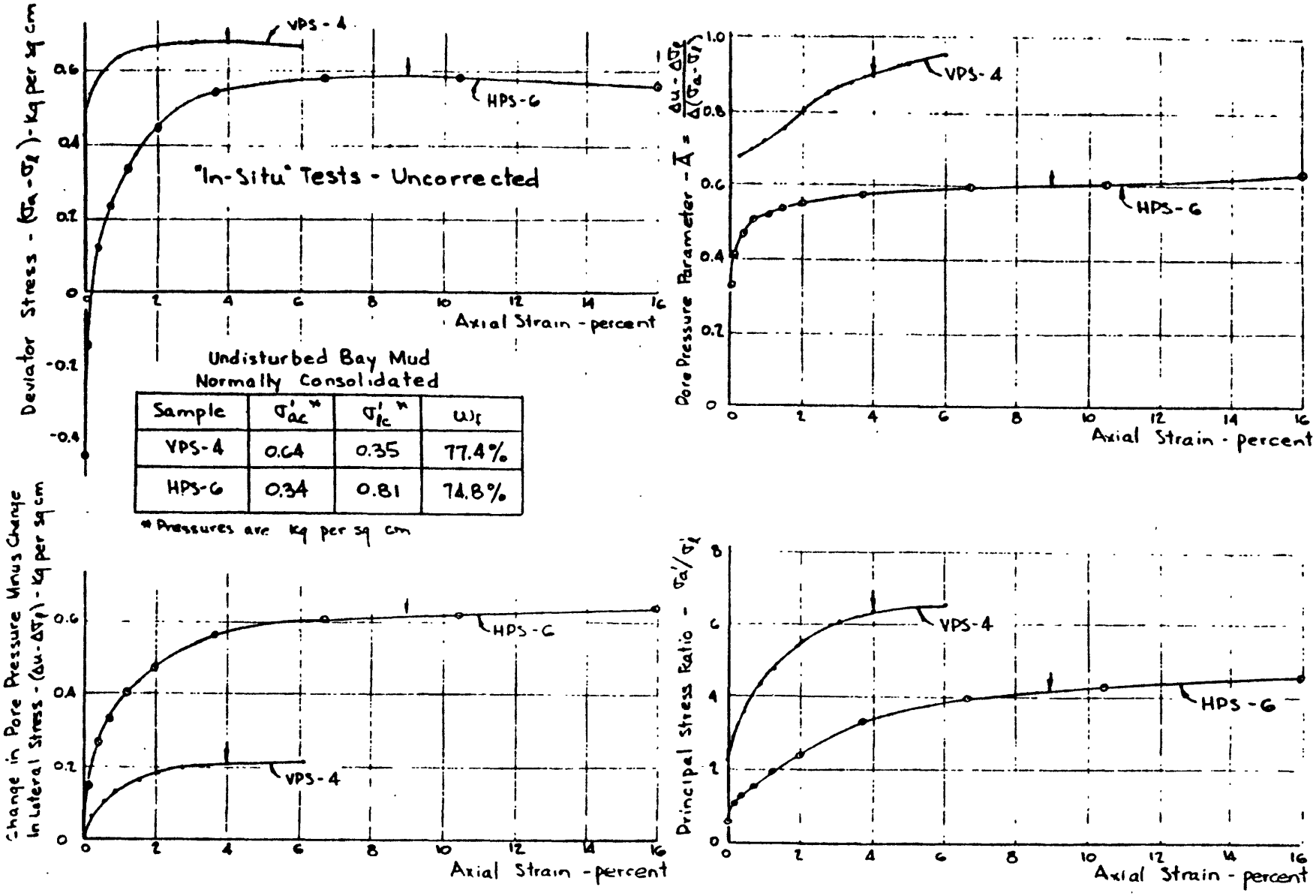
VARIATIONS OF DEVIATOR STRESS, PORE WATER PRESSURE, PORE PRESSURE COEFFICIENT $\bar{A}$, AND EFFECTIVE PRINCIPAL STRESS RATIO WITH AXIAL STRAIN FOR HORIZONTAL AND VERTICAL "IN-SITU" PLANE STRAIN TESTS.

FIGURE 80 PLANE STRAIN $\overline{AC\text{-}U}$ TESTS PERFORMED BY DUNCAN (1965)



VARIATIONS OF DEVIATOR STRESS, PORE WATER PRESSURE, PORE PRESSURE COEFFICIENT $\bar{A}$, AND EFFECTIVE PRINCIPAL STRESS RATIO WITH AXIAL STRAIN FOR HORIZONTAL AND VERTICAL "IN-SITU" PLANE STRAIN TESTS.

FIGURE 81 PLANE STRAIN $\overline{AC-U}$ TESTS PERFORMED BY DUNCAN (1965)



VARIATIONS OF DEVIATOR STRESS, PORE-WATER PRESSURE, PORE PRESSURE COEFFICIENT $\bar{A}$, AND EFFECTIVE PRINCIPAL STRESS RATIO WITH AXIAL STRAIN FOR HORIZONTAL AND VERTICAL "IN-SITU" PLANE STRAIN TESTS.

FIGURE 82 PLANE STRAIN $\overline{AC}$-$\bar{U}$ TESTS PERFORMED BY DUNCAN (1965)

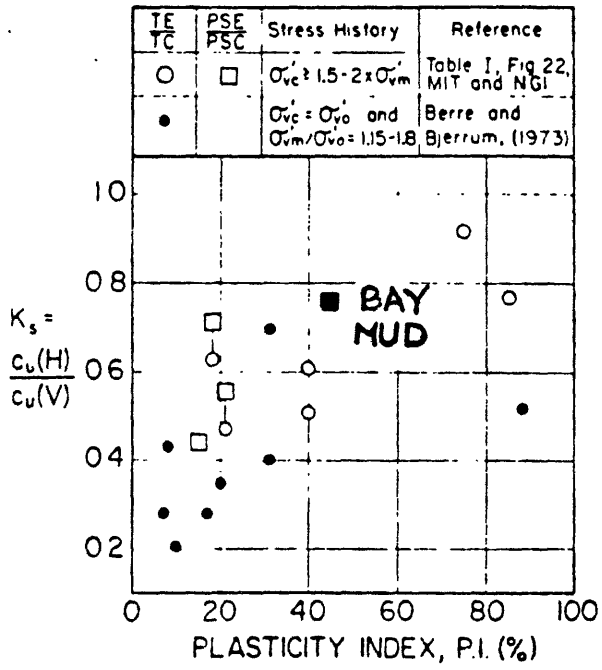


FIGURE 83 ANISOTROPIC UNDRAINED STRENGTH RATIO VS PLASTICITY INDEX

From Ladd (1977)

6. STRESS-STRAIN-TIME BEHAVIOR

Introduction

The effect of time on the behavior of Bay Mud manifests itself in many forms. These include creep, both drained and undrained, of soils subjected to a deviatoric stress component, creep rupture, stress relaxation, the effect of strain rate on strength and stress-strain behavior and the time dependent decrease in volume of soil undergoing one dimensional consolidation (secondary compression). Several of these factors have already been discussed. For instance, it was found that the coefficient of lateral earth pressure increased with time due to stress relaxation, a 10-fold increase in strain rate during shear caused an increase in strength of about 10 to 15 percent and as Figure 21 shows, the virgin compression curve which a soil follows is a function of the time that it has been subjected to a given set of stresses. In this section of the report the primary emphasis will be placed on the creep behavior of Bay Mud.

Creep Behavior of Bay Mud

Singh and Mitchell (1968) suggested that a general stress-strain-time function of the form given below, could be used to describe the creep behavior of cohesive soils. It is applicable to soils in which the stress level is great enough to cause sustained creep but is not so high that creep rupture is imminent, which is typically about 80 to 90% of the initial shear strength of the soil. The equation is,

$$\dot{\varepsilon} = Ae^{\alpha D} (t_1/t)^m$$

and upon integrating,

$$\varepsilon = \varepsilon_1 - \left(\frac{A}{1-m}\right) e^{\alpha D} + \left(\frac{A}{1-m}\right) e^{\alpha D} t^{(1-m)}; \; m \neq 1$$

$$\varepsilon = \varepsilon_1 + Ae^{\alpha D} \ln(t); \; (m = 1)$$

ε_1 = strain measured at unit time $t_1 = 1$

t = time

D = deviator stress

α = slope of the linear portion of the logarithm of strain rate vs. deviator stress plot

m = absolute value of the slope of the straight line relationship between the log of strain rate and the log of time

A = extrapolated value of strain rate for zero stress level in the linear plot of log strain rate vs. deviator stress for time t_1.

The parameter A is related to the soil and reflects the soils composition, structure and stress history. The parameter α, reflects the effect of stress intensity on creep rate. The speed with which the strain rate decreases with time is governed by the parameter m, which is found to lie between .75 and 1.25 for most soils. It is also a measure of the nonlinearity of a plot of strain vs. log time. For m = 1, strain will plot as a linear function of log time. For values other than 1, the relationship will be nonlinear. This behavior is illustrated in Figure 85. Furthermore, values of m less than 1 are indicative of soils succeptible to high strength loss during creep and eventual creep rupture (Singh and Mitchell, 1969).

Lacerda (1976) ran a series of creep tests on San Francisco Bay Mud and determined values for m, α and A. The tests were carried out in standard triaxial cells using the technique outlined by Singh and Mitchell (1968). The

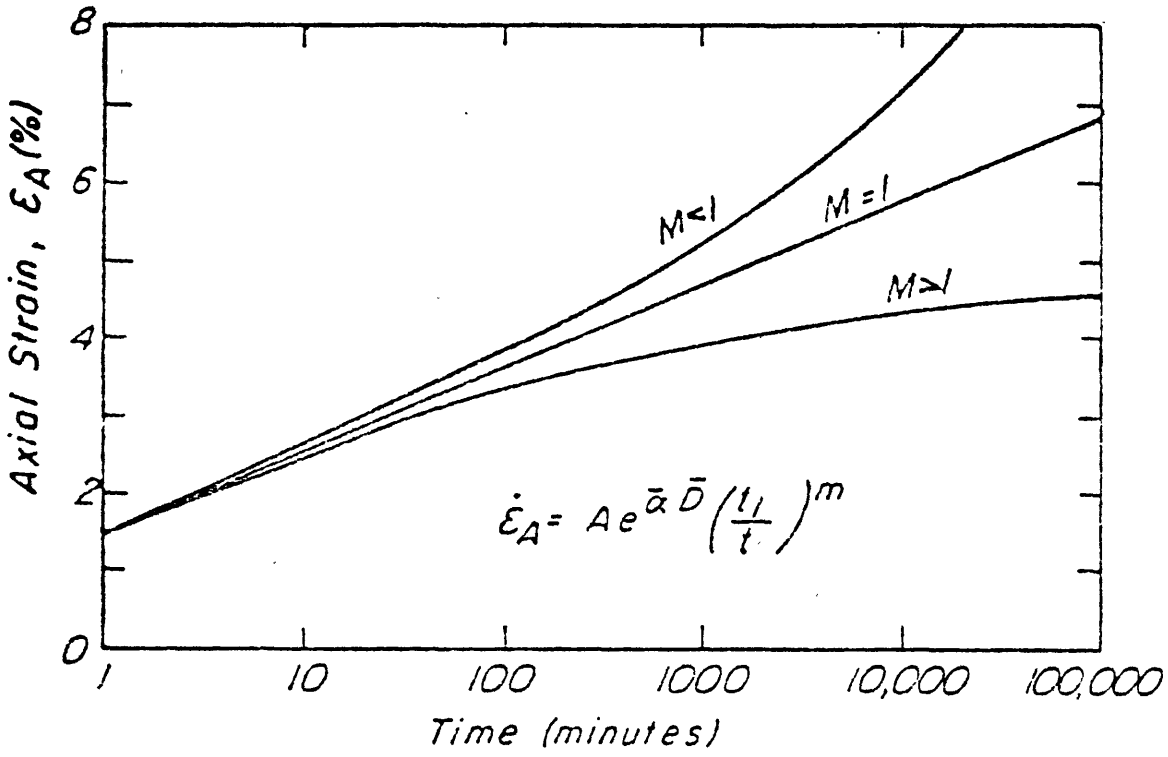


FIG. 85 EFFECT OF VALUE OF m IN SINGH-MITCHELL EQUATION ON SHAPE OF CREEP CURVE

From Kavazanjian (1978)

test specimens were trimmed from 5 inch diameter undisturbed piston samples obtained from the normally consolidated, unweathered zone of the Bay Mud profile. Samples were allowed to consolidate under isotropic conditions at pre-selected pressures and were then tested in one of two ways. At a consolidation pressure of .8 kg/cm^2 two creep tests were run in the conventional manner, whereby the minor principal stress is held constant and the major principal stress is increased to some value. At the same consolidation pressure six more creep tests were run holding the major principal stress constant and decreasing the minor principal stress. Creep tests with increasing major principal stress were also run on samples consolidated to pressures of 2.0 and 3.2 kg/cm^2. A series of tests on UU specimens were also performed.

The results of the tests performed by Lacerda are summarized in Table 18. Test results are shown in Figures 86 through 94. As can be seen in Figure 94 almost all of the results for the consolidated undrained specimens lie on a line with a value of $\bar{\alpha}$ of 4.45 ($\bar{\alpha} = \alpha$ x strength of sample before creep) and an intercept A = .0035%/minute. The results of the UU tests plot on a parallel lower line with $\bar{\alpha}$ = 4.45 and A = .0026%/minute. These results are in good agreement with the results of creep tests on Bay Mud presented by Mitchell and Singh (1968). They are also in agreement with the results of Holzer et al. (1973) for Bay Mud that was obtained from a location near the southern end of San Francisco Bay. The Bay Mud at this southern site had an L.L. = 99% and a P.L. = 47%. Its in-situ water content varied between 86% and 97% and its sensitivity was about 7. Holzer et al. obtained a value of A = .0030%/minute, m = .84 and $\bar{\alpha}$ = 5.8.

Lacerda concluded that for Bay Mud soil creep was not strongly influenced by the type of loading, the results being similar whether σ_1 is

TABLE 18 CREEP TESTS - SAN FRANCISCO BAY MUD

σ_c' kg/cm^2	Test	D kg/cm^2	D_f kg/cm^2	$\bar{D}$	m	$\dot{\varepsilon}$ (t=1) %/min	A %/min	α cm^2/kg	$\bar{\alpha}$
0.8	SR-1-3	.312	.625	.50	.810	.032	.0035	7.2	4.5
	CR-1-3	.375		.60	.781	.055 σ_1 = const		6.7	
	SR-1-2	.437		.70	.775	.077 σ_3 decreasing			4.45
	CR-1-4	.500		.80	.790	.13			
	CR-1-5	.562		.90	-	.21			
	CR-1-6	.595		.95		.26			
0.8	CR-1-1	.375	.625	.60	.860	.065 σ_3 = const			4.45
	CR-1-2	.500		.80	.755	.115 σ_1 increasing			
2.0	CR-71-1	1.125	1.5	-.75	.707	.110		3.0	4.45
	CR-71-2	0.75	1.5	-.50	.733	.032			
2.5	9-7-PD-1	1.4	1.7	-.82	.71	.13			
3.2	CR-10	.96	2.24	.43	.74	.028	.0038	2.0	4.48
	CR-11	1.68	2.24	.75	.76	.1			
UU		.217	.395	.55	.89	.032	.0026	11.22	4.45
		.276	.395	.70	.88	.055			
		.336	.395	.85	-	.12			

FROM LACERDA (1977)

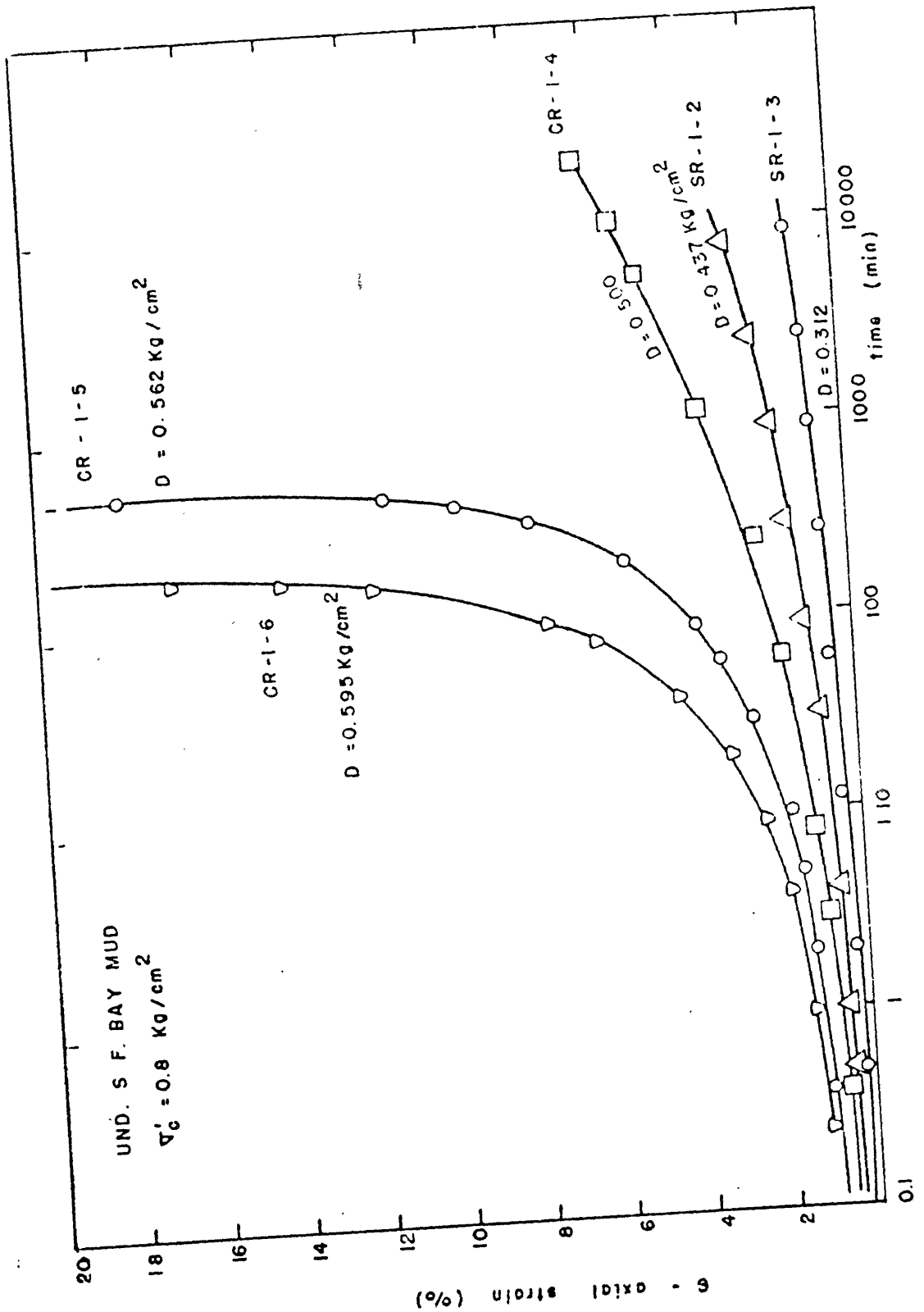


FIGURE 86 STRAIN X LOG TIME FOR CREEP TESTS ON S.F. BAY MUD

From Lacerda (1976)

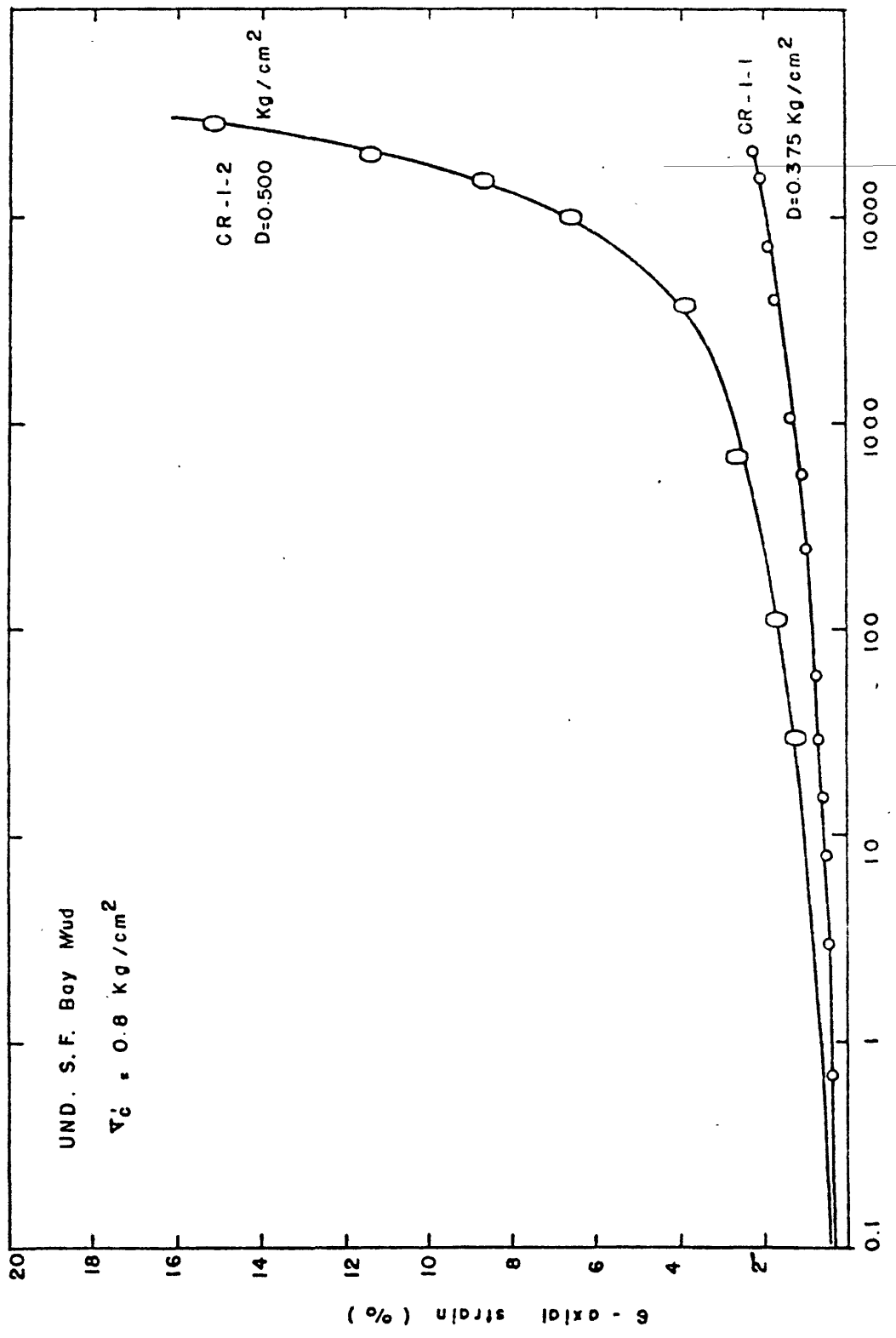


FIGURE 87 STRAIN X LOG TIME FOR CREEP TESTS ON S.F. BAY MUD

From Lacerda (1976)

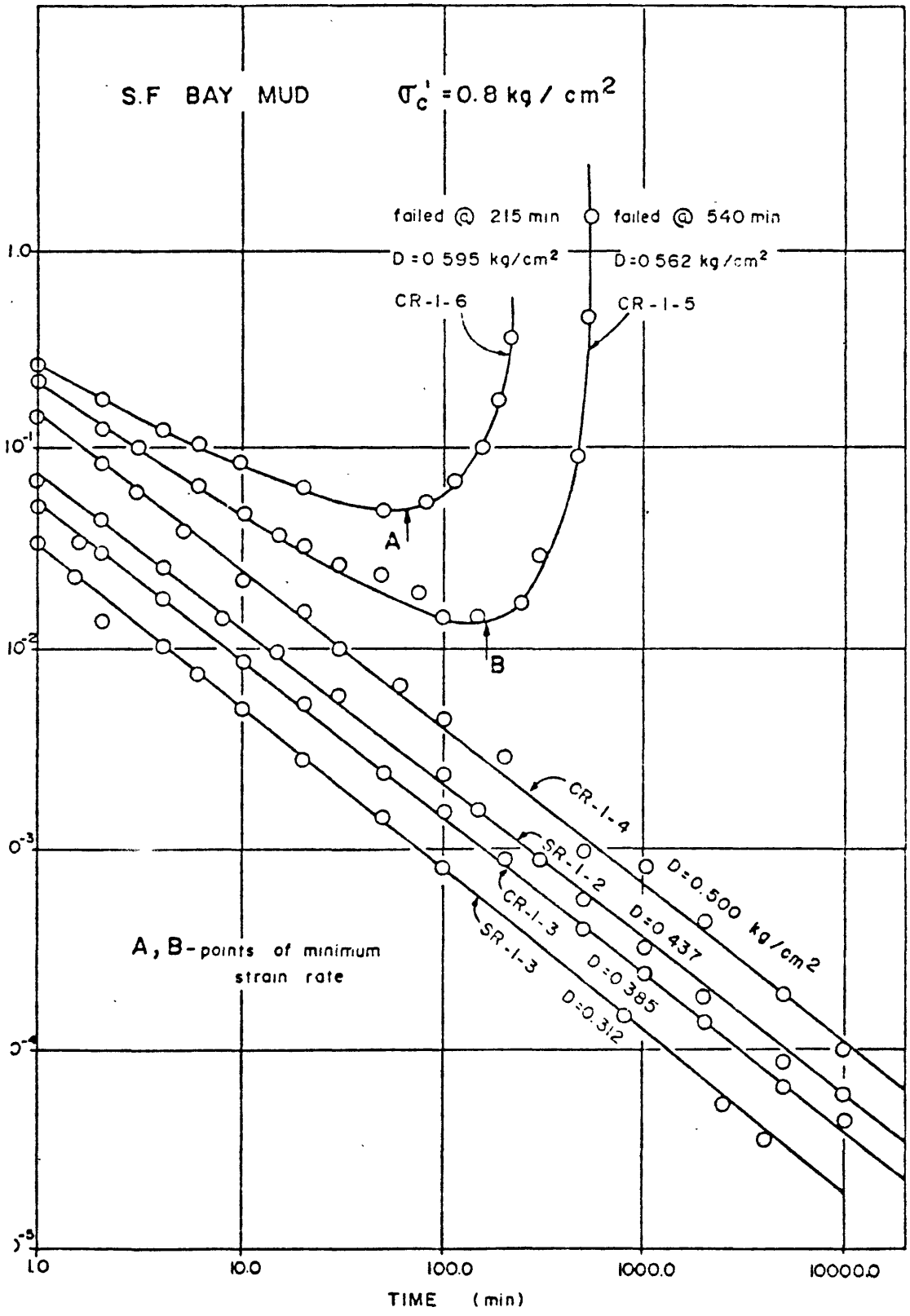


FIGURE 88 LOG STRAIN RATE X LOG TIME - S.F. BAY MUD TESTS WITH σ_1 = CONST.

From Lacerda (1976)

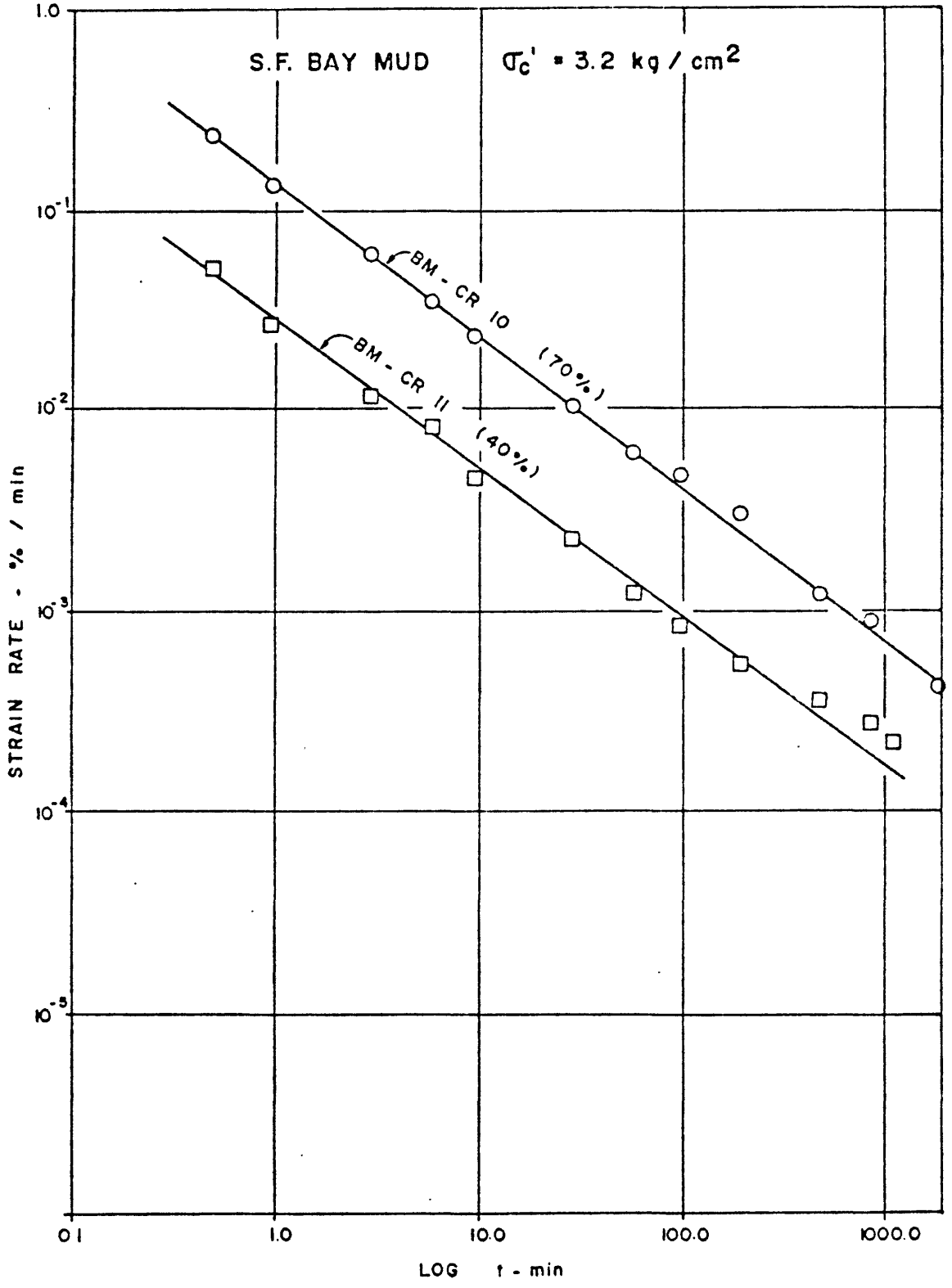


FIGURE 91 LOG STRAIN RATE X LOG TIME S.F. BAY MUD σ_c' = 3.2 kg/cm²

From Lacerda (1976)

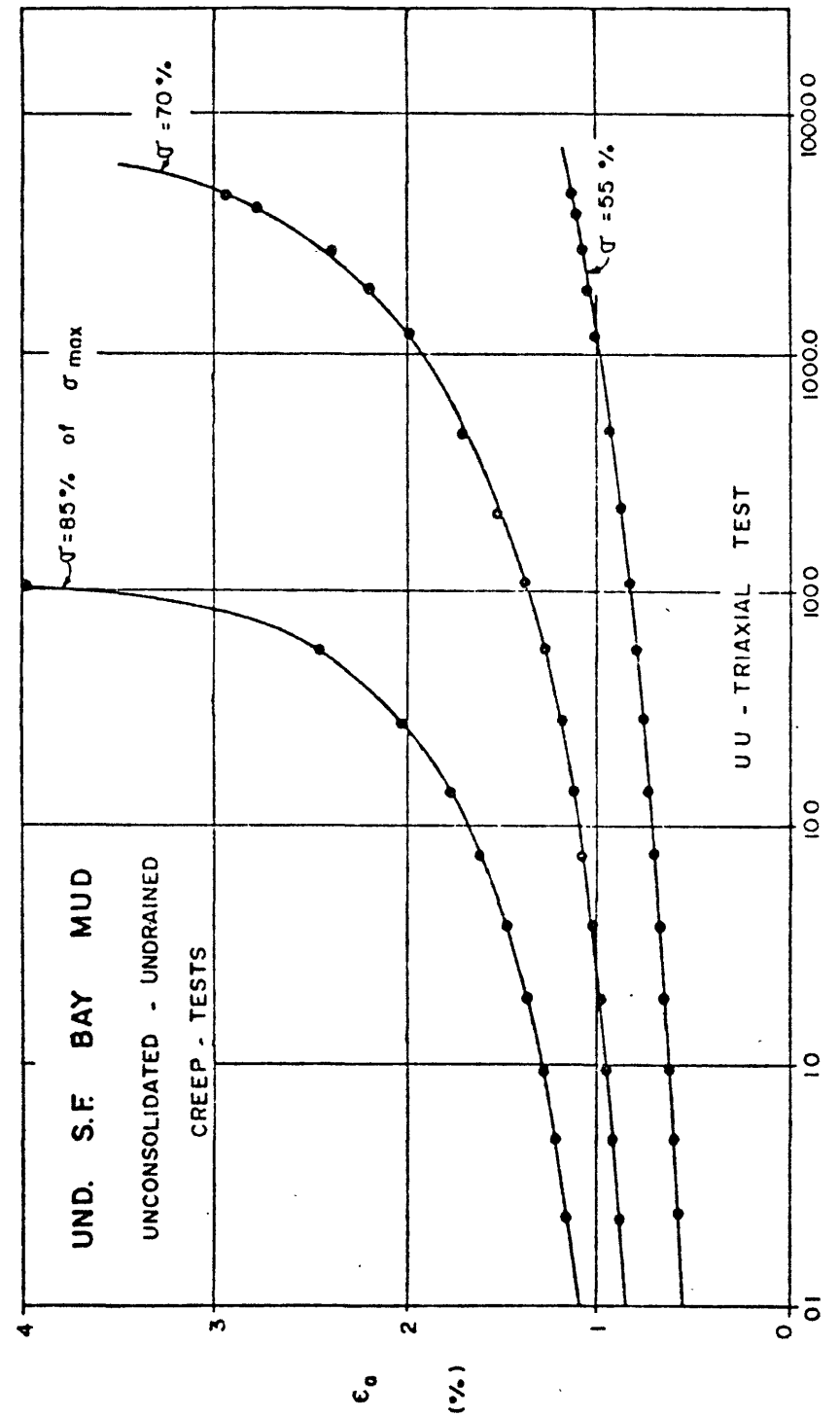


FIGURE 92 AXIAL STRAIN X LOG t CURVES FOR CREEP TESTS ON UU SPECIMENS OF S.F. BAY MUD

From Lacerda (1976)

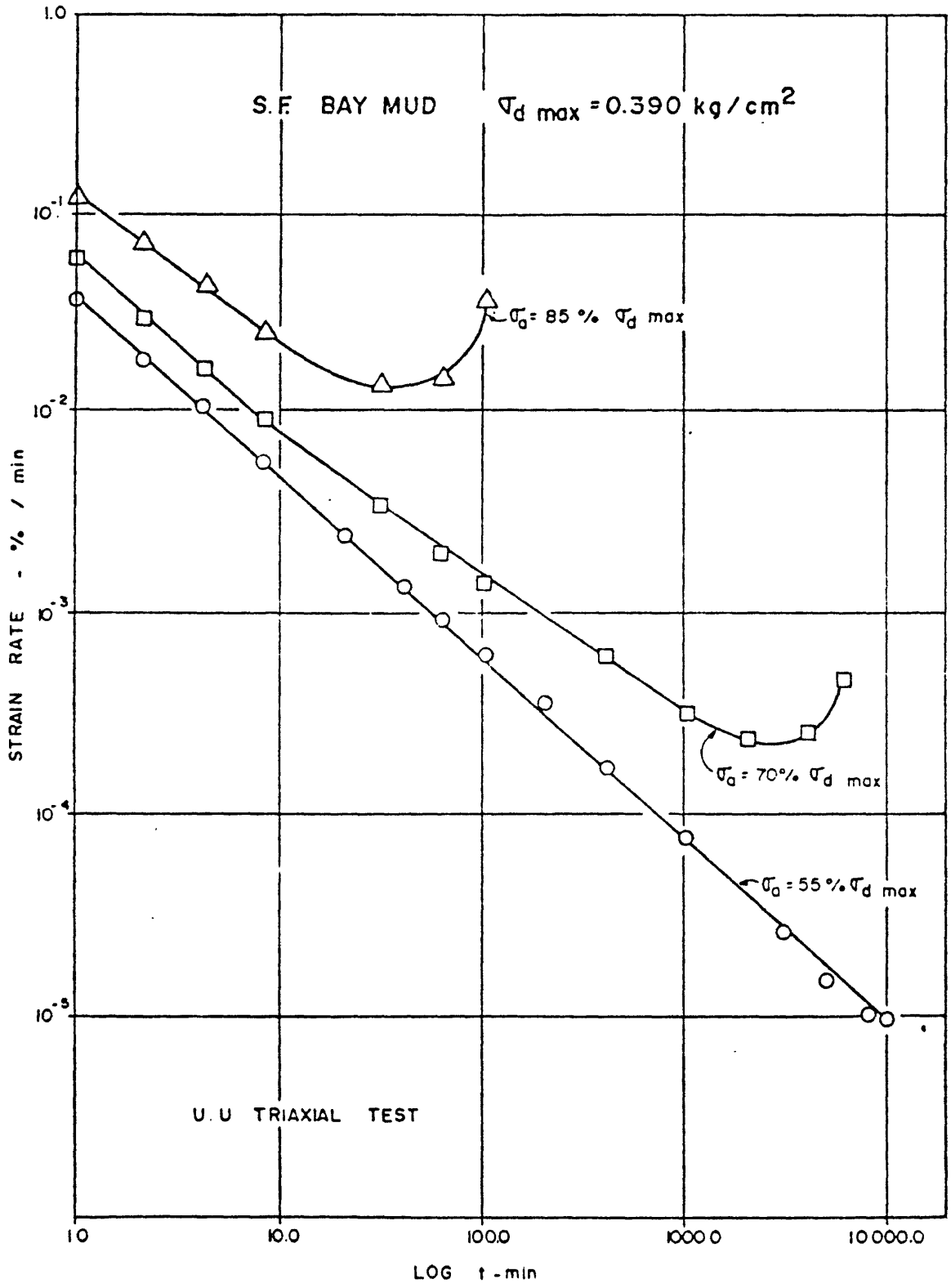


FIGURE 93 LOG STRAIN RATE X LOG TIME S.F. BAY MUD UU SPECIMENS

From Lacerda (1976)

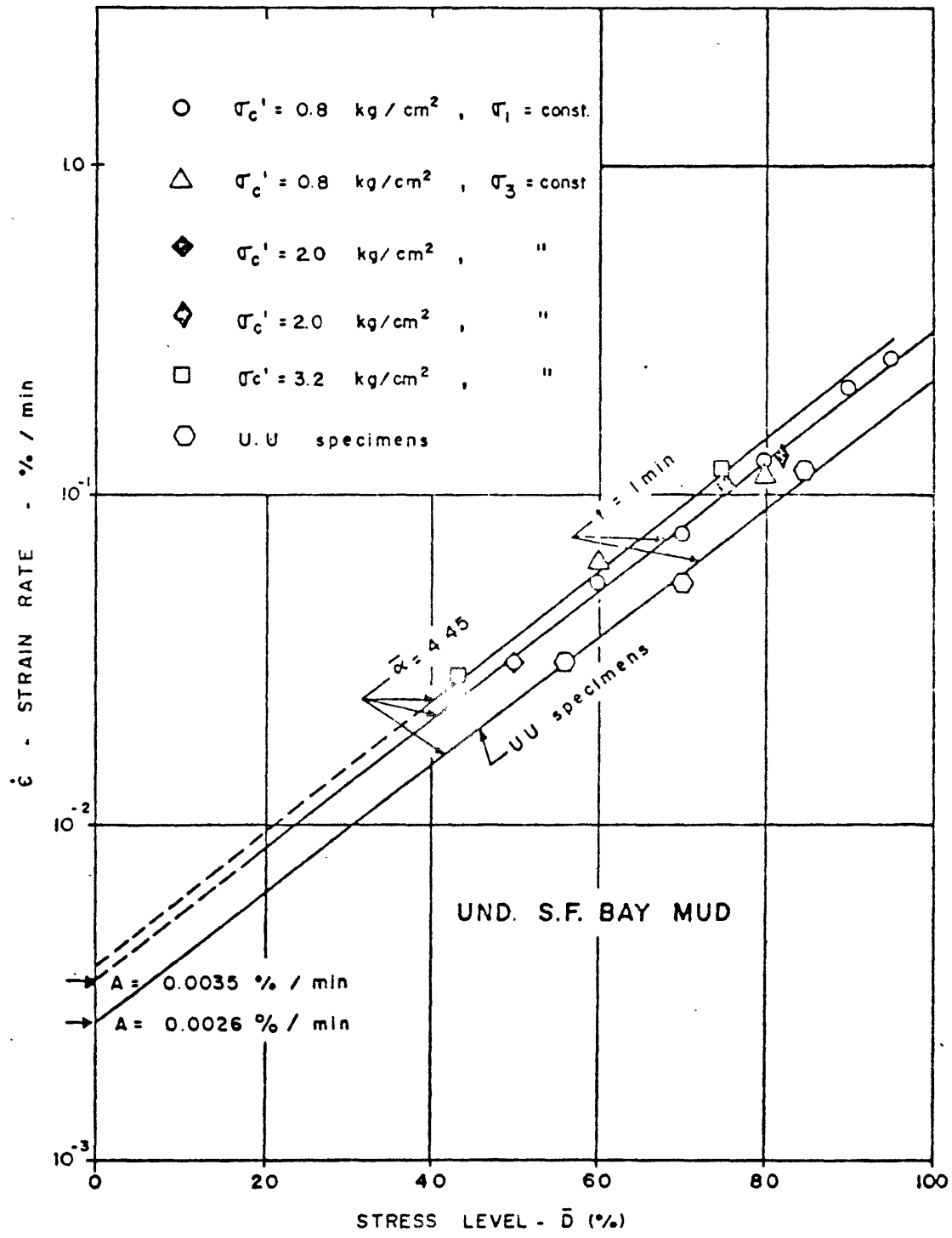


FIGURE 94 STRESS LEVEL X LOG STRAIN RATE FOR UNDISTURBED S.F. BAY MUD

From Lacerda (1976)

increased and σ_3 is held constant or σ_3 is decreased while σ_1 is held constant. The effects of partial drainage were studied and it was found that drainage of an element of soil subjected to a given shear stress yields lower creep strain rates than for an element of soil subjected to the same shear stress and with the same initial water content and no drainage during the test.

Singh (1967) carried out tests to determine the importance of stress path and temperature path on creep behavior. He concluded that although the short term creep behavior was influenced by stress and temperature changes, the long term creep behavior is fairly independent of stress and temperature path, and is instead primarily a function of the maximum, final stress and temperature to which the soil is subjected. This is an important conclusion in regard to foundation construction. In actual construction the load is applied in steps. The results of Singh's work indicates that when it is not possible or practical to simulate the entire temperature-load history of a foundation soil element, a reasonable approximation can probably be achieved by simulating the ultimate temperature-load conditions.

As part of his thesis work, Singh (1967) ran several undrained creep tests on Bay Mud from HAFB. His tests were performed on soil samples consolidated to pressures of .5, 1, 2, 4 kg/cm^2 in conventional triaxial cells. The soils were then subjected to various deviatoric stress intensities and the deformation of the samples with time were measured under undrained conditions. His results are given in Figures 95 and 96 and compare well with the results obtained by Lacerda.

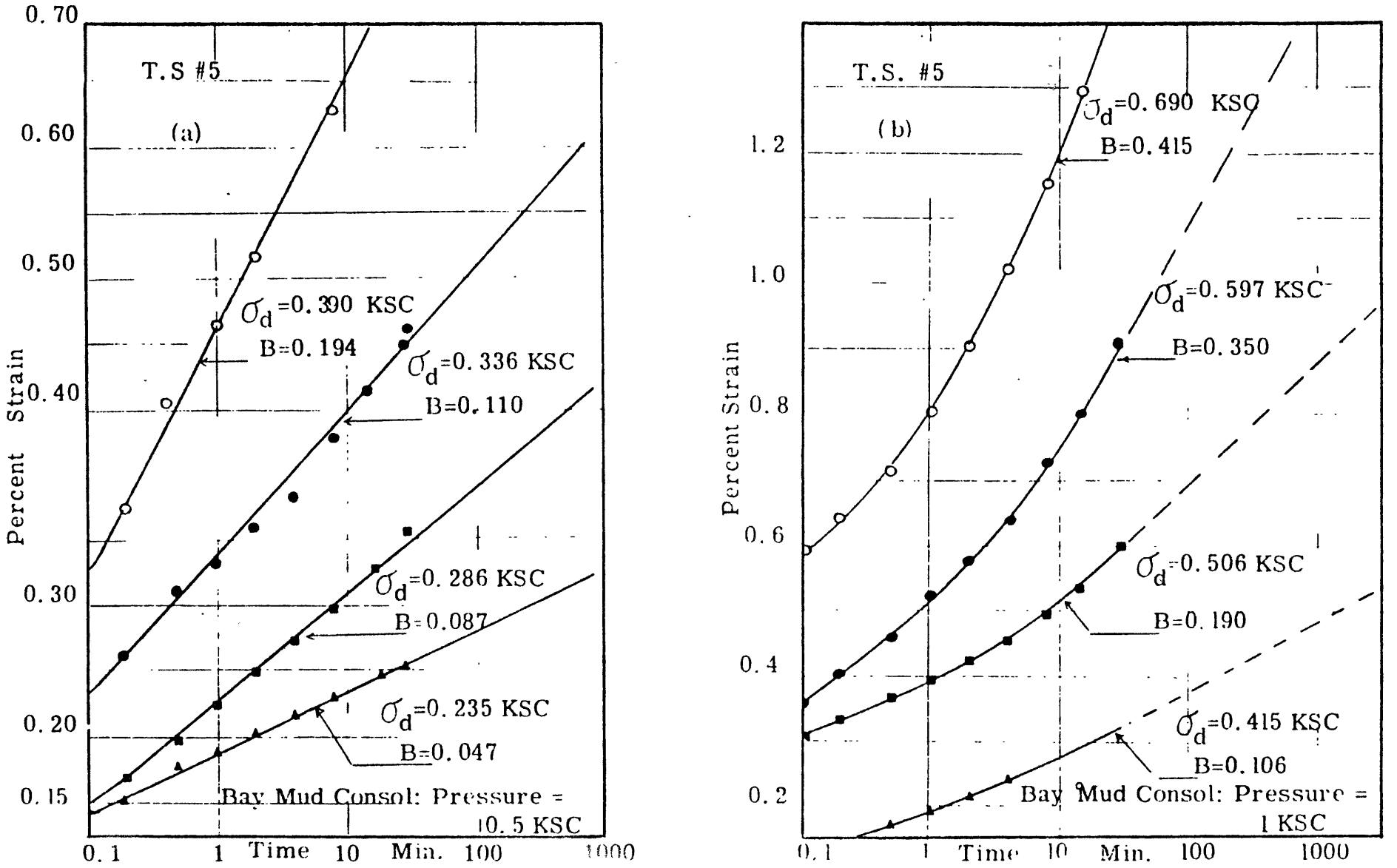
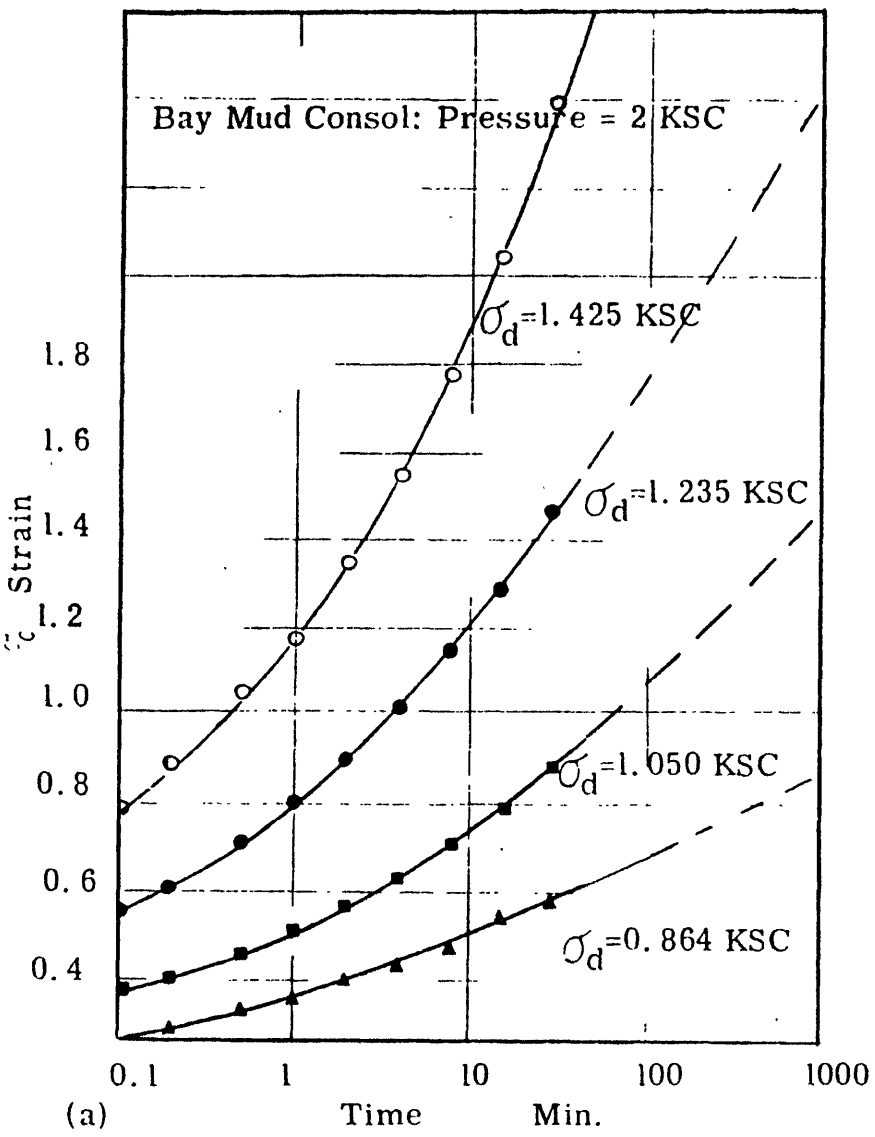


FIGURE 95 CREEP CURVES FOR NORMALLY CONSOLIDATED BAY MUD

From Singh (1967)



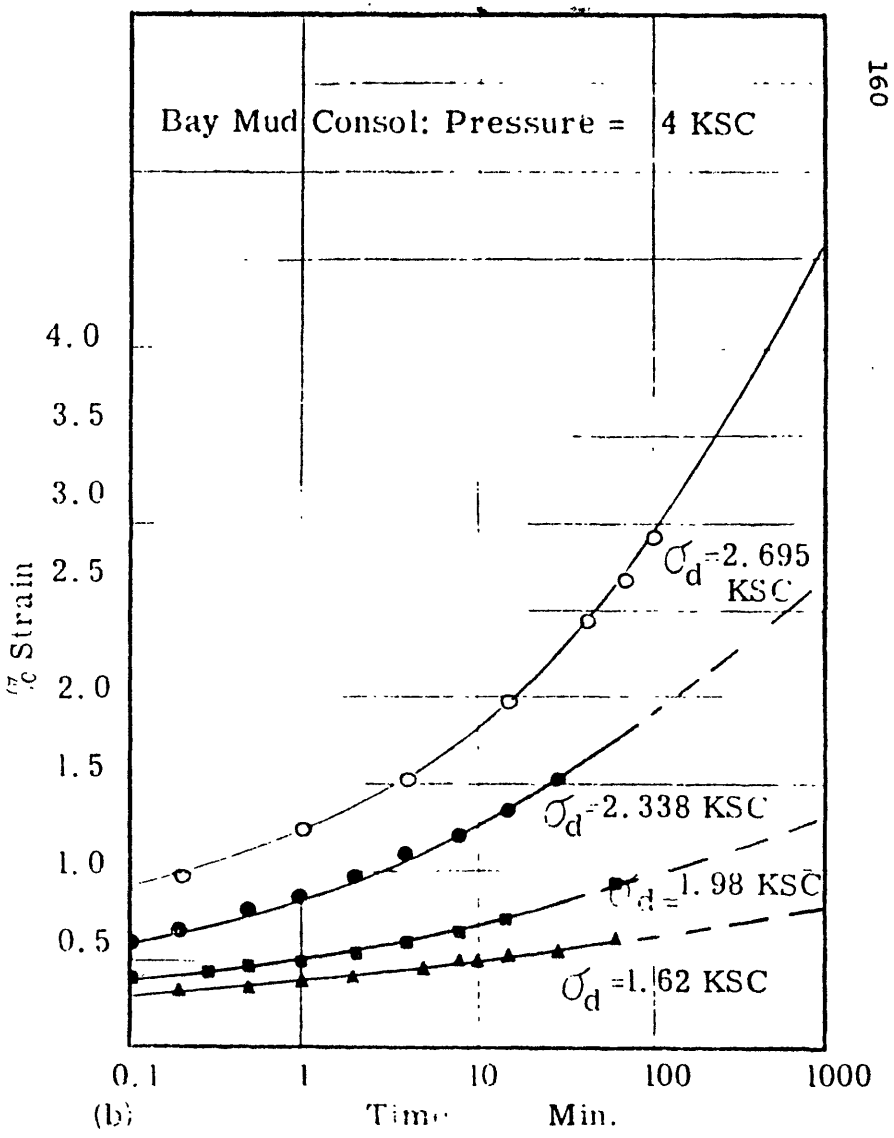


FIGURE 96 CREEP CURVES FOR NORMALLY CONSOLIDATED BAY MUD

From Singh (1967)

Creep Behavior of Remolded Bay Mud

Kavazanjian (1978) and Singh (1966) ran undrained creep tests on remolded samples of Bay Mud. Kavazanjian's results are shown in Figures 97 through 99, while Singh's results are shown in Figure 100. Using Kavazanjian's results along with the Singh-Mitchell phenomenalogical equation, values of m = .73

$$\varepsilon = \varepsilon_1 + \frac{A}{1-m} e^{\alpha D} \left[(t)^{1-m} - 1 \right]$$

$\bar{\alpha}$ = .54 and A = 8.8 x 10^{-4}%/minute were obtained.

With these results the undrained creep behavior of remolded Bay Mud under a given deviatoric stress can be calculated.

Creep Rupture

Creep rupture may be an important consideration for geotechnical designs in Bay Mud. This point was made clear by Duncan and Buchignani (1973) in their investigation of the failure of an underwater slope in San Francisco Bay. In investigating the failure at the LASH terminal, Port of San Francisco the authors ran a series of UU triaxial creep tests. The soil at the site was Bay Mud with properties reasonably similar to those at the HAFB site. The results of these tests are shown in Figure 101.

As can be seen in this figure the shearing resistance decreases with increasing time to failure, and for loads maintained for a week or longer the shear strength of the soil is reduced to about 70% of the value measured in conventional UU triaxial tests. This reduction in shear strength was enough to cause failure of the underwater slope.

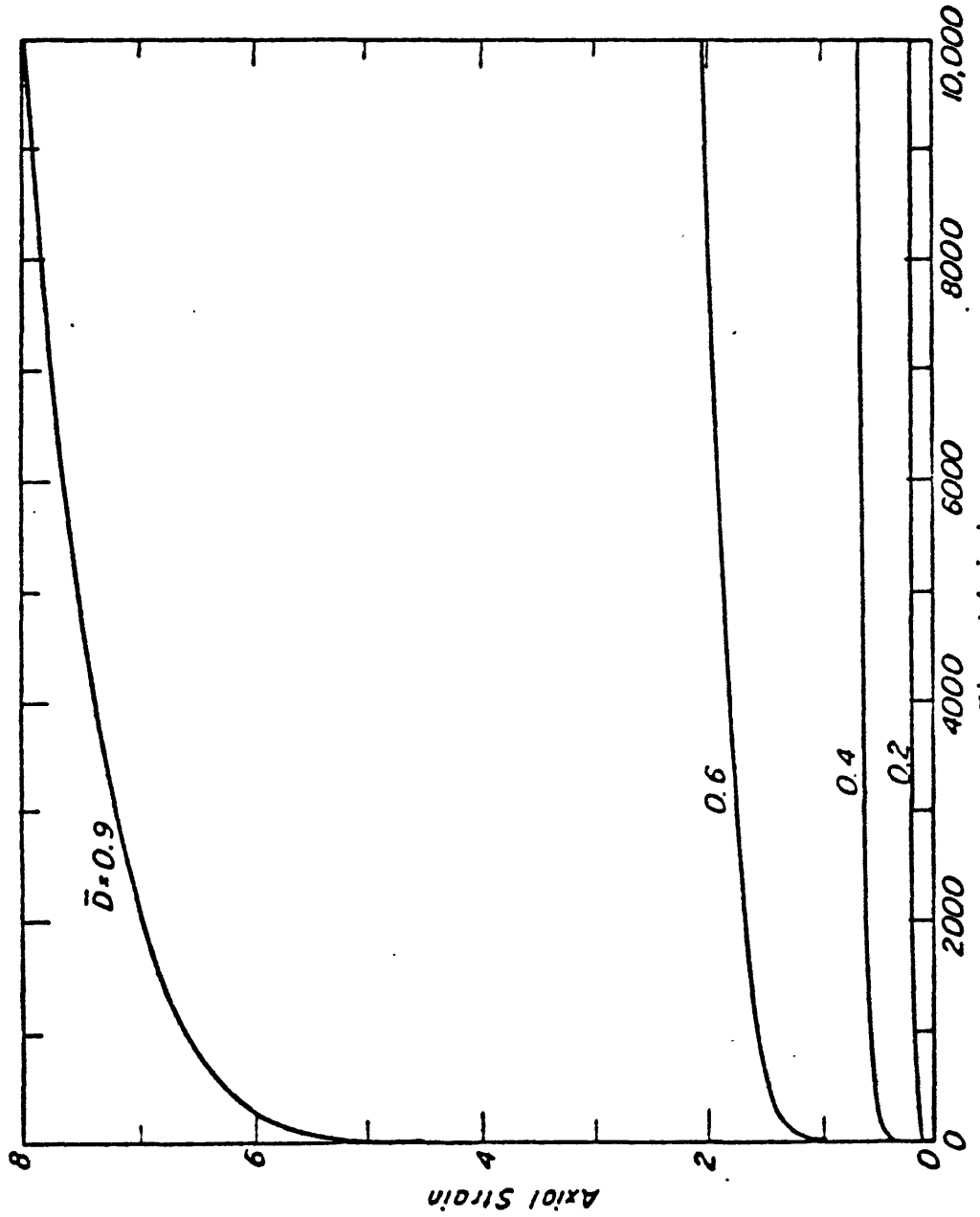


FIGURE 97 AXIAL STRAIN VERSUS TIME FOR UNDRAINED CREEP OF REMOLDED SAN FRANCISCO BAY MUD

From Kavazanjian (1978)

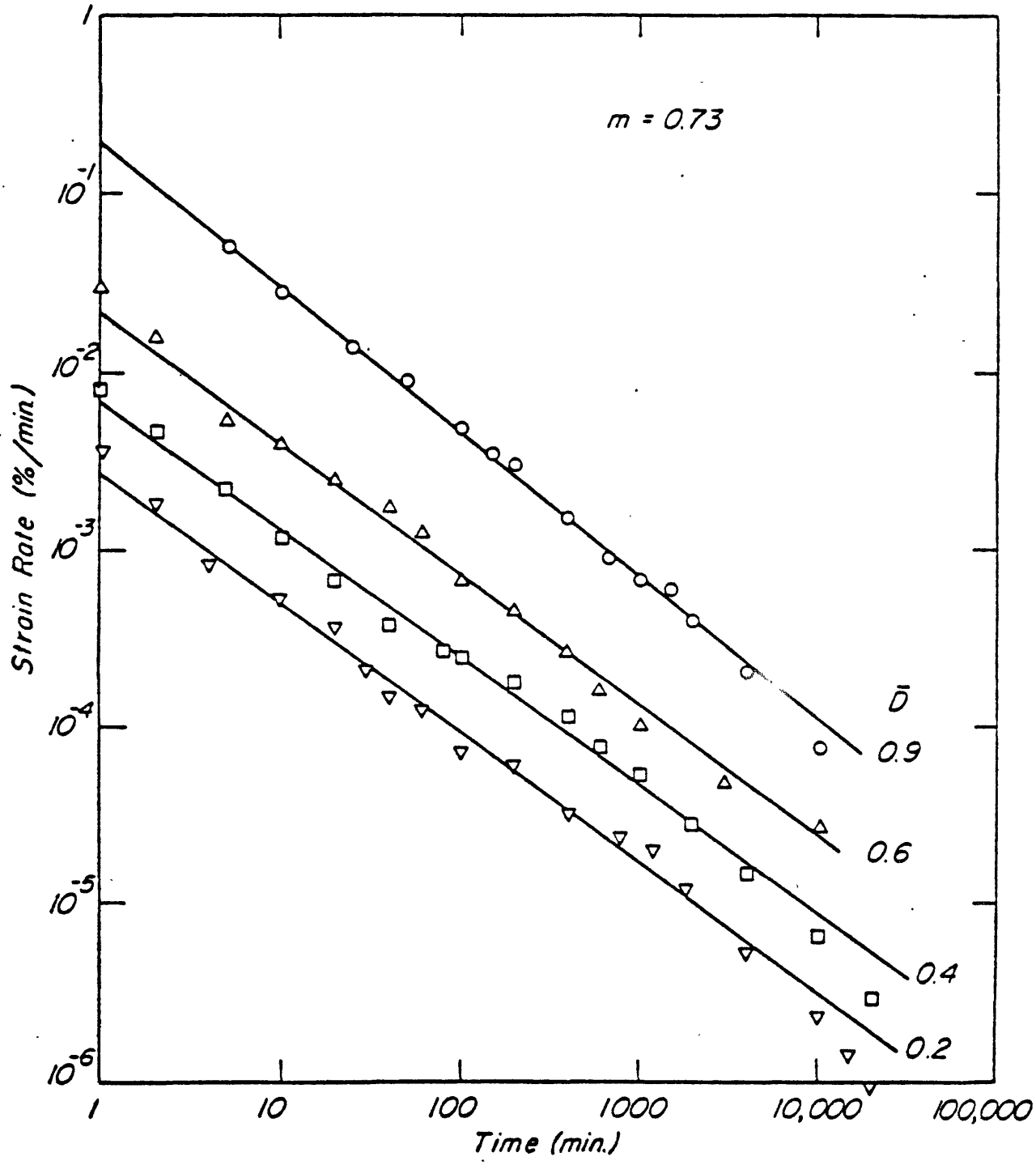


FIGURE 98 LOG STRAIN RATE VERSUS LOG TIME FOR UNDRAINED CREEP OF REMOLDED SAN FRANCISCO BAY MUD

From Kavazanjian (1978)

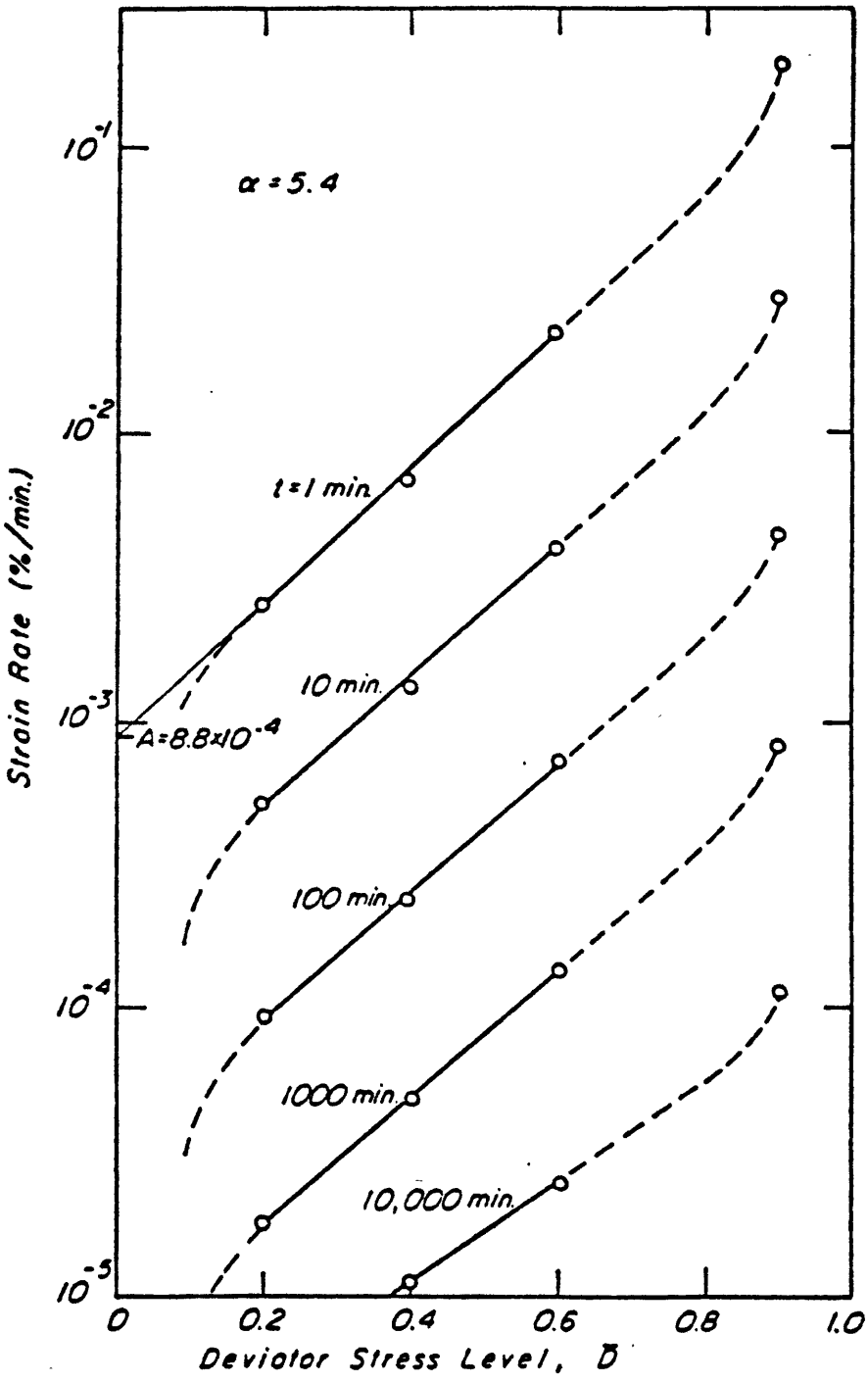


FIGURE 99 DEVIATOR STRESS LEVEL VERSUS LOG STRAIN RATE FROM UNDRAINED CREEP TESTS ON REMOLDED SAN FRANCISCO BAY MUD

From Kavazanjian (1978)

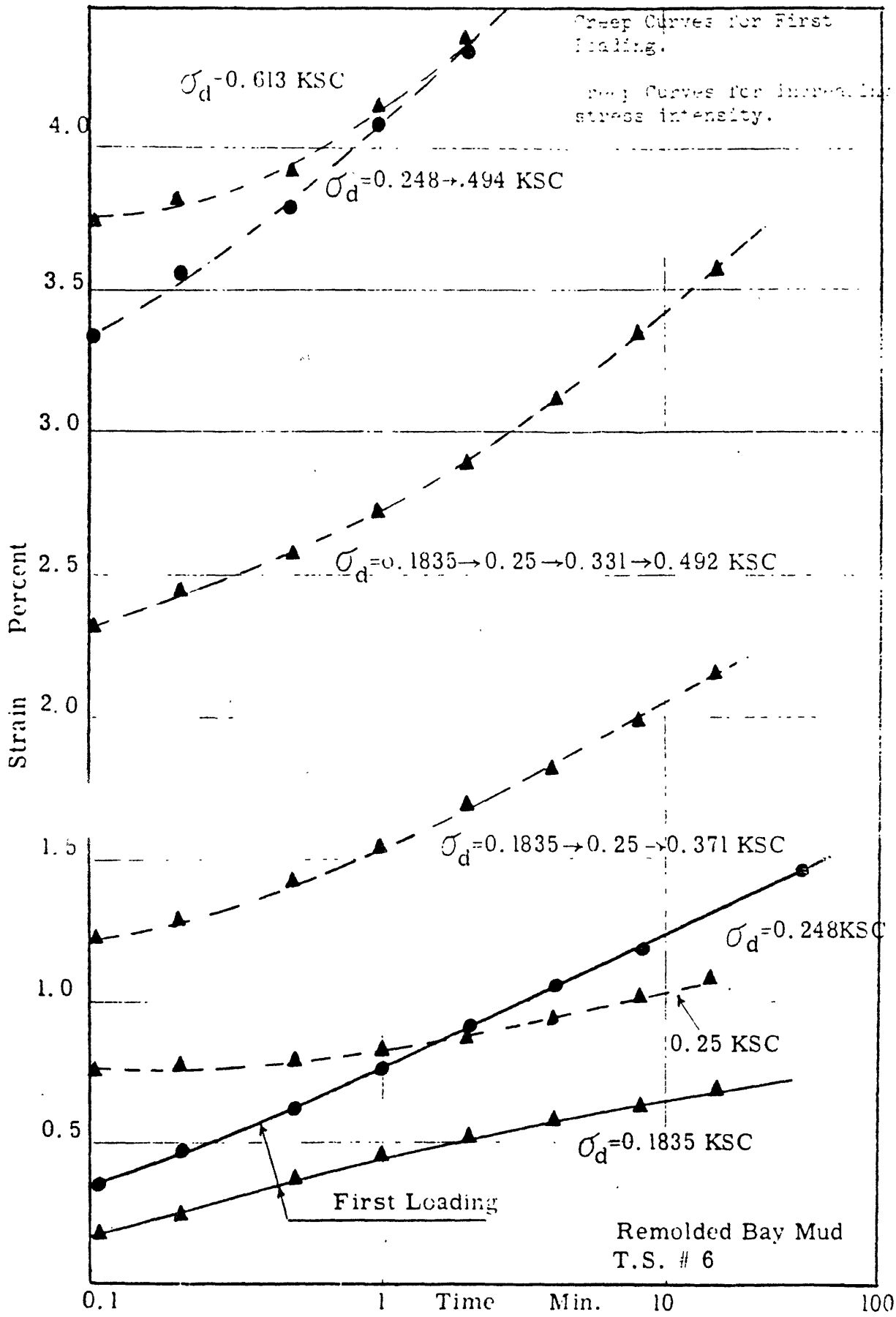


FIGURE 100 CREEP CURVES FOR REMOLDED BAY MUD

From Singh (1967)

Singh and Mitchell (1969) present a method for predicting the time for creep rupture to occur in soils. It involves plotting the log of ($\dot{\varepsilon}t$) versus the log of time and observing the time at which a certain critical value of ($\dot{\varepsilon}t$) is reached. Details of the method are not included here, however, it is noted that their analysis shows that for $m < 1$ (Bay Mud falls into this category), the logarithmic time to failure is a linear function of the stress intensity; the higher the stress level the shorter being the time to failure. For a more complete discussion of creep rupture reference should be made to Mitchell (1976).

To date, no comprehensive study of the creep rupture characteristics of Bay Mud has been performed. However, the results of creep tests that have ended in failure, from the work of Duncan and Buchignani (1973), Arulanandan et al. (1971), Holzer et al. (1973) and Lacerda (1976), can be used to obtain an estimate of the time to failure of Bay Mud when subjected to sustained loads. These results are plotted in Figure 101.

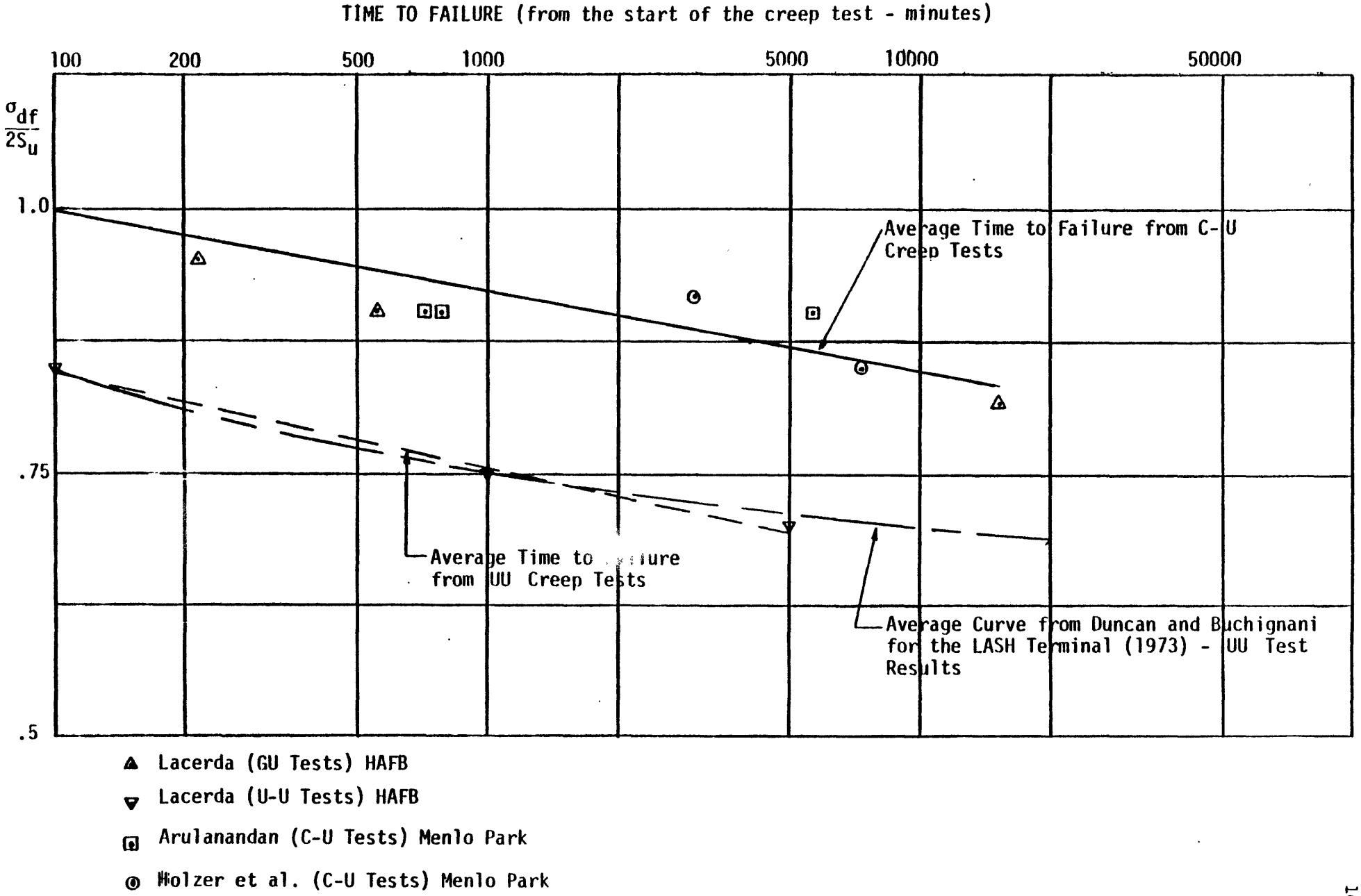


FIGURE 101 CREEP RUPTURE BEHAVIOR OF UNDISTURBED BAY MUD. DATA FROM VARIOUS SOURCES.

7. SUMMARY

This report summarizes the engineering properties of the San Francisco Bay Mud that underlies Hamilton Air Force Base, Novato, California.

At this site the Bay Mud is a soft to very soft, gray silty clay with some small silt lenses and microscopic pieces of shells and other matter. The depth of the deposit is about 58 feet and the water table fluctuates seasonally between 0 and 12 feet, at most times being between 4 and 8 ft. The upper few feet of the deposit are weathered and desiccated. Preconsolidation pressures indicate that the effect of desiccation extends to a depth of between 15 and 18 feet. Below 18 to 20 feet the deposit is very nearly normally consolidated.

A summary of some of the pertinent engineering properties of the Bay Mud are presented in Table 19. These results have been presented in detail in the text. It has been observed that the effective stress-sensitivity-liquidity index interrelationship found in Bay Mud is similar to that obtained for other soft clays, while the effective stress strength parameter, ϕ', is somewhat larger than for many other soils with similar index properties. The Bay Mud is a highly compressible soil and has a compressibility that decreases somewhat with increases in the logarithm of effective stress. The soil has been found to have a high secondary compressibility. It also exhibits significant creep under sustained loads, and under very high stress levels may undergo creep rupture. The creep behavior of Bay Mud has been characterized herein by means of the Singh-Mitchell (1968) creep equation.

TABLE 19 SUMMARY OF ENGINEERING PROPERTIES OF S.F. BAY MUD AT THE UNIVERSITY OF CALIFORNIA HAMILTON AIR FORCE BASE TEST SITE

Property	Value
Thickness of Deposit	55-58 ft
Depth of Water Table	0-12 ft
Winter Average	4-6 ft
Summer Average	8 ft
Saturated Unit Weight	94 pcf
Natural Water Content (%)	90
Liquid Limit (%)	88
Plasticity Index (%)	40
Liquidity Index (%)	1
Organic Content (Total carbon - %)	1.5
Compression Index C_c	
Just past p_p'	1.2-1.8 (1.5~average)
For $p' > 2\text{-}3$ kg/cm^2	.8-.9
Recompression Index C_r	.10-.15
Coefficient of Secondary Compression C_α	.01-.02
Coefficient of Consolidation, C_v	8-10 ft^2/year
Effective Stress Friction Angle, ϕ'	
Consolidated undrained triaxial	32.5°-35° (34° average)
Vertical Plane Strain C-U	38°
Horizontal Plane Strain C-U	35°
Consolidated Drained	31°
Undrained Strength Ratio $S_u/\bar{p}'$	
IC-U	.34
AC-U (K_o)	.35
UU	.32
Field Vane	.31-.32
Cone Penetrometer	.31-.32
Self Boring Pressuremeter	.40
IC-U Data Extrapolated (to an OCR of 1.1-1.5)	.36-.42

TABLE 19 (Cont'd.)

Property	Value
Undrained Strength Ratio-Continued	
Vertical Plane Strain	.29
Horizontal Plane Strain	.37
Creep Parameters (Undrained Creep on CU Samples)	
α	4.45
A	.0035%/minute
m	.7-.8
Overconsolidation Ratio	
Crust	3
"Normally Consolidated Zone	1.0-1.5
In-Situ Lateral Stresses	See Text
Modulus Multiplier M ($E = MS_u$)	See Text

BIBLIOGRAPHY

1) Arulanandan, K., Shen, C. K., and Young, R. B. (1971), "Undrained Creep Behavior of a Coastal Organic Silty Clay," Geotechnique, 21(4), pp. 359-375.

2) ASCE (1975), "Proceedings of the Conference on In Situ Measurement of Soil Properties," Raleigh, N.C.

3) Bjerrum, L. (1954), "Geotechnical Properties of Norwegian Marine Clays," Geotechnique, Vol. 4, pp. 49-69.

4) Bjerrum, L. (1967), "Engineering Geology of Norwegian Normally Consolidated Clays as Related to Settlement of Buildings," Geotechnique, Vol. 17, pp. 81-118.

5) Bjerrum, L. (1973), "Problems of Soil Mechanics and Construction on Soft Clays and Structurally Unstable Soils," General Report, Session 4, Proceedings of the Eighth International Conference on Soil Mechanics and Foundation Engineering, Vol. 3, pp. 111-159.

6) Denby, G. M. (1978), "Self Boring Pressuremeter Study of San Francisco Bay Mud," Technical Report No. CE-232, Dept. of Civil Engineering, Stanford University.

7) Duncan, J. M. (1962,1963) Consolidation Tests Performed at the University of California, Berkeley.

8) Duncan, J. M. (1965), e Effect of Anisotropy and Reorientation of Principal Stresses on e Shear Strength of Saturated Clays," Ph.D. Thesis, University of California, Berkeley.

9) Duncan, J. M. and Seed, H. B. (1966) "Strength Variation Along Failure Surfaces in Clay," Journal of the Soil Mechanics and Foundation Division, ASCE, Vol. 92, No. SM6, November, pp. 81-104.

10) Duncan, J. M. and Seed, H. B. (1967) "Corrections for Strength Test Data," Journal of the Soil Mechanics and Foundations Division, ASCE, Vol. 93, No. SM5, September, pp. 121-137.

11) Duncan, J. M. and Buchignani, A. L. (1973) "Failure of an Underwater Slope in San Francisco Bay," Journal of the Soil Mechanics and Foundations Division, ASCE, Vol. 99, No. SM5, September, 1973.

12) Duncan, J. M. and Buchignani, A. L. (1976) "An Engineering Manual for Settlement Studies," Department of Civil Engineering, University of California, Berkeley, June.

13) Holzer, T. L., Hoeg, K. and Arulanandan, K. (1973) "Excess Pore Pressures During Undrained Creep," Canadian Geotechnical Journal, Vol. 10, No. 1, pp. 12-24.

14) Houston, W. N. (1979) Personal Communication, University of California, Berkeley.

15) Kavazanjian, E. (1978) "A Generalized Approach to the Prediction of the Stress-Strain-Time Behavior of Soft Clay," Ph.D. Thesis, University of California, Berkeley.

16) Lacerda, W. J. (1976) "Stress Relaxation and Creep Effects on the Deformation of Soils," Ph.D. Thesis, University of California, Berkeley.

17) Ladd, C. C. (1971) "Strength Parameters and Stress-Strain Behavior of Saturated Clays," Department of Civil Engineering, M.I.T., Report R71-23, Soils Publication 278.

18) Ladd, C. C. (1971) "Settlement Analyses for Cohesive Soils," Dept. of Civil Engineering, M.I.T., Report R71-2, Soils Publication 272.

19) Ladd, C. C. and Foott, R. (1974) "New Design Procedures for the Stability of Soft Clays," Journal of the Geotechnical Division, ASCE, Vol. 100, No. GT7, pp. 763-786, July.

20) Ladd, C. C., Foott, R., Ishihara, K., Schlosser, F. and Poulos, H. G. (1977) "Stress-Deformation and Strength Characteristics," Proceedings of the Ninth International Conference on Soil Mechanics and Foundation Engineering, Tokyo, Vol. 2, pp. 421-494.

21) Lo, K. Y. (1969) "The Pore Pressure-Strain Relationship of Normally Consolidated Undisturbed Clays, Part 2 Experimental Investigation and Practical Applications," Canadian Geotechnical Journal, Vol. 7, pp. 395-412.

22) Mejia, L. H. (1979) "Consolidation Tests - Comparison of Results," Report for the completion of requirements for course CE 299, Individual Study, University of California, Berkeley.

23) Mitchell, J. K. (1963) "Engineering Properties and Problems of San Francisco Bay Mud." California Division of Mines and Geology, Special Report 82, pp. 25-32.

24) Mitchell, J. K., Campanella, R. G. and Singh, A. (1968) "Soil Creep as a Rate Process," Journal of the Soil Mechanics and Foundation Division, ASCE, Vol. 94, No. SM1, pp. 231-253.

25) Mitchell, J. K. (1976) Fundamentals of Soil Behavior, John Wiley & Sons, New York, 422 p.

26) Mitchell, J. K. and Lunne, T. (1977) Unpublished study of several in-situ soil tests at H.A.F.B., University of California, Berkeley.

27) Mitchell, J. K., Guzikowski, F. and Villet, W.C.B. (1978) "The Measurement of Soil Properties In-situ, Present Methods - Their Applicability and Potential," Lawrence Berkeley Laboratory Report LBL-6363, University of California, Berkeley.

28) Oakeshott, G. B. (1966) "San Francisco Bay Area - It's Geologic Setting," Geotimes, October, 1966, pp. 11-19.

29) Schlocker, J. (1974) "Geology of the San Francisco North Quadrangle, California," Geological Survey Professional Paper 782, U. S. Government Printing Office, Washington, D.C.

30) Seed, H. B., Noorany, I. and Smith, I. M. (1964) "Effect of Sampling and Disturbance on the Strength of Soft Clays," Soil Mechanics and Bituminous Materials Research Laboratory, Report No. TE 64-1, University of California, Berkeley.

31) Singh, A. (1967) "Creep Phenomena in Soils," Ph.D. Thesis, University of California, Berkeley.

32) Singh, A. and Mitchell, J. K. (1968) "General Stress-Strain-Time Function for Soils," Journal of the Soil Mechanics and Foundations Division, ASCE, Vol. 94, No. SM1, pp. 21-46.

33) Singh, A. and Mitchell, J. K. (1969) "Creep Rupture and Creep Potential of Soils," Proceedings of the Seventh International Conference on Soil Mechanics and Foundation Engineering, Vol. 1, pp. 379-384.

34) Stratton, T. (1975) "Bay Mud Test Data - An Attempt at Correlation," Report for the completion of requirements for course CE 299, Individual Study, University of California, Berkeley.

35) Trask, P. D. and Rolston, J. W. (1951) "Engineering Geology of the San Francisco Bay, California," Geological Society of Ameri[illegible] Bulletin, Vol. 62, pp. 1078-1109.

36) Treasher, R. C. (1963) "Geology of the Sedimentary Deposits in San Francisco Bay," California Division of Mines and Geology, Special Report 82, pp. 11-19.

37) Tringale, P. T. (1978) Personal Communication.

38) University of California, Berkeley (1977) Results of work done by the CE 273 Soil Behavior class, J. K. Mitchell, Instructor.

39) University of California, Berkeley (1978) Results of work done by the CE 270L Soil Mechanics Laboratory testing class, W. N. Houston, Instructor.

APPENDIX 1 - CORRECTIONS OF STRENGTH DATA

Triaxial Tests

In any triaxial test that uses a rubber membrane and filter paper drains it is necessary to apply corrections to the test results in order to account for the load that the membrane and drains carry. Depending on the testing system it may also be necessary to apply a correction for the friction developed by the loading piston passing through the head of the triaxial chamber. These statements also apply to plane strain tests. In this appendix a brief outline of the methods used in this report to correct some of the triaxial test data is presented. These corrections have been applied selectively because of the amount of time it takes to make the corrections. Usually corrections were applied only to the ultimate values measured, such as peak strength, $\bar{A}_f$, etc. Only rarely were the actual stress-strain, pore pressure-strain, $\bar{A}$-strain and principal stress ratio-strain curves corrected. This appendix enables the reader to apply the test corrections to the results as his needs demand. For a thorough discussion of shear strength test corrections refer to Duncan and Seed (1967).

Piston Friction Corrections

The piston friction corrections need only be applied to the $\overline{\text{IC-U}}$ and $\overline{\text{AC-U}}$ test results performed at the University of California, Berkeley, prior to 1970. The type of piston and seal in use at Berkeley during this time and the appropriate correction factors to apply to the strength data are shown in Figure A1. As can be seen, the required correction is a linearly increasing function of the confining pressure. This correction

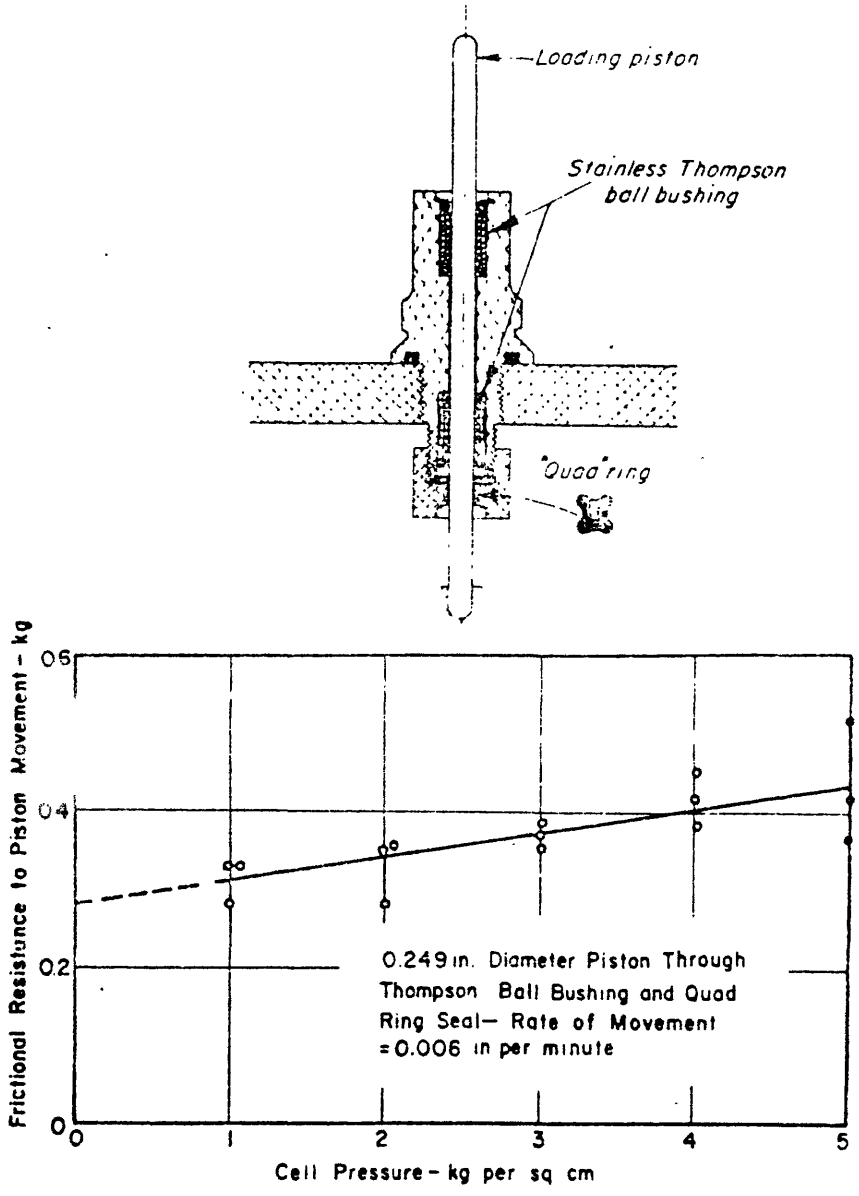


FIGURE A1 VARIATION OF FRICTIONAL RESISTANCE TO PISTON MOVEMENT WITH CHAMBER PRESSURE

From Duncan and Seed (1967)

should be applied at all strain levels. The triaxial cells presently in use at Berkeley have virtually no piston friction, eliminating any need for a piston friction correction.

Rubber Membranes

Rubber membrane corrections are calculated within acceptable accuracy by assuming that the membrane behaves elastically and the sample deforms as a right circular cylinder. The load carried by the membranes is very nearly a linear function of strain, small deviations from linearity arising out of changes in the cross sectional areas of the sample and the membrane. The rubber membrane corrections can be calculated using the following formulas. For a derivation of these equations refer to Duncan (1965).

$$\Delta\sigma_{AM} = -C_{am} \times (2/3) \times E_m \times 4\ t_{om}/D_{os}$$

$$\Delta\sigma_{LM} = -C_{\ell m} \times (2/3) \times E_M \times 2\ t_{om}/D_{os}$$

where $\Delta\sigma_{AM}$ = correction to axial stress for membrane strength

σ_{LM} = correction to lateral stress for membrane strength

E_M = Young's modulus of the membrane

t_{om} = initial thickness of the membrane

D_{os} = initial diameter of the sample

C_{am}, $C_{\ell m}$ = correction factors from Figure A2.

The usual type of rubber membrane used are Trojans, for which $t_{am} \simeq .002"$ and $E_m = 1400\ kN/m^2$. For the case of two membranes around a 1.4" diameter triaxial sample the corrections reduce to:

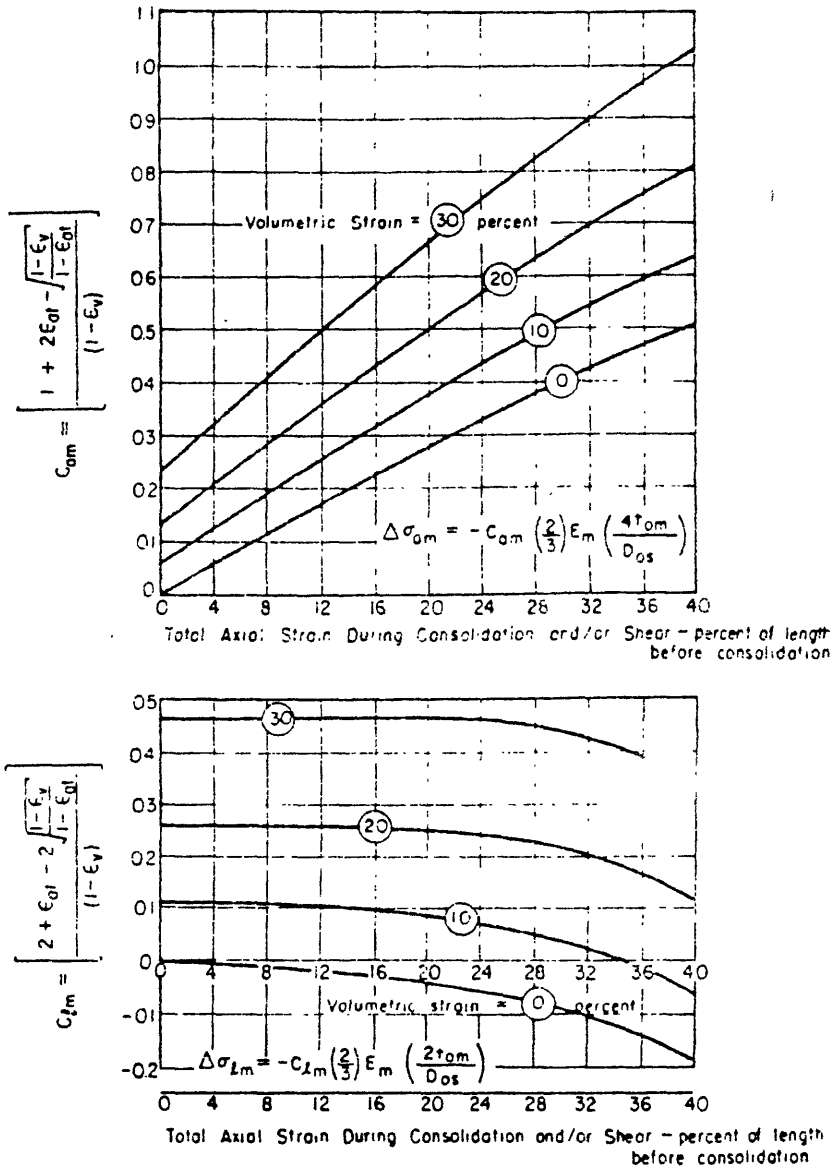


FIGURE A2 CORRECTION FACTORS C_{am} AND $C_{\ell m}$ FOR CORRECTIONS TO AXIAL AND LATERAL STRESS FOR MEMBRANE STRENGTH

From Duncan and Seed (1967)

$$\Delta\sigma_{AM} = -C_{AM} \times .107 \text{ kg/cm}^2$$

$$\Delta\sigma_{\ell m} = -C_{\ell m} \times .054 \text{ kg/cm}^2.$$

These corrections should be applied to all consolidated undrained and consolidated drained triaxial test data presented in this report.

Filter Paper Drains

The consolidated-undrained and consolidated-drained triaxial test data presented herein must be corrected for the load carried by filter paper drains. The appropriate correction to apply is given by the equation

$$\Delta\sigma_{afp} = K_{fp} \left(\frac{p}{A_s}\right)$$

$\Delta\sigma_{afp}$ = correction to axial stress for compressive strength of filter paper drains

p = length of perimeter covered by filter paper

A_s = area of specimen

K_{fp} = load carried by filter paper covering a unit length of the specimen perimeter.

For typical triaxial tests Whatman's No. 54 filter paper is used and covers 1/2 of the specimen perimeter with alternating 1/4 inch wide strips. For these test conditions values of K_{fp} between .06 and .19 kg/cm have been suggested. Houston (1979) recommends K_{fp} = .09 kg/cm, which is the value that has been used in this report. The filter paper drain correction should be applied at all strains greater than 2%. For strains between 0 and 2% the correction should vary linearly from 0 at 0% strain to its full value at 2% strain.

Plane Strain Tests

The corrections applied to plane strain tests are similar to those applied in triaxial tests, with some differences arising due to differences in geometry and possible end plate friction. For a discussion of the actual corrections applicable to plane strain tests, the reader is referred to either Duncan (1965) or Duncan and Seed (1967).